ACTA SILVATICA
&
LIGNARIA
HUNGARICA

Acta Silvatica & Lignaria Hungarica

An International Journal in Forest, Wood and Environmental Sciences

Volume 17, Nr. 1
Volume 17, Nr. 2
2021

UNIVERSITY OF SOPRON PRESS

ACTA SILVATICA ET LIGNARIA HUNGARICA
AN INTERNATIONAL JOURNAL IN FOREST, WOOD AND ENVIRONMENTAL SCIENCES
issued by the Forestry Commission of the Hungarian Academy of Sciences

The journal is financially supported by the
Hungarian Academy of Sciences (HAS),
Faculty of Forestry, University of Sopron (FF-US),
Faculty of Wood Engineering and Creative Industries, University of Sopron (FWECI-US),
Forest Research Institute, University of Sopron (FRI-US),
Sopron Scientists' Society of the Hungarian Academy of Sciences (SSS).

HU ISSN 1786-691X (Print)
HU ISSN 1787-064X (Online)

Manuscripts and editorial correspondence should be addressed to
TAMÁS HOFMANN, ASLH EDITORIAL OFFICE
UNIVERSITY OF SOPRON, PF. 132, H-9401 SOPRON, HUNGARY

Phone: +36 99 518 311
E-mail: aslh@uni-sopron.hu
Information and electronic edition: http://aslh.nyme.hu

The journal is indexed in the CAB ABSTRACTS database of CAB International; by SCOPUS, Elsevier's Bibliographic Database and by EBSCOhost database.

Published by UNIVERSITY OF SOPRON PRESS,
BAJCSY-ZS. U. 4., H-9400 SOPRON, HUNGARY
Cover design by ANDREA KLAUSZ
Printed by LŐVÉR-PRINT KFT., SOPRON

ACTA SILVATICA ET LIGNARIA HUNGARICA

Vol. 17, Nr. 1

Contents

ACTA SILVATICA ET LIGNARIA HUNGARICA

Vol. 17, Nr. 2

Contents

ACTA SILVATICA ET LIGNARIA HUNGARICA

Vol. 17, Nr. 1

Tartalomjegyzék

Vol. 17, Nr. 2

https://doi.org/10.37045/aslh-2021-0001 *Acta Silv. Lign. Hung., Vol. 17, Nr. 1 (2021) 9–20*

Photodegradation Properties of Earlywood and Latewood Spruce Timber Surfaces

Edina PREKLET[a] – László TOLVAJ[a*] – Satoru TSUCHIKAWA[b] – Dénes VARGA[a]

[a] Institute of Physics and Electrotechnics, University of Sopron, Sopron, Hungary
[b] Graduate School of Bioagricultural Sciences, Nagoya University, Nagoya, Japan

Abstract – Spruce (*Picea abies* Karst.) samples were irradiated using an ultraviolet light emitter mercury vapour lamp. The examined specimen surfaces contained earlywood or latewood to determine the photodegradation properties of these two tissue types. The generated chemical changes were monitored by diffuse reflectance Fourier transformed infrared spectroscopy. The difference spectrum method was used to present absorption changes. The earlywood suffered considerably greater degradation than the latewood during the UV irradiation. Most of the lignin molecules in the examined surface layer degraded during the first 11 days of UV irradiation for both earlywood and latewood. Results demonstrated that two types of unconjugated carbonyls absorbing at 1705 and 1764 cm^{-1} wavenumbers were created during the photodegradation. Time dependence of the absorption changes showed correlation between the guaiacyl lignin degradation and the generation of unconjugated carbonyl group absorbing at 1764 cm^{-1} wavenumber.

lignin / ultraviolet irradiation / infrared spectroscopy

Kivonat – A lucfenyő faanyag korai és késői pásztájának fotodegradációs tulajdonságai. Luc (*Picea abies* Karst.) famintákat világítottunk meg higanygőz lámpa által kibocsátott ultraibolya fénnyel. A vizsgált minták felszíne korai- vagy késői pásztát tartalmazott, hogy meghatározhassuk a kétféle pászta fotodegradációs tulajdonságait. A diffúz visszaverődésen alapuló Fourier transzformációs infravörös spektroszkópia segítségével követtük nyomon a kémiai változásokat. Az abszorpcióban bekövetkező módosulásokat a kalkulált különbségi színképek tükrözik. A korai pászta számottevően nagyobb degradációt szenvedett az UV besugárzás hatására, mint a késői pászta. A vizsgált felületi rétegben lévő lignin molekulák többsége degradálódott az UV besugárzás első 11 napja során. Az eredmények azt mutatják, hogy kétfajta nemkonjugált karbonil csoport keletkezett a fotodegradáció során, melyek abszorpciója az 1705 és az 1764 cm^{-1} hullámszámoknál jelentkezett. A kezelési idő függvényében vizsgált gvajacil lignin degradációja és az 1764 cm^{-1} hullámszámnál abszorbeáló nemkonjugált karbonil csoportok keletkezése között ok-okozati összefüggést találtunk.

lignin / ultraibolya besugárzás / infravörös színképelemzés

[*] Corresponding author: tolvaj.laszlo@uni-sopron.hu; H-9400 SOPRON, Bajcsy-Zs. u. 4, Hungary

1 INTRODUCTION

Colour harmony is one of nature's most beautiful creations. Machined wood surfaces in any anatomical plane present the colour diversity of the interior lumen surfaces, cell wall, earlywood, and latewood zones. The colour hue of wood between red and yellow generates a feeling of warmth.

This colour harmony of solid wood is sensitive to light, heat and humidity. Wood surfaces may degrade due to the combination of these factors and subsequently erode and become grey. Outdoor weathering tests of wood are highly complex. Outdoor weathering tests have some unavoidable disadvantages for scientific research because weather conditions are neither controllable nor repeatable. Therefore, the weathering properties of wood are usually investigated under artificial conditions.

The main factor causing the greatest changes in wood colour is exposure to sunlight (Tolvaj – Mitsui 2005, Zivkovic et al.2014). The ultraviolet (UV) part of sun radiation causes the main degradation of wooden surfaces (Agresti et al. 2013, Yildiz et al. 2013, Borda – Popescu 2019, Liu X et al. 2016, 2019, Liu R et al. 2019). Chemical analyses showed that the deterioration is mainly related to lignin decomposition (Pandey 2005, Teaca et al. 2013, Timar et al. 2016, Arpaci et al. 2020). The chromophoric groups of lignin are strong UV light absorbers. The energy of the absorbed UV photons is enough to create free phenoxyl radicals. These free radicals react with oxygen to produce carbonyl groups (Tolvaj – Faix 1995, Bonifazi et al. 2017, Varga et al. 2017, Jankowska et al. 2020). Rain is able to leach out some parts of the degradation products. The chemical background of leaching was recently investigated (Kannar et al. 2018, Bejó et al. 2019, Varga et al. 2020, Pásztory et al. 2020). The infrared (IR) spectrum analysis showed that the leached surface suffered greater lignin degradation than the dry surface. The photodegradation-generated compounds, containing unconjugated carbonyl groups, were leachable. According to the Arrhenius law, increasing temperatures intensify the effect of photodegradation (Tolvaj et al. 2013, 2015, Varga et al. 2017, Preklet et al. 2018).

Differences in the weathering properties of earlywood and latewood are well visible after long-term outdoor exposure. Earlywood surfaces became more eroded than latewood surfaces. Though this phenomenon is mentioned in some papers (Turkulin – Sell 2002, Tolvaj et al. 2014, Sandak et al., Štěrbová et al. 2020), the chemical background has not been investigated yet.

The aim of this study was to monitor chemical changes of photodegraded earlywood and latewood surfaces. IR spectroscopy was the applied analytical tool.

2 MATERIALS AND METHODS

Spruce (*Picea abies* Karst.) specimens with low extractive content were chosen for the degradation test. The specimen dimensions were 30 mm x 10 mm x 5 mm (long. x tang. x rad.). Both investigated series were represented by three samples. IR measurement was completed on two fixed locations of the tangential surface of each sample (both earlywood and latewood samples). The tangential surface of the specimens contained only earlywood or latewood. A double mercury vapour lamp, with a total electric power of 800 W, as a strong UV light emitter, generated the light irradiation. The UV radiation was 80% of the total emission of the lamps. Specimens were located at a distance of 64 cm from the lamp. The temperature in the chamber was 50°C during the irradiation. The duration of the first UV irradiation period was 24 hours. After this period, UV radiation time was doubled (48 hours), and the 48-hour period of UV radiation was repeated up to 20 days (the last period was 36 hours). The shorter UV

radiation time was chosen at the beginning of the treatment because the degradation effect of UV radiation is very intensive at the beginning of the treatment.

Diffuse reflectance infrared Fourier transform (DRIFT) spectrum of the samples was measured before and after each treatment period. Measurements were carried out with an IR spectrophotometer (JASCO FT/IR 6300). The resolution was 4 cm^{-1} and 64 scans were measured and averaged. The background spectrum was obtained against an aluminium plate. Two-point baseline correction at 3800 cm^{-1} and at 1900 cm^{-1} was executed. The spectral intensities were calculated in Kubelka-Munk (K-M) units. The spectra were normalised to the band maximum around 1375 cm^{-1}. The intensity of spectra was adjusted to 1.0 by this normalisation at a maximum of around 1375 cm^{-1}. This C-H band of cellulose is often used as an internal standard because of its high intensity, central position, and strong stability during photodegradation. The difference spectrum was calculated by subtracting the initial IR data from the data of the treated sample. In this case, absorption increase is represented by positive band while negative band represents absorption decrease. Details are described in a previous work (Csanady et al. 2015). The band assignment is presented in *Table 1*.

Table 1. Characteristic IR bands of wood (place of maximum) and band assignments (Csanády et al. 2015)

Wavenumber (cm^{-1})	**Assignment**
3600–3550	Intramolecular hydrogen bond in a phenolic group (in lignin) and weakly bounded absorbed water
3360–3310	O(3)H. .O(5) intramolecular hydrogen bonds in cellulose
2928	CH_2 stretching asymmetric
2854	Symmetric CH_2 stretching
1770–1757	C=O stretching vibration of non-conjugated ketones and γ lactones
1736–1705	C=O stretching vibration of carboxyl groups and acetyl groups in hemicelluloses (xyloglucan)
1660–1653	conjugated C-O in quinines coupled with C=O stretching of various groups (flavones)
1628–1618	C=O stretching in flavones
1604–1594	aromatic skeletal breathing with CO stretching (syringil lignin)
1512–1505	aromatic skeletal (guaiacyl lignin)
1478–1476	C–H deformation in lignin
1465–1457	C–H deformation in xylan
1435	C–H deformation in lignin and carbohydrates
1390–1380	C–H deformation in cellulose and hemicellulose
1369–1366	Aliphatic C-H stretching in methyl and phenol OH
1333–1342	C–H deformation, C-OH stretching, syringyl ring
1319	$C–H_2$ wagging, C–H deformation (conifers)
1285	C–H bending mode in cellulose
1285–1275	C_{aryl}-O, guaiacyl ring breathing with CO stretching
1240–1230	C–O linkage in guaiacyl aromatic methoxyl groups and acetyl groups in xyloglucan
1183–1175	C-O-C stretching (asymm.) in cellulose and hemicelluloses
1158–1156	C–O–C stretching in pyranose rings, C=O stretching in aliphatic groups
1138–1131	C-O-C stretching (symm.), arom. C-H i.p. deformation, glucose ring vibration
1108–1106	C-O-C stretching
1078–1076	C−O stretching mainly from C(3)−O(3)H in cellulose I
1050–1045	C−O and C−C stretching in cellulose and hemicelluloses
898	C-H deformation of cellulose

3 RESULTS AND DISCUSSION

Infrared spectroscopy is a good measurement technique to determine the chemical changes of wood caused by light irradiation. *Figure 1* illustrates the IR absorption spectrum of spruce earlywood before and after three days of UV irradiation. Absorption intensities are presented in Kubelka-Munk (KM) units. The left half of the spruce absorption spectrum consists of two broad bands. The higher peak around 3450 cm^{-1} belongs to the absorption of hydroxyl groups. Hydroxyl groups are located at various places in cellulose, hemicellulose, and lignin. The OH groups are located in many different positions surrounded by diverse chemical compounds. Surrounding chemical groups perturb the vibration of hydroxyl groups, which slightly modifies the wavenumber of the absorption band. That is why the hydroxyl groups have absorption at different wavenumbers causing a rather wide absorption band. Water in the wood also results in absorption in this region. The next band around 2900 cm^{-1} represents the absorption of different methyl groups. This is also a multiple absorption band.

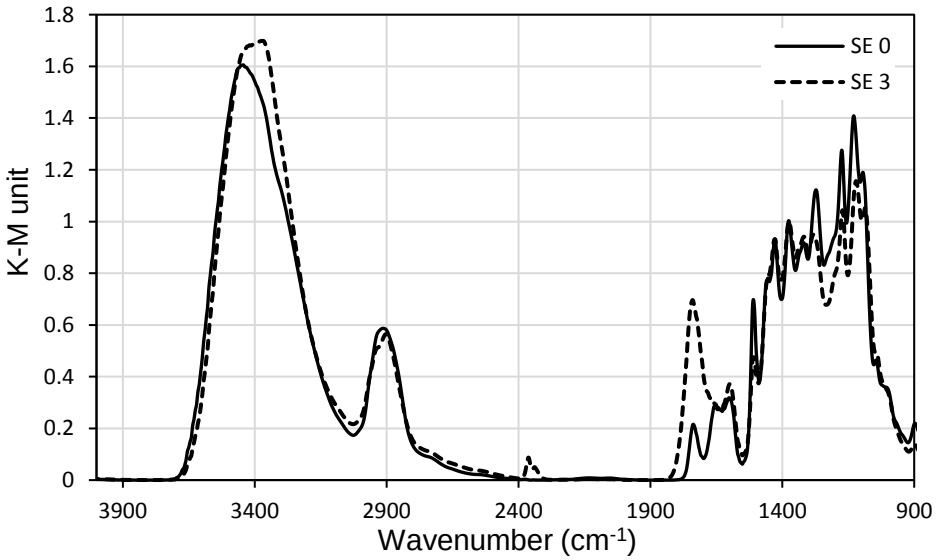

Figure 1. Absorption spectra of spruce (S) earlywood (E) before treatment (0) and after three days of UV irradiation

The right side of the spectrum (fingerprint region between 900–1900 cm^{-1}) consists of several overlapping bands generated by the absorption of cellulose, hemicelluloses, and lignin. As the bands highly overlap each other, most of the peak maxima are not real due to the superposition of two or more individual bands. (This phenomenon is clearly visible when comparing the form of the bands around 1740 cm^{-1} in *Figures 2–4*.)

The unconjugated carbonyl band is located between 1650 and 1820 cm^{-1}. This carbonyl band is the superposition of some individual bands. A previous study determined four bands in the unconjugated carbonyl region (Varga et al. 2017). Hence most publications treat the band of unconjugated carbonyls as a single absorption band with a maximum around 1740 cm^{-1}. The region between 950–1550 cm^{-1} wavenumbers has many overlapping bands. The most important peaks are the following: the peaks of the aromatic ring vibrations arising from lignin are at 1510 cm^{-1}; the peaks of the aromatic C-H deformation are at 1469 and 1428 cm^{-1}; the absorption of the guaiacyl ring breathing is located at 1270 cm^{-1}.

The absorption wavenumbers of the asymmetric and symmetric stretching of ether bond in cellulose are located around 1170 and 1130 cm^{-1}. The aromatic C-H deformation and the glucose ring vibration also generate absorption around 1130 cm^{-1}.

Chemical changes created by UV irradiation can be seen in *Figure 1*. The number of hydroxyl groups absorbing around 3400 cm^{-1} increased and the groups absorbing around 3600 cm^{-1} decreased during the three-day UV irradiation period. A great absorption increase appeared around 1740 cm^{-1}. The place of maximum shifted towards smaller wavenumbers and the band became wider. The absorption decrease of aromatic skeletal vibration of lignin at 1510 cm^{-1} is hardly visible together with the absorption decrease of ether bonds between 1120–1180 cm^{-1}. The difference spectrum method solves these problems. Creating the difference spectrum (irradiated minus initial) provides a more transparent figure since only those absorption bands appear where actual changes occurred. (The absorption increase is represented by positive band while negative band represents the absorption decrease.) The real changes are clearly visible in *Figure 2*, where the difference spectra are presented for both earlywood and latewood generated by one-day and three-day UV irradiation. The negative peak at 1510 cm^{-1} belongs to the aromatic skeletal vibration of guaiacyl lignin. This negative peak is detectable together with the absorption decrease of the aromatic C-H deformation at 1470 and 1430 cm^{-1} and with the absorption decrease of the guaiacyl ring breathing at 1270 cm^{-1}. The greatest absorption decrease is visible at 1174 and 1133 cm^{-1}. The first decrease belongs to the asymmetric stretching of ether bond in cellulose. The second decrease belongs to the symmetric stretching of ether bond, the aromatic C-H deformation, and to the glucose ring vibration. These absorption decreases indicate the ether splitting and the depolymerisation of cellulose.

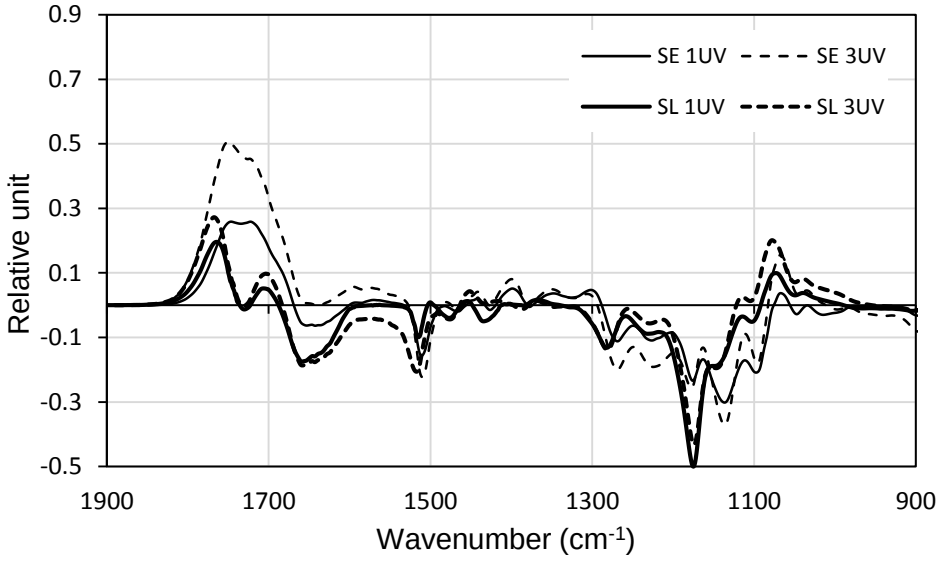

Figure 2. Absorption difference spectrum of spruce (S) earlywood (E) and latewood (L) generated by UV irradiation (in days).

Free radicals were generated during lignin degradation. These free radicals react with oxygen to produce carbonyl groups. The absorption increase of unconjugated carbonyls is visible in *Figures 2–4* in the 1680–1820 cm^{-1} wavenumber interval. Two bands rose in this region for both earlywood and latewood at 1705 and 1764 cm^{-1} wavenumbers. The band at 1764 cm^{-1} represents the absorption of CO stretching for unconjugated ketones and γ lactones generated by the oxidation after the splitting of the aromatic ring. The band at 1705 cm^{-1} represents the absorption of aliphatic carboxyl groups. Although the locations of these peaks should be the same, the intensities and the apparent places of the peaks are different for earlywood and latewood. Latewood produced a smaller absorption increase than earlywood. Great intensity difference was found between the two peaks. The peak intensity at 1705 cm^{-1}

was small compared to the neighbouring peak. The two bands are well separated because of the low intensities. In contrast, the peak intensity at 1705 cm^{-1} for earlywood is almost equal to that of the neighbouring peak at 1764 cm^{-1}. The superposition of the two bands is visible in *Figure 2.* The real positions of the peaks are not visible since the superposition pulled the locations of the peaks toward each other. These two bands finally joined into one single band after 20-day UV irradiation (*Figure 4*). The negative intensity change of the peak at 1510 cm^{-1} increased during UV irradiation. (Time dependence of this intensity will be discussed later.)

The intensity of the two types of ether bond at 1174 and 1133 cm^{-1} decreased, but in different ways for earlywood and latewood. The two negative peak intensities were almost equal for earlywood. The peak at 1133 cm^{-1} was a little greater than the peak at 1174 cm^{-1}. Latewood showed opposite peak intensities. The peak at 1174 cm^{-1} presented the greatest negative change and the peak at 1133 cm^{-1} is visible as a shoulder. There is a visible positive peak at 1068 cm^{-1}. This positive peak is associated with the C-O bonds stretching in cellulose and hemicelluloses.

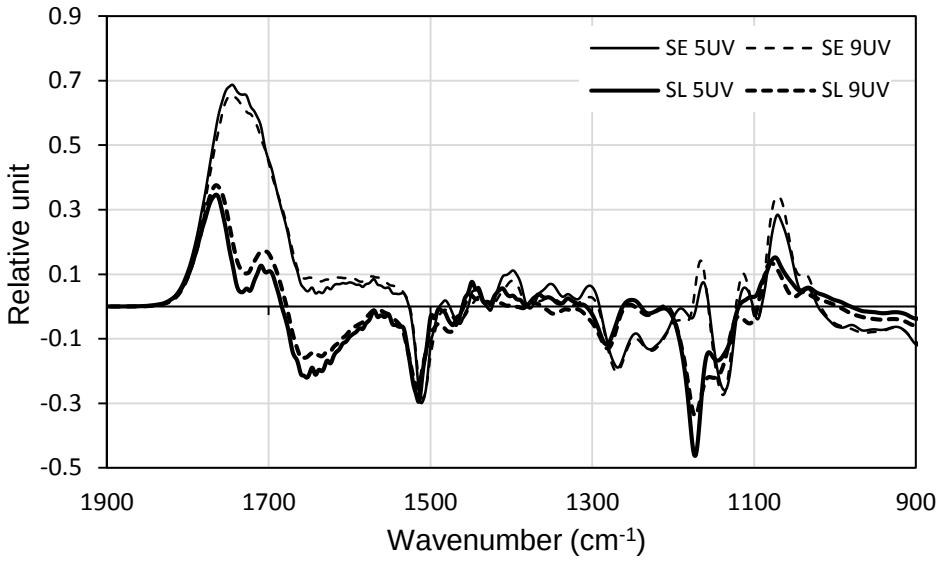

Figure 3. Absorption difference spectrum of spruce (S) earlywood (E) and latewood (L) generated by UV irradiation (in days)

The prolonged treatment time intensified the absorption changes *(Figures 3 and 4).* The absorption intensities of the two types of unconjugated carbonyl groups at 1705 and 1764 cm^{-1} wavenumbers increased with longer irradiation. (The time dependence of these intensities will be discussed later.) The two bands composed a single band after nine days of irradiation for earlywood, which remained up to the end of treatment. The peak intensity at 1705 cm^{-1} was growing faster than the peak intensity at 1764 cm^{-1} for latewood, and it became only a shoulder after 20 days of irradiation.

The evaluation of the changes in the ether bond region is difficult because the Kubelka-Munk equation does not provide the absorption spectrum properly if the absorption is high and the surface roughness changes. A previous study showed that photodegradation increases the surface roughness of wood (Tolvaj et al. 2014). The roughness increase lifts up the intensities due to the increasing scattering. A detailed discussion of this phenomenon can be found in a previous study (Tolvaj et al. 2011). The lifting effect overlaps the real absorption changes, interfering with the evaluation of IR spectrum in the 1000–1200 cm^{-1} wavenumber interval.

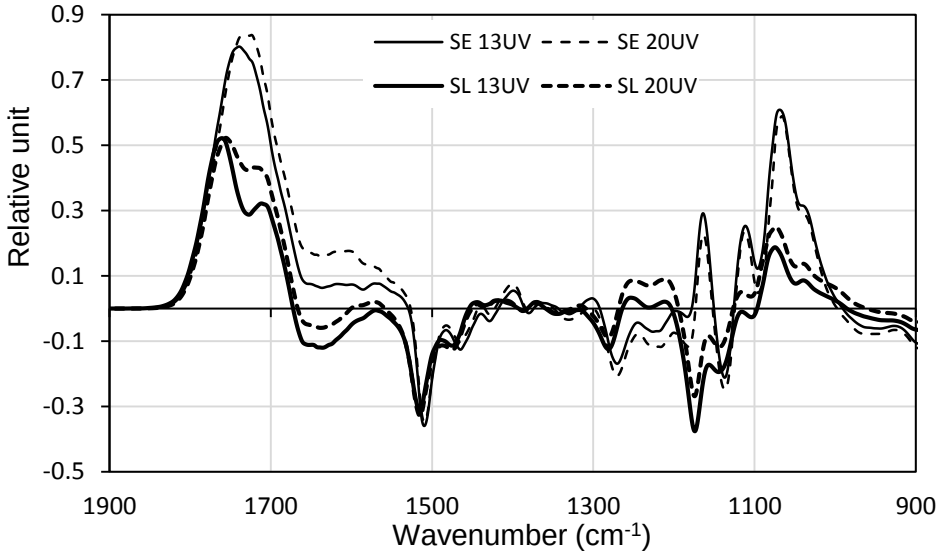

Figure 4. Absorption difference spectrum of spruce (S) earlywood (E) and latewood (L) generated by UV irradiation (in days).

Figures 2–4 present the absorption decrease of guaiacyl lignin. However, due to overlapping, these figures do not clearly show the intensity changes of this negative peak. *Figure 5* clearly demonstrates the absorption change at 1510 cm^{-1} in all investigated situations. The results show that earlywood suffered greater lignin degradation than latewood. The higher extractive content in latewood provided greater protection for lignin than the lower extractive content in earlywood. The protecting effect of the extractives was demonstrated by previous studies (Németh et al. 1992, Varga et al. 2020). Lignin degradation was fast at the beginning of the treatment and stopped after 11 days of UV irradiation for both earlywood and latewood. The reason could be that most of the lignin molecules of the examined surface layer degraded during the first 11 days of UV irradiation.

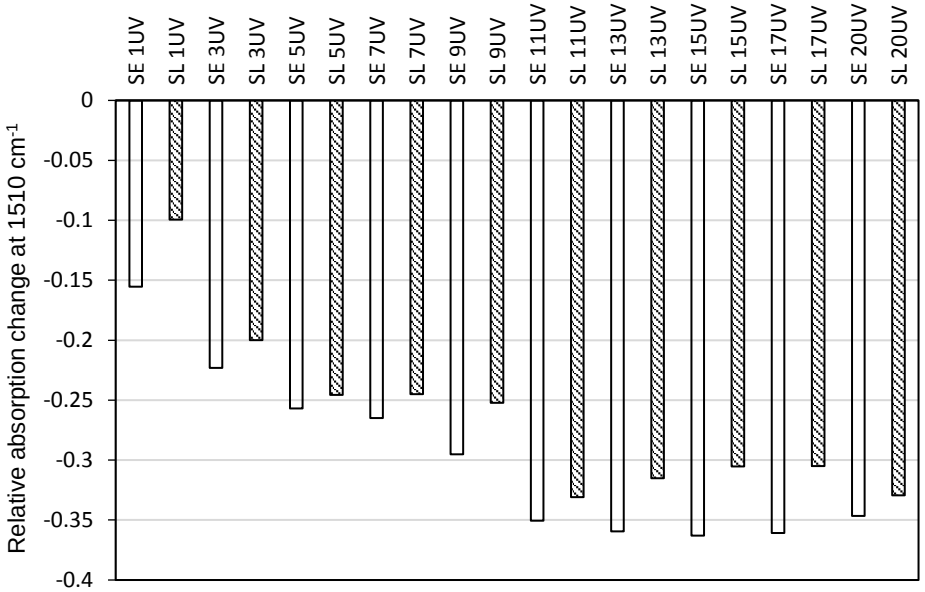

Figure 5. Absorption band intensity change of guaiacyl lignin in spruce (S) earlywood (E) and latewood (L) at 1510 cm^{-1} wavenumber generated by UV irradiation (in days)

Figure 6 presents the intensity changes of the unconjugated carbonyl groups absorbing at the 1764 cm^{-1} wavenumber. Absorption intensity increased continuously for both earlywood and latewood up to the thirteenth day of UV irradiation, and decreased slightly after that. The decrease after the thirteenth day of treatment might not be a real decrease. The values were read exactly at 1764 cm^{-1} wavenumber; however, changes in the overlapping band at the 1705 cm^{-1} wavenumber probably modified the real values. UV irradiation generated greater absorption increase for earlywood than for latewood. The trend seems to be opposite for one-day treatment, while *Figure 2* clearly shows that earlywood produced greater absorption increase than latewood during the first day of irradiation. The tendency of the absorption changes at 1764 cm^{-1} was a mirror image of lignin degradation at 1510 cm^{-1}. This fact demonstrates the correlation between lignin degradation and the generation of unconjugated carbonyl groups absorbing at 1764 cm^{-1}. Many studies deal with the correlation between lignin degradation and the generation of new unconjugated carbonyl groups (Pandey 2005, Agresti et al. 2013, Timar et al. 2016, Bonifazi et al. 2017, Reinprecht et al. 2018). However, all of these publications use the complete integrated unconjugated carbonyl band as the participant in the correlation. Our results demonstrate that only one component of unconjugated carbonyl band (at 1764 cm^{-1} wavenumber) participates in this correlation.

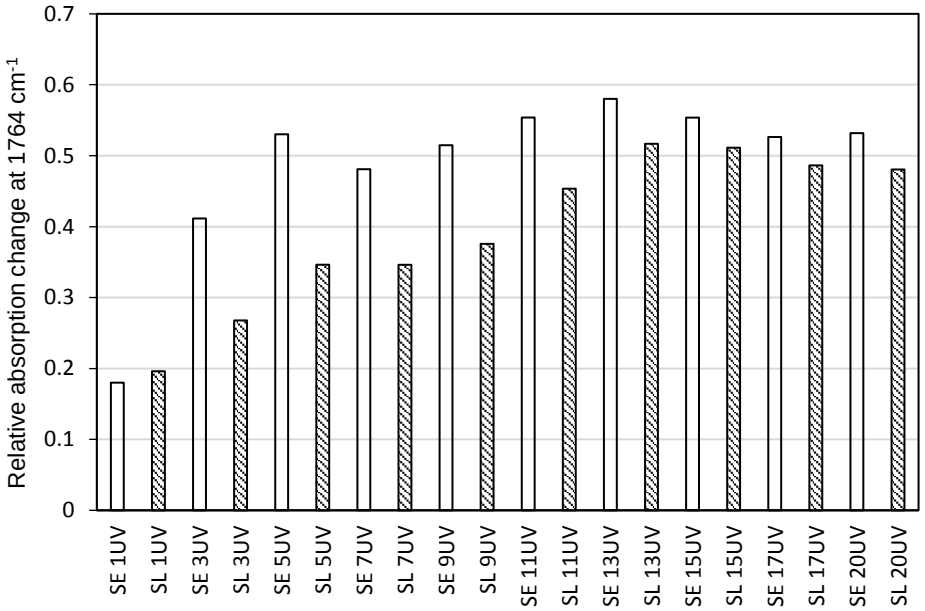

Figure 6. Absorption band intensity change of the unconjugated carbonyls at 1764 cm^{-1} for spruce (S) earlywood (E) and latewood (L) generated by UV irradiation (in days)

Figure 7 shows the irradiation time dependence of the unconjugated carbonyls absorbing at the 1705 cm^{-1} wavenumber. Earlywood presented rapid absorption increase at the beginning of the UV irradiation, followed by a moderate increase up to the end of the treatment. Latewood produced only a small absorption increase during the first day of irradiation. This small value was followed by continuous absorption increase throughout the whole investigated treatment period. In the second part of the treatment, latewood produced more intensive absorption increase than the earlywood. The absorption increase at 1705 cm^{-1} does not show similar time dependence to the lignin degradation. This finding raises the question of whether the unconjugated carbonyls absorbing at 1705 cm^{-1} are derived from the degradation of lignin. This phenomenon requires further chemical investigations.

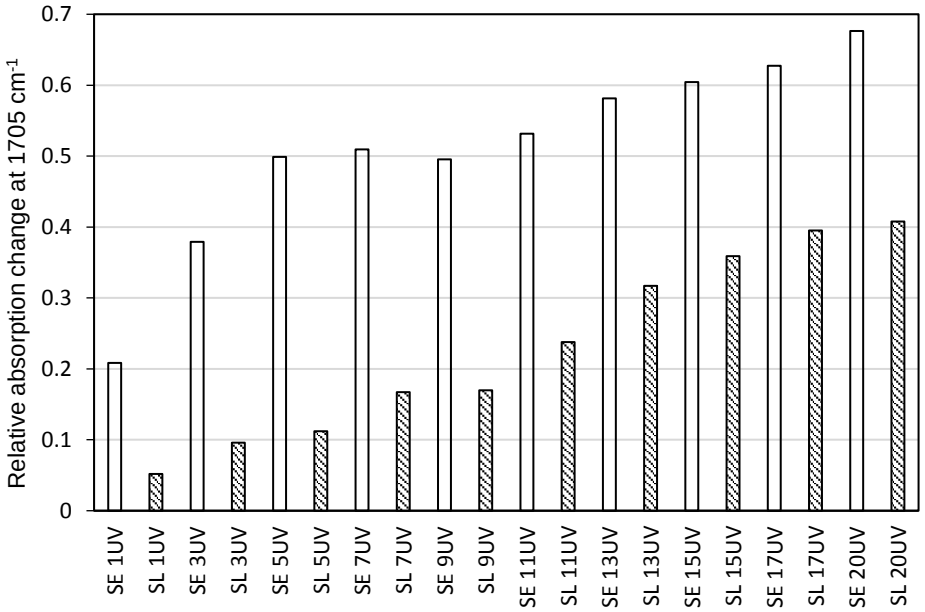

Figure 7 Absorption band intensity change of the unconjugated carbonyls at 1705 cm^{-1} for spruce (S) earlywood (E) and latewood (L) generated by UV irradiation (in days)

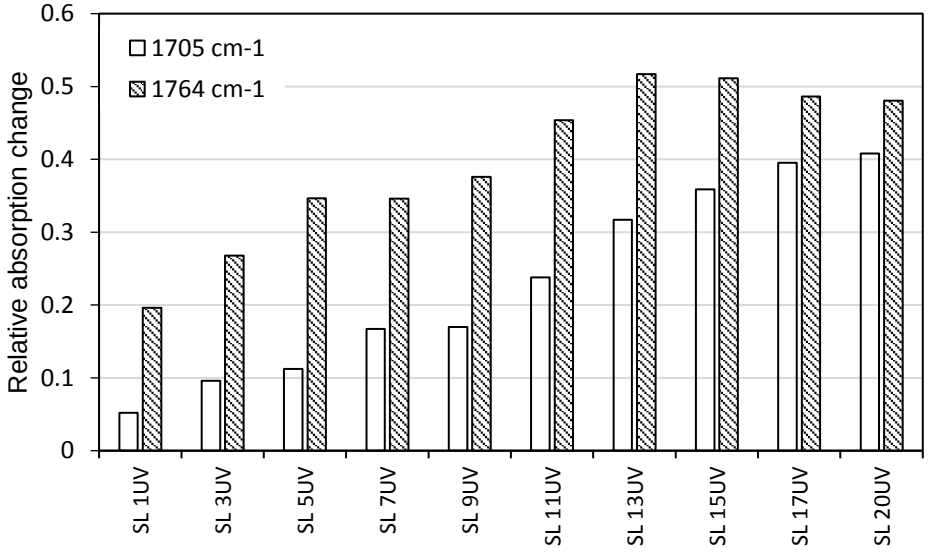

Figure 8. Absorption band intensity change of the unconjugated carbonyls at 1705 cm^{-1} and 1764 cm^{-1} wavenumbers for spruce (S) latewood (L) generated by UV irradiation (in days)

Figure 8 represents the differences between the absorption properties of the two types of unconjugated carbonyl groups absorbing at 1705 and 1764 cm^{-1}. The time dependence of these two absorption increases is completely different. The band at 1764 cm^{-1} showed a rapid increase at the beginning of the UV irradiation. The change of the absorption increase produced a maximum on the thirteenth day of the treatment. In contrast, the band at 1705 cm^{-1} presented continuous increase during the whole investigated period. This difference in the growing tendency shows that the generation of these two types of unconjugated carbonyl groups (at 1705 and 1764 cm^{-1}) has two different pass ways or different origins.

4 CONCLUSIONS

Spruce samples with earlywood or latewood surfaces were irradiated using a strong ultraviolet light emitter mercury lamp. Chemical changes were monitored by DRIFT IR spectroscopy. The difference spectrum method was applied to determine the changes. Lignin deterioration and unconjugated carbonyl compound generation were found to be the main changes during UV irradiation. Earlywood suffered greater degradation than latewood. Most of the lignin molecules of the examined surface layer degraded during the first 11 days of UV irradiation in both earlywood and latewood. Results demonstrated that two types of unconjugated carbonyls absorbing at 1705 and 1764 cm^{-1} wavenumber were created during photodegradation. The time dependence of the absorption changes showed correlation between the guaiacyl lignin degradation and the generation of unconjugated carbonyl group absorbing at 1764 cm^{-1} wavenumber. There is no correlation between the lignin degradation and the generation of unconjugated carbonyl group absorbing at 1705 cm^{-1} wavenumber.

Acknowledgements: This article was made in frame of the "EFOP-3.6.1-16-2016-00018 – Improving the role of research+development+innovation in the higher education through institutional developments assisting intelligent specialization in Sopron and Szombathely".

REFERENCES

AGRESTI, G. – BONIFAZI, G. – CALIENNO, L. – CAPOBIANCO, G. – LO MONACO, A. – PELOSI, C. – PICCHIO, R. – SERRANTI, S. (2013): Surface investigation of photo-degraded wood by colour monitoring, infrared spectroscopy, and hyperspectral imaging. Journal of Spectroscopy 1: Paper: 380536. https://doi.org/10.1155/2013/380536

ARPACI, S.S. – TOMEK, E.D. – ERMEYDAN, M.A. – YILDIRIM, I. (2020): Natural weathering of sixteen wood species: Changes on surface properties. Polymer Degradation and Stability Paper id:109415. https://doi.org/10.1016/j.polymdegradstab.2020.109415

BEJO, L. – TOLVAJ, L. – KANNAR, A. – PREKLET, E. (2019): Effect of water leaching on photodegraded spruce wood monitored by IR spectroscopy. Journal of Photochemistry and Photobiology A: Chemistry 382: Paper: 111948. https://doi.org/10.1016/j.jphotochem.2019.111948

BONIFAZI, G. – CALIENNO, L. – CAPOBIANCO, G. – LO MONACO, A. – PELOSI, C. – PICCHIO, R. – SERRANTI, S. (2017): A new approach for the modelling of chestnut wood photo-degradation monitored by different spectroscopic techniques. Environmental Science and Pollution Research 24: 13874–13884. https://doi.org/10.1007/s11356-016-6047-0

BRODA, M. – POPESCU, C.M. (2019): Natural decay of archaeological oak wood versus artificial degradation processes – An FT-IR spectroscopy and X-ray diffraction study. Spectrochimica Acta A: Molecular and Biomolbiomolecular Spectroscopy 209: 280–287.

CALIENNO, L. – LO MONACO, A. – PELOSI, C. – PICCHIO, R. (2014): Colour and chemical changes on photodegraded beech wood with or without red heartwood. Wood Science and Technology 48:1167–1180. https://doi.org/10.1007/s00226-014-0670-z

CSANÁDY, E., MAGOSS, E., TOLVAJ, L., (2015): Quality of Machined Wood Surfaces, Springer pp 41–90.

JANKOWSKA, A. – RYBAK, K. – NOWACKA, M. – BORUSZEWSKI, P. (2020): Insight of Weathering Processes Based on Monitoring Surface Characteristic of Tropical Wood Species. Coatings 10: 877. https://doi.org/10.3390/coatings10090877

KÁNNÁR, A. – TOLVAJ, L. – MAGOSS, E. (2018): Colour change of photodegraded spruce wood by water leaching. Wood Research 63: 935–946.

LIU, X.Y. – TIMAR, M.C. – VARODI, A.M. – YI, S.L. (2016): Effects of Ageing ont he Color and Surface Chemistry of Paulownia Wood (*P. elongata*) from Fast Growing Crops. BioResources 11(4): 9400–9420.

LIU R, ZHU H, LI K, YANG Z (2019) Comparison on the Aging of Woods Exposed to Natural Sunlight and Artificial Xenon Light. Polymer 11(4): Paper: 709. https://doi.org/10.3390/polym11040709

LIU, X.Y. – LIU, M. – LV, M.Q. – LV, J.F. (2019): Photodegradation of Three Hardwood Species by Sunlight and Xenon Light Source. BioResources 14(3): 6969–6922.

NÉMETH, K. – VANÓ, V. – FAIX, O. (1992): The effect of wood extractives on the photodegradation of wood. EWLP Conf. Grenoble, France. 191–192.

PANDEY, K.K. (2005): Study of the effect of photo-irradiation on the surface chemistry of wood. Polymer Degradation and Stability 90(1): 9–20. http://doi.org/10.1016/j.polymdegradstab.2005.02.009

PÁSZTORY, Z. – TOLVAJ, L. – VARGA, D. (2020): Effect of water leaching on photodegraded poplar wood monitored by IR spectroscopy. Wood Research 65 (6): 885–894. http://doi.org/10.37763/wr.1336-4561/65.6.885894

REINPRECHT, L.·– MAMOŇOVÁ, M.·– PÁNEK, M.·– KAČÍK, F. (2018): The impact of natural and artificial weathering on the visual, colour and structural changes of seven tropical woods. European Journal of Wood and Wood Products 76: 175–190. https://doi.org/10.1007/s00107-017-1228-1

ŠTĚRBOVÁ, I. – OBERHOFNEROVÁ, E. – PÁNEK, M. – DVOŘÁK, O. – PAVELEK, M. (2020): Influence of different exposition of larch wood facade models on their surface degradation processes. Central European Forestry Journal.

SANDAK, A. – BURUD, I. – FLØ, A. – THIIS, T. – ROSS GOBAKKEN, L. – SANDAK, J. (2017): Hyperspectral imaging of weathered wood samples in transmission mode. International Wood Products Journal 8: Sup. 1. https://doi.org/10.1080/20426445.2016.1237079

TEACA, C.A. – ROSU, D. – BODIRILAU, R. – ROSU, L. (2013): Structural Changes in Wood under Artificial UV Light Irradiation Determined by FTIR Spectroscopy and Color Measurements – A Brief Review. BioResources 8: 1478–1507.

TIMÁR, M.C. – VARODI, A.M. – GURAU, L. (2016): Comparative study of photodegradation of six wood species after short-time UV exposure. Wood Science and Technology 50(1): 135–163. https://doi.org/10.1007/s00226-015-0771-3

TURKULIN, H. – SELL, J. (2002): Investigations into the photodegradation of wood using microtensile testing. Part 4: Tensile properties and fractography of weathered wood. Holz als Roh- und Werkstoff 60: 96–105.

TOLVAJ, L. – FAIX, O. (1995): Artifical ageing of wood monitored by drift spectroscopy and CIE L*a*b* color measurements. I. effect of UV light. Holzforschung 49(5): 397–404. https://doi.org/10.1515/hfsg.1995.49.5.397

TOLVAJ, L. – MITSUI, K. (2005): Light source dependence of the photodegradation of wood. Journal of Wood Science 51(5): 468–473. http://doi.org/10.1007/s10086-004-0693-4

TOLVAJ, L. – MITSUI, K. – VARGA, D. (2011): Validity limits of Kubelka–Munk theory for DRIFT spectra of photodegraded solid wood, Wood Science and Technology 4: 135–146. https://doi.org/10.1007/s00226-010-0314-x

TOLVAJ, L. – MOLNÁR, ZS. – NÉMETH, R. (2013): Photodegradation of wood at elevated temperature: Infrared spectroscopic study. Journal of Photochemistry and Photobiology B: Biology 121:32–36. http://doi.org/10.1016/j.jphotobiol.2013.02.007

TOLVAJ, L. – MOLNÁR, ZS. – MAGOSS, E. (2014): Measurement of photodegradation-caused roughness of wood using a new optical method. Journal of Photochemistry and Photobiology B: Biology 134: 23–26. https://doi.org/10.1016/j.jphotobiol.2014.03.020

TOLVAJ, L. – TSUCHIKAWA, S. – INAGAKI, T. – VARGA, D. (2015): Combined effects of UV light and elevated temperatures on wood discoloration. Wood Science and Technology 49: 1225–1237. https://doi.org/10.1007/s00226-015-0749-1

VARGA, D. – TOLVAJ, L. – TSUCHIKAWA, S. – BEJÓ, L. – PREKLET E. (2017): Temperature dependence of wood photodegradation monitored by infrared spectroscopy. Journal of Photochemistry and Photobiology A: Chemistry 348: 219–225. http://doi.org/10.1016/j.jphotochem.2017.08.040

VARGA, D. – TOLVAJ, L. – MOLNÁR, ZS. – PÁSZTORY, Z. (2020): Leaching effect of water on photodegraded hardwood species monitored by IR spectroscopy. Wood Science and Technology 54: 1407–1421. https://doi.org/10.1007/s00226-020-01204-2

YILDIZ, S. – TOMAK, E.D. – YILDIZ, U.C. – USTAOMER, D. (2013): Effect of artificial weathering on the properties of heat treated wood. Polymer Degradation and Stability 98:1419–1427. https://doi.org/10.1016/j.polymdegradstab.2013.05.004

ZIVKOVIC, V. – ARNOLD, M. – RADMANOVIC, K. – RICHTER, K. – TURKULIN, H. (2014): Spectral sensitivity in the photodegradation of fir wood (Abies alba Mill.) surfaces: colour changes in natural weathering. Wood Science and Technology 48(2): 239–252. https://doi.org/10.1007/s00226-013-0601-4

https://doi.org/10.37045/aslh-2021-0002 *Acta Silv. Lign. Hung., Vol. 17, Nr. 1 (2021) 21–35*

Comparative Study of Conventional and Zero-joint Edgebanding

Mária Réka ANTAL[a] – Levente DÉNES[ab] – Zsigmond András VAS[a] – András POLGÁR[c*]

[a] Institute of Wood Based Products and Technologies, Simonyi Károly Faculty of Engineering, Wood Sciences and Applied Art, University of Sopron, Sopron, Hungary
[b] Transylvanian Furniture Cluster, Cluj-Napoca, Romania
[c] Department of Environmental Protection, Institute of Environmental and Earth Sciences, Faculty of Forestry, University of Sopron, Sopron, Hungary

Abstract – Edgebanding affects both the visual appearance and edge protection of wood-based panels. In order for edgebanding to provide the desired protection, it must adhere strongly to the entire surface of the panel edges and maintain this adhesion throughout the life of the product. The present research compares conventional and so-called zero-joint edgebandings in terms of water and steam resistance, and examines the environmental impacts of edgebanding technologies using Life Cycle Assessment (LCA). In-line with our hypothesis, our test results showed that corners are the critical points of edgebanded furniture fronts, especially when exposed to moisture. Due to high variations in measurements, there is no significant difference between the two edgebanding methods at the beginning. However, differences become more significant after longer treatment times. These differences amount to two quality categories after 6 hours and three quality categories after 12 and 24 hours. The edgebanded fronts exposed to water for less than 30 minutes experience no significant deteriorations with any of the edgebanding methods. In the case of steam resistance, zero-joint edgebanding provides better protection, especially after the second and third treatment cycle. We can state that the surplus costs of zero-joint technology are 1.45 times greater than costs associated with conventional technology. Both show the considerable costs of edging materials, chipboard, and electrical energy. The applied environmental life cycle assessment (LCA) method corresponds to the requirements of ISO 14040:2006 and ISO 14044:2006 standards. We built up the environmental inventory and the life cycle model of the manufacturing technology using the GaBi Professional LCA software. In the impact assessment, we analysed the specific environmental impact categories of the differing production processes by technology according to the operation order of the manufacturing technology. In relation to traditional and the zero-joint edging technologies, according to all impact assessment methods, the life-cycle contribution rate was uniformly 47% traditional – 53% zero-joint by impact category. The higher indicator values of the zero-joint method are due to larger edge material consumption and higher energy demand. Zero-joint technology appears to avoid the application of conventional hot melt adhesives, but replacing these adhesives does not necessarily result in better environmental indicators. Nevertheless, zero-joint egdebanding does not just improve aesthetic appearance but also exceeds the durability provided by conventional edgebanding technology.

edgebanding / resistance to water and steam / environmental impact / LCA

[*] Corresponding author: polgar.andras@uni-sopron.hu; H-9400 SOPRON, Bajcsy-Zs. u. 4, Hungary

Kivonat – Hagyományos és fugamentes élzárás összehasonlító vizsgálata. A faalapú lemezek élzárása nemcsak esztétikailag, hanem az élek védelme szempontjából is fontos. Ahhoz, hogy az élzárás a kívánt védelmet nyújtsa erősen kell tapadnia a lemezek éleinek teljes felületéhez, és ezt a tapadást meg kell őriznie a termék teljes életciklusa alatt. Jelen kutatás a hagyományos és az ún. nullfugás élzárásokat hasonlítja össze a vízzel és gőzzel szembeni ellenállás szempontjából, valamint az élzárási technológiák környezeti hatásait vizsgálja. A vizsgálati eredmények azt mutatják, hogy a hipotézisünknek megfelelően a sarkok a kritikus pontok, a víz és gőz behatolása itt a leggyorsabb. A mérési adatok nagy szórása miatt a vízzel szembeni ellenállás esetén a két élzárási technológia között nincs szignifikáns különbség, azonban a 6 órás kitettség után két, a 12 és 24 órás kitettség után pedig három minőségi osztálykülönbség tapasztalható. Ha a víz csak maximum 30 percig érintkezik az éllel, nem tapasztalhatók elváltozások egyik élzárási módszernél sem. A gőzzel szembeni ellenállás esetén a nullfugás élzárás jobb védelmet nyújt különösen a második és harmadik gőzölési ciklus után. A kutatás során elvégeztük az életciklus költségszámítást is: a nullfugás technológia 1,45-szörös költségtöbbletet mutatott a hagyományoshoz képest. Nagyságrendileg mindkét esetben az élzáró anyag, a forgácslap és az elektromos energia költségei voltak jelentősek. A környezeti életciklus elemzés (LCA) során az ISO 14040-44:2006 szabványok alapján kizárólag az élzárási alternatívák műveleteit vizsgáltuk. Szoftveres támogatással felépítettük a gyártástechnológiák környezeti leltáradatbázisát és LCA modelljét. A hatásértékelés során technológiánként elemeztük a gyártási folyamatok jellemző környezeti hatáskategóriáit. A hagyományos és nullfugás élzárási technológiát illetően hatásértékelési módszerenként egységesen 47% hagyományos - 53% nullfugás arány volt tapasztalható az életciklus hozzájárulásban hatáskategóriánként. A nullfugás eljárás magasabb értékei a nagyobb mennyiségű felhasznált élanyagnak és a nagyobb energiaigénynek tudhatók be. A nullfugás technológia a hagyományos ragasztóanyag alkalmazását mellőzi, ám ennek kiváltása nem eredményezett kedvezőbb környezeti mutatókat. Az élzárások esetén életciklus elemzéssel vizsgált környezeti hatásokat nemcsak az alkalmazott gyártástechnológiák jellemzői befolyásolják, hanem emellett meghatározó szerepe van az élzárt termék igénybevételekkel szembeni tartósságának is, amely az élzárási alternatíva sajátossága.

élzárás / vízzel és gőzzel szembeni ellenállás / környzeti hatás / LCA

1 INTRODUCTION

Wood and wood-based materials are a renewable resource and are considered ‘environmentally friendly’ compared to other materials (Lippke et al. 2004). Wood product manufacturing results in lower emissions than the manufacturing of other materials (Lippke et al. 2019).

The furniture industry has been increasing its use of particleboard over the past few decades. Many studies support the main importance of edging as a mandatory technological step for protecting sides of wood composite panels such as particleboard (Jivkov 2002; Tankut & Tankut 2010; Saçli 2015; Merdzhanov 2018).

Different technologies are currently employed for edgebanding. Gluing edgebands, which has become a key technology in furniture production, is completed through a conventional bonding process: hot melt glues are applied using rollers in edgebanding woodworking machines (Rechner et al. 2009). Technological modernization has led to the quick spread of innovative processes in furniture manufacturing. One such innovation is zero-joint edgebanding, which is considered an important technological operation in the wood industry. The main differences between the two edgebanding technologies are aesthetical appearance and adhesive spreading. The zero joint glue line is almost invisible due to the coextruded functional layer. Moreover, an additional bonding agent is unnecessary *(Figure 1)*. Consequently, the environmental significance of the method is beyond question.

In edgebanding that incorporates laser technology, laser radiation melts a predetermined layer of the edging material. According to Rechner et al. (2009), laser technology for the edgebanding process in furniture manufacturing provides the same strength as conventional gluing, all without the adhesive joints that affect visual appearance. The transition between the

edgeband and the board surface provides a flawless appearance to the human eye. At the same time, the impact of external influences (like water or dirt) is reduced to a minimum. This increases the resistance of the adhesive bond to ageing (Rechner et al. 2009).

According to Tankut and Tankut (2010), the purpose of edgebanding is to suppress the absorption of water and humidity and provide an aesthetic finish for all decorative surfaces.

Edgebanding has two main functions: to cover the aesthetically unfavorable core panels like particleboard, fiberboard, etc., and to protect these panels from mechanical and physical impacts (Molnárné 2002). To fulfill these requirements, edgebanding materials (coiled foils from polyvinyl chloride [PVC], acrylonitrile butadiene styrene [ABS], polypropylene [PP], polymethylmethacrylate [PMMA], or strips from solid wood) must be perfectly bonded to the panel edges without voids or loose parts, leveled to the thickness of the panels, and trimmed to the desired dimensions and shapes. Several factors influence the durability of the adhesion line between edgebanding materials and panels. Among these we find the resistance to moisture, which affects edgebanding in two main forms i.e., liquid and vapor.

In addition to durability, the quality (conformity) factors of the product include other characteristics, such as aesthetics or environmental impacts. Life-Cycle Assessment (LCA) is the most suitable method for determining the environmental impacts of a product. According to Fava et al. (1994), the development of the LCA methodology has helped to quantify and provide information about products where environmental qualities were lacking.

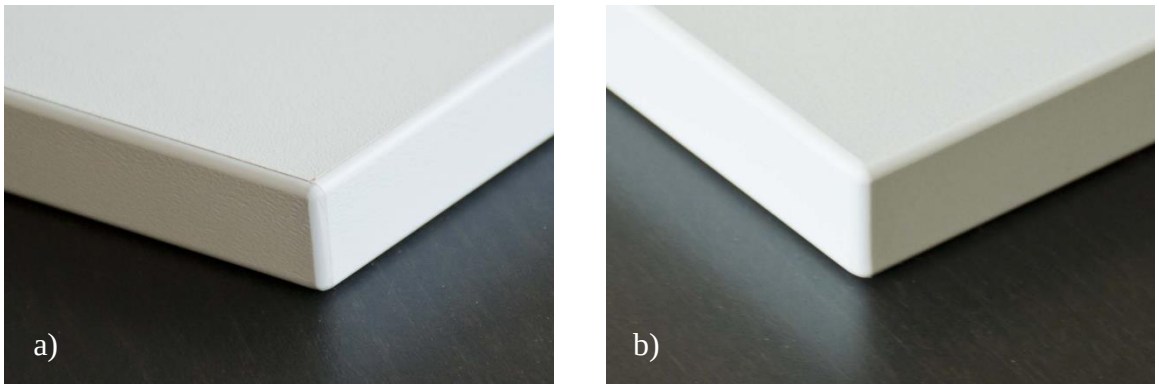

Figure 1. Aesthetic comparison of conventional (a) and zero-joint (b) ABS edgebanding

The first main goal of this research was to examine how moisture affects the durability and aesthetics of edgebanded panels. Moisture came into contact with the surface in two forms: cold liquid and hot steam. Conventional (EVA) and zero-joint technologies were used to determine the effect of edgebanding type on thickness swelling. The second goal of our study was to use the LCA method to determine and compare the environmental impacts of conventional and the zero-joint edgebanding technologies in the wood industry. Durability affects the environmental impacts additionally. If the edgebanding is more durable, the edgebanded panel is favourable in terms of environmental impacts.

2 MATERIALS AND METHODS

Hungarian furniture manufacturers most frequently use 18 mm-thick laminated particleboards; hence, these were selected for both the durability and environmental studies. Acrylonitrile butadiene styrene (ABS) was the material selected for edgebanding. The edgebanding methods employed were the conventional (using hot melt adhesive EVA) and zero-joint technology methods. A Roxyl 6.0 edgebander wood machine was used for both conventional and zero-joint edgebanding. Life-Cycle Analysis (LCA) was used to determine environmental impacts. We

used the GaBi Professional LCA software, which is the most trusted product for Life Cycle Assessment.

2.1 Durability study

All tests were performed according to the IOS-TM-0002 IKEA specification.

2.1.1 Assessment of edges' resistance to water

This test simulates the water resistance of the edgebanded furniture fronts used in locations with elevated humidity levels such as kitchens and bathrooms. Five specimens were used per edgebanding technology. The 400x300 mm edgebanded specimens were conditioned at 23 ± 2 °C and 50 ± 5% humidity prior to testing. Seven measuring points were selected for specimen' thickness determination: five at the edge and two at a distance of 20 mm from the edge. The first and last measuring points at the edge were located at the corners of the specimens, and the distance between each point was 100 mm. *Figure 2* shows the placement of the measuring points.

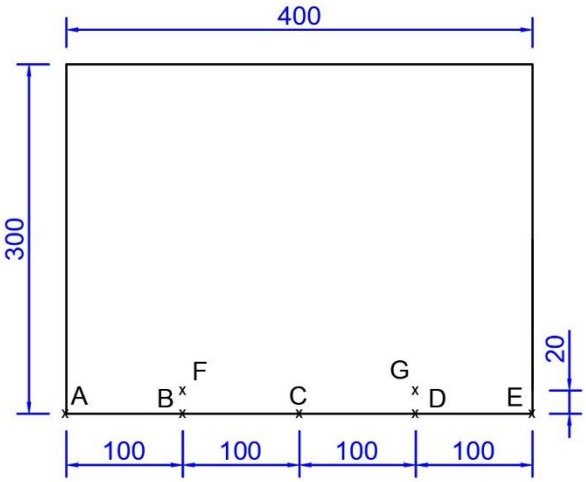

Figure 2. Measuring points of water and steam resistance

Sample thickness was determined at the measuring points to the nearest 0.01 mm using a digital caliper after conditioning and before the tests began. A 50 mm-thick, open-cell polyurethane foam with a density of 20 kg/m^3 was placed in a flat tub equipped with spacer plates of the same height as the tub height (50 mm), and the tub was filled with distilled water at 23 ± 2 °C. Water level was kept constant at 12 mm below the upper edge of the spacers throughout the entire test period. The edgebanded specimens were placed vertically on the partition plates and exposed for the time corresponding to the test periods *(Figure 3a)*. A total of seven test periods with the following values were used: 5 min, 30 min, 2 h, 6 h, 12 h, 24 h, and 48 h. The last period consisted of 24 hours of soaking and 24 hours of conditioning. After each test period, the specimen edges were wiped dry and the thickness was measured at the measurement points. After visual inspection of the edges, the thickness swelling results were evaluated on a scale of 1 to 5 as defined in the specification *(Table 1).*

Table 1. Assessment criteria for water resistance (IOS 2017)

Rating	Criteria
5	**No visible damage** can be seen; thickness swelling is less than 0.05 mm.
4	**Minor damage** that does not affect function or appearance essentially is accepted. The maximum thickness swelling is 0.1 mm, but without visible cracking or opening between edge bands.
3	**Moderate damage** with thickness swelling from 0.1 to 0.25 mm. The glue line may have become soft, but there is still enough adhesive to keep the edging in place. The edging may loosen to mechanical strain and few narrow cracks are allowed.
2	**Significant damage** with thickness swelling from 0.25 to 1.0 mm. Open glued joint or partly loose edging. Several narrow cracks may appear.
1	**Severe damage**: thickness swelling is over 1 mm. Loose edging, totally or partly damaged surface finish. Many narrow cracks or one or more broad cracks.

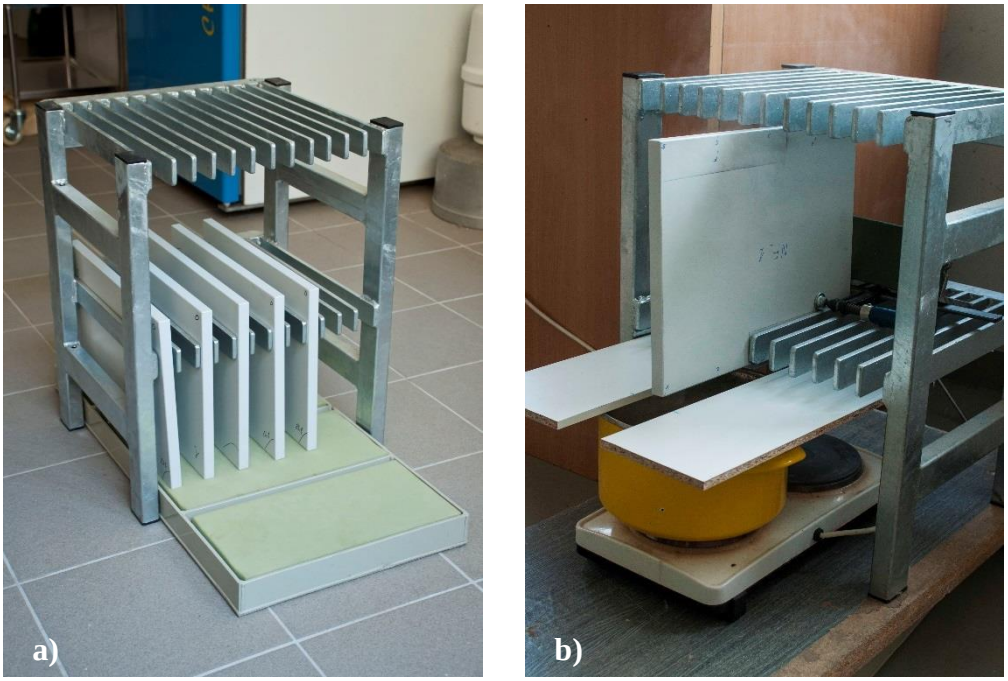

Figure 3. Determination of edge resistance to water and steam (a – to water; b – to steam)

2.1.2 Assessment of edges' resistance to steam

The test method simulates the effect of steam and condensation on edgebanded furniture fronts. Edgebanded specimens with dimensions of 400x300 mm were cleaned prior to conditioning (see the test method for water resistance test) and examined for defects. Sample thickness was measured at the corner and at a distance of 100 mm from the corner. Specimens were mounted on the jig using a clamp with the tested edge facing downward and resting on the water-bath with the corner at a distance of 50 mm from bath side. The length of the exposed edge was about 150 mm. The water bath placed beneath specimens was heated using an electric hob, with the water level set at 70 mm below the edge of the test samples. The water bath was covered with two panels allowing a 70 mm wide gap for specimens (*Figure 3b*). After five minutes of steam exposure and 24 hours conditioning, specimen thickness was measured at two measuring points. This cycle was repeated two more times, with the cumulated steam exposure time

reaching 15 minutes. After each cycle, the tested edges were examined for damage. At the end of the three cycles, the tested edges were assessed according to *Table 2*.

Table 2. Assessment criteria for steam resistance (IOS 2017)

Rating	Criteria
5	**No visible damage**.
4	**Minor change:** slight discoloration, rough surface, minor gloss change.
3	**Moderate change:** minor blistering, small cracks and opening (maximum 1 mm), visible/noticeable thickness swelling.
2	**Significant change:** opening of maximum 2 mm, large cracks, the edge band is partly loose.
1	**Severe change:** large opening (>2 mm), large cracks along/across the edge, edge band completely detached.

2.2 Environmental study

The objective of the environmental study was to perform a comparative life cycle analysis of conventional and zero-joint edgebanding technologies. The study refers of 3.5 m^3 quantity chipboard, edgebanded with two different types of ABS materials for conventional and zero-joint edging technologies. The input and output data for this study are presented in *Table 4.* The data sources stem from Hungarian manufacturing data, our own data, expert estimations, and published data. Reference period: 2016.

The applied environmental life cycle assessment *(LCA)* method corresponds to the requirements of ISO 14040:2006 (ISO 2006a) and ISO 14044:2006 (ISO 2006b) standards.

The environmental life cycle assessment (LCA) method plays an important role in the analysis of environmental impacts. Life cycle assessment enables the determination of the sustainability and environmental quality of wood products and the related manufacturing technologies.

Life-cycle methods allow for the evaluation of environmental burdens such as air and water pollution, solid waste, and ecosystem impacts (Lippke et al. 2019).

To run LCA, we examined the flow of material and energy on the input and output side during the conventional and zero-joint wood edgebanding operations. We also examined each material cost during the analysis.

We built up the environmental inventory and the life cycle model of the manufacturing technology using the GaBi Professional LCA software. In the impact assessment, we analysed the specific environmental impact categories of the differing production processes by technology according to the order of operation of the manufacturing technology. For a reliable analysis, we calculated the impact-category indicator results by using several impact assessment methods and models (CML2001, Primary energy).

Functional unit: edgebanding the chipboard elements of the specific furniture family with ABS edgebanding material

- reference flow (conventional): ABS edge material, 1006.98 m long, 2.00 mm thick, 22.65 mm wide
- reference flow (zero-joint): ABS edge material, 1006.98 m long, 2.35 mm thick, 23.15 mm wide

As regards the transport of raw materials, we considered 100 tkm and a EURO 4 truck. In the case of electrical energy, we used the Hungarian energy mix.

The edgebanding process steps (operational steps) of the Roxil 6.0 edgebander wood machine, which are also the LCA boundaries, comprise the following: raw materials transport – loading of banding material – chipboard surface handling – chipboard edge milling – applying glue (gluing) (*omitted for zero-joint technology*) – applying banding material by pressing (bonds the edge banding to the substrate) – end-cutting banding material – rough and fine trimming – edge rounding – ABS edge refining – glue scraping (*omitted for zero-joint technology*) – cutting grooves or rabbets (if necessary) – edge polishing using brush – edge heating for colour correction using air blower – panel transport (Kozák 2006).

3 RESULTS AND DISCUSSION

3.1 Water resistance

Specimen thicknesses were measured in the assigned points after each treatment. F-tests and Student t-tests were employed for the statistical analysis of the data. *Figure 4* presents the variation of thickness swelling in function of treatment time, edgebanding technologies, and measurement points. From the three-dimensional column diagram, we can deduce that visible changes occur only at the corners (points A and E) and at a distance of 100 mm from the left corner (point B). The thickness swelling at point B is remarkable only in conventional joints; there are no visible changes at zero joints. Both joint types were waterproof for 30 minutes. The first noticeable deviations occurred after two hours of exposure. The maximum thickness swelling of 1.31 mm was measured at the corner of the conventional joints after 24 hours of treatment. In point A (specimens' left corner) there were no statistically significant differences between conventional and zero joints. However, at a distance of 100 mm from the corner (point B) after 2 hours of water exposure, the conventional joints swelling was 0.112 mm and increased gradually with the exposure time, but the zero joints showed no changes in thickness. At the right corner (point E), the visible changes appeared just after 6 hours of exposure and the zero joints had higher swelling values than conventional joints. After 24 hours of exposure and 24 hours of conditioning, the specimens started to lose water in the conditioning phase and the thickness values began to decline; however, this change was not statistically significant.

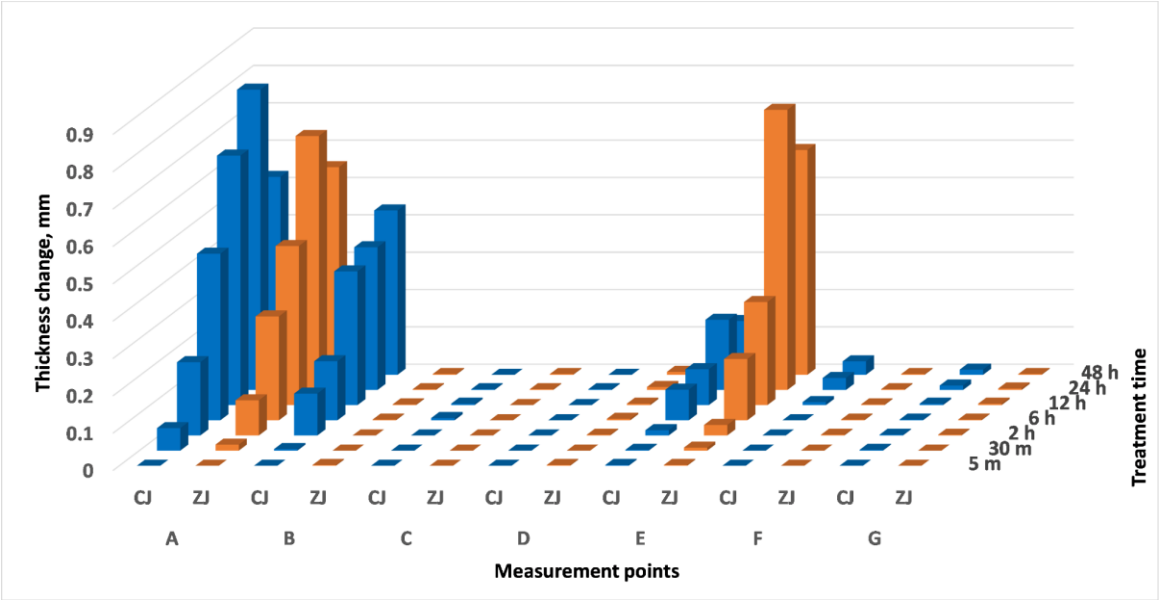

Figure 4. The average thickness swelling of specimens with conventional (CJ) and zero joints (ZJ) at the measurement points (A-G) after different moisture exposure times

Table 3 contains the average rating values of the measuring points in function of treatment time and joint type. The values confirm the statements related to *Figure 4.* The first differences in rating values (see *Table 1*) between conventional and zero joints appeared after 2 hours of exposure at the left corner, and after 12 hours both joints showed significant changes, the value decreased from 5 to 2. Rating differences between the two joint types were less accentuated at the opposite corner; however, zero joint values were worse than conventional joint values. In point B, the conventional joint degraded gradually, but the zero joints remained intact after 2 hours of exposure. This contradiction needs to be analysed further on a larger sample to discover if it is local gluing defects or the variation is too high.

Table 3. Classification of measuring points based on the assessment criteria

Measuring points	Treatment duration													
	5min		30min		2h		6h		12h		24h		48h	
	CJ	ZJ	CJ	ZJ	CJ	ZJ	CJ	ZJ	CJ	ZJ	CJ	ZJ	CJ	ZJ
A	5	5	4	5	3	4	2	2	2	2	2	2	2	2
B	5	5	5	5	3	5	3	5	2	5	2	5	2	5
C	5	5	5	5	5	5	5	5	5	5	5	5	5	5
D	5	5	5	5	5	5	5	5	5	5	5	5	5	5
E	5	5	5	5	5	5	4	3	4	2	3	2	3	2
F	5	5	5	5	5	5	5	5	5	5	5	5	5	5
G	5	5	5	5	5	5	5	5	5	5	5	5	5	5

3.2 Steam resistance

Figure 5 displays the thickness swelling values of the edgebanded specimens exposed to steaming. The thickness increases were visible after each treatment cycle, reaching a maximum of 1.75 mm at the corner of one of the conventionally edgebanded specimens. After 5 minutes, the differences between the two joint types were noticeable, but after 10 minutes, this difference attained 40%. The corner was more affected by steaming than the edges; however, after 15 minutes of exposure the average thickness swelling of the conventional joint at a distance of 100 mm reached 1 mm. This value is 80% higher than the value of the zero joint (0.2 mm). The measured values demonstrate that the conventional joints are more sensitive to steaming.

Statistical evaluations revealed that thickness-swelling values were significantly higher at the corner than at a distance of 100 mm from the corner. No significant difference appeared between the conventional and zero joint after one cycle; however, after 10 and 15 minutes of steam exposure the zero joint swelling values were considerably lower (with 39% and 37%). A gradually increasing thickness swelling can be observed by extending the exposure time from 5 to 15 minutes. At 100 mm from the corner, there is a significant difference between the two joint types after 10 minutes treatment, and the conventional joint thickness increased considerably at the end of the total exposure. *Figure 6* shows the effect of moisture and steam on the edgebanded samples.

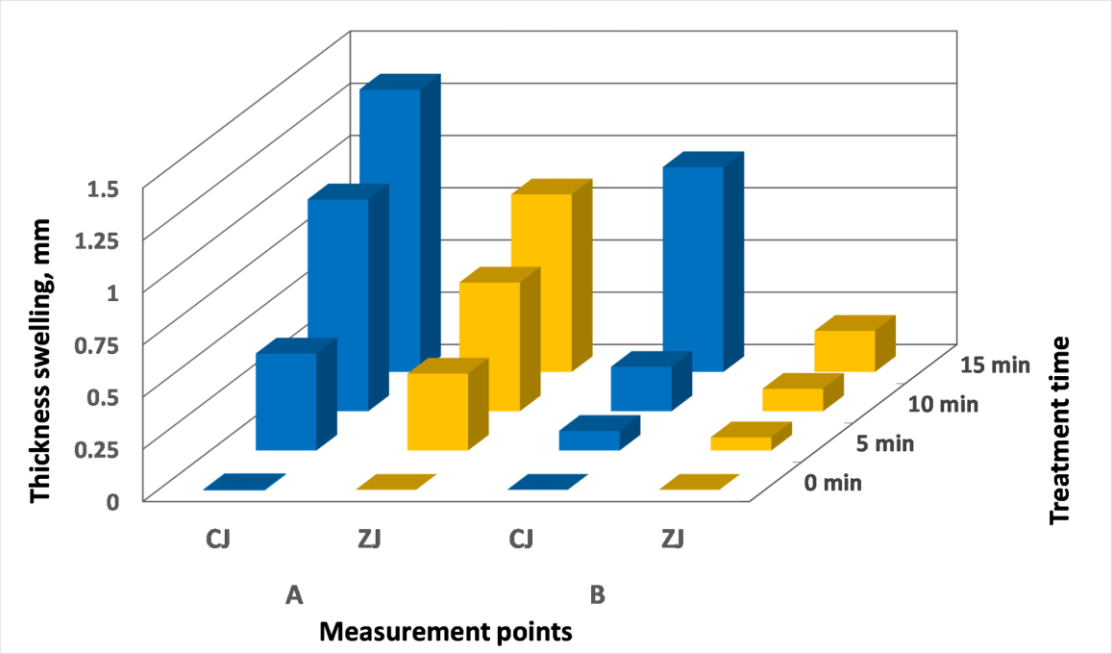

Figure 5. The average thickness swelling of specimens with conventional (CJ) and zero joints (ZJ), in the measurement points (A and B) after different steam exposure times

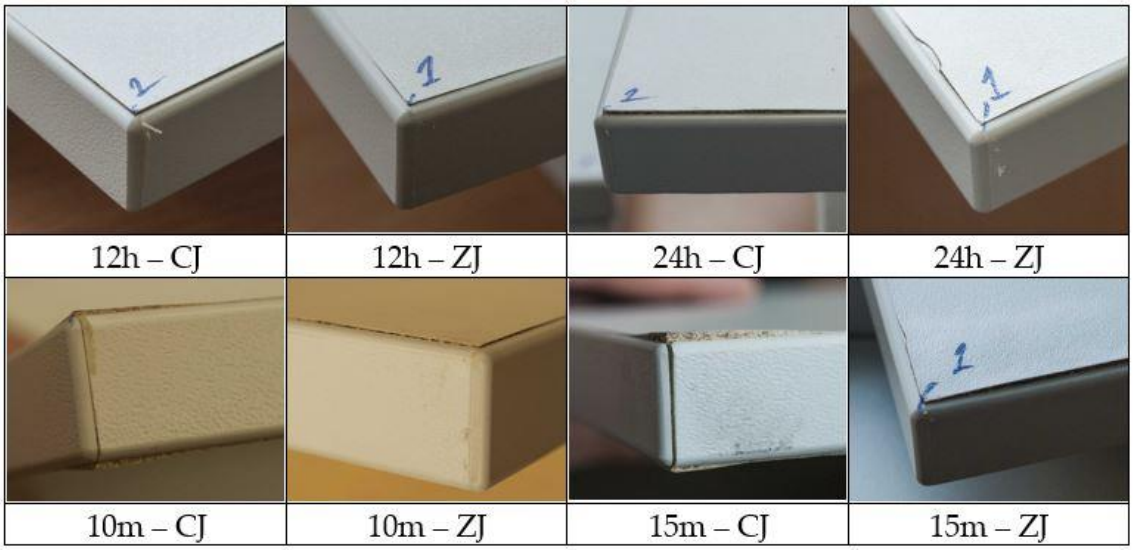

Figure 6. The effect of moisture and steam on the edgebanded samples

3.3 Environmental impacts

In *Table 4*, we collected the most important environmental inventory data, namely the inputs and outputs specific to the process. According to standard ISO 14044:2006 (ISO 2006b), the inputs could be product, material, or energy flow that enters a unit process. The output could be product, material or energy flow that leaves a unit process (products and materials include raw materials, intermediate products, co-products, and releases).

These inputs and outputs were the environmental factors (material and energy abstractions and emissions during the technology) that define the system boundaries of the analysis. The inputs and outputs were empirical data as well as data based on Hungarian manufacturing technology. These data were collected in the reference year 2016.

Table 4. Total environmental inventory data of edgebanding technologies (our own data were collected from manufacturing technology in Hungary, reference period: 2016)

Environmental inventory	Unit	Edgebanding	
		Conventional	Zero-joint
Input			
Acrylonitrite-Butadiene-Styrene (ABS) edge material	kg	48.50	53.69
Electrical energy	kWh	171.68	246.59
Treatment fluid (ethanol)	ml	458.10	458.10
Chipboard 18 mm	kg (m^3)	2277.99 (3.50)	2277.9 (3.50)
Ethylene-vinyl acetate copolymers, adhesive granulate (EVA)	kg	0.10	–
Lubricating oil	kg	0.0016	0.0016
Package of adhesive (plastic)	kg	0.002	0.002
Package of edging material (cardboard)	kg	3.65	3.65
Output			
Acrylonitrite-Butadiene-Styrene (ABS) edge material	kg	35.42	39.84
Treatment fluid (ethanol)	ml	343.56	343.56
Chipboard 18 mm	kg (m^3)	2257.44 (3.47)	2257.4 (3.47)
Ethylene-vinyl acetate copolymers, adhesive granulate (EVA)	kg	0.09	–
Packaging waste material	kg	0.011	–
Edge material waste	kg	13.08	13.85
Chipboard waste	kg (m^3)	20.55 (0.032)	20.55 (0.032)
Treatment fluid waste	ml	114.54	114.54
Package of adhesive (plastic)	kg	0.002	0.002
Package of edging material (cardboard)	kg	3.65	3.65
Waste oil (recycled)	kg	0.0016	0.0016

Based on the environmental inventory data, costs emerging in the examined life cycle can also be included in the life cycle costing (LCC) method. LCC analysis provides an appropriate basis for calculating the costs in the life cycle. Through this, profit can be maximized at all stages of the life cycle. One of the advantages of LCC analysis is that all investment costs and cost structures can be demonstrated. This enables a more accurate calculation, which leads to better decision making (Laáb 2021).

In the case of the environmental inventory data, we assigned the costs primarily to the inputs (the prices of the inputs come from the raw material distribution companies, July 2020 prices). According to this, the total cost of inputs for conventional edgebanding technology were HUF 792,896; while the total cost of inputs for the zero-joint edging technology were HUF 1,152,642. We can state that zero-joint technology displays a 1.45 times surplus compared to conventional technology. Both technologies showed considerable costs of the edging material, the chipboard, and the electrical energy. Concerning the input, significant differences (more than doubled value) occurred from the quantity of acrylonitrite-butadiene-styrene (ABS) edge material (in the case of 1006.98 m, traditional: HUF 213,480, zero-joint: HUF 568,950). The costs of ABS edge material waste by technologies were the following: traditional, HUF 57,574 (27%); zero-joint, HUF 146,768 (28%).

Differences in electricity consumption also arose. Zero-joint technology requires 1.44 times more energy input compared to conventional technology, which results in additional costs.

The usage of ethylene-vinyl acetate copolymers, adhesive granulate (EVA) in the conventional technology results in only HUF 226,300 extra cost compared to the zero-joint technology.

In the impact assessment process, the environmental impact categories of the specific production processes were analysed by technology according to the operational sequence of the edgebandings.

The following results in Figure 7 were based on the CML 2001 (version: April 2015) problem-oriented impact assessment method.

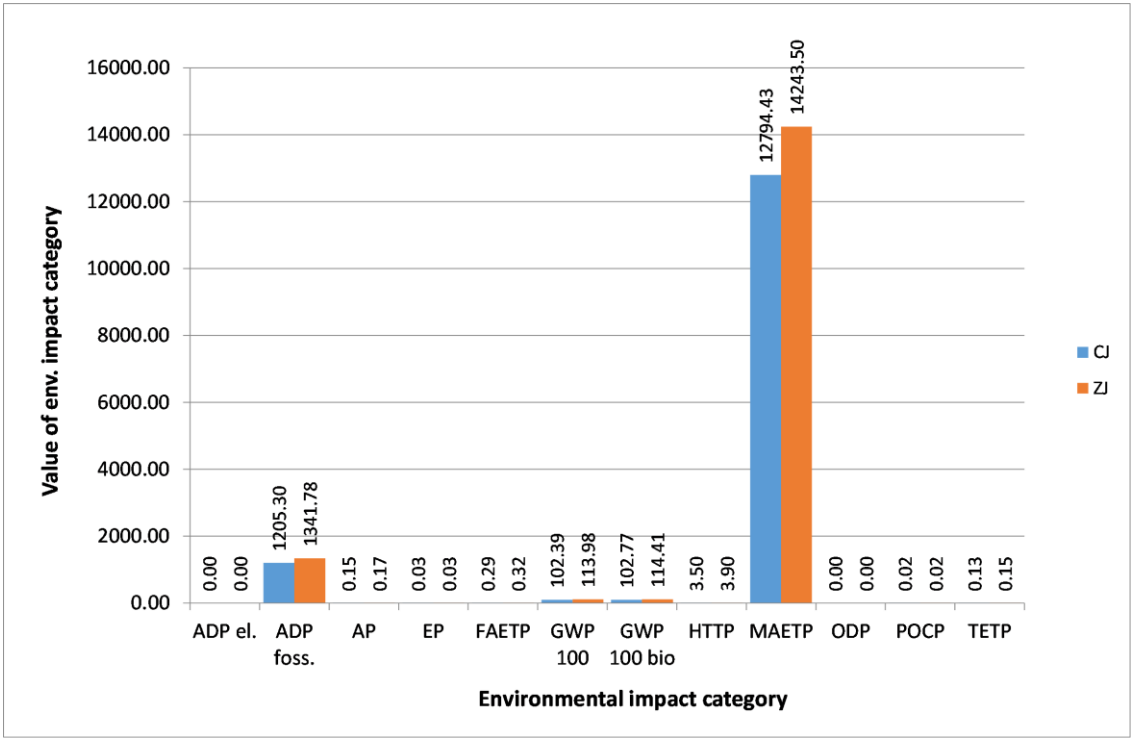

Abbreviations: Conventional (CJ) and Zero joints (ZJ) edgebanding;
ADP el. – Abiotic Depletion (ADP elements) [kg Sb-Equiv.]; ADP foss. – Abiotic Depletion (ADP fossil) [MJ]; AP – Acidification Potential (AP) [kg SO2-Equiv.]; EP – Eutrophication Potential (EP) [kg Phosphate-Equiv.]; FAETP – Freshwater Aquatic Ecotoxicity Pot. (FAETP inf.) [kg DCB-Equiv.]; GWP 100 – Global Warming Potential (GWP 100 years) [kg CO2-Equiv.]; GWP 100 bio – Global Warming Potential (GWP 100 years), excl biogenic carbon [kg CO2-Equiv.]; HTTP – Human Toxicity Potential (HTP inf.) [kg DCB-Equiv.]; MAETP – Marine Aquatic Ecotoxicity Pot. (MAETP inf.) [kg DCB-Equiv.]; ODP – Ozone Layer Depletion Potential (ODP, steady state) [kg R11-Equiv.]; POCP – Photochem. Ozone Creation Potential (POCP) [kg Ethene-Equiv.]; TETP – Terrestric Ecotoxicity Potential (TETP inf.) [kg DCB-Equiv.]

Figure 7. Environmental impacts of edgebanding technologies in the impact categories of the CML 2001 (April 2015) impact assessment methodology

The technologies had the greatest impact on *Marine Aquatic Ecotoxicity Pot. (MAETP)* during their entire life cycle based on the CML 2001 (April 2015) problem-oriented (focusing on midpoints) assessment method. This can be explained by the edge material consumption of the technologies and by the transport. *ADP foss.-Abiotic Depletion (ADP fossil)* emerged as a significant impact category.

GWP 100-Global Warming Potential (GWP 100 years) values were negligible. *The life cycle contribution evolved in the proportion of 47% conventional – 53% zero-joint according to the impact categories.*

Figure 8 displays the contribution of the different operational steps within the conventional and zero-joint edgebanding technologies to the above environmental impact categories.

Operational steps (conventional): 1) Placing and feeding the edgebanding material roll into the machine + handling of the chipboard surfaces; 2) 1 mm milling of chipboard edge; 3) Melting, adding EVA granulate and applying glue + pressing the edgebanding onto the workpiece edge (bonds the edge banding to the substrate); 4) End-cutting banding material; 5) Trimming excess material at the bottom and top of edges; 6) Fine trimming excess material at the bottom and top of edges; 7) Rounding of edges; 8) Scraping any surplus of glue and banding materials; 9) Milling of workpiece on the edges; 10) Polishing of the edge surface + heating the edge of the workpiece for colour correction using hot air blower; 11) Lubricant oil; 12) Raw materials transport 1; 13) Raw materials transport 2

*Operational steps (zero-joint):*1) Loading of banding material + handling of the chipboard surfaces with anti-adhesive fluid; 2) 1 mm milling of chipboard edge; 3) Pressing the edgebanding onto the workpiece edge (bonds the edge banding to the substrate); 4) End-cutting banding material; 5) Trimming excess material at the bottom and top of edges; 6) Fine trimming excess material at the bottom and top of edges; 7) Rounding of edges; 8) Scraping any surplus of banding materials; 9) Milling of workpiece on the edges; 10) Polishing of the edge surface + heating the edge of the workpiece for colour correction using hot air blower; 11) Lubricant oil; 12) Raw materials transport 1; 13) Raw materials transport 2

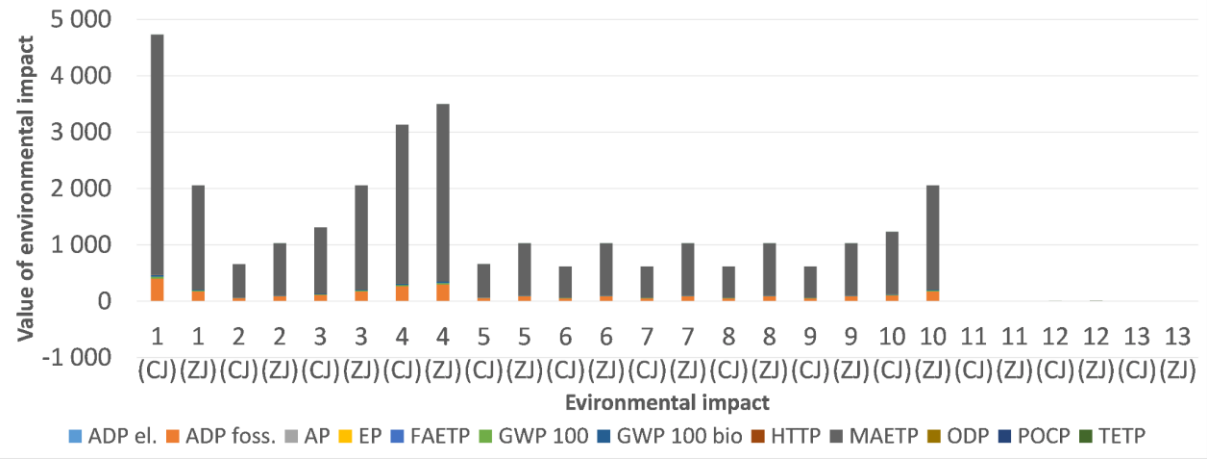

Abbreviations: Conventional (CJ) and Zero joints (ZJ) edgebanding;
ADP el. – Abiotic Depletion (ADP elements) [kg Sb-Equiv.]; **ADP foss. – Abiotic Depletion (ADP fossil) [MJ]**; AP – Acidification Potential (AP) [kg SO2-Equiv.]; EP – Eutrophication Potential (EP) [kg Phosphate-Equiv.]; FAETP – Freshwater Aquatic Ecotoxicity Pot. (FAETP inf.) [kg DCB-Equiv.]; GWP 100 – Global Warming Potential (GWP 100 years) [kg CO2-Equiv.]; GWP 100 bio – Global Warming Potential (GWP 100 years), excl biogenic carbon [kg CO2-Equiv.]; HTTP – Human Toxicity Potential (HTP inf.) [kg DCB-Equiv.]; **MAETP – Marine Aquatic Ecotoxicity Pot. (MAETP inf.) [kg DCB-Equiv.]**; ODP – Ozone Layer Depletion Potential (ODP, steady state) [kg R11-Equiv.]; POCP – Photochem. Ozone Creation Potential (POCP) [kg Ethene-Equiv.]; TETP – Terrestric Ecotoxicity Potential (TETP inf.) [kg DCB-Equiv.]

Figure 8. Contribution to environmental impact categories of operational steps of conventional and zero-joint edgebanding according to impact categories of CML 2001 (April 2015) impact assessment methodology

According to our examination (Figure 8), the following operational steps in the edgebanding technologies demonstrated considerable environmental impacts:

- Operational steps marked with the number 1. This is due to the electrical energy intake, meaning an extra energy demand compared to the other steps in the case of both alternatives. There is a strong indicator of this as regards the impact categories.
- Operational steps marked with the number 3. In the case of conventional technology, the step of "Melting, adding EVA granulate and applying glue + pressing the edgebanding onto the workpiece edge (bonds the edge banding to the substrate)" while in the zero-joint technology, the step of "Pressing the edgebanding onto the workpiece edge (bonds the edge banding to the substrate)" had higher energy demand compared to the others.
- Operational steps marked with the number 4. We have higher energy demand here in our model as well due to the extra energy demand of the compressor in addition to the energy demand of "End-cutting banding material" in both the conventional and the zero-joint technology.
- Operational steps marked with the number 10. In both alternatives, the extra energy demand of heat transfer of colour correction need to be counted.

Calculation of the primary energy demand of the technologies is a built-in module in the GaBi Professional LCA software as well. *Figure 9* illustrates the primary energy demand of the examined edging technologies. Life-cycle *contribution rate developed as 47% conventional – 53% zero-joint* according to the model of energy consumption.

The constructed life cycle models have the attribute that *the usage of the renewable energy sources (8.41%) is only a fraction of the non-renewable energy sources used in the manufacturing technologies*. This demonstrates a high potential of environmental development.

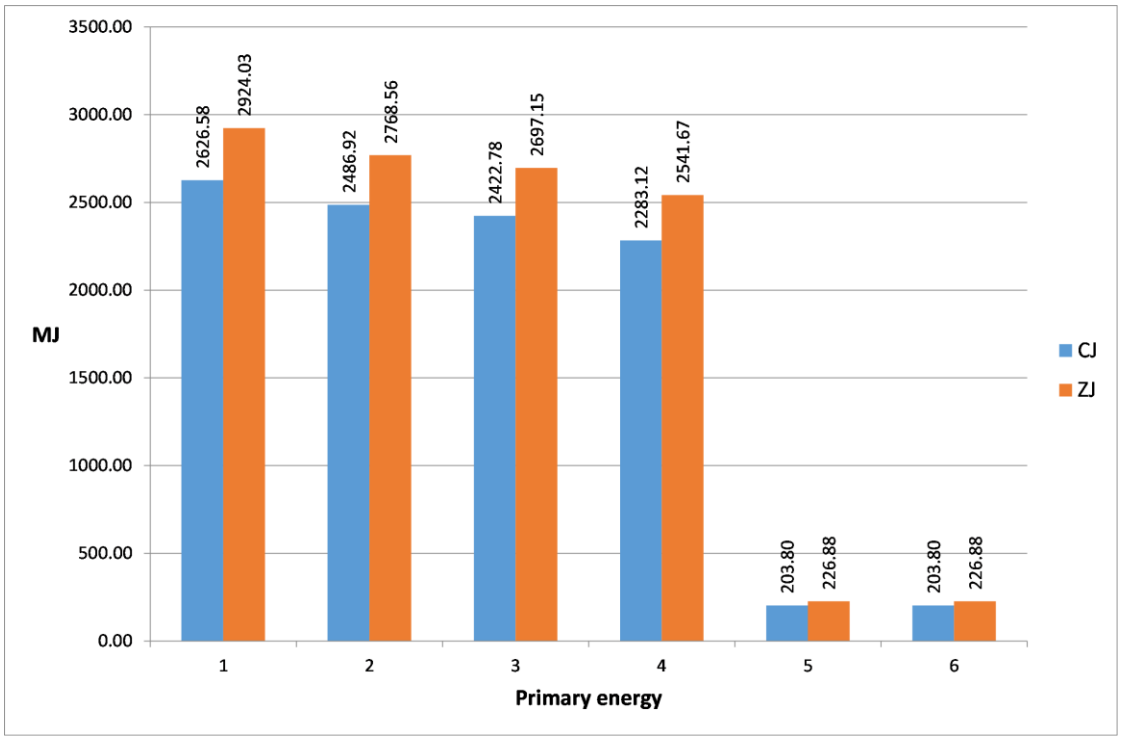

Abbreviations: Conventional (CJ) and Zero joints (ZJ) edgebanding;
1 – Primary energy demand from renewable, and non-renewable resources (gross cal. value) [MJ];
2 – Primary energy demand from renewable, and non-renewable resources (net cal. value) [MJ];
3 – Primary energy from non-renewable resources (gross cal. value) [MJ];
4 – Primary energy from non-renewable resources (net cal. value) [MJ];
5 – Primary energy from renewable resources (gross cal. value) [MJ];
6 – Primary energy from renewable resources (net cal. value) [MJ]

Figure 9. Primer energy demand of edgebanding technologies [MJ]

4 CONCLUSIONS

In our durability study, the edgebanded furniture fronts were the most sensible at the corners when exposed to moisture. Due to the high variations, the differences between conventional and zero joints were not statistically significant; however, there was a difference of two to three classes based on the assessment criteria for water resistance (Table 1). There was no consistency between the thickness swelling values of the two corners, since the conventional joints had higher values at the left corner. The edgebanded fronts exposed to moisture for a short period of time did not suffer significant deteriorations. In the case of steaming, the specimen' corners were affected the most and the thickness swelling of zero joints was significantly lower after the second and third treatment cycle. At 100 mm from the corners, the deterioration of edgebanding was considerably smaller and the visible differences between the joint types appeared after longer exposure.

The life cycle cost assessments revealed that zero-joint technology displays a 1.45 times surplus cost compared to conventional technology. Both technologies showed considerable costs of the edging material, the chipboard, and the electrical energy.

In our environmental study, we examined the environmental impact of edgebanding in woodwork by following the technological operation of a modern edgebander machine. In relation to conventional and the zero-joint edging technologies, according to all impact assessment methods, the life-cycle contribution rate was uniformly *47% conventional – 53% zero-joint* by impact category. *The higher indicator values of zero-joint method are due to the larger edge material consumption and the higher energy demand.* The constructed life cycle models have the attribute that *the usage of the renewable energy sources (8.41%) is only a fraction of the non-renewable energy sources used in the manufacturing technologies*. This demonstrates a high potential of environmental development.

Zero-joint technology appears to avoid the application of hot melt adhesive, but replacing these does not necessarily result in better environmental indicators. Nevertheless, zero-joint egdebanding does not just improve the appearance from an aesthetic point of view (invisible gluing joint line on the panels), but also exceeds the conventional edgebanding technology when durability aspects are considered.

Of course, the results obtained by the LCA examinations also depend on the nature of the model constructed in the analysing program and on how the electrical energy demand is distributed among the specific operational steps.

Not only are zero-joint edges aesthetically pleasing, but they also provide stronger, longer-lasting edges and anti-bacterial benefits. The LCA method considers the environmental impact of the manufacturing technology, but it also addresses product durability. In the latter, the two technologies examined in this study demonstrated significant differences.

Acknowledgements: This article was made in frame of the "EFOP-3.6.1-16-2016-00018 – Improving the role of research+development+innovation in the higher education through institutional developments assisting intelligent specialization in Sopron and Szombathely". This research was supported also by Competitiveness Operational Program 2014–2020 Priority Axis 1 - Research, Technological Development and Innovation (RDI) in support of Economic Competitiveness and Business Development Action 1.1.1 - Large CD infrastructures, Project type: Innovation clusters Project title: "Transylvanian Furniture Cluster – an innovative cluster of European interest" by the Sectoral Operational Programme Human Resources Development (SOP HRD), ID134378 financed from the European Social Fund and by the Romanian Government.

REFERENCES

CML 2001 METHODOLOGY: GUINÉE, J.B. – GORRÉE, M. – HEIJUNGS, R. – HUPPES, G. – KLEIJN, R. – KONING, A. DE – OERS, L. VAN – WEGENER SLEESWIJK, A. – SUH, S. – UDO DE HAES, H.A. – BRUIJN, H. DE – DUIN, R. VAN – HUIJBREGTS, M.A.J.(2002): Handbook on life cycle assessment. Operational guide to the ISO standards. I: LCA in perspective. IIa: Guide. IIb: Operational annex. III: Scientific background. Kluwer Academic Publishers. Dordrecht. 692 p., https://www.universiteitleiden.nl/en/research/research-projects/science/cml-new-dutch-lca-guide

FAVA, J. A. – JONES, B. – DENISON, R. – CURRAN, M. A. – VIGON, B. – SELKE, S. – BARNUM, J. (1994): A Technical Framework for Life-Cycle Assessment. SETAC Foundation for. Washington, DC. 134 p.

IOS (2017): IOS–TM–0002. Test method. Surface resistance – test methods. Inter IKEA Systems B.V. 1993–017. Sweden. 52 p.

ISO (2006a): ISO 14040:2006. Environmental management. Life cycle assessment. Principles and framework (ISO 14040:2006). International Organization for Standardization, Geneva, Switzerland. 20 p.

ISO (2006b): ISO 14044:2006. Environmental management. Life cycle assessment. Requirements and guidelines (ISO 14044:2006). International Organization for Standardization, Geneva, Switzerland. 46 p.

JIVKOV, V (2002): Influence of Edge Banding on Banding Strength of End Corner Joints from 18 mm Particleboard. In: Conference Nabytok 2002 (CD – ROM). At: Technical University Zvolen. Volume: IV. Slovakia. October 2002, https://www.researchgate.net/publication/311391217

KOZÁK, J. (2016): Életciklus elemzés alkalmazása faipari élzáró gépen [Using Life Cycle Assessment method for an edgebanding machine]. University of Sopron, Sopron. 88 p. (in Hungarian), http://diploma.nyme.hu/id/eprint/2028

LAÁB, Á. (2021): Life Cycle Costing. ELTE, Budapest, Hungary. http://www.laabagnes.hu/wp-content/uploads/2008/04/life-_cycle_costing1.pdf

LIPPKE, B. – WILSON, J. – PEREZ-GARCIA, J. –BOWYER J. –MEIL, J. (2004): CORRIM: Life-cycle environmental building materials. Forest Products Journal. 54 (6): 8–19. https://www.researchgate.net/publication/238776944_CORRIM_Life-Cycle_Environmental_Performance_of_Renewable_Building_Materials

LIPPKE, B.R.– WILSON, J. – MEIL, J. – TAYLOR, A. (2019): Characterizing the importance of carbon stored in wood products. Society of Wood Science and Technology 42: 5–14. https://www.researchgate.net/publication/228714657_Characterizing_the_importance_of_carbon_stored_in_wood_products

LUGOSI, A. (1976): Faipari kézikönyv [Wood industry manual]. Műszaki Könyvkiadó [Technical Publishing], Budapest. 1095 p. (in Hungarian)

MERDZHANOV, V. (2018): Comparative study of tensile bond strength for melted EVA glue on particle boards with different edge banding materials. In: Proceedings of the 5th International Conference on Processing Technologies for the Forest and Bio-based Products Industries (PTF BPI 2018). Germany. September 2018. 1–6. https://www.researchgate.net/publication/328964901_Comparative_study_of_tensile_bond_strength_for_melted_EVA_glue_on_particle_boards_with_different_edge_banding_materials

MOLNÁRNÉ POSCH, P. (2002): Faipari kézikönyv II. [Wood industry manual II.] Faipari Tudományos Alapítvány [Wood Industry Science Foundation], Sopron. 461 p. (in Hungarian)

RECHNER, R. – JANSEN, I. – BEYER, E. (2009): Using lasers in edge banding. Adhesion Adhesives&Sealants 6: 36–40., https://doi.org/10.1007/BF03250465

SAÇLI, C. (2015): The effect of time and edge banding type and thickness on the bending and tensile strength of melamine coated particleboard. In: Proceedings of the 27th International Conference Research for Furniture Industry. Turkey. September 2015. 469–480.

TANKUT, A.N. – TANKUT, N. (2010): Evaluation the effects of edge banding type and thickness on the strength of corner joints in case-type furniture. Materials and Design 31 (6): 2956–2963. https://doi.org/10.1016/j.matdes.2009.12.022

https://doi.org/10.37045/aslh-2021-0003 *Acta Silv. Lign. Hung., Vol. 17, Nr. 1 (2021) 37–50*

Using Different Approaches of Particle Size Analysis for Estimation of Water Retention Capacity of Soils: Example of Keszthely Mountains (Hungary)

Orsolya SZECSŐDI[a] – András MAKÓ[b,c] – Viktória LABANCZ[d] – Gyöngyi BARNA[b] – Borbála GÁLOS[a] – András BIDLÓ[a] – Adrienn HORVÁTH[a*]

[a] Institute of Environmental Protection and Natural Conservation, University of Sopron, Sopron, Hungary
[b] Centre for Agricultural Research, Institute for Soil Sciences, Budapest, Hungary
[c] Georgikon Campus, Hungarian University of Agriculture and Life Sciences (MATE), Keszthely, Hungary
[d] Gödöllő Campus, Hungarian University of Agriculture and Life Sciences (MATE), Gödöllő, Hungary

Abstract – PSD (particle size distribution) is a key factor affecting soil hydro-physical properties (e.g. hydraulic conductivity and water retention), which makes its determination essential. Climate change increases the importance of water retention and permeability as extreme weather events can severely impair the water supply of drought-sensitive vegetation. The amount of water in soils is expected to decrease. The modified Thornthwaite model considers soil properties such as root depth, topsoil layer thickness and particle size distribution (silt and clay fraction) of soil particles combined with the most significant soil properties. At the beginning of the research, we developed a laser diffraction method to replace the standard based "pipette" sedimentation method. The theoretical background of laser diffraction measurements is already known, but their practical application for estimating soil water retention capacity is still poorly understood. The pre-sieving of soil aggregates, the pre-treatment (disaggregation and dispersion) of the samples greatly influence the obtained results. In addition to the sedimentation method, laser diffraction measurements (Malvern Mastersizer 3000) were applied with three variants of pre-treatment. For comparison, the results of a Leptosol, a Cambisol, and a Luvisol were prepared for the first modified Thornthwaite water balance model. Significant differences appeared, especially during drought periods, which could be a basis for studying soil drought sensitivity. The development of our method can estimate the water retention capacity of soil, which could support adaptive forest management plans against climatic and pedological transformations.

paricle size analysis / pipette method / laser diffraction

Kivonat – A talaj víztartó-képességének értékelése szemcseanalízissel Keszthelyi-hegységi talajokon. A Soproni Egyetem Környezet- és Földtudományi Intézetében végzett jelen kutatás fő témája a talajok szemcseméret eloszlásának a vizsgálata, melynek több célja is van. Egyik kitűzött cél a laboratóriumban jelenleg használt hagyományos és időigényes „pipettás módszer" lecserélése a gyorsabb és modernebb lézerdiffrakciós mérési módszerre. A másik cél annak vizsgálata, hogy a talajokat miként befolyásolják a klímaváltozás hatására végbemenő változások, illetve a talajok vízfelvevő- és megtartó képessége hogyan hat az erdőállományok vitalitására. A jelen cikk a kezdeti lépéseket hivatott részletesebben bemutatni három különböző talajtípuson. Egyrészt összehasonlítjuk a pipettás módszer és három különböző módon előkezelt minta lézerdiffrakciós módszerrel mért mechanikai összetétel eredményeit, másrészt bemutatjuk a mérési eredményeken alapuló vízmérleg

[*] Corresponding author: horvath.adrienn@uni-sopron.hu; H-9400 SOPRON, Bajcsy-Zs. u. 4, Hungary

modell pontosítását, mely az analitikai módszerek gyakorlati alkalmazását és erdészeti jelentőségét is szemléleti.

granulometria / pipettás módszer / lézerdiffrakció

1 INTRODUCTION

The Russian pedologist Vasily Dokuchaev was the first to define soil-forming factors. He identified the five main factors, namely geological, climatic, biological, topographical, and soil age. The massive impact of human activities is considered the sixth factor today. Soil formation processes include humus formation, leaching, and clay formation, but the most basic formation process is weathering (Blaskó 2011). Soil can be characterized as primary mineral residues mixed with secondary minerals formed by weathering and fragmentation. Mineral particle sizes in the composition vary greatly depending on the quality of the minerals and their formation or mode of fragmentation.

Different soil-forming factors and processes cause different-sized soil particles. The particle size distribution (PSD), or the qualitative characteristic expressing this (soil texture), and the relative position of the particles of different sizes are among the most important soil indicators (Stefanovits 1971). This influences many soil properties, particularly the size of the interfaces between the soil phases (specific surface area) and, consequently, the major physical and chemical processes taking place on these surfaces. In addition to the soil structure, this also affects porosity, which, in turn, affects water retention and hydraulic conductivity (Bieganowski et al. 2018). Soil porosity can be described by the total volume of soil pores and by pore size distribution. We can distinguish two main pore types: structural (inter-aggregate) and textural (intra-aggregate) pores (Beven – Germann 1982, Schlotter – Schack-Kirchner 2013). The pores can also be divided according to size, e.g. micropores, macropores, and other differentiated divisions (SSSA, 1997). Using the capillary tube model described by the Young-Laplace equation, the matric potential (water retention) can be related to effective pore diameter as follows: macropores: > 75 μm, < 1.6 pF; mesopores: 30–75 μm, 1.6–2 pF; micropores: 5–30 μm, 2–2.78 pF; ultramicropores: 0.1–5 μm, 2.78–4.47 pF and cryptopores < 0.1 μm, > 4.47 pF (Rajkai et al. 2015).

Though sedimentation methods (sieve-pipette or hydrometer method) are the most commonly used methods to determine PSD, the use of laser diffraction methods (LDMs) is also presently widespread (di Stefano et al. 2010). The pipetting method is a classical sedimentation method in which a certain amount from the suspension is pipetted after the settling time has elapsed. The dried mass of the particle fractions is then measured (*MSZ 08-0206, 1978).* Calculations are completed according to the Stokes-law. Spherical grains are usually assigned with the density of quartz (ρ*=2.65 g/cm*^{3}). Although the particle shapes are not uniformly spherical, for calculation purposes they should be considered as such. Most silt and clay particles possess a plate or tubular structure rather than a spherical structure, so the direction of movement is perpendicular to the maximum cross-section. Thus, as the settling rate of the particle decreases, the expected *tensile strength* of the particle increases, denoting that the particle shapes affect the result (Polakowski et al. 2014).

Laser diffraction particle analysis is an efficient procedure because it takes significantly less time, covers larger size ranges, and requires a smaller amount of sample (Bieganowski et al. 2018). The definition is based on the relationship between light and surface. Light impinges on the particle surface, allowing light to refract, bend, reflect, and absorb on the surface (according to *Lambert-Beer* law). Laser diffraction particle analysis is based on the fact that the particle reflects the light beam at a certain angle, and that this angle increases as the particle size decreases. The beam of monochromatic light passes through the suspended sample, and

the beam of curved light thereby generated enters the multi-element sensor. The most commonly used PSD calculation method also assumes that the particles are spherical, i.e., the diameter of a given particle is an optical sphere (Eshel et al. 2004).

Site factors determine the occurrence and distribution of each tree species. By field factors, we mean the totality of factors that affect the growth and health of plants. Climatic factors, hydrological conditions (amount of available water from the soil), and soil properties (genetic soil types, physical diversity, and crop layer thickness) significantly influence the classification of Hungarian forest sites. Furthermore, altitude, exposure, slope, and the role of bedrock must also be considered (Babos 1966).

Site changes have accelerated in recent decades. Experts have noticed a rapid change in hydrological conditions such as groundwater level subsidence (Csáki et al. 2018). Hydrological factors change relatively quickly, but for the time being, they are mostly local problems. Climate is also a rapidly changing factor, but this change already affects the entire domestic forest population. Extreme changes in precipitation and temperature averages significantly impact the forest ecosystem and often leads to contiguous periods of drought. We can also expect climatic condition changes and soil transformation, both of which are expected to accelerate in the future due to temperature fluctuations. Two important changes in soils are directly related to climate change; an increase in soil temperature, which precipitates a decrease in soil moisture content; and altered soil moisture contents, which influences evapotranspiration and the rate of groundwater formation (Bidló – Horváth 2018).

Based on the research conducted at the University of Sopron in recent years, the spatial shift of certain climatic categories can be predicted (Führer et al. 2011, Führer 2018). In the future, the appearance of site type variants that have not occurred in Hungary must also be expected (Czimber – Gálos 2016, Mátyás et al. 2018). In order to prepare for the projected changes, the four forest climate categories used thus far had to be extended by a fifth, the so-called steppe climate category. In addition, the spatial shift of climate is accompanied by the emergence of soil types, whose formation conditions are related to other climates, plants, e.g. forest steppe. Applying planned forest management in advance of the new site type variants is crucial (Bidló – Horváth 2018).

Climate sensitive tree species and tree stand types should characterize classes of production site typology in forestry practice. Precisely measured meteorological parameters can determine climate classes (Beech, Hornbeam-oak, Sessile oak - Turkey oak, and Forest-steppe climates). Models indicate that forest climate classes will shift by the middle of the 21st century; forest-steppe climate class areas will increase, while closed forests are expected to decrease (Führer et al. 2017). The importance of individual soil properties will increase due to climate change. Concerning groundwater retention capacity, only forests with access to adequate water supplies will be able to survive longer rainfall-free periods. This ability is mainly determined by the physical soil variety and the thickness of the topsoil layer. Therefore, conducting the widest possible PSD measurements is vital to the health of our soils and forests.

The complex excavations performed in Hungary revealed that the effects of unfavourable soil properties, such as the physical variety or aggregates of coarse sand, are further aggravated by long dry and warm periods, which have been typical recently. For these reasons, the water holding capacity of our soils will become one of the most important production factors in the changing climate. The analysis of temperature and precipitation time series for a given area is suitable for detecting the effects of dry and warm periods in recent periods. The frequency of these is expected to increase in the future, especially in extreme weather situations, as well as the importance of microclimate conditions, in which exposure and forest structure will play key roles. Although weather is the primary cause of individual deforestation, soil conditions also play a very important role, as the water holding capacity of extremely shallow and shallow soils is exceedingly poor. As precipitation events have become more intense but less frequent in the

recent period, only a small portion of the precipitation that falls in this way can be stored in the soil. For this reason, we can expect that no water that can be taken up by the vegetation will remain in the soil during long dry periods between heavy rains. By predicting the expected negative effects, we can already conclude to what extent drought can aggravate the given unfavorable soil properties. Due to the long dry periods already mentioned, the declining amount of water in the soil causes so-called drought stress.

Significant deforestation occurred in the Keszthely Mountains in 2012. The devastation continued in subsequent years and appears to be ongoing even today. The destruction mainly affected the planted black pine stands, but the health of other tree species has also deteriorated. Primary studies have detected biotic pests as a damage cause, but also indicate that abiotic factors are the main causes of the destruction. Since the damage affected black pine, which has been present in the area for several decades (centuries), questions concerning abiotic factor changes arose. A chief goal of our work is to detect the changes and facilitate a solution. At the same time, questions concerning future possibilities also arise. Expected future changes may render currently reversible damage irreversible, which in turn prompts concerns about adapting to expected future site conditions as well as which tree species to use. This current paper presents the first steps of an analytical methodology development, which provides a basis for a more accurate estimation of the water retention capacity of soils. The final aim of this research is to help afforestation. More specifically, to aid climate-resistant tree species selection on a precise amount of silt and clay particle determination. The main questions of the current study are the following:

1. How can the time-consuming pipette method be efficiently replaced with a timesaving measuring instrument based LDM PSD? Furthermore, what are the advantages and disadvantages of LDM?
2. Do instrumental measurement results have better accuracy? Are those results optional for the water balance model?

2 MATERIALS AND METHODS

2.1 Durability study

Based on the previously stated objectives, we selected the Keszthely Mountains as the study area. The bedrock here is mainly dolomite. The soils of these mountains are very diverse, which makes them particularly suitable for our measurements. Due to the geological and topographical features of the area, the forests of the Keszthely Mountains have no access to surplus water, which means that the vegetation is dependent on precipitation. Most of the mountainous and hilly areas here are not under intensive land use and no upcoming land use changes are expected. Leaking wetlands in the loess areas and valleys, where oxygen-rich water moves under the cover or in the soil almost parallel to the surface, may exist to a small extent. The amount varies, but excess water is always beneficial for the local populations (Bidló et al. 2015).

In the sampling area, three soil profiles with different structures were selected to examine the organic matter content influencing the measurement in as varied a manner as possible (*Figure 1*). The topsoil layer thickness of black rendzina (BRE) is 30 cm, of which the reduced thickness is only 10 cm, which can be defined as shallow. The humus form of the soil is mull-humus. The topsoil contains organic plant residuals parts. The parent material is dolomite. Soil pH was 7.5 and was determined according to the Hungarian Standard (MSZ-08-0205/2-1978). The field capacity and the permanent wilting point of the topsoil layer was also significant. This layer hass a loam texture with a crumbly structure, containing highly humus-rich rock fragments, richly networked by roots.

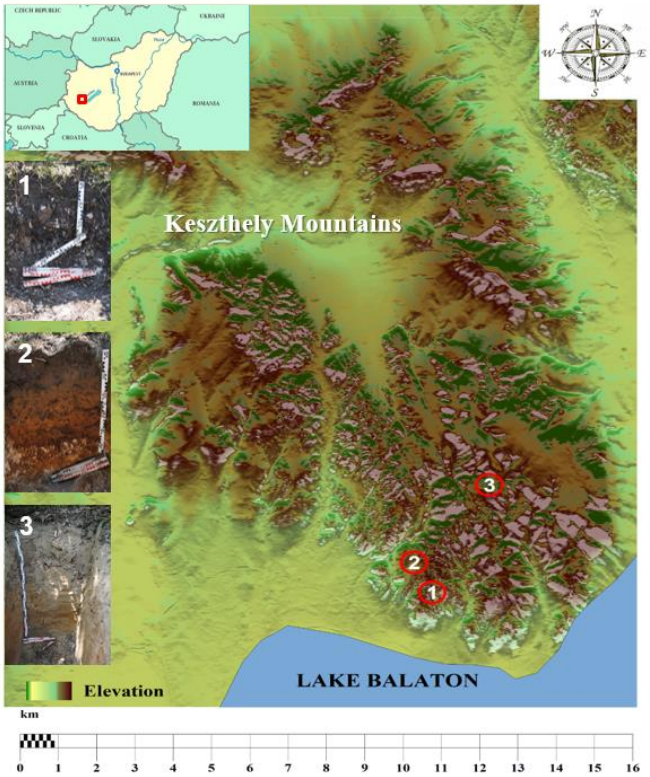

Figure 1. Location of the examined soil profiles in Hungary with the elevation information and the pictures of the investigated soil types

The topsoil layer thickness of brown earth (BEARTH) is 40 cm, of which the reduced thickness is also 40 cm, which can be defined as middle deep. The humus form of the soil is mull-humus. The parent material is loess (deposited on dolomite). Soil pH was 7.6 . The texture was loam. Water conditions were favourable, water permeability was medium, and water-holding capacity was suitable. Nutrient supply was adequate. The supply of nitrogen, phosphorus, and potassium in the non-eroded section were also appropriate.

The topsoil layer thickness of lessivated brown forest soil (LBFS) is 100 cm, of which the reduced thickness is 100 cm, which can be defined as deep. The humus form of the soil is mull-humus. The parent material is loess. Soil pH was 5.8−7.9, slightly acidic in the topsoil, and the pH increased with soil depth (effect of loess). The texture was sandy loam. A typical three-layered soil. The water management of such soils was excellent, the water permeability is medium, and the water field capacity is adequate. The water storage capacity increased by the fact that the B horizon has a weak water retention effect.

2.2 Analytical methods

Standard based pipette sedimentation method (PSM)

The samples for both procedures were prepared according to a modified version of the Hungarian Standard (MSZ-08-0206, 1978). After weighing the soil sample, the organic matter was removed with hydrogen peroxide until the soil turned grey and the humus materials decomposed into water and carbon dioxide (the original standard does not suggest to destroy the organic matter). Then Na-pyrophosphate solution was added to the sample as dispersing agent and shaken for 6 hours. The soil suspension was then washed through a 0.2 mm mesh sieve into a large porcelain bowl using warm distilled water and a rubber brush. This process should be repeated until the water that drips off is transparent. The coarse sand fraction remaining on the sieve was washed into a small porcelain dish of known weight without loss

using distilled water. The suspension of silt and clay passed through a 0.2 mm sieve was washed into a 1000 ml settler, then filled with distilled water and pipetted out from the given depth after given time.

Laser diffraction method (LDM)
Since three types of treatment were conducted, a more detailed description of these follows. The previously mentioned Malvern Mastersizer 3000 particle analyser was used for the laser diffraction particle size analysis. The device itself consists of a laser light source, light processing optics, a cell, a lens, and a multi-element detector. The multi-element detector provides the diffraction pattern. A data processing unit is also needed for the deconvolution of the diffraction data, as well as for volumetric particle size distribution, related data processing, and reporting (Malvern 2013). The optical unit is the center of the system, designed to transmit red laser light and blue light through the sample. The light is transmitted to a detector, which generates data from light scattering caused by particles in the sample. The measuring cell functions as an interface between the dispersion unit and the optical unit. Wet dispersion units are designed to circulate a liquid sample through the measuring cell. Measuring range: 0.01µm – 3500 µm. The measurement is quite simple: a Hydro EV dispersion unit is placed in a 1000 ml beaker, filled with 800 ml of distilled water, and a soil sample is added to the distilled water accompanied by ultrasound. Ultrasound prevented settling to the bottom of the beaker for heavier aggregates and prevented re-agglomeration in the samples. The blue light (λ=470 nm) was used to capture the background, while the red light (λ=632.8 nm) was used to detect particles. The rotation speed was 2750 rpm and Mie theory was applied, refraction index 1.52 and absorption index 0.1 for the dispersed phase, and refraction index of 1.33 for water as the dispersing phase.

The treatments used were as follows for instrumental measurement:

- **M1** = Sample containing organic matter: In the case of the soil samples, the organic matter content was not destroyed; only the soil was suspended and the solution was homogenized. The prepared sample was added from the shake flask to the dispersing unit.
- **M2** = $NaPO_3$ dispersed sample, pre-treated with hydrogen peroxide (H_2O_2): The second treatment is the same as the preparation for the pipette method. Adhesives in the soil include humus, iron and alumina oxides and hydroxides, and calcium carbonates ($CaCO_3$). H_2O_2 treatment is used to destroy humic substances, while diluted hydrochloric acid (HCl) should be used to remove $CaCO_3$. $NaPO_3$ was used for dispersion. Complexing agents are used to form iron and aluminium oxides (oxide hydroxides). To prevent re-coagulation of the particles, a peptizing agent (NaOH and Na brine, in rare cases Li brine) is added to the soil sample and soil suspension.
- **M3** = Sample pre-treated with hydrogen peroxide (H_2O_2) and hydrochloric acid: In the third preparation, we only destroyed the soil organic matter content. The humic substances are destroyed with hydrogen peroxide, while diluted hydrochloric acid is used to remove the calcium carbonate.

The PSD measurement results of the pipette method, considered as a standard, were compared with the LDM results obtained with different treatments using SPSS statistical software package to found find the best reliable (best correlated) LDM procedure.

2.3 Water balance model calculations

To detect drought stress, the Thornthwaite water balance model (Thornthwaite – Mather 1955) was used, which, in addition to monthly temperature and precipitation data, also includes soil

physical diversity, rooting depth, available water (EW) and maximum water uptake (EWm) (1). Monthly precipitation was reduced by an interception to determine the annual drought stress index (Is) (2). Granier et al. (1999) assumed stress when the relative recoverable moisture content (REW) of the soil drops below 40%. In the case of long-term drought period, this percentage could be higher in Hungary. Model parameters: monthly temperature and precipitation, reduced topsoil layer thickness, and root depth. Furthermore, the relative extractable water amount was refined with the data of the measured silt and clay fractions of the soils. At this point, we used the PSD results previously measured by different analytical methods. The models were prepared in MS Excel program.

$$REW = EW / EWm \quad (1)$$

$$Is = \sum SWD / EWm \quad (2)$$

$$SWD = EWm \cdot 0.4 - EW \quad (3)$$

Where:

REW:	the relative extractable water content
EW:	the available water volume
EWm:	the maximum of water absorption
Is:	the annual drought stress index
SWD:	the water deficit stored in the soil.

3 RESULTS AND DISCUSSION

3.1 Particle size distribution

All measurement results were compared during the evaluation. The focus was on the correlation between the results of pipette (PSM) and laser diffraction (LDM) particle analysis. Moreover, the connection between the three data groups measured with the instrument was considered as well. In comparing the results, the different fractions were compared separately using correlation diagrams for conclusions. *Table 1* summarizes the sums of silt% and clay%.

Table 1. Results of the silt+clay fraction (%) determined with PSM and LDM

Soil type	Depth (cm)	S+C % (Pi)	S+C % (M1)	S+C % (M2)	S+C % (M3)
LBFS	0 – 5	25	20	12	40
LBFS	5 – 25	27	36	54	17
LBFS	25 – 60	35	40	62	33
LBFS	60 – 100	27	36	60	27
LBFS	100 – 120	11	29	48	43
BRE	0 – 15	39	13	33	56
BRE	15 – 30	17	13	32	8
BEARTH	0 – 10	49	24	69	60
BEARTH	10 – 40	43	25	31	63

S+C %: summarized value of Silt%+ Clay%; Pi: Pipette measurement; M1: Sample containing organic matter; M2: Dispersed sample treated with Hydrogen-peroxide (H_2O_2); M3: Sample treated with hydrogen-peroxide (H_2O_2) and hydrochloric acid; LBFS: lessivated brown forest soil; BRE: Black rendzina; BEARTH: Brown earth

Differently measured clay and silt fractions were compared. The clay content is interesting because it is the best efficiency indicator of the preparation methods (Kun et al. 2013, Yang et

al. 2015, Makó et al. 2017). The clay + silt fraction is one of the most fundamental input soil parameters of water balance models. For clay content, the 2 µm clay/silt fraction boundary (*Figure 2*) and the 7 µm clay/silt fraction boundary (Figure 3) were determined (Makó et al. 2019). In addition, only filtered values were entered into the program, with "obscuration" greater than 25 and "residual" results greater than 2.5 selected. Two statistical numbers were considered for the samples, the Coefficient of Determination (R^2) and the Root Mean Square Error (RMSE). The RMSE number shows both an underestimation and overestimation of the results, while R^2 value means a close or weak correlation between the pipette and the laser methods. Figures clearly indicated that the extent of RMSE varied depending on pre-treatments and fraction boundaries. The smallest underestimation or overestimation was measured for untreated suspensions by choosing the 7 µm fraction limit. The samples without pre-treatment had the highest R^2, while the lowest R^2 values were obtained for the only destroyed samples, for both limits. The highest RMSE value was observed for the destroyed and dispersed samples at the 7 µm clay boundary. Considering all the pre-treatments, it can be said that the R^2 values were slightly higher for the 7 µm fraction limit, while for the 2 µm fraction limit we found a smaller underestimation or overestimation on average.

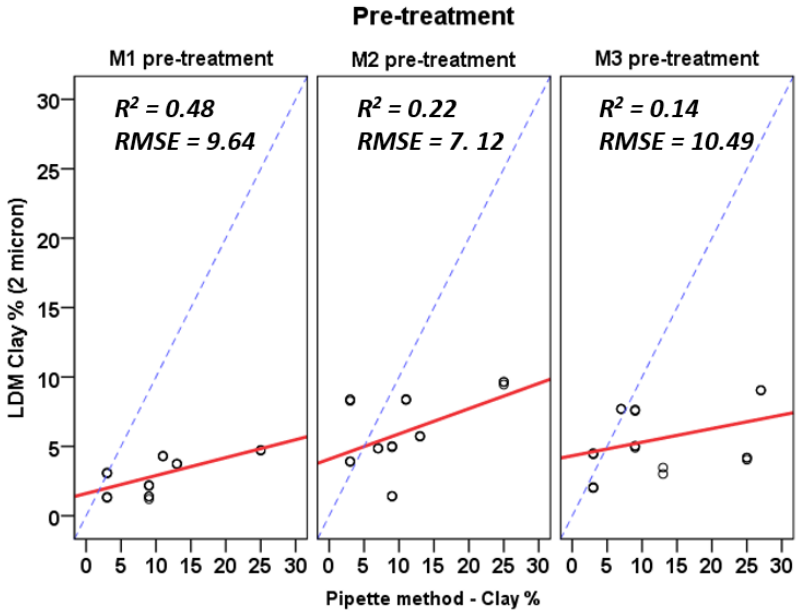

Figure 2. Comparison of clay content at 2 µm fraction limit determined with pipette and laser diffraction method

The 2 and 7 micron limits do not require separate evaluation for this fraction, as their sums are the same. On Figure 4. values marked in brown represent samples with high organic matter content from the upper horizons. The values show a low regression at first glance and a rather large overestimation. The only acceptable value (R^2 = 0.41) is shown for M3 due to the high soil organic matter (SOM) content of each sample. However, the confounding effect of SOM did not appear in this sample because if we take out the data marked in brown, we still obtain a good regression fit. In the case of the M1 sample, the data with a high organic matter content stand out from the other values. There are two possible reasons for this. It is possible that some of the clay + silt content remained in the form of aggregates and that the incorporation of ultrasound did not help to separate the aggregates. Another possibility is that the undestroyed organic debris, which remained in the suspension, hindered the laser measurement. The coexistence of these two options interfered with the poor regression relationship (R^2 = 0.08). If

the data marked in brown are taken out of the analysis, a high regression line is obtained (R^2 = 0.94).

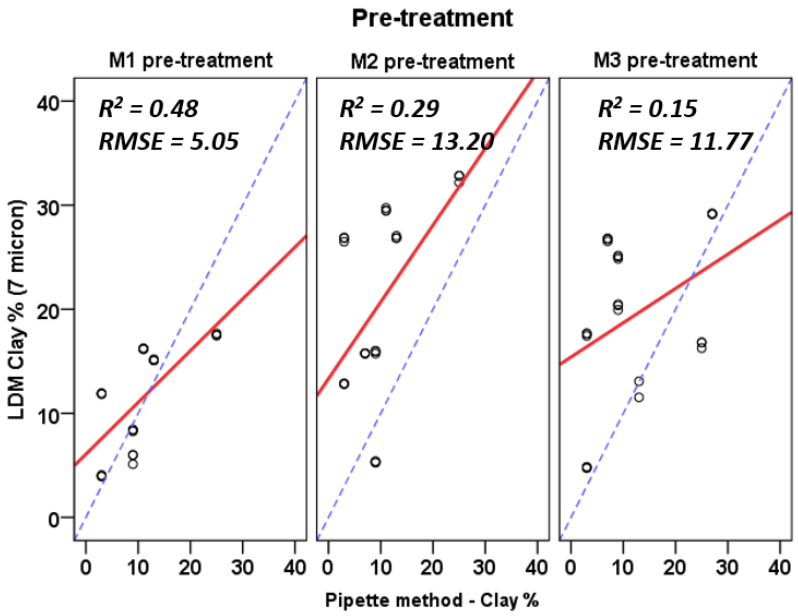

Figure 3. Comparison of clay content at 7 µm fraction limit determined with pipette and laser diffraction method

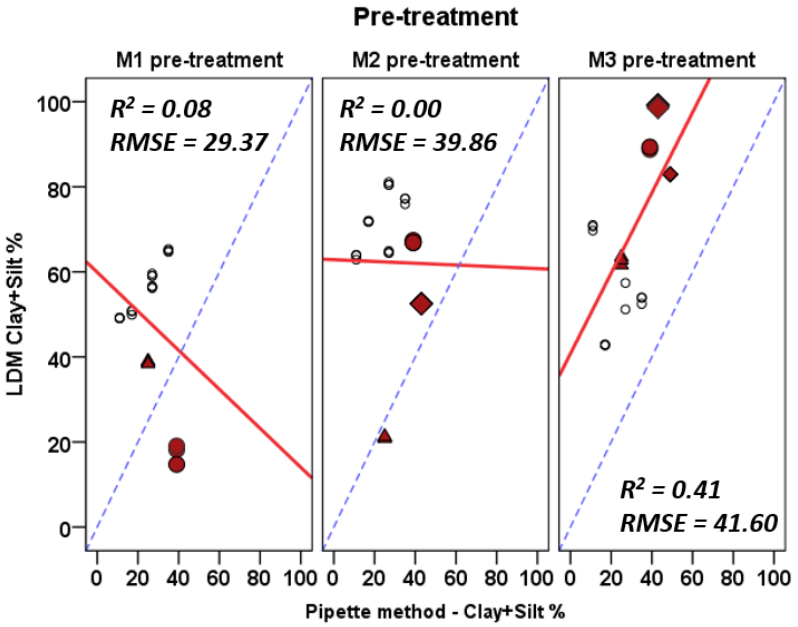

Figure 4. Comparison of three type of instrumental measurement

The destroyed and dispersed (M2) sample displays the same behaviour (*Figure 4*). The value of R^2 (= 0.00) is weak as well, but if we take these high organic matter contents out of the evaluation, we get a better fit (R^2 = 0.42). To conclude, the clay + silt content always overestimates the pipette clay + silt content in laser diffraction measurements. In the cases of M1 and M2, this occurred even without the samples with high SOM content, and in the case of M3, it even occurred in the samples with high SOM content. Promisingly, Igaz and colleagues (2020) performed PSM and LDM comparisons on 542 soil samples and found that a

polynomial-based regression model is adequate for obtaining an approximation of the pipette method and laser tools (Malvern Mastersizer 2000, Fritsch Analysette22) after recalculation of the data.

For practical applicability, the obtained results were used to construct the Thornthwaite monthly water balance model. To prepare the water scales, we first used the pipette measurements followed by the values obtained with the laser instrument. Following the measurements, water scales for the three studied soil types were prepared to investigate the relationships between the soil particle properties and the water retention capacity. Water balance diagrams were prepared using the properties of the soils and the climatic conditions of the area (Gálos et al. 2017, Bidló et al. 2019). It is important to note that below a certain limit, plants cannot absorb enough water and water stress develops.

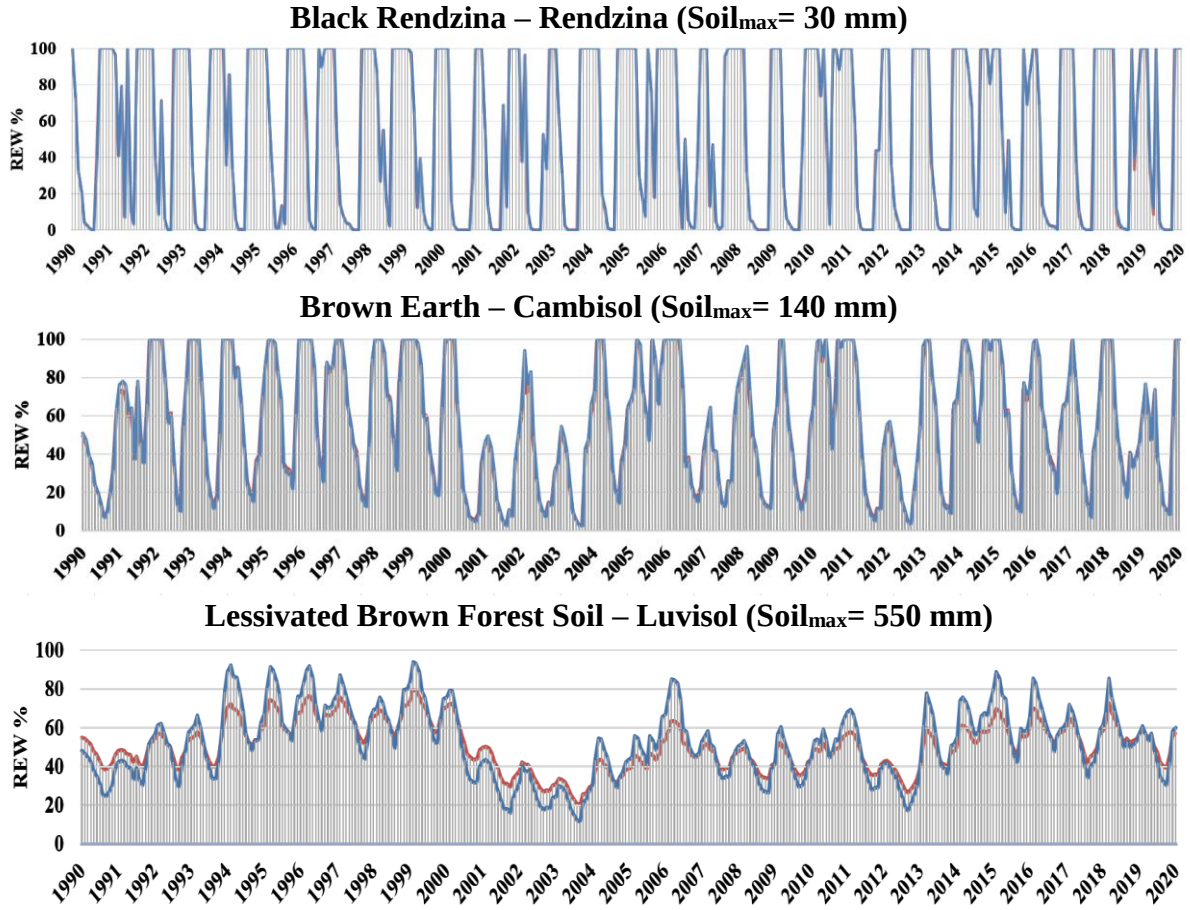

Figure 5. Water balance models derived from results of pipette (red line) and M2 laser diffraction measurements (blue line) (Soil$_{max}$: maximum amount of water that can be stored for an emptied soil during a precipitation event, REW%: relative extractable water amount)

Figure 5 displays the comparison of the Pipette method (blue colour) and M2 (red colour) measurements made by the similar pre-treatment.

In the case of LBFS, the water was well retained and evaporated slowly during the drought periods, of which there were three (1990-1993; 2000-2003; 2011-2013). These conditions ensured continuous forest cover. Mention should also be made of the amount of water stored in the soil, which is 500 mm, and the thickness of the reduced topsoil is 100 cm.

BEARTH absorbs water relatively quickly, but it releases it just as quickly due to the physical variety of the soil. The maximum amount of water that can be stored in the soil is 100 mm, which is already significantly less than LBFS. During drought periods, this soil type was

already much less able to store enough water for vegetation. The figure also clearly shows the difference in years with very high rainfall (e.g. 2010), when plants were relieved from water stress.

For the BRE soil type, Figure 5 illustrates that the soil saturates quickly, but also loses water content quickly, especially during drought periods. The maximum amount of water that can be stored is small (30 mm) due to the shallow (15 cm) thickness of the crop layer, which, however, has an exceptionally high organic matter content. The water retention capacity of the soil is no longer enough to maintain closed forests.

The three different figures clearly show that LBFS with a deep topsoil layer thickness is much more sensitive to water loss during drought periods. The measurement differences are mainly visible in the LBFS water balance, especially in drought years when the instrument over-measures. After 2-3 years of drought, the Mastersizer measurements underestimate, and then the difference in measurements decreases in the following years. Therefore, analytical studies require further investigation to draw further conclusions.

4 CONCLUSIONS

Determining the particle size distribution of soils helps to monitor the hydro-physical properties of the soil (e.g. hydraulic conductivity or water retention). Climate change increases the importance of water retention and permeability as extreme weather events can severely impair the water supply of drought-sensitive vegetation. Overall, the amount of water is expected to decrease in the future.

As a first step of this research, we developed the laser diffraction method, which is a faster and more reliable pre-treatment measurement method than the classical "pipette" sedimentation method. The theoretical background of laser diffraction measurements is well known, but their practical application for estimating soil water retention is still poorly understood. (Yudina et al. 2020). The modified Thornthwaite model considers soil properties (e.g. root depth, topsoil layer thickness) and particle size distribution (silt and clay fraction). In addition to the sedimentation method, laser diffraction measurements (Malvern Mastersizer 3000) were conducted with three variants of pre-treatment.

- The pre-sieving and pre-treatment of the samples greatly influence the obtained results. Weak regression lines and high underestimations are possible due to sources of error from pre-treatments.
  Explanation: During organic matter decomposition, it is likely that not only the humus content decomposed. The undegraded organic debris from the topsoil in the samples may have remained in large quantities. The aggregates and the mineral phase may also have been destroyed by removing organic materials and carbonates, which may have resulted in the decomposition and transformation of some of the clay minerals.
- For laser diffraction measurements, sampling from the suspension can also be a source of error, as a significant part of the sand fraction presumably settles down, which means the suspension could not be dispersed evenly.
  Explanation: This can be seen in the determination of the clay + silt content when overestimating the samples. Another possible source of error is that the soil suspension could not be completely washed out. After decomposition, dissolved, possibly semi-decomposed, organic substances such as hydrogen peroxide may have formed, which may have formed a precipitate with the dispersant during sonication. Therefore, the correlation between pipette and laser diffraction measurements may be weak.
- Based on our results, the particle size distribution has great importance in determining the water retention capacity of soils. We obtained lower-than-expected correlation

values for the particle size distribution determined in different ways, which could be due to several reasons (Yang et al. 2015, Bieganowski et al. 2018).
Explanation: One such reason is that the laser diffraction instrument gives a volume percentage, while pipetting measurements give weight percentages. The density of soil particles greatly influences pipette measurements. This parameter is negligible with laser diffraction measurement. However, in the latter case, the refractive index of the particles can be a significant factor.

The current study indicates that laser diffraction measurement can replace the classical sedimentation (pipette) method in the near future. These facts are sufficient to obtain different results. In addition, the removal of organic matter also worsened the correlation of the results. For comparison, the results of a Leptosol, a Cambisol, and a Luvisol were prepared for the first modified Thornthwaite water balance model. Significant differences appeared, especially during drought periods, which could provide a basis for studying the drought sensitivity of soils. The development of our method allows for the estimation of the water retention capacity of soil, which could help forest management in planning adaptations to climatic and pedological changes.

Acknowledgements: The research was conducted by the Faculty of Forest Engineering of the University of Sopron within the framework of the EFOP-3.4.3-16-2016-00022 project "QUALITAS Quality Higher Education Development in Sopron, Szombathely and Tata". We would like to thank Bernadett Bolodár-Varga and Bakonyerdő Zrt. for their help in the field sampling. This research was partly funded by the National Research, Development and Innovation Office—NKFIH grant number OTKA 119475, and by the ÚNKP 20-3 New National Excellence Program of the Ministry for Innovation and Technology from the source of the National Research, Development and Innovation Fund.

REFERENCES

BABOS, I. – HORVÁTHNÉ PROSZT, S. – JÁRÓ, Z. – KIRÁLY, L. – SZODFRIDT, I. – TÓTH, B. (1966): Erdészeti termőhelyfeltárás és térképezés [Site surveying and soil mapping in forestry] (in Hungarian) Akadémiai Kiadó. Budapest.

BEVEN, K.L. – GERMANN, P.F. (1982): Macropores and water flow in soils. Water Resources Research 18 (5) 1311–1325. https://doi.org/10.1029/WR018i005p01311

BIDLÓ, A. – CZIMBER, K. – GÁLOS, B. – GYULÁS, K. – HORVÁTH, A. – VARGA, ZS. (2015): Részletes erdészeti termőhelyfeltárási szakvélemény. [Detailed soil site survey]. Nyugat-Magyarországi Egyetem. Környezet- és Földtudományi Intézet. Termőhelyismerettani Intézeti Tanszék. Sopron. 24–39. pp. (in Hungarian)

BIDLÓ, A. – HORVÁTH, A. (2018): Talajok szerepe a klímaváltozásban. [Role of soils in climate change]. Erdészettudományi Közlemények 8 (1): 57–71. (in Hungarian) https://doi.org/10.17164/EK.2018.004

BIDLÓ, A. – HORVÁTH, A. – VEPERDY, G. (2019): The soil conditions of the forests of Zala County and their impact on the growth of beech. Agrochemisty and Soil Science 68: 1–13. https://doi.org/10.1556/0088.2019.00010

BIEGANOWSKI, A. – RYŻAK, M. – SOCHAN, A. – BARNA, GY. – HERNÁDI, H. – BECZEK, M. – POLAKOWSKI, C. – MAKÓ, A. (2018): Laser diffractometry in the measurements of soil and sediment particle size distribution. Advances in Agronomy 151: 215–279. https://doi.org/10.1016/bs.agron.2018.04.003

BLASKÓ, L. (2011): Soil science. University of Debrecen. 170. p

CALLESEN, I. – KECK, H. – ANDERSEN, T.J. (2018): Particle size distribution in soils and marine sediments by laser diffraction using Malvern Mastersizer 2000—method uncertainty including the

effect of hydrogen peroxide pretreatment, Journal of Soils Sediments 18 (7): 2500–2510. https://doi.org/10.1007/s11368-018-1965-8

CSÁKI, P. – SZINETÁR, M.M. – HERCEG, A. – KALICZ, P., GRIBOVSZKI, Z. (2018): Climate change impacts on the water balance - case studies in Hungarian watersheds. Időjárás 122 (1): 81–99. pp. https://doi.org/10.28974/idojaras.2018.1.6

CZIMBER, K. – GÁLOS, B. (2016): A new decision support system to analyse the impacts of climate change on the Hungarian forestry and agricultural sectors. Scandinavian Journal of Forest Research 31 (7): 664–673. https://doi.org/10.1080/02827581.2016.1212088

DI STEFANO, C. – FERRO, V. – MIRABILE, S. (2010): Comparison between grain-size analyses using laser diffraction and sedimentation methods. Biosystems Engineering 106 (2): 205–215. https://doi.org/10.1016/j.biosystemseng.2010.03.013

ESHEL, G. – LEVY, G.J. – MINGELGRIN, U. – SINGER, M.J. (2004): Critical evaluation of use of laser diffraction for particle-size distribution analyses. Soil Science Society of America 68: 736–743. https://doi.org/10.2136/sssaj2004.7360

FÜHRER, E. – HORVÁTH, L. – JAGODICS, A. – MACHON, A. – SZABADOS, I. (2011): Application of a new aridity index in Hungarian forestry practice. Időjárás 115: 205–216.

FÜHRER, E. (2017): Az erdészeti klímaosztályok új lehatárolása öko-fiziológiai alapon. [New delimitation of forest climate classes on an ecophysiological basis] Erdészeti Lapok 152 (6): 173–174. (in Hungarian)

FÜHRER, E. (2018): A klímaértékelés erdészeti vonatkozásai [Forestry aspects of climate evaluation] Erdészettudományi Közlemények 8 (1): 27–42. (in Hungarian) https://doi.org/10.17164/EK.2018.002

GÁLOS, B. – CSÁKI, P. – GRIBOVSZKI, Z. – KALICZ, P. – TIBORCZ, V. – ZAGYVAI, G. – BARTHA, D. – HOFMANN, T. - VISI RAJCZI, E. – BALÁZS, P. – BIDLÓ, A. – HORVÁTH, A. (2017): Multidisciplinary aspects of adaptation to climate extremes in forestry. *In*: GRIBOVSZKI, Z. – HLAVČOVÁ, K. – KALICZ, P. – KOHNOVÁ, S. (eds). Catchment Processes in Regional Hydrology: Experiments, Modeling and Predictions in Carpathian Drainage Basins. 1–5 p.

GRANIER, A. – BRÉDA, N. – BIRON, P. – VILLETTE S. (1999): A lumped water balance model to evaluate duration and intensity of drought constraints in forest stands. Ecological Modelling 116: 269– 283. https://doi.org/10.1016/S0304-3800(98)00205-1

HUNGARIAN STANDARD MSZ-08-0205, 1978. Determination of soil pH, total salinity and $CaCO_3$ content. Hungarian Standard Association, Budapest (in Hungarian)

HUNGARIAN STANDARD MSZ-08-0206, 1978. Determination of particle size distribution of soils. Hungarian Standard Association, Budapest (in Hungarian)

IGAZ, D. – AYDIN, E. – ŠINKOVIČOVÁ, M. – ŠIMANSKÝ, V. – TALL, A. – HORÁK, J. (2020): Laser diffraction as an innovative alternative to standard pipette method for determination of soil texture classes in central Europe. Water 12 (5): 1232. https://doi.org/10.3390/w12051232

KUN, Á. – KATONA, O. – SIPOS, GY. – BARTA, K. (2013): Comparison of pipette and laser diffraction methods in determining the granulometric content of fluvial sediment samples. Journal of Environmental Geography 6: 49–54. https://doi.org/10.2478/jengeo-2013-0006

MAKÓ, A. – SZABÓ, B. – RAJKAI, K. – SZABÓ, J. – BAKACSI, ZS. – LABANCZ, V. – HERNÁDI, H. – BARNA, GY. (2019): Evaluation of soil texture determination using soil fraction data resulting from laser diffraction method. International Agrophysics 33: 445–454. https://doi.org/10.31545/intagr/113347

MAKÓ, A. – TÓTH, G. – WEYNANTS, M. – RAJKAI, K. – HERMANN, T. – TÓTH, B. (2017): Pedotransfer functions for converting laser diffraction particle-size data to conventional values. European Journal of Soil Science 68 (5): 769-782. http://doi.org/10.1111/ejss.12456

MALVERN INSTRUMENTS LIMITED (2013): Mastersizer 3000 user manual. 2–13.; 131–132. pp.

MÁTYÁS, CS. – BERKI, I. – BIDLÓ, A. – CSÓKA, GY. – CZIMBER, K. – FÜHRER, E. – GÁLOS, B. – GRIBOVSZKI, Z. – ILLÉS, G. – HIRKA, A. – SOMOGYI, Z. (2018): Sustainability of forest cover under climate change on the temperate-continental xeric limits. Forests 9 (8): 489. https://doi.org/10.3390/f9080489

POLAKOWSKI, C. – SOCHAN, A. – BIEGANOWSKI, A. – RYZAK, M. – FÖLDÉNYI, R. – TÓTH, J. (2014): Influence of the sand particle shape on particle size distribution measured by laser diffraction method. International Agrophysics 28: 195–200. https://doi.org/10.2478/intag-20014-0008

RAJKAI, K. – TÓTH, B. – BARNA, GY. – HERNÁDI, H. – KOCSIS, M. – MAKÓ, A. (2015): Particle-size and organic matter effects on structure and water retention of soils. Biologia 70: 1456–1461. https://doi.org/10.1515/biolog-2015-0176

SCHLOTTER, D. – SCHACK-KIRCHNER, H. (2013): Intra-aggregate CO_2 enrichment: a modelling approach for aerobic soils. Biogeosciences 10: 1209–1218. https://doi.org/10.5194/bg-10-1209-2013

SOIL SCIENCE SOCIETY OF AMERICA (1997): Glossary of Soil Science Terms. Soil Science Society of America, Madison.

STEFANOVITS, P. (1971): Brown forest soils of Hungary. Akadémiai Kiadó. Budapest. p. 261.

THORNTHWAITE, C.W. – MATHER, J.R. (1955): The water budget and its use in irrigation. In Water, The Yearbook of Agriculture. US Department of Agriculture: Washington DC. pp. 346–358.

YANG, X. – ZHANG, Q. – LI, X. – JIA, X. – WEI, X. – SHAO, M. (2015): Determination of soil texture by laser diffraction method. Soil Science Society of America Journal 79: 1556–1566. https://doi.org/10.2136/sssaj2015.04.0164

YUDINA, A.V. – FOMIN, D.S. – VALDES-KOROVKIN, I.A. – CHURILIN, N.A. – ALEKSANDROVA, M.S. – GOLOVLEVA, YU.A. – PHILLIPOV, N.V. – KOVDA, I.V. – DYMOV, A.A. – MILANOVSKIY, E.YU. (2020): The ways to develop soil textural classification for laser diffraction method. Eurasian Soil Science 53 (11): 1579–1595. https://doi.org/10.1134/S1064229320110149

https://doi.org/10.37045/aslh-2021-0004 Acta Silv. Lign. Hung., Vol. 17, Nr. 1 (2021) 51–61

Growing of Black Locust (*Robinia pseudoacacia* L.) Candidate Cultivars on Arid Sandy Site

Zsolt KESERŰ [a*] – Attila BOROVICS[a] – Tamás ÁBRI[a,b] – Károly RÉDEI[b] – Il Hwan LEE[c] – Hyemin LIM[c]

[a] Forest Research Institute, University of Sopron, Sopron, Hungary
[b] Faculty of Agricultural and Food Sciences and Environmental Management, University of Debrecen, Debrecen, Hungary
[c] Division of Forest Improvement, National Institute of Forest Science, Suwon, Republic of Korea

Abstract – In the late 1990s, Hungarian Forest Research Institute researchers produced 15 micropropogated black locust (*Robinia pseudoacacia* L.) clones as part of a program to select clones that could be successfully grown on arid sites. Five of these clones (R.p. 'Vacsi', R.p. 'Szálas', R.p. 'Oszlopos', R.p. 'Homoki' and R.p. 'Bácska') have been categorized as cultivar candidates. The current study presents information concerning the 'Bácska', 'Vacsi' and 'Homoki' candidate cultivars. Based on research results obtained thus far, the three aforementioned candidate cultivars seem the most promising. The cultivars, aged 6-15 years, were tested in a variety comparison trial under arid, sandy soil conditions in the Danube–Tisza Interfluve near the town of Helvécia. Significant differences ($p<0.05$) were observed during results evaluation of full inventories and during the comparison of candidate cultivars partly with common black locust and partly with 'Jászkiséri' cultivars. The 15-year-old 'Homoki' outperformed common black locust in diameter and mean tree volume; 'Vacsi' outperformed in stem quality. The 14-year-old 'Bácska' candidate cultivar was compared with the 'Jászkiséri' cultivar and the 'Oszlopos' cultivar candidate. 'Bácska' proved to be significantly better in diameter and mean tree volume than Jászkiséri', but weaker in trunk quality.
The South Korean National Institute of Forest Science has supported this research for several years. The growing technology of the mentioned candidate cultivars are also examined in Korea, taking local ecological conditions into account.

***Robinia pseudoacacia* / micropropagation / selection / black locust growing**

Kivonat – Akácfajtajelöltek termesztése szárazodó homoki termőhelyen. Az 1990-es évek végén az Erdészeti Tudományos Intézet kutatói a szárazodó termőhelyeken is eredményesen termeszthető akácklónok szelektálását célul kitűző program keretében 15 klónt állítottak elő, amelyből öt (R.p.'Vacsi', R.p.'Szálas', R.p.'Oszlopos', R.p.'Homoki' és R.p.'Bácska') fajtajelölti minősítést kapott. Jelen tanulmányban, a fentebb említett fajtajelöltek közül, a 'Bácska', a 'Vacsi' és a 'Homoki' kerülnek bemutatásra. Az eddigi vizsgálati eredmények alapján ez a három fajtajelölt tűnik a legígéretesebbnek. A fajtajelölteket a Duna–Tisza közi homokhátságon (Helvécia település közelében), szárazodó, gyenge homoki termőhelyen létesült fajta összehasonlító kísérletben vizsgáltuk 6-15 éves korban. Az állomány-felvételek eredményeinek kiértékelése, a fajtajelölteknek részben a közönséges akáccal, részben a 'Jászkiséri' akáccal történő összehasonlítása során szignifikáns különbségeket tapasztaltunk. A 15 éves 'Homoki' átmérő, és átlagfa-térfogat, a 'Vacsi' törzsminőség tekintetében múlta felül a közönséges akácot. A 'Bácska' fajtajelöltet a 'Jászkiséri' fajtával, valamint az 'Oszlopos' fajtajelölttel hasonlítottuk

[*] Corresponding author: keseru.zsolt@uni-sopron.hu; H-4150 PÜSPÖKLADÁNY, Farkassziget 4, Hungary

össze, ahol a 14 éves ’Bácska’ átmérőben és átlagfa-térfogatban szignifikánsan jobbnak, törzsminőségben viszont gyengébbnek bizonyult a ’Jászkisérinél’.
Ezt a kutatómunkát több éve támogatja a Dél-Koreai Erdészettudományi Intézet, ahol az említett fajtajelöltek termesztési technológiai tulajdonságait szintén vizsgálják az ottani ökológiai feltételek figyelembevétele mellett.

***Robinia pseudoacacia* / mikroszaporítás / szelekció / akáctermesztés**

1 INTRODUCTION

Black locust (*Robinia pseudoacacia* L.), a hard broadleaved tree species, originates from North America. The estimated area of black locust plantations beyond the native range is approx. 3 million ha globally (Schneck 2010). The fast spread of black locust can be expected in two continents in the future: Asia, primarily in the countries of China and South Korea; and Europe, with Hungary, Romania, Poland and some Mediterranean countries (mostly Bulgaria, Italy, France, Turkey) being the most prominent black locust growers (Li et al. 2014, Nicolescu 2020).

Black locust was introduced to Europe more than 400 years ago (Demené – Merzeau 2007). In Hungary, the first records of black locust introduction date back to the 18th century. Since then, black locust area has been steadily increasing (Vadas 1911, Keresztesi 1988). Currently the species covers approx. 24% of forested area in Hungary (HCSO 2019). Black locust was introduced to South Korea in the 19th century. After the Korean War in the 1960s, it was heavily used in the reforestation of denuded mountains. Recently, black locust is one of the most extensively established exotic tree species in Hungary and South Korea. Its widespread growth can be attributed to its drought tolerance, frequent and abundant seed production, rapid growth, relatively high tree yielding potential, good honey production, excellent vegetative regeneration ability, and low susceptibility to pest and pathogens. Its role in soil protection (erosion and deflation control) is also decisive. Black locust wood is durable, high quality, and is utilized for many purposes (Keresztesi 1988, Lee et a. 2004, Noh et al. 2010, Rédei 2013, Lee et al. 2019, Nicolescu et al. 2020). In addition to its many advantageous properties, its ability to propagate aggressively and its inability to associate due to its high light demand and strong root competition should not be overlooked (Vítková et al. 2015, 2017). Furthermore, common black locust may also possess negative tree characteristics to varying degrees. These include warped and space-curved trunks as well as forking and low industrial wood yields, all of which are disadvantageous for growing (Keresztesi 1988).

Hungarian Forest Research Institute (FRI) staff have been improving black locust growing technology for decades, including the creation and introduction of selected black locust cultivars, the primary goal of which is to improve stem quality as well as increase yield and nectar production. Thanks to this research work, we have several black locust cultivars and candidate cultivars available for use in industrial plantations (Keresztesi 1983, 1988; Rédei et al. 2001, 2002, 2008, 2017).

In the late 1990s, FRI researchers produced 15 micropropogated clones as part of a research programme to select clones that could be successfully grown on arid sites. Five of these (*Robinia pseudoacacia* ‘Vacsi’, *Robinia pseudoacacia* ‘Szálas’, *Robinia pseudoacacia* ‘Oszlopos’, *Robinia pseudoacacia* ‘Homoki’ and *Robinia pseudoacacia* ‘Bácska’) have been granted a provisionally approved cultivar candidate category by the Hungarian National Food Chain Safety Office (Rédei et al. 2002, 2006, 2008, 2013a, 2013b).

Apart from Hungary, several countries have initiated research programmes that aim to improve black locust wood quality and/or increase biomass production for energy purposes. Black locust breeding and improvement is undertaken in the USA (Bongarten et al. 1991,

Straker et al. 2015), Germany (Liesebach et al. 2004, Böhm et al. 2011), Poland (Szyp-Borowska et al. 2016), Bulgaria (Kalmukov 2005, 2014), Greece (Dini-Papanastasi – Panetsos 2000), Turkey (Dengiz et al. 2010), India (Sharma et. al. 2006), China (Dunlun et al. 1995, Li et al. 2021), and South Korea (Lee et al. 2007). Countries are increasingly interested in black locust improvement and management, with special attention focused on the species' response to climate change impacts.

The main goals of this paper are as follows:

- providing a brief review of the international aspects of black locust propagation and improvement,
- documenting available knowledge about black locust candidate cultivars,
- presenting the most important results of growing black locust within the Hungarian-South Korean cooperation as a reference work.

2 ORIGIN AND BOTANICAL DESCRIPTION OF THE BLACK LOCUST CANDIDATE CULTIVARS

The black locust improvement (selection) programme launched in 1996 has two aims: to help quality development of black locust propagation material and to complete the variety choice of particular regions producing new black locust cultivars that can be grown effectively under unfavourably changed ecological conditions. The following are the main selection step processes: choice of black locust population containing trees of good phenotype; choice of plus trees; seed collection from the plus trees; seedling production, establishing a collection with the progenies of the plus trees; organizing a collection of seedlings selected from the progenies; clonal selection from the seedlings' collection by tissue culture (micropropagation) method; initiating clone trials for selecting the best clones. The programme has improved 15 new black locust clones (Rédei 2013). As mentioned above, five of these clones have recently been designated as candidate cultivars.

The following segment presents the botanical description of R. p. 'Homoki', R. p. 'Bácska', R. p. 'Vacsi' and R. p. 'Oszlopos' (R. p. 'Szálas' is not subject of this paper).

2.1 Bácska (*Robinia pseudoacacia* 'Bácska')

The breeding label for Bácska is KH 56A 2/5, which indicates the origin of the clone (KH means Kéleshalom). Bácska has medium density foliage, with 11-17 leaflets per leaf stalk. In most cases the leaflet is orderly elliptical possibly inversely egg-shaped, of which the tip is rounded or indented without any splinter. The length of spines ranges from 6 to 12 mm. The base is small, possibly medium-sized, and evenly acuminate toward its point. The shoot is ribbed and uniformly salad-green. It develops many, relatively short shoots (not determining features, these depend mostly on the environment). The rod of 'Bácska' is strongly ribbed and spines, which subtend 90° with the rod, cover its full length. These decrease evenly in size toward the apical part. Generally, 21 to 24 nodes are situated along the length of the 50 cm part of shoot. The bark is smooth and steel-grey in colour. The flower is white. The flowering-axis is green with medium-length. The flower cluster is loose; a cluster consists of 23-31 pieces of flowers. The calyx is green with brown pigmentation, but green-toned determinatively. After flowering, the colour changes to brownish-red. Bácska's flowering intensity was average at Kecskemét-Méheslapos in 2006 and in 2007. Its flowering began three days later than and lasted two days longer than the common black locust at Gödöllő (Osváth-Bujtás – Rédei 2007).

2.2 Homoki (*Robinia pseudoacacia* 'Homoki')

The breeding label for this cultivar is MB 17D ¾, which indicates the origin of the clone (MB means Mikebuda). 'Homoki' makes a dense foliage impression. The compound, which consists of 13-19 leaflets, is of an average length. Mid-positioned leaves are the largest ones. The leaflet is drawn; sometimes it is orderly elliptical-shaped of which the form factor is 3-3.5. The tip of the leaflet is mildly indented and lacks splinter. The spines are small, bodkin-like, and 5-8 mm in length. 'Homoki' black locust shoots are reddish, greenish-brown and are typically ribbed. Rods are strongly ribbed with a medium number of nodums (15-21). Tiny spines subtend at an acute angle (approx. 30°) with the rod. The bark is greyish-brown, with lenticels of scattered position emerging from the surface. Often longitudinal brown stripes can be seen on sapling bark. The flowering-axis is dull green with purple discoloration. The petals are white with mild greenish-yellow colour in the middle of the vexil. 'Homoki' began flowering at average time at Kecskemét-Méheslapos in 2006 but lasted 2-4 days longer than the common black locust at Gödöllő. Its flowering was abundant in 2006 and in 2007 (Osváth-Bujtás – Rédei 2007).

2.3 Vacsi (*Robinia pseudoacacia* 'Vacsi')

This clone is labelled as PV 201E2/1, which indicates the origin (PV means Pusztavacs). 'Vacsi' develops olive-green, relatively sparse foliage after leafing. On average, there are 15-21 leaflets per leaf stalk. With the exception of the lowest leaflets, the mostly egg-shaped leaflets are identical in size. The form factor is 2.5-3. The leaf tips are rounded or indented and are ordered in an opposite leaf arrangement. Spines are mouse ear-like and small. Shoots are green, greenish-brown, and ribbed only on 5-15 cm of length on the youngest segments. The next part of shoot is cylindrical. The rod is covered by medium strong ribs, with an average number of nodums (19-21). Tiny spines are situated only on the lower part of the shoot. The bark of 'Vacsi' black locust is dark grey with scattered lenticels. It has white flowers and the flowering-axis is green. The calyx is light green and occasionally displays pink pigment; the petals are white with an olive-green spot. Flowering intensity was average at Kecskemét-Méheslapos in 2006 and was weak-medium in 2007 (Osváth-Bujtás – Rédei 2007).

2.4 Oszlopos (*Robinia pseudoacacia* 'Oszlopos')

The breeding label for this clone is PV 233A/1. It develops medium green rich foliage after vernal leafing. The compound leaf consists of 15-19 leaflets. The leaflet is elongated elliptical (its form factor is 3-3.5) with an acuminate tip, sometimes with splinter. The leaf base of leaflets is wedge-shaped. The 1-3 mm-long spines are situated on the underside of the rod. Their shape is uncharacteristic and nondescript. Shoots are light green, ribbed along 15-20 cm of length, while the other part of the shoot is cylindrical. Medium strong ribs, with many (27-30) nodums and little spines, cover the rods. Spines do not or hardly develop on the apical – longer – part of the rod and occur only along the lower 15-20 cm. The bark is greenish-grey with scattered lenticels. Flowering intensity was average at Kecskemét-Méheslapos in 2006 and in 2007. The same applies to flower quantity (Osváth-Bujtás – Rédei 2007).

2.5 Experiences of clone trials

The Hungarian Forest Research Institute has three clone trials (Helvécia, Kecskemét and Hajdúhadház) where 'Bácska' and 'Homoki' candidate cultivars proved to be the best (Rédei et al. 2013a, 2013b).

3 MATERIALS AND METHODS

3.1 Site and stand parameters

Data used in this study emanated from black locust clone trials established in the forest subcompartment Helvécia 22 E (two experimental plots) in Danube–Tisza Interfluve, "Homokhátság" (sandy ridge) region (*Figure 1*). In the past three decades, the mean annual precipitation at the site was 574 mm while the mean annual temperature was 11.4 °C (Tölgyesi et al. 2016). The FOA has recognized this region as an increasingly arid zone in its long-term forecast. The most pessimistic assessments predict the risk of desertification (UNCCD 2006).

The experimental plots are located in a forest-steppe climate. The soil is slightly humous, sandy, and free-draining (according to the Hungarian forest site classification by Járó, 1972). The black locust stands at the site ranged from 6 to 15 years.

In experimental plot 1, we compared 'Vacsi', 'Homoki' candidate cultivars and the common black locust (control). The examined trees were 15 years old at the time (January 2021) of the full inventory (Laar – Akca 2007).

In experimental plot 2, 'Jászkiséri' cultivar and 'Bácska' and 'Oszlopos' candidate cultivars were compared. These were 14-year-old trees.

In the experimental plots, 30 stems/clone were examined.

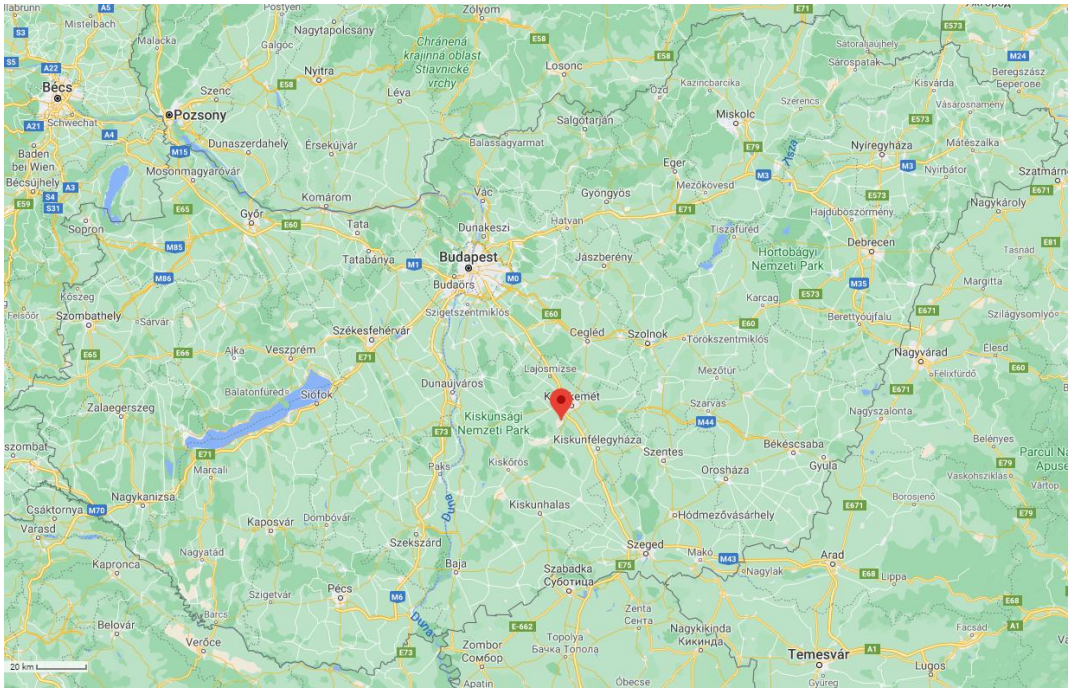

Figure 1. Location of the research site (Helvécia)

The location (forest subcompartment) and the most important dendrometric characteristics, including age, mean height (H), mean diameter at breast height (DBH), mean tree volume (v) and stem form value (SFV), extended by data from previous full inventories (6-year-old and 7-year-old trees) are compiled in *Table 1*. The stem volume was calculated using the following volume function based on the volume table for black locust (Sopp – Kolozs 2013):

$$v = 10^{-8} \cdot d^2 \cdot h^1 \cdot (h/[h-1.3])^2 \cdot (-0.6326 \cdot d \cdot h + 20.23 \cdot d + 3034), \quad (1)$$

where v is stem volume (m^3), d is diameter at breast height (cm), h is tree height (m). The mean tree volume (v, m^3/tree) was calculated using the means of stem volume for each of the

experimental plots. The following classifications were used for the evaluation of stem form value (SFV): 1 – stem form is straight, 2 – more or less straight, 3 – crooked, 4 – very crooked.

Table 1. Parameters of black locust candidate cultivars, 'Jászkiséri' cultivar, and common black locust (control) at 6-15 years old

Clones	Experimental plot	Age (yr)	H_m (m)	DBH (cm)	v (m^3)	SFV
Homoki	1	7	8.7	6.2	0.0227	1.78
Vacsi	1	7	7.8	5.3	0.0147	1.36
Common black locust	1	7	6.36	3.86	0.0081	2.45
Homoki	1	15	10.5	9.8	0.0626	2.32
Vacsi	1	15	9.0	7.7	0.0327	1.66
Common black locust	1	15	9.77	7.56	0.0343	2.37
Bácska	2	6	7.1	6.3	0.0131	1.74
Oszlopos	2	6	3.9	3.5	0.0034	2.23
Jászkiséri	2	6	6.28	5.81	0.0105	1.68
Bácska	2	14	11.4	11.2	0.0790	2.50
Oszlopos	2	14	6.7	7.6	0.0312	2.32
Jászkiséri	2	14	11.66	9.85	0.0616	1.96

Note: PV 233 A/1 ('Oszlopos') candidate cultivars are situated on the poorest spot of the site

3.2 Statistical analysis

Microsoft Excel 2016 and IBM SPSS Statistics 25 software packages were used for the statistical analysis of experimental results. Candidate cultivars were compared using one-way ANOVA and Fisher's least significance difference (LSD) test (p<0.05).

4 RESULTS AND DISCUSSION

Figure 2 presents the distribution of the candidate cultivars in the site index curves of the black locust yield table. As the figure shows, at 6 and 7 years old, the candidate cultivars (except 'Oszlopos' – PV 233A/1) belong to yield class I to III, and to yield class IV to VI at 14 and 15 years old.

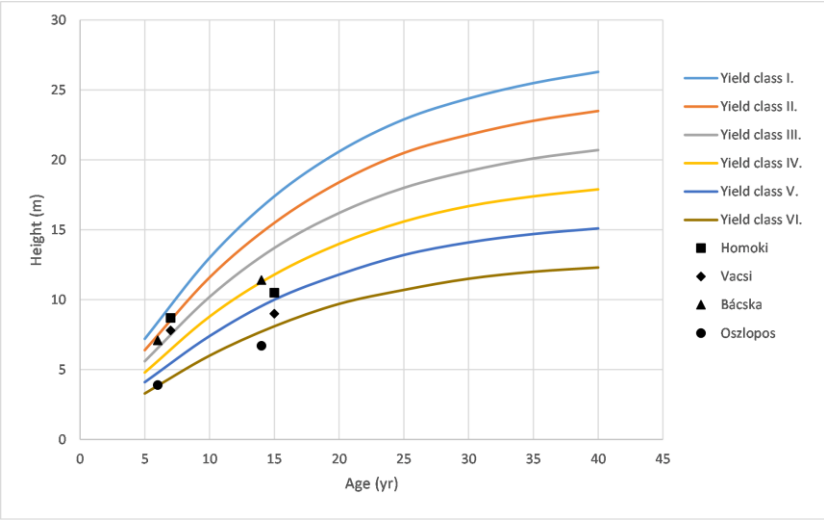

Figure 2. 6-15-year-old black locust candidate cultivars in the site index curves of black locust yield table (based on Rédei 1984*)*

In this study, significant (p<0.05) differences were observed between the examined candidate cultivars. More specifically, 15-year-old 'Homoki' outperformed the common black locust in diameter and mean tree volume; 'Vacsi' outperformed in stem quality (*Table 2*). The 14-year-old 'Bácska' cultivar candidate was compared with the 'Jászkiséri' cultivar and 'Oszlopos' cultivar candidate where 'Bácska' proved to be significantly better in diameter and mean tree volume, but weaker in stem quality than 'Jászkiséri' (*Table 3*).

Table 2. The result of one-way ANOVA (Helvécia 22 E/1)

	Clone		Mean Difference	Std. Error	Sig.	95% Confidence Interval Lower Bound	95% Confidence Interval Upper Bound
DBH (cm)	Control	Homoki	-2.2785*	0.5463	0.000	-3.3611	-1.1959
		Vacsi	-0.1372	0.5037	0.786	-1.1353	0.8609
	Homoki	Control	2.2785*	0.5463	0.000	1.1959	3.3611
		Vacsi	2.1413*	0.4848	0.000	1.1806	3.1021
	Vacsi	Control	0.1372	0.5037	0.786	-0.8609	1.1353
		Homoki	-2.1413*	0.4848	0.000	-3.1021	-1.1806
Based on observed means. *The error term is Mean Square (Error) = 4.757*							
Height (m)	Control	Homoki	-0.7480	0.4746	0.118	-1.6886	0.1925
		Vacsi	0.7267	0.4376	0.100	-0.1404	1.5938
	Homoki	Control	0.7480	0.4746	0.118	-0.1925	1.6886
		Vacsi	1.4747*	0.4212	0.001	0.6401	2.3093
	Vacsi	Control	-0.7267	0.4376	0.100	-1.5938	0.1404
		Homoki	-1.4747*	0.4212	0.001	-2.3093	-0.6401
Based on observed means. *The error term is Mean Square(Error) = 3.590*							
Mean tree volume (m^3)	Control	Homoki	-0.0282*	0.0066	0.000	-0.0413	-0.0151
		Vacsi	0.0017	0.0061	0.785	-0.0104	0.0137
	Homoki	Control	0.0282*	0.0066	0.000	0.0151	0.0413
		Vacsi	0.0299*	0.0059	0.000	0.0183	0.0415
	Vacsi	Control	-0.0017	0.0061	0.785	-0.0137	0.0104
		Homoki	-0.0299*	0.0059	0.000	-0.0415	-0.0183
Based on observed means. *The error term is Mean Square(Error) = 0.001*							
Stem form value	Control	Homoki	0.0431	0.1419	0.762	-0.2381	0.3243
		Vacsi	0.7067*	0.1308	0.000	0.4474	0.9659
	Homoki	Control	-0.0431	0.1419	0.762	-0.3243	0.2381
		Vacsi	0.6635*	0.1259	0.000	0.4140	0.9131
	Vacsi	Control	-0.7067*	0.1308	0.000	-0.9659	-0.4474
		Homoki	-0.6635*	0.1259	0.000	-0.9131	-0.4140
Based on observed means. *The error term is Mean Square(Error) = 0.321*							

*. The mean difference is significant at the 0.05 level

Table 3. The result of one-way ANOVA (Helvécia 22 E/2)

	Clone		Mean Difference	Std. Error	Sig.	95% Confidence Interval Lower Bound	95% Confidence Interval Upper Bound
DBH (cm)	Bácska	Jászkiséri	1.3181*	0.5360	0.015	0.2567	2.3795
		Oszlopos	3.5695*	0.5581	0.000	2.4642	4.6747
	Jászkiséri	Bácska	-1.3181*	0.5360	0.015	-2.3795	-0.2567
		Oszlopos	2.2514*	0.5360	0.000	1.1900	3.3127
	Oszlopos	Bácska	-3.5695*	0.5581	0.000	-4.6747	-2.4642
		Jászkiséri	-2.2514*	0.5360	0.000	-3.3127	-1.1900
Based on observed means. *The error term is Mean Square(Error) = 5.919*							
Height (m)	Bácska	Jászkiséri	-0.2203	0.3351	0.512	-0.8839	0.4433
		Oszlopos	4.7763*	0.3489	0.000	4.0853	5.4673
	Jászkiséri	Bácska	0.2203	0.3351	0.512	-0.4433	0.8839
		Oszlopos	4.9966*	0.3351	0.000	4.3331	5.6602
	Oszlopos	Bácska	-4.7763*	0.3489	0.000	-5.4673	-4.0853
		Jászkiséri	-4.9966*	0.3351	0.000	-5.6602	-4.3331
Based on observed means. *The error term is Mean Square(Error) = 2.313*							
Mean tree volume (m^3)	Bácska	Jászkiséri	0.0174*	0.0073	0.018	0.0030	0.0317
		Oszlopos	0.0479*	0.0076	0.000	0.0329	0.0628
	Jászkiséri	Bácska	-0.0174*	0.0073	0.018	-0.0317	-0.0030
		Oszlopos	0.0305*	0.0073	0.000	0.0161	0.0448
	Oszlopos	Bácska	-0.0479*	0.0076	0.000	-0.0628	-0.0329
		Jászkiséri	-0.0305*	0.0073	0.000	-0.0448	-0.0161
Based on observed means. *The error term is Mean Square(Error) = 0.001*							
Stem form value	Bácska	Jászkiséri	0.5444*	0.1210	0.000	0.3047	0.7842
		Oszlopos	0.1842	0.1260	0.147	-0.0654	0.4338
	Jászkiséri	Bácska	-0.5444*	0.1210	0.000	-0.7842	-0.3047
		Oszlopos	-0.3602*	0.1210	0.004	-0.5999	-0.1205
	Oszlopos	Bácska	-0.1842	0.1260	0.147	-0.4338	0.0654
		Jászkiséri	0.3602*	0.1210	0.004	0.1205	0.5999
Based on observed means. *The error term is Mean Square(Error) = 0.302*							

*. The mean difference is significant at the 0.05 level

5 CONCLUSIONS

This study compared black locust candidate cultivars with common black locust and 'Jászkiséri' cultivars. After the evaluation of statistical analysis (one-way ANOVA) of experimental results, the present study found significant differences (p<0.05) between the

candidate cultivars and common black locust or 'Jászkiséri' locust. More specifically, 15-year-old 'Homoki' and 14-year-old 'Bácska' proved to be the best in diameter at breast height (9.8 cm and 11.2 cm) and mean tree volume (0.0626 m^3 and 0.0790 m^3).

The evaluation of the experiment addresses the important fact of whether it is worthwhile to grow selected black locust cultivars and candidate cultivars on marginal sites. Detailed economic studies are needed to determine this, especially with regard to the expected added value (stem quality) of the candidate cultivars.

The Hungarian Forest Research Institute and the South Korean National Institute of Forest Science have been cooperating on the improvement of black locust cultivation in Hungary and South Korea for over ten years. The South Korean National Institute of Forest Science fully supports the project. Candidate cultivars evaluated in this manuscript are also available in South Korea and have been experimentally vegetative propagated and placed in variety comparison trials in recent years. The focus of our study was to investigate the growth relationships of the candidate cultivars on marginal sites, as the potential for future black locust propagation in such sites is under primary consideration in South Korea.

The systematic evaluation of the cultivation experiments and the selection of black locust clones and candidate cultivars to be proposed for public cultivation should be further extended to the following main fields:

- better definition of their site (ecological) requirements;
- development of a large-scale, profitable technology for their vegetative propagation (from root cuttings);
- further data collection and evaluation of the cultivation technological factors (planting spacing, mixing, cutting age, etc.) which are not yet sufficiently understood;
- extension of productivity (yield) studies, development of new yield models for groups of candidate cultivars;
- continued monitoring and evaluation of the resistance of candidate cultivars to biotic and abiotic pests;
- more consistent use of landscape ecology in species selection.

Acknowledgements: Prepared with the professional support of the Doctoral Student Scholarship Program of the Co-operative Doctoral Program of the Ministry of Innovation and Technology financed from the National Research, Development and Innovation Fund. Furthermore, the work is supported by the South Korean National Institute of Forest Science (NIFoS).

REFERENCES

BONGARTEN, B.C. – MERKLE, S.A. – HANOVER, J.W. (1991): Genetically improved black locust for biomass production in short-rotation plantations. *In*: Energy from Biomass and Wastes XV (KLASS, D.L. ed.), Institute of Gas Technology, Chicago, IL. 391–409.

BÖHM, C. – QUINKENSTEIN, A. – FREESE, D. (2011): Yield prediction of young black locust (*Robinia pseudoacacia* L.) plantation for woody biomass production using allometric relations. Annals of Forest Research 54: 215–227.

DEMENÉ, J.M. – MERZEAU, D. (2007): Le robinier faux acacia, Historique et caractéristiques biologiques. Forêt-entreprise 177: 10–12. (in French)

DENGIZ, O. – GOL, C. – SARIOGLU, F. E. – EDIS, S. (2010): Parametric approach to land evaluation for forest plantation: A methodological study using GIS model. African Journal of Agricultural Research 5 (12): 1482–1496.

DINI-PAPANASTASI, O. – PANETSOS, C.P. (2000): Relation between growth and morphological traits and genetic parameters of *Robinia pseudoacacia var. monophylla* DC in northern Greece. Silvae Genet. 49: 37–44.

DUNLUN, Z. – ZHENFEN, Z. – FANGQUAN, W. (1995): Progress in clonal selection and breeding of black locust (*Robinia pseudoacacia* L.) *In*: Forest Tree Improvement in the Asia-Pacific Region (Xihuan Shen): China Forestry Publishing House, Beijing, 152–156.

HUNGARIAN CENTRAL STATISTICAL OFFICE (HCSO) (2019): A faállománnyal borított erdőterület és az élőfakészlet megoszlása fafajcsoportok és korosztályok szerint (2010-2019) online: https://www.ksh.hu/docs/hun/xstadat/xstadat_eves/i_ome002b.html (in Hungarian)

JÁRÓ, Z. (1972): A termőhely fogalma. *In*: Danszky I. (ed.): Erdőművelés I. Mezőgazdasági Kiadó, Budapest, 47–87. (in Hungarian)

KALMUKOV, K. (2005): Growth and yield of pure and mixed black locust cultures. *In*: Proceedings of the symposium forest and sustainable development. Transylvania University of Braşov, Braşov, pp 91–96.

KALMUKOV, K. (2014): Improvement of black locust stands in Bulgaria. Gora 6–7: 24–26 (in Bulgarian)

KERESZTESI, B. (1983): Breeding and cultivation of black locust (*Robinia pseudoacacia* L.) in Hungary. Forest Ecology and Management 6: 217–244.

KERESZTESI, B. (Ed.) (1988): The Black Locust. Akadémiai Kiadó, Budapest.

LAAR, A. – AKÇA, A. (2007): Forest Mensuration. City, Springer: 377.

LEE, C.S. – CHO, H.J. – YI, H. (2004): Stand dynamics of introduced black locust (Robinia pseudoacacia L.) plantation under different disturbance regimes in Korea. Forest Ecology and Management 189: 281–293. https://doi.org/10.1016/j.foreco.2003.08.012

LEE, H. – LIM, H. – KANG, J.-W. (2019): Growth Performance of Exotic Trees in Korea. Journal of Forest and Environmental Science 35 (2): 115–120. https://doi.org/10.7747/JFES.2019.35.2.115

LEE, K.J. – SOHN, J.H. – RÉDEI, K. – YUN, H.Y. (2007): Selection of early and late flowering *Robinia pseudoacacia* from domes-ticated and introduced cultivars in Korea and prediction of flowering period by accumulated temperature. Journal of Korean Forest Society 96: 170–177.

LI, G. – XU, G. – GUO, K. – DU, S. (2014): Mapping the global potential geographical distribution of black locust (*Robinia Pseudoacacia* L.) using herbarium data and a maximum entropy model. Forests 5: 2773–2792. https://doi.org/10.3390/f5112773

LI, X. – ZHANG, Z. – REN, Y. – FENG, Y. – GUO, Q. – DONG, L. – SUN, Y. – LI, Y. (2021): Induction and early identification of tetraploid black locust by hypocotyl in vitro. In Vitro Cellular and Developmental Biology – Plant 57: 372–379. https://doi.org/10.1007/s11627-020-10133-5

LIESEBACH, H. – YANG, M. S. – SCHNECK, V. (2004): Genetic diversity and differentiation in a black locust (*Robinia pseudoacacia* L.) progeny test. Forest Genetics 11 (2): 151–161.

NICOLESCU, V.N. – RÉDEI, K.–MASON, W.L. ET AL. (2020): Ecology, growth and management of black locust (*Robinia pseudoacacia* L.), a non-native species integrated into European forests. Journal of Forestry Research 31: 1081–1101. https://doi.org/10.1007/s11676-020-01116-8

NOH, N.J. – SON, Y. – KOO, J.W. – SEO, K.W. – KIM, R.H. – LEE, Y.Y. – YOO, K.S. (2010): Comparison of nitrogen fixation for north- and south-facing Robinia pseudoacacia stands in central Korea. Journal of Plant Biology 53: 61–69. https://doi.org/10.1007/s12374-009-9088-9

OSVÁTH-BUJTÁS, Z. – RÉDEI, K. (2007): Akác fajtaismertető. Agroinform Kiadó. Budapest. 36. (in Hungarian)

RÉDEI, K. – OSTVÁTH-BUJTÁS, Z. – BALLA, I. (2001): Propagation methods for black locust (*Robinia pseudoacacia* L.) improvement in Hungary. Journal of Forestry Research 12 (4): 215–219. https://doi.org/10.1007/BF02856710

RÉDEI, K. – OSTVÁTH-BUJTÁS, Z. – BALLA, I. (2002): Clonal approaches to growing black locust (*Robinia pseudoacacia* L.) in Hungary: a review. Forestry 75 (5): 548–552. https://doi.org/10.1093/forestry/75.5.547

RÉDEI, K. – OSVÁTH-BUJTÁS, Z. – VEPERDI, I. (2006): Black locust (*Robinia pseudoacacia* L.) clonal seed orchards in Hungary. Silva Balcanica 7 (1): 63–68.

RÉDEI, K. – OSVÁTH-BUJTÁS, Z. – VEPERDI, I. (2008): Black locust (*Robinia pseudoacacia* L.) improvement in Hungary: a review. Acta Silvatica et Lignaria Hungarica 4:127–132.

RÉDEI, K. (1984): Akácosok fatermése. ERTI Kutatási jelentés. Kecskemét (in Hungarian)

RÉDEI, K. (Ed.) (2013): Black locust (*Robinia pseudoacacia* L.) Growing in Hungary. Agroinform Kiadó, Budapest.

RÉDEI, K. – KESERŰ, Z. – RÁSÓ, J. (2013a): Early evaluation of micropropagated black locust (*Robinia pseudoacacia* L.) clones in Hungary. Forest Science and Practice 15: 81–84.

RÉDEI, K. – KESERŰ, ZS. – CSIHA, I. – RÁSÓ, J. – KAMANDINÉ VÉGH, Á. – ANTAL, B. (2013b): Juvenile growth and morphological traits of micropropagated black locust (*Robinia pseudoacacia* L.) clones under arid site conditions. Acta Silvatica et Lignaria Hungarica 9: 35–42.

RÉDEI, K. – CSIHA, I. – RÁSÓ, J. – KESERŰ, ZS. (2017): Selection of promising black locust (*Robinia pseudoacacia* L.) cultuvars in Hungary. Journal of Forest Science 63 (8): 339–343. https://doi.org/10.17221/23/2017-JFS

SHARMA, K.R. – PUNEET, S. (2006): Variation in wood character-istics of *Robinia pseudoacacia* Linn. managed under high density short rotation system. *In*: Verma K.S., Khurana D.K., Christersson L. (eds): Proceedings of IUFRO In-ternational Conference on World Perspective on Short Rotation Forestry for Industrial and Rural Development, Nauni-Solan, Sept 7–13, 2003: 233–237.

SCHNECK, V. (2010): Robinie - Züchtungsansätze und Begründungsverfahren. In: Deutschland / Bundesministerium für Ernährung, Landwirtschaft und Verbraucherschutz (eds) Beiträge - Agrarholz 2010: Symposium am 18. und 19. Mai 2010 in Berlin. Bonn: BMELF, pp 1-8, online: http://veranstaltungen.fnr.de/fileadmin/allgemein/pdf/veranstaltungen/Agrarholz2010/11_2_Beitrag_Schneck.pdf. Accessed 15th April 2021 (in German)

SOPP L. – KOLOZS L. (2013): Fatömegszámítási táblázatok. 4th Ed. Budapest, National Food Chain Safety Office, State Forest Service: 280 (in Hungarian)

STRAKER, K.C. – QUINN, L.D. – VOIGT, T.B. – LEE, D.K. – KLING, G.J. (2015): Black Locust as a bioenergy feedstock: A review. Bioenergy Research 8: 1117–1135. https://doi.org/10.1007/s12155-015-9597-y

TÖLGYESI, CS. – ZALATNAI, M. – ERDŐS, L. – BÁTORI, Z. – HUPP, N.R. – KÖRMÖCZI, L. (2016): Unexpected ecotone dynamics of a sand dune vegetation complex following water table decline. Journal of Plant Ecology 9 (1): 40–50. https://doi.org/10.1093/jpe/rtv032

UNCCD (2006): Second National Report of the Republic of Hungary on the implementation of the United Nation Convention to Combat Desertification. Budapest: Ministry of Environment and Water of the Republic of Hungary.VADAS, J. (1911): Az ákácfa monográfiája. Budapest. 236. (in Hungarian)

VÍTKOVÁ, M. – TONIKA, J. – MÜLLEROVÁ, J. (2015): Black locust – successful invader of a wide range of soil conditions. Science of the Total Environment 505: 315–328. https://doi.org/10.1016/j.scitotenv.2014.09.104

VÍTKOVÁ, M. – MÜLLEROVÁ, J. – SÁDLO, J. – PERGL, J. – PYŠEK, P. (2017): Black locust (*Robinia pseudoacacia*) beloved and despised: A story of an invasive tree in Central Europe. Forest Ecology and Management 384: 287–302. https://doi.org/10.1016/j.foreco.2016.10.057

https://doi.org/10.37045/aslh-2021-0005 *Acta Silv. Lign. Hung., Vol. 17, Nr. 2 (2021) 65–82*

The Role of Grassy Habitats in Agroforestry

Nóra SZIGETI[a*] – Imre BERKI[b] – Andrea VITYI[b] – Dániel WINKLER[c]

[a] Institute of Advanced Studies, Kőszeg, Hungary
[b] Institute of Environmental Protection and Natural Conservation, University of Sopron, Sopron, Hungary
[c] Institute of Wildlife Biology and Management, University of Sopron, Sopron, Hungary

Abstract – Planting shelterbelts on agricultural fields has long traditions in Hungary. The biodiversity-enhancing effect of this type of agroforestry is intensively researched, but most of the results concentrate on tree species diversity and specific animal communities such as insects and birds. The characteristics of herbaceous vegetation and soil mesofauna related to shelterbelts are understudied; however, both communities play key roles in agricultural productivity. This study aimed to explore the diversity and species composition of these groups in shelterbelts and adjacent grassy and cropped habitats. Samples were taken inside and adjacent to a native and a non-native shelterbelt in an agricultural landscape. The results highlight that shelterbelt edges are at least as important as tree stands in preserving soil-related diversity. Native tree species composition shows slightly more favorable conditions concerning the examined communities. While the positive impact of shelterbelts on the agricultural productivity and the diversity of several animal communities has been proven, the appearance of forest-related herbaceous species in tree stands planted on cultivated fields is not expected, even after decades have passed. The research was supported by the Blue Planet Climate Protection Foundation.

agroforestry / diversity / species composition / herbaceous vegeatation / soil mesofauna

Kivonat – A gyepes élőhelyek szerepe az agrár-erdészetben. Magyarországon nagy hagyományokkal rendelkezik a mezőgazdasági területek védelme erdősávokkal. Az agrár-erdészet e típusának a biodiverzitást fokozó hatása intenzíven kutatott terület, de az eredmények többsége a fafajok sokféleségére és az állatközösségek szűkebb körére, például rovarokra és madarakra koncentrál. Az erdősávok lágyszárú növényzete és a talajlakó mezofauna jellemzői még kevéssé vizsgált, holott mindkét közösség kulcsszerepet játszik a mezőgazdaság termelés eredményességében. A tanulmány célja ezen csoportok diverzitásának és fajösszetételének feltárása az erdősávokban és a csatlakozó gyepes és kultivált területeken. A mintavételezés mezőgazdasági területre ültetett őshonos és nem honos erdősávokban és környezetükben történt. Az eredmények azt tükrözik, hogy az erdősávok gyepes szegélyei legalább olyan fontosak a talajhoz kötődő diverzitás megőrzésében, mint maga a faállomány. Az őshonos fafajösszetételű erdősáv kissé kedvezőbb képet mutat a vizsgált közösségek szempontjából. Míg az erdősávok pozitív hatása a szántóföldi termesztésre és számos állatközösség diverzitására bizonyított, az erdőhöz kötődő lágyszárú fajok megjelenése még évtizedek után sem várható a mezőgazdasági területekre ültetett faállományokban. A kutatást a Kék Bolygó Klímavédelmi Alapítvány támogatta.

agrár-erdészet / diverzitás / fajösszetétel / lágyszárú növényzet / talajlakó mezofauna

[*] Corresponding author: szigetinora31@gmail.com; H-9730 KŐSZEG, Chernel u. 14, Hungary

1 INTRODUCTION

Agroecological systems can provide the opportunity to maintain productivity in a sustainable form (Ball et al. 2018). Agroforestry, a promising aspect of climate change adaptation, integrates woody vegetation into agricultural cultivation, thereby exploiting its various economic, social and ecological benefits. Agroforestry can even revive degraded lands by improving the physical quality of soil once the characteristics of soil aggregate and biological activity are taken into account (Cherubin et al. 2019).

Based on several research results (Feliciano et al. 2018, Jezeer et al. 2019, Elagib – Al-Saidi 2020, Tschora – Cherubini 2020), the advantages of agroforestry can be summarised as follows:

- Soil erosion and runoff control, defending soil from losses of water and nutrients
- Maintaining biological activity, physical properties, and nutrient content of soil for fertility
- Micro-climate regulating
- Providing fodder and shelter for livestock
- Insect pest control
- Eroded and degraded land rehabilitation
- Diversification and stabilisation of farm economy via multiple products
- Promoting nature conservation and biodiversity by providing a framework for above ground and belowground biodiversity

Shelterbelts are the most significant representatives of arable agroforestry in Hungary. While the weed vegetation of intensively cultivated agricultural areas has been widely researched (Pinke − Pál 2005, Pinke et al. 2012, Király – Király 2012, Nagy et al. 2017, Krähmer et al. 2019), research concentrated on shelterbelts has been largely limited to tree species composition and structure surveys (Takács 2008, Jánoska 2012).

According to the technical development of weed management, the number of species adapted to agricultural land use has experienced a significant decline in recent decades (Marshall 2002, Pinke – Pál 2005). Field edges that form a boundary structure with associated habitats can positively affect the weed flora (Marshall – Moonen 2002). These edges offer refuges for many weed species in intensely cultivated environments (Marshall – Arnold 1995).

In appropriate conditions, shelterbelts produce a corridor effect by providing connectivity between woody patches, thereby increasing tree stand area and offering an edge habitat in agricultural landscapes (Damschen 2013). As these corridors increase the number of native plant species, they are an essential tool for biodiversity preservation (Damschen et al. 2006). The presence, absence, or diversity of herbaceous plants can strongly influence the composition and richness of the food chain upon which it is based, and thus the overall biodiversity of the agroforestry system. Therefore, the study of the herbaceous diversity of shelterbelts in agricultural environments is sensible. Acari and Collembola communities play key roles in support productivity under nutrient-poor conditions. Nevertheless, even minor changes in the composition and abundance of these species can significantly affect the local mobilization of nutrients (Heneghan – Bolger 1998). Several studies highlight the role of the food chain and the presence of natural enemies of pests, or even alien, invasive species in agriculture (Schonrogge et al. 1996, Willis – Memmott 2005, Morris et al. 2004). While some weeds can uniquely support the life cycle of a range of insect species, weed diversity strictly correlates with the heterogeneity of plant communities, which affects insectivorous bird communities and other animal communities (Marshall et al. 2003). Also, the presence of seeds is of key importance for granivorous bird species, especially during winter (Buckingham et al. 2011). Many bird species feed primarily on seeds and other parts of plants

as adults, but young individuals need invertebrate food. In addition to the diversity and species composition of vegetation, the density and structure of a plant community are very important for many arthropods that, in turn, provide nutrients for vertebrate animals (Marshall et al. 2003). According to the dispersal of the hedge flora, Marshall (1989) found that the majority of the plants do not spread into the crop field. Some species have limited dispersal into crop areas, and a lower number of species occur as serious field weeds. The field margin, as ecotone, often supports species characteristic to the adjacent habitats and other species that are not present in either adjacent habitats. Thus, a field margin containing grassland, woodland, and ruderal or segetal plants can be more diverse than either the crop field or the woody boundary. Thus, if woody vegetation (trees or shrubs as hedges) border the agricultural fields, the ideal structure of the margin consists of the woody boundary, a nature conservation strip, and the crop edge, which should be completed with a grassy or wildflower margin strip for wildlife or environmental objectives, between the boundary and the crop field. This strip should be free of chemicals (Marshall – Moonen 2002). The aim of the study was to assess the role of shelterbelts and their grassy edges in increasing the soil-related diversity in an intensively managed agricultural area.

2 MATERIALS AND METHODS

2.1 Location of the study area

Surveys were conducted in an intensively managed agricultural landscape in northwest Hungary (*Figure 1*). Mosonszolnok and its surroundings are typical of the Little Hungarian Plain. An important feature of the sample area is the significant climatic drought, which is caused by the frequent descending westward airflow from the Eastern Alps (Péczeli 1975). In addition, the sediments and alluvium in this area are calcareous, which can increase the effect of climatic drought.

Figure 1. Location of the test site

Sandy muddy loess covers the gravel-based flat alluvial cone (Pécsi 1975). Topsoil depth determines the land use: 40-70 cm deep topsoil is only suitable for poor quality pastures, or where other conditions allow, peach and grape cultivation (Miklay – Molnár 1968). This explains the presence of former pasture fragments on the test site. Agricultural cultivation determines the current appearance of the landscape. The few existing semi-natural habitats are

highly fragmented. A variety of grains are grown on the monocrop fields. Shelterbelts with different tree species compositions provide a poor diversity of the landscape. The shelterbelts here consist of tree stands that are approximately 50 years old and were established primarily field protection. The current study examined two of these shelterbelts.

Surveys were conducted within the two shelterbelts and in the adjacent habitats: in the grassy edge on both sides of the shelterbelts (EDGE) and in the cultivated fields, 10 m distance from the trees (CULT), with tree repeats (*Figure 2*).

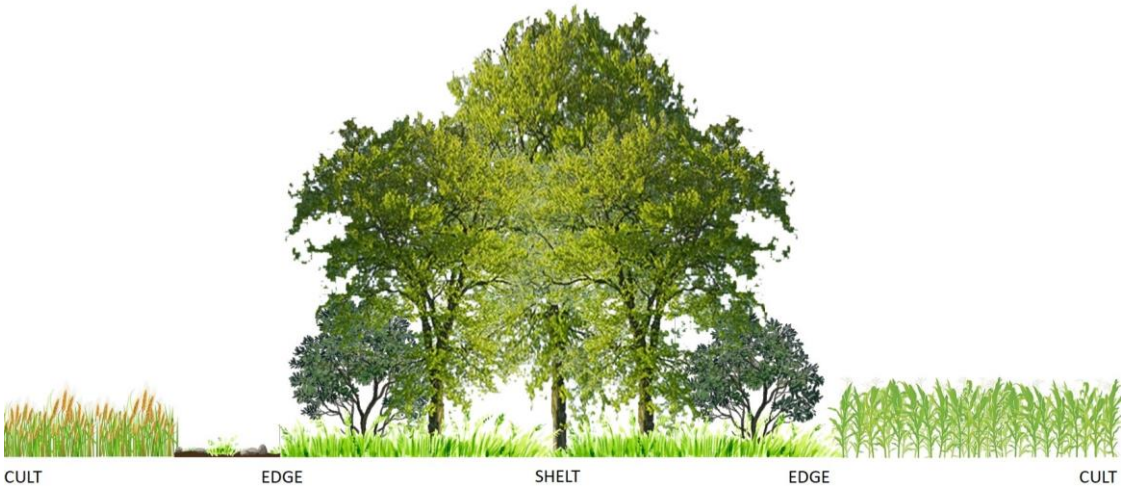

Figure 2. Location of the sampling plots in the shelterbelts and adjacent habitats

2.2 Soil properties

Soil samples were taken from the soil surface (0-10 cm depth) to measure soil parameters. *Table 1* summarises the examined characteristics and the measuring methods.

Table 1. Measured soil parameters and methods

Soil parameter	Measuring method
pH	Ratio of 1:5 soils to distilled water
Soil organic matter content (SOM)	Potassium dichromate capacity method (Búzás 1988)
Available nitrogen (NO_3^- + NH_4^+)	Parnas-Wagner distillation apparatus (Houba et al. 1986)
Available phosphorus	Ammonium-lactate solution (Hungarian Standard MSZ 20135:1999
Available potassium	
Particle size distribution	Robinson's pipette method (Pansu – Gautheyrou 2007)
Soil moisture	Gravimetric method, after heating the samples at 105 ^oC for 24 h (Black 1965)

2.3 Vegetation

Coenological data were collected in 25 m^2 quadrats with three repeats in all plots (*Figure 2*). Diversity profiles were used to compare the herb layers of the different habitats, calculated with PAST software. PAST uses the exponential of the so-called Renyi index, including the number of species, Shannon diversity, quadratic diversity, and Berger-Parker diversity. The value of the index depends upon the parameter "alpha". The diversity of the studied communities can be ranked in a partial order with this method (Tóthmérész 2013).

The social behaviour type (SBT) categories are derived from the CSR plant functional system (Grime 1979), adapted to the Pannonian flora by Borhidi (1995). The category of each

plant species was determined based on the role the plant species plays in the communities. The naturalness of the species as well as how it linked to the habitat were also considered. The number and proportion of categories represented in a habitat provide information about the stability, the level of disturbance, or the deviation from the natural state of the community. The specialists (S), competitors (C), generalists (G), and natural pioneers (NP) – with naturalness values of +6, +5, +4, and +3, respectively – are all characteristic to natural habitats. Disturbance tolerants (DT) and weeds (W) appear in disturbed, secondary, and artificial habitats, but still have a positive (2 and 1) naturalness value. Introduced alien species (I), adventives (A), ruderal competitors (RC), and aggressive alien species (AC) represent the most unfavorable categories with negative values: -1, -1, -2 and -3, respectively. The classification of each species was obtained from the Hungarian Flora Database (Horváth et al. 1995). The proportion of species belonging to the different categories in a habitat is displayed with stacked column charts, where the total species number of the examined habitat and the distribution of the species numbers by the SBT categories can be examined simultaneously. (In the case of a small number of species, the SBT categories are not given in the database, which results in a difference between the SBT total number of species and the total number in diversity analysis).

RDA was chosen to analyse the relationship between species composition environmental descriptors observed at the same locations. The species abundance matrix was transformed with the Hellinger method. Hellinger transformation is recommended as a basis for ordination as permits the exploration of the relationships of species to explanatory variables (Legendre – Gallagher 2001). The environmental factors included in the analysis were the impact of measured soil parameters (Table 2), the cover of the different tree species, exposure, and the presence or absence of an earth road separating the examined plot from the cultivated area.

2.4 Soil mesofauna

One hundred cubic centimetres of soil samples were collected with a cylindrical soil core sampler in each coenological quadrat. The microarthropods were extracted with Berlese-Tullgren funnels to 96% ethanol for two weeks. The specimens were classified into major taxonomic groups, while Collembola individuals were determined to the species level. Collembolan diversity was measured with the same method used for herbaceous diversity.

QBS-ar index was employed to evaluate the soil's biological quality (Parisi 2001, Menta et al. 2017). Based on their adaptation to the soil environment, microarthropods are classified into different morphotypes, and characterized with an ecomorphological (EMI) value. The sum of the obtained EMI scores gives the QBS-ar index of the examined sample (Annex IV).

Redundancy analysis was applied to assess the impact of environmental factors on collembolan species composition, with the same method used for herbaceous plants.

3 RESULTS AND DISCUSSION

3.1 Soil habitat condition

The soil parameters (*Table 2*) show that all of the plots have a neutral to slightly alkaline pH. The texture of the soils is sandy-silty with a low carbonate content. Cultivated plots have the lowest SOM value and, at the same time, the highest phosphorus and potassium content due to fertilization.

3.2 Woody vegetation

The non-native tree stand (ROBINIA) is dominated by black locust (*Robinia pseudoacacia*) and green ash (*Fraxinus pennsylvanica*) in the canopy layer. The shrub layer is poor in species; *Ligustrum vulgare, Elaeagnus angustifolia,* and *Maclura pomifera* can be found with low cover. The native shelterbelt (ACER) is composed of native tree species, where field maple (*Acer campestre*), field elm (*Ulmus minor*), Norway maple (*Acer platanoides*) and Turkey oak (*Quercus cerris*) form the canopy layer. The shrub layer is weak, similar to the non-native stand; besides *Ligustrum vulgare*, only *Sambucus nigra* and *Prunus spinosa* appear. The cover values of the canopy and shrub layers in the shelterbelts can be found in *Table 3.*

Table 2. Measured values of the soil parameters

	Plot	pH (H_2O)	$CaCO_3$ (%)	SOM	$NH_4^+ + NO_3^-$ N (mg/kg)	AL P (mg P_2O_5/kg)	AL K (mg K_2O/kg)	A%	I%	FH%	DH%	Moist
ROBINIA	CULT	7.76	3.28	0.90	7.10	542.00	614.67	29.33	23.00	43.33	4.33	15.87
	EDGE	7.46	5.51	1.57	8.80	413.67	541.00	27.33	18.00	47.00	7.67	13.73
	SHELT	7.43	3.33	2.10	9.70	125.33	615.67	25.33	23.00	48.00	3.67	13.67
	EDGE	7.42	4.96	1.77	8.43	449.67	523.00	27.67	17.00	48.00	7.33	13.04
	CULT	7.71	2.52	0.87	7.27	561.33	688.00	30.00	22.67	41.67	5.67	14.46
ACER	CULT	7.51	1.63	0.93	6.63	584.67	770.00	31.33	26.33	38.00	4.67	12.13
	EDGE	7.50	7.20	1.67	8.57	314.33	434.00	29.33	19.67	42.33	8.67	11.42
	SHELT	7.51	5.99	1.97	10.07	133.67	513.67	23.33	22.67	43.00	10.67	10.76
	EDGE	7.52	7.08	1.67	8.13	369.67	463.00	29.33	20.33	42.33	8.00	12.70
	CULT	7.49	2.37	0.97	7.17	537.33	735.33	32.00	26.33	36.67	5.00	12.50

Table 3. Cover values of the canopy (A) and shrub (B) layers in the shelterbelts

Layer	Cover (%) of layer		Species	Cover (%) of species	
	ROBINIA	ACER		ROBINIA	ACER
A (10-15 m)	80%	80%	*Robinia pseudoacacia*	60	
			Fraxinus pennsylvanica	20	
			Acer platanoides	5	
			Maclura pomifera	5	
			Gleditsia triacanthos	5	
			Acer campestre		50
			Ulmus minor		10
			Acer platanoides		10
			Quercus cerris		10
B	40%	20%	*Ligustrum vulgare*	20	20
			Sambucus nigra		10
			Prunus spinosa		10
			Elaeagnus angustifolia	10	
			Maclura pomifera	5	

3.3 Herbaceous diversity

In total, 50 herbaceous species appeared in the examined quadrats. Only 14 of these were present inside the shelterbelts, while 44 species were found in the grassy edges (Annex II).

In both non-native (ROBINIA) and native (ACER) shelterbelts, the herbaceous diversity of the woody habitat (SHELT) is lower than that of grassy edges (EDGE). Both shelterbelts are very poor in species. This is similar to the results of Carlier – Moran (2019), who found

the herbaceous vegetation of hedgerows very poor in species. The cultivated areas adjacent to ROBINIA were almost totally weed-free in all of the three periods (*Figure 3*). This may indicate a more intensive weed management activity in the surroundings of this shelterbelt and can explain the lower diversity of the edges and field margins compared to ACER.

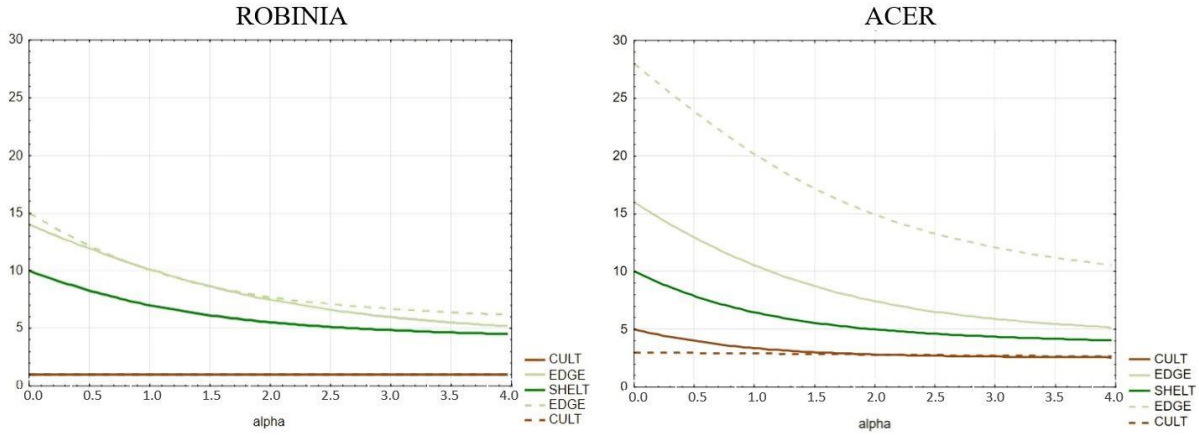

Figure 3. The diversity profiles of the herbaceous vegetation in the shelterbelts and adjacent habitats

The non-woody field margins, grassy edges, and roadside habitats contribute significantly more to the weed diversity of the landscape than shelterbelts do. Romero et al. (2008) also reflected the significance of field margins in enhancing the diversity of the agricultural land, especially in the case of organic farming. Besides increasing weed diversity, Fried et al. (2009) found that field margins act as a refuge for agricultural weed species. A similar phenomenon was experienced at our test site, where numerous segetal weed species were found in the grassy edges, but none of these appeared inside the shelterbelts. Typically forest-related species were not found in the shelterbelts either, which can be explained by the effect of fragmentation and by the fact that most of the forest-related herbaceous species colonise the newly planted woodlands very slowly (Wilson 2019). On the other hand, the agricultural weeds are adapted to open habitats and extensive cultivation (Pinke – Pál 2005). Thus, the conditions in the core of a shelterbelt are not appropriate for these species. This results in lower diversity in the shelterbelts than in the adjacent open habitats.

The herbaceous layer of black locust forests is typically poor in species due to the allelopathic effect of this tree species (Ferus et al. 2019), which causes the homogenization of the plant forest biota (Benesperi et al. 2012). This phenomenon is not evident in the case of the examined shelterbelts. Morrison – Flores (2013) found a significant difference regarding diversity and species composition in the understorey layer for native windbreaks; the appearance of invasive herbaceous species was higher in non-native shelterbelts. This survey was not limited to herbaceous species, but included tree seedlings as well. This method naturally results in a more favourable species construction of the native tree plantations.

3.4 Soil microarthropods

Fifty-five Collembola species were found in the examined soil samples. Four of these appeared only in the native shelterbelts, four in the non-native shelterbelts, and 18 only in non-woody habitats. Six of the species were found only in the grassy edges of the shelterbelts, and three were uncial to cultivated plots (Annex III). According to collembolan diversity, the native shelterbelt (ACER) exhibits slightly better conditions than the non-native belt (ROBINIA). The cultivated plots (CULT) are very poor in species, but the grassy edges of the shelterbelts are quite diverse in most cases (*Figure 4*).

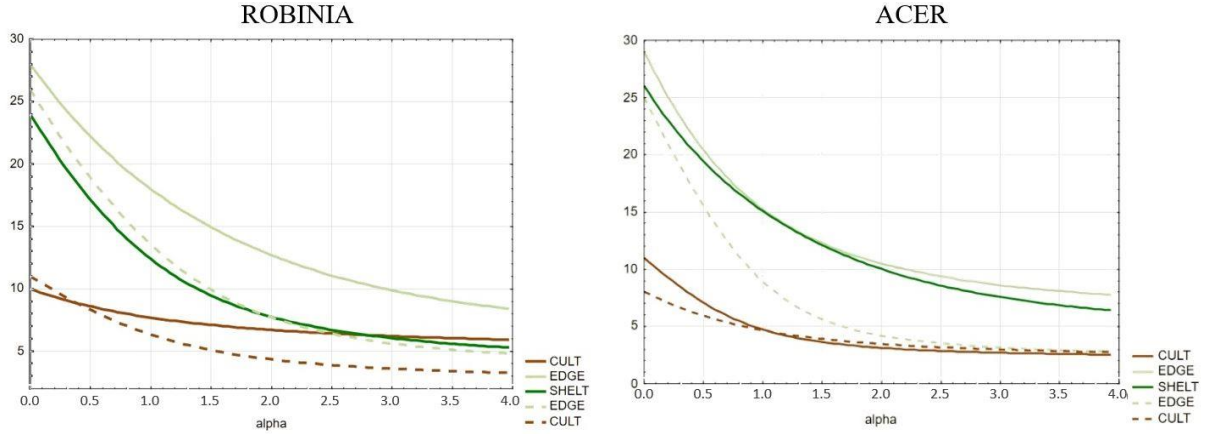

Figure 4. The diversity profiles of springtails (Collembola) in the shelterbelts and adjacent habitats

The grassy edges of shelterbelts are at least as favourable a habitat for Collembola communities as the core of the shelterbelts are, which is similar to the results of herbaceous diversity examinations. Just a few forest-related Collembola species appeared in the soil of the shelterbelts. The reason for this phenomenon is the lack of forest habitats in the landscape and, similar to forest-related herb species, the weak dispersal ability of euedaphic Collembola species (Auclerc et al. 2009). The majority of the Collembola species are pioneers in both native and non-native shelterbelts, which coincides with the results of Olejniczak (2007). In terms of species richness and diversity, the maple shelterbelt is in a slightly more favourable condition than the black locust stand. Lazzaro et al. (2018) reported that this phenomenon is more significant in forest stands; the study found a remarkable decrease in hemiedaphic and euedaphic microarthropod groups, such as Protura, Acarina, Collembola, Diplopoda, Coleoptera, and Thysanoptera in black locust forests, which also can be explained with the allelopathic effect of black locust. Secondary metabolites (e.g., toxalbumins, robin) produced and released by black locust (Hui et al. 2004) often limit the diversity and abundance of microarthropods (Nasiri et al. 2005, Litt et al. 2014). Overall, both shelterbelt types play an essential role in collembolan diversity in agricultural landscapes. Several studies highlight the impact of tree rows in the migration of springtails from woody habitats to cultivated fields (Alvarez et al. 2000, Olejniczak 2007), which positively affects organic degradation and nutrient recycling processes (Menta 2012).

3.5 Qualitative parameters

The majority of the herbaceous plants appearing in the environment of the examined shelterbelts are disturbance tolerant (DT) and weed (W) species, such as *Arrhenatherum elatius, Veronica arvensis*, *Lolium perenne, Galium aparine,* or *Lamium purpureum.* The specialist (S) and natural competitor (C) categories are totally absent, while ruderal competitors (RC), like *Amaranthus retroflexus, Bromus sterilis,* and *Convulvulus arvensis* appear in all examined plots. The cultivated fields are extremely poor in herbaceous species due to weed management. The only generalist appearing in the maple shelterbelt is *Symphytum officinale,* while in the grassy edges, this category is represented by two species: *Poa pratensis* and *Thymus glabra*. Segetal weed species *Consolida regalis, Fumaria vaillantii,* and *Viola arvensis* appeared only in the grassy edges.

Regarding microarthropods, 20 taxa were present in the examined soil samples, of which Collembola and Acari are the most abundant groups. Both the biological quality of soil (QBS-ar index) and the distribution of herbaceous plant species by social behaviour type (SBT)

categories reveal the importance of shelterbelts and grassy edges in agroforestry as these habitats increase soil-related diversity in the agricultural land (*Figure 5*).

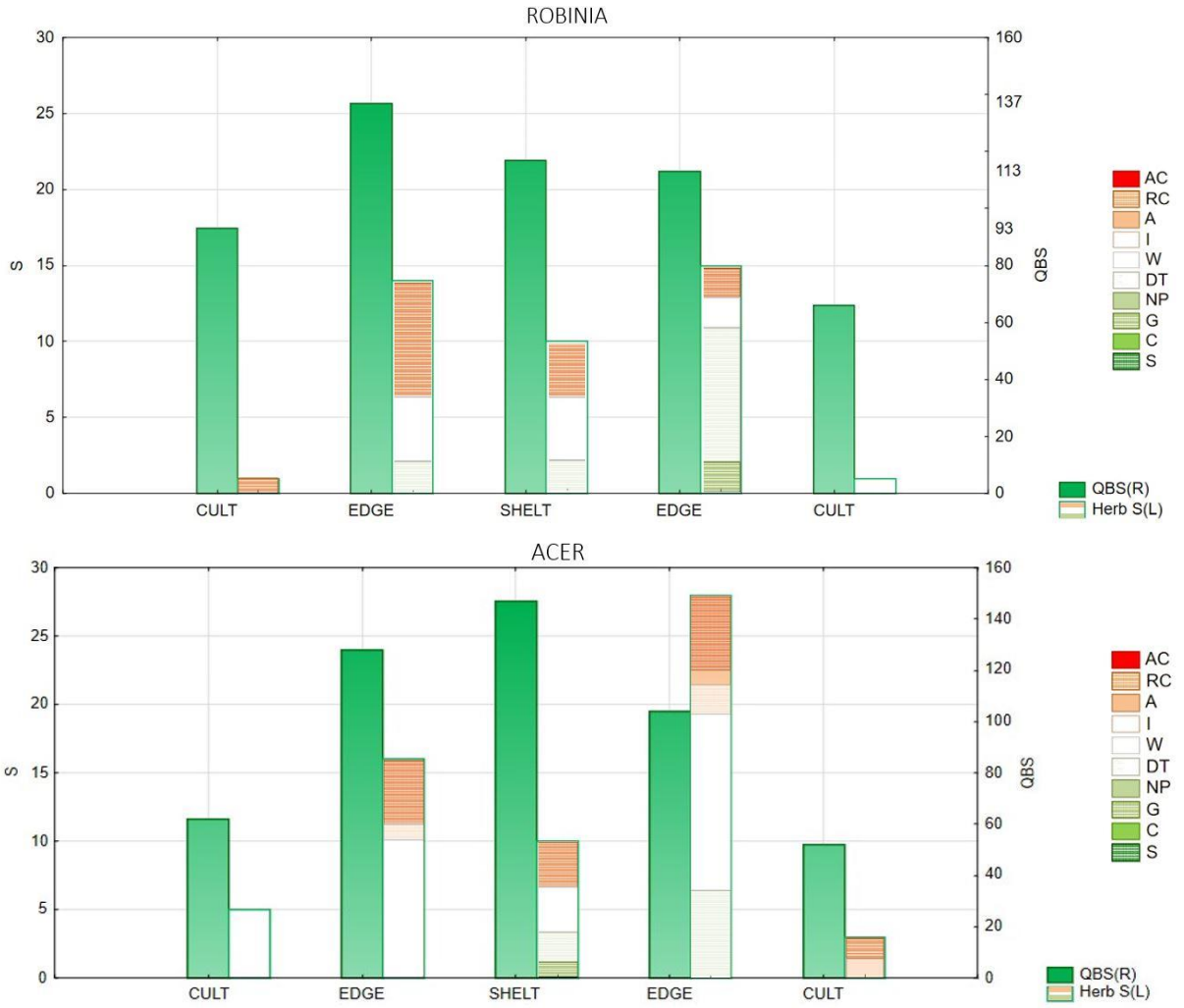

Figure 5. QBS-ar index and the distribution of herbaceous species by SBT categories in the non-native (ROBINIA) and native (ACER) shelterbelts and adjacent habitats

The qualitative traits of herbaceous and microarthropod communities show slightly more favourable conditions in the native shelterbelt. The QBS-ar index of the maple shelterbelt is the highest among the examined plots, while in some cases, this value is higher in the grassy edges than in the black locust belt. The number of ruderal competitor (RC) herbaceous species is similar in the different plots, but the number of native weeds is significantly higher in the edges than it is in the shelterbelts or cultivated fields.

3.6 Species composition

Among soil parameters, $CaCO_3$ and pH are inversely correlating and determining factors for both communities (*Figure 6*). However, in the case of vegetation, this relation should be indirect, as the differences in the values are negligible. In practice, this linkage can result from differences in the level of disturbance, which cannot be measured and added to the analysis as a determining factor. The grassy vegetation and the presence of an earth road between the crop field and the edge are also important features. Black locust strongly affects the

collembolan community, contrary to the herbaceous species composition, which is not determined by the tree species primarily.

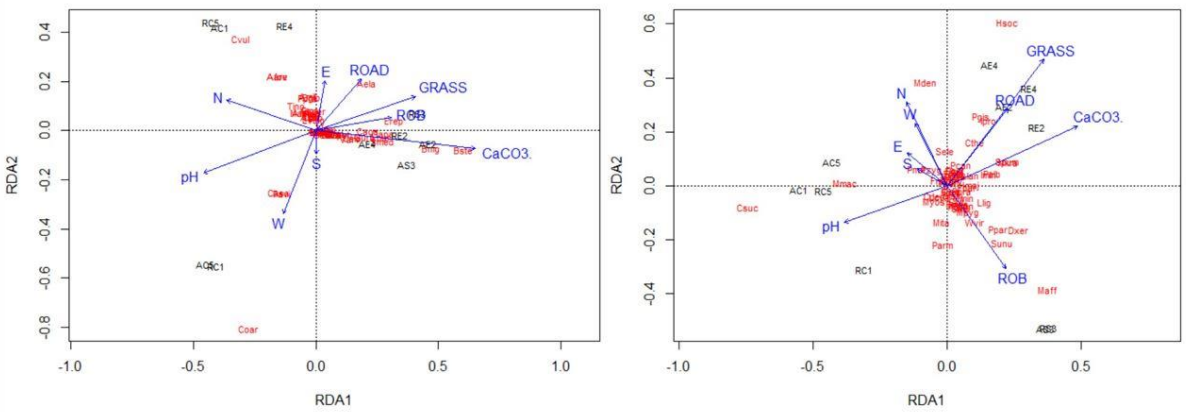

Figure 6. Redundancy analysis of the herbaceous (left) and collembolan (right) communities. Abbreviations: pH: soil pH; $CaCO_3$: calcium carbonate content of the soil; N, E, W: northern, western and eastern exposure; ROAD: an earth road separating the shelterbelt edges from crop field; GRASS: the vegetation cover is grass, ROB: the cover value of black locust.

Several studies confirm the positive correlation between herbaceous and Collembola communities (Salamon et al. 2004, Eisenhauer et al. 2011, Perez et al. 2013). The impact of the presence of an earth road between the cultivated field and the edge on the edge flora is confirmed by Sutyinszki et al. (2013), who found that line facilities mitigate the negative effects coming from cultivated fields and, thereby, support the formation of a more diverse edge flora. The sensitivity of Collembola species to herbicides (Frampton et al. 2006) explains that the presence of an earth road determines collembolan species composition. The majority of the herbaceous plants appearing in the environment of the examined shelterbelts are disturbance tolerant (DT) and weed (W) species, such as *Arrhenatherum elatius, Veronica arvensis.*

4 CONCLUSIONS

The results showed that the herbaceous flora of shelterbelts planted in agricultural areas is weak, and forest-related herbaceous species do not appear in such tree stands. Despite the allelopathic and nitrogen-fixing effect of black locust, which can lead to habitat transformations, the herbaceous layer is similar to that of the native shelterbelts. The cause of the species-poor herbaceous vegetation in shelterbelts is complex. The main factors are fragmentation, the negative effects of the agricultural surroundings, and the lack of immediate connections to former semi-natural habitats. In addition, the drying climate and the increased game population may contribute to the degradation of the herbaceous flora. The role of non-woody habitats in preserving the agricultural weed flora is higher than that of the shelterbelts. The herbaceous diversity of an agroforestry system can be increased with grassy edges, where a species-rich, even segetal weed community can develop. However, some forest-related Collembola species appeared in the shelterbelts, and the grassy edges are also important habitats for soil mesofauna. The choice of tree species has a greater impact on microarthropods than on herbaceous plants. Overall, chemical-free, extensively mowed grassy strips can contribute significantly to the diversity of the soil-related communities of an agroforestry system.

Acknowledgements: The project was supported by the EFOP-3.6.2-16-2017-00018 in University of Sopron project.

REFERENCES

ALVAREZ, T. – FRAMPTON, G.K. – GOULSON, D. (2000): The role of hedgerows in the recolonization of arable fields by epigeal Collembola. Pedobiologia 44: 516–526. https://doi.org/10.1078/S0031-4056(04)70068-2

AUCLERC, A. – PONGE, J-F. – BAROT, S. – DUBS, F. (2009): Experimental assessment of habitat preference and dispersal ability of soil springtails. Soil Biology and Biochemistry 41 (8): 1596–1604. https://doi.org/10.1016/j.soilbio.2009.04.017

BALL, B.C. – HARGREAVES, P.R. – WATSON, C.A. (2018): A framework of connections between soil and people can help improve sustainability of the food system and soil functions. Ambio 47: 269–283. https://doi.org/10.1007/s13280-017-0965-z

BENESPERI, R. – GIULIANI, C. – ZANETTI, S. – GENNAI, M. – LIPPI, M.M. – GUIDI, T. – NASCIMBENE, J. – FOGGI, B. (2012): Forest plant diversity is threatened by *Robinia pseudoacacia* L. (Black locust) invasion. Biodiversity and Conservation 21 (14): 3555–3568. http://doi.org/10.1007/s10531-012-0380-5.

BERKI, I. (2020): A Mosoni-sík természetföldrajzi tényezőinek összhatása [The combined effect of the natural geographical factors of the Moson plain]. *In*. FÜHRER, E. (ed): Magyarország erdészeti tájai III. Kisalföld Erdészeti Tájcsoport. Kézirat (in Hungarian)

BLACK, C.A. (1965): Methods of Soil Analysis: Part I Physical and mineralogical properties. American Society of Agronomy, Madison, Wisconsin, USA.

BORHIDI, A. (1995): Social behaviour types, the naturalness and relative ecological indicator values of the higher plants in the Hungarian flora. Acta Botanica Hungarica 39: 97–181.

BUCKINGHAM, DL. – BENTLEY, S. – DODD, S. – PEACH, W.J. (2011): Seeded ryegrass swards allow granivorous birds to winter in agriculturally improved grassland landscapes. Agriculture, Ecosystems and Environment 142 (3–4): 256–265. https://doi.org/10.1016/j.agee.2011.05.017

BUZÁS, I. (ed). (1988): Soil- and agrochemical methods manual. Part 2. Mezőgazdasági Kiadó, Budapest. (in Hungarian)

CARLIER, J. – MORAN, J. (2019): Hedgerow typology and condition analysis to inform greenway design in rural landscapes. Journal of Environmental Management 247: 790–803. https://doi.org/10.1016/j.jenvman.2019.06.116

CHERUBIN, M.R. – CHAVARRO-BERMEO, J.P. – SILVA-OLAYA, A.M. (2019): Agroforestry systems improve soil physical quality in northwestern Colombian Amazon. Agroforestry Systems 93: 1741–1753 https://doi.org/10.1007/s10457-018-0282-y

DAMSCHEN, E.I. – HADDAD, N.M. – ORROCK, J.L. – TEWKSBURY, J.J. – LEVEY, D.J. (2006): Corridors Increase Plant Species Richness at Large Scales. Science 313: 1284–1286. https://doi.org/10.1126/science.1130098

DAMSCHEN, E.I. (2013) Lanscape corridors. In: LEVIN, S.A.: Encyclopedia of Biodiversity 467–475. Academic Press https://doi.org/10.1016/B978-0-12-384719-5.00385-3

EISENHAUER, N. – YEE, K. – JOHNSON, E.A. – MARAUN, M. – PARKONSON, D. – STRAUBE, D. – SCHEU, S. (2011): Positive relationship between herbaceous layer diversity and the performance of soil biota in a temperate forest. Soil Biology and Biochemistry 43: 462–465. https://doi.org/10.1016/j.soilbio.2010.10.018

ELAGIB, N.A. – AL-SAIDI, M. (2020): Balancing the benefits from the water–energy–land–food nexus through agroforestry in the Sahel. Science of the Total Environment 742: 140509. https://doi.org/10.1016/j.scitotenv.2020.140509

ERDÉLYI, M. – RÓNAI, A. – SOMOGYI, S. (1975): A Győri-medence felszín alatti vizei [Groundwater of the Győr basin]. *In*: ÁDÁM, L.– MAROSI, S (eds): Magyarország tájföldrajza 3. A Kisalföld és a Nyugat-magyarországi-peremvidék. p. 605 (in Hungarian)

FELICIANO, D. – LEDO, A. – HILLIER, J. – NAYAK, D.R. (2018): Which agroforestry options give the greatest soil and above ground carbon benefits in different world regions? Agriculture, Ecosystems and Environment 254: 117–129. https://doi.org/10.1016/j.agee.2017.11.032

FERUS, P. – BOSIAKOVA, D. – KONOPKOVA, J. – HOTKA, P. – KÓSA, G. – MELNYKOVA, N. – KOTS, S. (2019): Allelopathic interactions of invasive black locust (*Robinia pseudoacacia* L.) with secondary aliens: the physiological background. Acta Physiologiae Plantarum 41: 182. https://doi.org/10.1007/s11738-019-2974-y

FRAMPTON, G. K. – JÄNSCH, S –, SCOTT-FORDSMAND, J. J. – RÖMBKE, J. – VAN DEN BRINK, P. J. (2006): Effects of pesticides on soil invertebrates in laboratory studies: a review and analysis using species sensitivity distributions. Environmental Toxicology and Chemistry 25 (9): 2480. https://doi.org/10.1897/05-438R.1

FRIED, G. – PETIT, S. – DESSAINT, F. – REBOUD, X. (2009): Arable weed decline in Northern France: Crop edges as refugia for weed conservation? Biological Conservation 142 (1): 238–243. https://doi.org/10.1016/j.biocon.2008.09.029

GRIME, J.P. (1979): Plant Strategies, Vegetation Processes, and Ecosystem Properties. Wiley, New York.

HENEGHAN, L. – BOLGER, T. (1998): Soil microarthropod contribution to forest ecosystem processes: the importance of observational scale. Plant and Soil 205 (2): 113–124. https://doi.org/10.1023/A:1004374912571

HORVÁTH, F. – DOBOLYI, K. – MORSCHAUER, T. – LŐKÖS, L. – KARAS, L. – SZERDAHELYI, T. (1995): Flóra adatbázis [Flora database]. MTA ÖBKI, Vácrátót. (in Hungarian)

HOUBA, V.J.G. – NOVOZAMSKY, I. – HUIJBREGTS, A.W.M. – LEE VAN DER, J.J. (1986): Comparison of soil extractions by 0.01 $CaCl_2$ by EUF and by some conventional extraction procedures. Plant and Soil 96: 433–437. https://doi.org/10.1007/BF02375149

HUI, A. MARRAFFA, J.M. STORK, C.M. (2004): A rare ingestion of the Black Locust tree. Journal of Toxicology: Clinical Toxicology 42: 93–95. https://doi.org/10.1081/CLT-120028752

JÁNOSKA, F. (2012): A mezővédő erdősávok és erdőfoltok jellemzése [Characterization of shelterbelts and forest patches]. In: FARAGÓ, S. (szerk.): A Lajta Project: Egy tartamos mezei vad és ökoszisztéma vizsgálat 20 éve. [The Lajta Project: 20 years of a long-term field wildlife and ecosystem study], Nyugat-magyarországi Egyetem Kiadó, Sopron. pp.: 159–160. (in Hungarian)

JEZEER, R.E – SANTOS, M.J. – VERWEIJA, P.A. – BOOT, R.G.A. – COUGH, Y. (2019): Benefits for multiple ecosystem services in Peruvian coffee agroforestry systems without reducing yield. Ecosystem Services 40: 101033. https://doi.org/10.1016/j.ecoser.2019.101033

KIRÁLY, A. – KIRÁLY, G. (2012): A gyomnövény közösségek szerkezete [The structure of weed communities]. In: FARAGÓ, S. (szerk.): A Lajta Project: Egy tartamos mezei vad és ökoszisztéma vizsgálat 20 éve. [The Lajta Project: 20 years of a long-term field wildlife and ecosystem study] Nyugat-magyarországi Egyetem Kiadó, Sopron. pp.: 134–159. (in Hungarian)

KRÄHMER, H. – ANDREASEN, C. – ECONOMOU-ANTONAKA, G. – HOLEC, J., KALIVAS, D. – KOLÁŘOVÁ, M. – NOVÁK, R. – PANOZZO, S. – PINKE, G. – SALONEN, J. – SATTIN, M. – STEFANIC, E. – VANAGA, I. – FRIED, G. (2019): Weed surveys and weed mapping in Europe: State of the art and future tasks. Crop Protection 129: 105010. https://doi.org/10.1016/j.cropro.2019.105010.

LAZZARO, L. – MAZZA, G. – D'ERRICO, G. – FABIANI, A. – GIULIANI, C. – INGHILESI, A. F. – LAGOMARSINO, A. – LANDI, S. – LASTRUCCI, L. – PASTORELLI, R. – ROVERSI, P. F. – TORRINI, G. – TRICARIO, E. – FOGGI, B. (2018): How ecosystems change following invasion by *Robinia pseudoacacia*: Insights from soil chemical properties and soil microbial, nematode, microarthropod and plant communities. Science of the Total Environment 622–623: 1509–1518. https://doi.org/10.1016/j.scitotenv.2017.10.017

LEGENDRE, P. – GALLAGHER, E.D. (2001): Ecologically meaningful transformations for ordination of species data. Oecologia 129: 271–280. https://doi.org/10.1007/s004420100716

LITT, A.R. – CORD, E.E. – FULBRIGHT, T.E. – SCHUSTER, G.L. (2014): Effects of invasive plants on arthropods. Conservation Biology 28: 1532–1549. https://doi.org/10.1111/cobi.12350

MARSHALL, E.J.P. (1989): Distribution patterns of plants associated with arable field edges. Journal of Applied Ecology 26: 247–257. https://doi.org/10.2307/2403665

MARSHALL, E.J.P. – ARNOLD, G.M. (1995): Factors affecting field weed and field margin flora on a farm in Essex, UK. Landscape and Urban Planning 31 (1–3): 205–216. https://doi.org/10.1016/0169-2046(94)01047-C

MARSHALL, E.J.P. – MOONEN, A.C. (2002): Field margins in northern Europe: their functions and interactions with agriculture. Agriculture Ecosystems and Environment 89: 5–21. https://doi.org/10.1016/S0167-8809(01)00315-2

MARSHALL, E.J.P. – BROWN, V.K. – BOATMAN, N.D – LUTMAN, P.J.W. – SQUIRE, G.R. – WARD, L.K. (2003): The role of weeds in supporting biological diversity within crop fields. Weed Research 43: 77–89 https://doi.org/10.1046/j.1365-3180.2003.00326.x

MENTA, C (2012): Soil Fauna Diversity - Function, Soil Degradation, Biological Indices, Soil Restoration. In: LAMEED, G.A.: Biodiversity Conservation and Utilization in a Diverse World. IntechOpen https://doi.org/10.5772/51091

MIKLAY, F. MOLNÁR, L. (1968): A Mosoni-síkság talajviszonyai [Soil conditions in the Mosoni plain]. Agrokémia és Talajtan 17: 495–506. (in Hungarian)

MORRIS, R.J. – LEWIS, O.T. – GODFRAY, H.C.J. (2004): Experimental evidence for apparent competition in a tropical forest food web. Nature 428: 310–313. https://doi.org/10.1038/nature02394

MORRISON, B.M.L – FLORES S.A. (2013): Promoting biodiversity in agricultural landscapes: native windbreaks support greater understory plant diversity in Monteverde, Costa Rica. Journal of Young Investigators 25 (10). https://www.jyi.org/2013-october/2017/6/25/native-windbreaks-support-greater-understory-plant-diversity-in-monteverde-costa-rica

NAGY, K. – LENGYEL, A. – KOVÁCS, A. – TÜREI, D. – CSERGŐS, A.M. – PINKE GY. (2017): Weed species composition of small-scale farmlandsbears a strong crop-related and environmental signature. Weed Research 58 (1): 46–56. https://doi.org/10.1111/wre.12281

NASIRI, H. – IQBAL, Z. – HIRADATE, S. – FUJII, Y. (2005): Allelopathic potential of *Robinia pseudoacacia* L. Journal of Chemical Ecology 31: 2179–2192. https://doi.org/10.1007/s10886-005-6084-5

OLEJNICZAK, I. (2004): Communities of soil microarthropods with special reference to Collembola in midfield shelterbelts. Polish Journal of Ecology 52 (2): 123–133.

OLEJNICZAK, I. (2007): Soil mesofauna (Acarina and Collembola) along transects crossed shelterbelts of different age and adjacent fields. Polish Journal of Ecology 55 (4): 637–646.

PANSU, M. – GAUTHEYROU, J. (2007). Handbook of Soil Analysis: Mineralogical, Organic and Inorganic Methods. Springer Science and Business Media: Berlin, Heidelberg, The Netherlands.

PARISI, V. (2001): La qualità biologica del suolo. Un metodo basato sui microatropodi. Acta Naturalia de "L'Ateneo Parmense" 37 (3/4): 105–114.

PÉCSI, M. (1975): A Győri-medence felszínének kialakulása és domborzata [Formation and topography of the surface of the Győr basin]. *In*: ÁDÁM, L. – MAROSI, S. (Eds): Magyarország tájföldrajza 3. A Kisalföld és a Nyugat-magyarországi-peremvidék. p. 605 (in Hungarian)

PÉCZELI, Gy. (1975): A Sopron – Vasi-síkság éghajlata [The climate of the Sopron - Vas plain]. In: ÁDÁM, L. – MAROSI, S. (eds): Magyarország tájföldrajza 3.: A Kisalföld és a Nyugat-magyarországi-peremvidék. p. 605 (in Hungarian)

PEREZ, G. – DECAËNS, T. – DUJARDIN, G. – AKPA-VINCESLAS, M. – LANGLOIS, E. – CHAUVAT, M. (2013): Response of collembolan assemblages to plant species successional gradient. Pedobiologia 56 (4–6): 169–177. https://doi.org/10.1016/j.pedobi.2013.04.001

PINKE, G. – KARÁCSONY, P. – CZÚCZ, B. – BOTTA-DUKÁT, Z. – LENGYEL, A. (2012): The influence of environment, management and site context on species composition of summer arable weed vegetation in Hungary. Applied Vegetation Science 15: 136–144. https://doi.org/10.1111/j.1654-109X.2011.01158.x

PINKE, GY. – PÁL, R. (2005): Gyomnövényeink eredete, termőhelye és védelme. Alexandra Kiadó, Pécs, 231 p. (in Hungarian)

ROMERO, A. – CHAMORRO, L. – SANS, F. X. (2008): Weed diversity in crop edges and inner fields of organic and conventional dryland winter cereal crops in NE Spain. Agriculture, Ecosystems and Environment 124: 97–104. https://doi.org/10.1016/j.agee.2007.08.002

SALAMON, J.A. – SCAEFER, M. – ALPHEI, J. – SCHMID, B. – SCHEU, S. (2004): Effects of Plant Diversity on Collembola in an Experimental Grassland Ecosystem. Oikos 106 (1): 51–60.

SCHONROGGE, K. – STONE, G.N. – CRAWLEY, M.J. (1996): Alien herbivores and native parasitoids: rapid developments and structure of the parasitoid and inquiline complex in an invading gall wasp Andricus quercuscalicis (Hymenoptera: Cynipidae). Ecological Entomology 21: 71–80. https://doi.org/10.1111/j.1365-2311.1996.tb00268.x

SUTYINSZKI, ZS. – SZENTES, SZ. – KATONA, Z. – PUSZTA, E. – MARINKÁS, Á. – PENSZKA, K. (2013): Kondorosi mezsgyék növényzete és tájtörténete közötti összefüggések vizsgálata [Examination of the relations between the vegetation and landscape history of field margins in Kondoros]. Tájökológiai Lapok 11 (2): 379–388. (in Hungarian)

TAKÁCS, V. (2008): Útfásítások közlekedésbiztonsági vizsgálata a Sopron-Fertőd Kistérség területén. [Analysis of traffic safety of roadside afforestations in the Sopron-Fertőd region] Doctoral thesis, NyME, Sopron. (in Hungarian)

TÓTHMÉRÉSZ, B. (2013): Diversity. University of Debrecen.

TSCHORA, H. – CHERUBINI, F. (2020): Co-benefits and trade-offs of agroforestry for climate change mitigation and other sustainability goals in West Africa. Global Ecology and Conservation 22: e00919. https://doi.org/10.1016/j.gecco.2020.e00919

WILLIS, A.J. – MEMMOTT, J. (2005): The potential for indirect effects between a weed, one of its biocontrol agents and native herbivores: A food web approach. Biological Control 35: 299–306. https://doi.org/10.1016/j.biocontrol.2005.07.013

WILSON, P.J. (2019): Restoring pollinator communities and pollination services in hedgerows in intensively managed agricultural landscapes. *In*: The ecology of hedgerows and field margins. Dover, J.W. (ed.) Routledge, New York, USA. pp. 163–185.

APPENDIX

Annex I: GPS coordinates of the sampling plots

	ROBINIA	ACER
CULT	47.86473, 17.12453	47.86191, 17.19932
	47.86460, 17.12541	47.86250, 17.20066
	47.86444, 17.12718	47.86294, 17.20189
EDGE	47.86485, 17.12455	47.8621, 17.19919
	47.86473, 17.12541	47.86266, 17.20052
	47.86454, 17.12717	47.86313, 17.20165
SHELT	47.86501, 17.12457	47.86219, 17.19912
	47.86484, 17.1254	47.86277, 17.20043
	47.86467, 17.12718	47.86324, 17.20153
EDGE	47.86518, 17.12456	47.86229, 17.19904
	47.86503, 17.12538	47.86286, 17.20031
	47.86484, 17.12721	47.86332, 17.20145
CULT	47.86531, 17.12455	47.86248, 17.19887
	47.86519, 17.12537	47.86304, 17.20019
	47.86496, 17.12722	47.86352, 17.20121

Annex II: Herbaceous species list and cover (%)

Species	SBT	ROBINIA					ACER				
		CULT	EDGE	SHELT	EDGE	CULT	CULT	EDGE	SHELT	EDGE	CULT
Achillea millefolium	DT	0	0	0	20	0	0	0	0	0	0
Allium scorodoprasum subsp. scorodoprasum	DT	0	0	0	3	0	0	0	0	0	0
Amaranthus retroflexus	RC	0	7	0	0	0	0	0	0	5	0
Anagallis arvensis	W	0	0	0	0	0	17	0	0	3	0
Anagallis foemina	W	0	0	0	0	0	17	0	0	3	0
Arrhenatherum elatius	DT	0	13	33	30	0	0	0	0	3	0
Artemisia vulgaris	W	0	0	0	0	0	0	0	0	2	0
Avena fatua	W	0	0	0	0	0	2	0	0	0	0
Ballota nigra	W	0	7	13	0	0	0	27	30	27	0
Bromus sterilis	RC	0	13	33	0	0	0	50	40	17	0
Calamagrostis epigeios	RC	0	3	0	0	0	0	0	0	0	0
Cannabis sativa	A	0	0	0	0	0	0	0	0	3	3
Cardaria draba	W	0	0	0	0	0	0	2	0	8	0
Carduus acanthoides	W	0	7	8	0	0	0	12	0	0	0
Carex hirta	DT	0	0	0	3	0	0	0	0	0	0
Chenopodium album	RC	0	3	0	0	0	0	7	2	2	0
Chenopodium hybridum	W	0	0	0	0	0	0	10	0	7	0
Cirsium arvense	RC	0	3	0	0	0	0	0	0	0	0
Cirsium vulgare	W	0	0	0	0	3	0	0	0	0	0
Consolida regalis	W	0	0	0	0	0	0	0	0	3	0
Convolvulus arvensis	RC	5	7	2	0	0	0	3	7	7	5
Dactylis glomerata	DT	0	0	0	20	0	0	0	0	3	0
Elymus repens	RC	0	40	7	3	0	0	13	0	13	0
Euphorbia peplus	W	0	0	0	0	0	0	0	0	7	0
Falcaria vulgaris	W	0	0	0	0	0	0	2	0	0	0
Fumaria vaillantii	DT	0	0	0	0	0	0	0	0	5	0
Galium aparine	W	0	7	13	0	0	0	10	3	0	0
Geum urbanum	DT	0	0	0	2	0	0	7	17	17	0
Hypericum perforatum	DT	0	0	0	5	0	0	0	0	0	0
Lamium purpureum	W	0	15	5	0	0	0	7	7	0	0
Lathyrus tuberosus	W	0	0	0	0	0	0	0	0	2	0
Linaria vulgaris	W	0	0	0	2	0	0	0	0	0	0
Lolium perenne	DT	0	0	0	7	0	0	0	0	3	0
Medicago sativa	I	0	0	0	0	0	0	0	0	2	0
Mercurialis annua	W	0	0	0	0	0	2	0	0	0	0
Phacelia tanacetifolia	I	0	0	0	0	0	0	2	0	3	0
Plantago lanceolata	DT	0	0	0	5	0	0	0	0	0	0
Plantago major	W	0	0	0	7	0	0	0	0	0	0
Poa pratensis	G	0	0	0	17	0	0	0	0	0	0
Polygonum aviculare		0	0	0	0	0	0	0	0	7	3
Silene latifolia subsp. alba	W	0	0	0	0	0	0	3	0	5	0
Stellaria media		0	2	5	0	0	0	10	10	8	0
Symphytum officinale	G	0	0	0	0	0	0	0	2	0	0
Taraxacum officinale	RC	0	0	0	3	0	0	0	0	0	0
Thymus glabrescens	G	0	0	0	3	0	0	0	0	0	0
Tripleurospermum inodorum	W	0	0	0	0	0	3	0	0	0	0
Urtica dioica	DT	0	0	3	0	0	0	0	0	0	0
Veronica arvensis	DT	0	12	0	0	0	0	0	5	2	0
Veronica persica	W	0	0	0	0	0	0	10	0	3	0
Viola arvensis	W	0	0	0	0	0	0	0	0	2	0

Annex III: Collembola species list

Species	ROBINIA					ACER				
	CULT	EDGE	SHELT	EDGE	CULT	CULT	EDGE	SHELT	EDGE	CULT
Ceratophysella denticulata	0	0	0	0	0	2	0	2	0	0
Ceratophysella luteospina	0	0	7	0	0	0	0	0	0	0
Ceratophysella succinea	14	0	0	0	35	39	0	0	2	11
Hypogastrura socialis	0	54	0	92	4	2	29	0	104	0
Hypogastrura vernalis	0	0	0	0	0	0	3	0	0	0
Schoettella ununguiculata	0	14	47	0	0	0	0	17	0	0
Willemia virae	8	6	14	9	0	0	1	26	6	1
Friesea sp.	0	0	0	0	0	1	2	0	0	0
Deutonura conjuncta	0	0	6	0	0	0	1	2	0	0
Micranurida pygmaea	0	0	3	0	0	0	1	9	0	0
Pseudachorutes parvulus	0	4	28	1	0	0	2	19	0	0
Pseudachorutes pratensis	0	0	8	0	0	0	1	0	1	0
Superodontella lamellifera	0	0	0	0	0	0	0	2	0	0
Protaphorura armata	12	7	38	2	6	3	14	21	3	0
Protaphorura campata	0	0	12	0	0	0	0	0	0	0
Protaphorura cancellata	0	3	0	0	0	0	4	0	1	0
Protaphorura gisini	0	18	0	10	0	1	22	0	9	0
Doutnacia xerophyla	0	1	67	12	0	0	5	23	1	0
Mesaphorura critica	11	16	2	12	2	0	4	0	3	0
Mesaphorura italica	4	0	0	0	0	0	0	7	0	0
Mesaphorura krausbaueri	0	9	14	19	0	0	15	4	3	0
Mesaphorura macrochaeta	0	0	0	0	5	22	0	0	0	4
Mesaphorura yosii	3	0	0	0	0	0	0	0	0	0
Metaphorura affinis	0	11	126	9	0	0	0	87	0	0
Metaphorura denisi	0	12	5	39	2	3	52	0	21	26
Cryptopygus bipunctatus	0	0	0	0	0	0	0	12	0	0
Cryptopygus thermophilus	0	7	0	3	0	0	4	0	7	0
Folsomia manolachei	0	0	9	0	0	0	0	0	0	0
Folsomides parvulus	0	2	12	4	7	0	7	7	3	0
Isotomodes productus	0	11	0	14	0	0	14	0	8	0
Proisotoma minuta	0	0	0	0	0	0	0	8	0	0
Isotoma caerulea	0	2	0	0	0	0	2	0	0	0
Isotoma viridis	0	0	0	9	0	0	0	0	0	0
Parisotoma notabilis	7	17	12	11	19	3	53	27	21	9
Isotomiella minor	0	28	9	7	0	0	0	0	0	0
Entomobrya corticalis	0	0	1	0	0	0	0	0	0	0
Entomobrya multifasciata	0	4	0	6	0	0	0	2	0	2
Entomobrya quinqelineata	0	0	0	2	0	0	0	0	1	0
Orchesella cincta	1	3	4	1	3	0	1	2	3	0
Lepidocyrtus cyaneus	3	2	0	0	0	0	0	0	0	0
Lepidocyrtus lanuginosus	0	0	0	0	0	0	12	7	4	0
Lepidocyrtus cf. lignorum	0	0	6	0	0	0	7	19	5	0
Lepidocyrtus paradoxus	0	0	0	1	0	0	0	0	0	0
Heteromurus major	0	0	5	0	0	0	3	2	5	0
Tomocerus juv	0	0	0	0	0	0	0	1	0	0
Pseudosinella alba	0	18	13	8	0	2	11	8	3	0
Pseudosinella octopunctata	1	2	0	5	0	0	0	0	2	0
Pseudosinella petterseni	0	4	0	0	0	0	0	1	0	1
Pseudosinella zygophora	0	0	3	2	3	0	1	0	3	2
Cyphoderus albinus	0	1	0	3	0	0	0	0	0	0
Megalothorax minimus	0	0	0	0	0	0	4	9	0	0
Bourletiella arvalis	0	2	0	0	0	0	0	0	0	0
Sphaeridia pumilis	0	9	0	14	0	0	17	28	4	0
Sminthurinus elegans	0	7	0	6	1	2	2	0	2	0

Annex IV: calculation of QBS-ar index

Microarthropod taxa individuals	ROBINIA					*ACER*				
	CULT	EDGE	SHELT	EDGE	CULT	*CULT*	*EDGE*	*SHELT*	*EDGE*	*CULT*
ACARI	276	823	1128	530	214	329	643	1236	571	179
ARANEAE	1	3	2	1	0	0	3	4	2	0
CHILOPODA	0	1	2	0	0	0	0	1	0	0
COLEOPTERA	3	3	3	1	0	1	5	5	2	1
COLEOPTERA larvae	3	11	9	8	0	1	3	14	4	1
COLLEMBOLA	64	274	451	301	87	80	294	352	225	56
DIPLOPODA	0	2	0	0	0	0	0	1	0	0
DIPLURA	2	6	5	9	5	0	7	7	4	0
DIPTERA LARVAE	0	0	2	2	0	1	1	0	3	0
HEMIPTERA	0	0	0	1	0	0	0	0	2	0
HYMENOPTERA - ANTS	0	12	2	6	5	0	6	0	17	0
LARVA HYMENOPTERA	0	0	0	2	0	0	0	0	0	0
ISOPODA	0	0	0	0	0	0	0	0	0	0
LARVA LEPIDOPTERA	0	0	0	0	0	0	1	0	0	0
PAUROPODA	1	2	0	0	0	0	0	0	0	0
PROTURA	0	0	0	0	0	0	2	4	0	0
PSEUDOSCORPIONIDA	0	0	0	0	0	0	0	3	0	0
PSOCOPTERA	16	5	7	0	8	4	2	0	9	7
SYMPHYLA	0	5	3	2	0	0	6	7	2	0
THYSANOPTERA	0	2	7	2	0	0	1	3	4	0

Microarthropod taxa EMI scores	ROBINIA					*ACER*				
	CULT	EDGE	SHELT	EDGE	CULT	*CULT*	*EDGE*	*SHELT*	*EDGE*	*CULT*
ACARI	20	20	20	20	20	20	20	20	20	20
ARANEAE	1	5	5	1	0	0	5	1	5	0
CHILOPODA	0	10	10	0	0	0	0	10	0	0
COLEOPTERA	1	5	5	5	0	1	5	5	1	1
COLEOPTERA larvae	10	10	10	10	0	10	10	10	10	10
COLLEMBOLA	20	20	20	20	20	20	20	20	20	20
DIPLOPODA	0	10	0	0	0	0	0	10	0	0
DIPLURA	20	20	20	20	20	0	20	20	20	0
DIPTERA LARVAE	0	0	10	10	0	10	10	0	10	0
HEMIPTERA	0	0	0	1	0	0	0	0	1	0
HYMENOPTERA - ANTS	0	5	5	5	5	0	5	0	5	0
LARVA HYMENOPTERA	0	0	0	10	0	0	0	0	0	0
ISOPODA	0	0	0	0	0	0	0	0	0	0
LARVA LEPIDOPTERA	0	0	0	0	0	0	1	0	0	0
PAUROPODA	20	20	0	0	0	0	0	0	0	0
PROTURA	0	0	0	0	0	0	20	20	0	0
PSEUDOSCORPIONIDA	0	0	0	0	0	0	0	20	0	0
PSOCOPTERA	1	1	1	0	1	1	1	0	1	1
SYMPHYLA	0	10	10	10	0	0	10	10	10	0
THYSANOPTERA	0	1	1	1	0	0	1	1	1	0
QBS-ar	93	137	117	113	66	62	128	147	104	52

ACTA SILVATICA ET LIGNARIA HUNGARICA

Vol. 17, Nr. 2

Contents

ACTA SILVATICA ET LIGNARIA HUNGARICA

Vol. 17, Nr. 2

Tartalomjegyzék

https://doi.org/10.37045/aslh-2021-0006 *Acta Silv. Lign. Hung., Vol. 17, Nr. 2 (2021) 83–103*

Correspondence Between Vegetation Patterns and Soils in Wet and Wet-mesic Grasslands of Hanság and Tóköz (Hungary)

Győző HASZONITS* – Dávid HEILIG

Institute of Environmental Protection and Natural Conservation, University of Sopron, Sopron, Hungary

Abstract – Our research focused on the causes responsible for the fine mosaic pattern of plant associations on wet and wet-mesic meadows. The study area is located in the Little Hungarian Plain, including the former swamp basins of Hanság and Tóköz in Hungary. The vegetation survey data were evaluated by statistical methods (TWINSPAN method), and vegetation maps of the areas were prepared. Topsoil samples near the relevés were gathered for further laboratory tests. Soil profiles were opened by a Pürckhauer soil sampler for on-site description of the soil horizons and classification. Surface models provided a base for the preparation of contour maps that could be compared with the vegetation pattern. We found that of the two dominant vegetation types, mesotrophic wet meadows were associated with Mollic Gleysols, while non-tussock sedge beds were associated with Histic Gleysols. At the transitions of the two soil classes, the subgroup of non-tussock sedge beds is the dominant type. The soil class only determined the plant association on a habitat level, but it could not reason the fine pattern of the plant communities on the same soil class. Canonical correspondence analysis (CCA) was performed to investigate the relationship between the distribution of dominant species and soil parameters. Several soil parameters combined have a significant effect on the distribution of dominant species. In conclusion, we found that the formation of association types strongly depends on the soil characteristics of the area, and that it is closely related to it. However, in the formation of the fine mosaic pattern, the driving ecological factors are the microrelief and the length of the saturated or flooded soil conditions.

phytocoenology / soil factors / soil-plant relationships

Kivonat – Összefüggés a vegetációmintázat és talajok között nedves és üde-nedves gyeptársulásokon a Hanság és Tóköz területén (Magyarország). Kutatásunk a nedves rétek fitocönózisanak, finommozaikos mintázatáért felelős okok felderítésére irányult. A vizsgálatok a Kisalföld nagytájon, ezen belül a Tóközben és a Hanság egykori lápmedencéiben történtek, Magyarországon. A választott mintaterületeken cönológiai felméréseket végeztünk, melyek felvételi adatait statisztikai módszerekkel (TWINSPAN analízis) kiértékeltük. Elkészítettük a területek vegetációtérképeit. A kvadrátok közelében feltalajmintákat vettünk, melyeket laborvizsgálatoknak vetettünk alá, valamint Pürckhauer-féle szúróbotos mintavevő segítségével 1 méteres talajszelvényeket vettünk a talajtípusok helyszíni leírásához. Beszereztük a vizsgálati területek felületmodelljeit, melyekből szintvonalas térképeket generáltunk így a domborzati eltéréseket össze tudtuk vetni a növényzet mintázatával. Megállapítottuk, hogy a két meghatározó növényzettípus közül a mocsárrétek a típusos réti talajokhoz, míg a magassásrétek a lápos réti talajokhoz kötődnek. A két talajtípus átmenetein a magassásrétek alcsoportja a meghatározó típus. Kimutattuk, hogy a talajtípus csak

* Corresponding author: hasz.gjozo@gmail.com; H-9400 SOPRON, Bajcsy-Zs. u. 4, Hungary

élőhely szinten (láp-, magassás, mocsárrét) határozza meg a növényzetet, az asszociációk egymással kialakított finom mintázatáért nem felelős. Az azonos talajtípusokon kifejlődött eltérő növénytársulások hasonló képet mutattak, így a finom mintázat kialakulását nem magyarázzák. Kanonikus korrespondencia analízissel (CCA) kerestük a domináns fajok elterjedésének és a talajtani adottságoknak a kapcsolatát. Megállapítottuk, hogy a több tényező együttesen alakítja a fajok elterjedését. Összegezve, a társulástípusok kialakulása erősen függ a terület talajtani viszonyaitól, azzal szoros kapcsolatban áll. Azonban a finommozaikos mintázat kialakulásában a mikrodomborzat változatossága és az ezzel együtt járó vízborítottság különbség mértéke lehet a meghatározó ökológiai faktor.

fitocönológia / talajtulajdonságok / talaj-növény kapcsolatok

1 INTRODUCTION

The plant communities and soils of wet and wet-mesic grasslands formed water-rich environments (Scott et al. 1998). The saturated soil conditions and periodical flooding are important factors in these habitats. The common soil classes are Histosols (marsh soils) and Gleysols (meadow soils). In wet habitats, Histosols are formed as organic material accumulates, which is the result of persistent water saturation, anaerobic soil conditions, and the slowed decomposition of plant debris (Stefanovits et al. 2010). Wet to mesic habitats are affected by unsaturated soil conditions for shorter or longer periods of time, and flooding rarely occurs. The topsoil is well aerated under more mesic conditions, while wetter conditions lead to the accumulation of organic matter in the form of muck.

The distribution of species and their biomass production are highly determined by soils (Janssens et al. 1998, Duranel et al. 2007, Seabloom et al. 2021), but plants also affect the soils. Several studies aimed to answer whether this dynamic relationship could be detected between soil properties and vegetation diversity, but the relationship of soils and vegetation pattern is not explained completely (Scott et al. 1989, Ma et al. 2021).

The species composition of wet grassland plant associations is ruled by the nutrient contents, but pH, organic carbon content (TOC), and soil bulk density (BD) also play important roles (Bedforf et al. 1999). Extremely low BD (< 0.25 $g \cdot cm^{-3}$) signifies histic conditions where the nutrient levels are generally low while there is a vast amount of TOC. Higher BD informs us about the different porosity of the soil and about the different water regime. Low pH can indicate the limitation of nutrient uptake or toxic conditions, while slightly acidic or neutral values are seen under more aerated soil conditions (Ma et al. 2021). Along the changes of O_2 and redox gradients, Josselyn et al. (1990) and Pennington – Walters (2006) observed patterns in the composition of plant vegetation. Even soil microbial communities have a strong relation with soil conditions and vegetation characteristics (Li et al. 2021). Michener (1983) investigated catenas in the northeastern part of United States regarding the composition and diversity of plant associations. He discovered a close relationship between soil zonation and plant community patterns. Bartha et al. (1996) described the relationship of site parameters and plant associations in a meadow in Bozsok (Zsidó-rét). The geomorphology of the mesotrophic wet meadow involved in the research is diverse, and many associations are represented in the area accordingly. Bartha et al. (1996) found that the zonation of the vegetation closely followed the zonation of the habitat and of the soils. Rajkai (1978) reports on his research in the floodplain of the Szilas stream, in which he states that the water regime of the different soil classes is closely related to the species composition of the plant association developed on their surface. Microtopography was found to be an important organizing structure of vegetation pattern (Diamond et al. 2019). Diamond et al. (2020) even revealed a correlation between soil chemical properties and microtopography. These studies showed that plant associations and soil types, especially soil

chemical properties, and relief have a close relationship. Nevertheless, many blank spots remain.

Focusing on the plant communities of wet and wet-mesic grasslands, there are generally numerous associations which are mixtures of lowland or colline plant associations. They form stripe- or mosaic complexes with each other. Several different associations were found in the plains, especially on the wet and wet-mesic grasslands of Hanság and Tóköz. Zólyomi (1934) presented the plan associations and habitat of Hanság. Járai-Komlódi (1960) described the plant associations of south Hanság. Keszei – Takács (2008) completed an overview of north Hanság habitats.

Wetlands and wet grasslands are disappearing all over the world (Hu et al. 2017). In Hungary, the proportion of these habitats is in constant decline due to climate change and anthropogenic effects (Kovács 1957, Tasi et al. 2014). The longer and more frequent dry periods have been especially detrimental (Borhidi – Sánta 1999, Bartholy et al. 2011). Grassland and meadows are usually grazed or mowed, but the danger of overuse is always present (Janisova et al. 2013, Swacha et al. 2018, Bíró et al. 2020). Recording the current state of these habitats is also an important motivation.

The plant associations of the research area exhibited a mosaic pattern. Our research aims to find the reasons behind the observed pattern. We wanted to answer the following research questions: (1) Does the plant association pattern follow the soil diversity of the research area? (2) Is there any soil parameter or groups of parameters that show direct relationship with species composition? (3) Is there a relationship between the vegetation pattern and microrelief?

2 MATERIALS AND METHODS

2.1 Study area

The Hanság and Tóköz (Csorna plain) are plains formed by tectonic subsidence and subsequent refilling of the area. Non-runoff areas are common due to topography. Groundwater is generally close to the surface. The variability of the microrelief can have a large influence on vegetation. According to the Köppen-Geiger classification, the region is characterised by a warm temperate, fully humid, and hot summer climate (*Cfb*). (Berki et al. 2019a, b). Between 1961 and 2010, the annual mean temperature was 10.2°C and the annual rainfall was 564 mm. June is the wettest month. The forest aridity index (FAI) is 6.70, indicating a forest climate class with Turkey oak and sessile oak (Führer et al. 2019a, b).

The treeless plant communities of the micro-regions are characterized by mesotrophic wet meadows, non-tussock tall-sedge beds, mesotrophic wet meadows, and their transition parts. There are also mesic hay meadows, uncharacteristic wetlands, uncharacteristic mesic grasslands, and uncharacteristic dry and semi-dry grasslands that have become uncharacteristic due to anthropogenic effects. Our research investigated relatively small (< 10ha) areas in which the current treeless plant associations show a high degree of mosaic pattern. The visible difference in species composition was obvious even in the flat meadows. Depending on the location, the various treeless associations alternated in the form of stripe complexes or mosaic complexes. Closely related coenoses are also separated in most cases (based on physiognomy, species composition).

2.2 Methods of botanical survey and soil investigation

We conducted field surveys within the village boundaries of Barbacs and Osli in 2020 (*Figure 1*). The vegetation sampling is based on a modified Braun-Blanquet method – plant

cover percentage is used (Braun-Blanquet 1932). During the survey on the research area previously described, seven association types were searched and sampled. As a first step, satellite imagery was obtained and observed to delineate the plant community units. Then the field assessment, where the actual plant communities were identified and delineated, began. Altogether 94 relevés were collected. In 21 relevés, topsoil sampling and description were also performed: three relevés from every plant association. The relevés were 5×5 meters. The location of the relevés was recorded by GPS-based point determination using a Trimble Geo XT field computer.

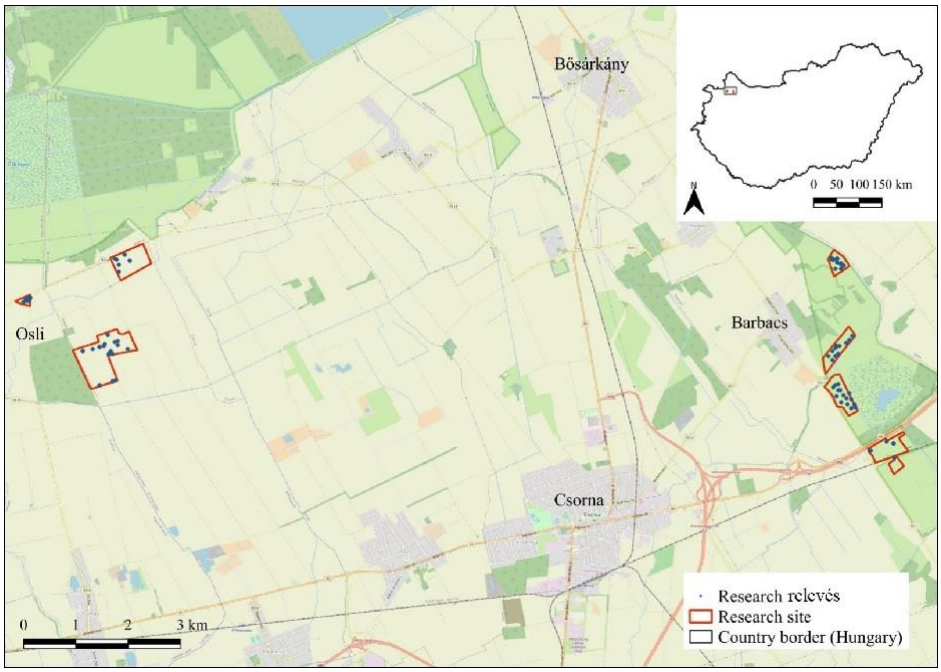

Figure 1. Map of the study area with the research sites and relevés

The nomenclature of plant species follows the work of Király (2009). We considered Borhidi's (2003) work relevant in determining the associations. During the survey, we prepared a species list of the plants within the relevé and estimated the total cover, the percent of the open soil surface and the litter cover, and average vegetation height.

To determine the genetic soil type, we took soil profiles with a Pürckhauer sampler at the 21 selected relevés. The properties of genetic soil levels were recorded at the sites during the description. When naming soil types, we use both the Hungarian genetic system (Stefanovits 2010) and the nomenclature of the World Reference Base for Soil Resources (WRB) (FAO 2015). During field days, momentary soil moisture content (VWC) was measured at depths of 0-10 cm (VWC1), 10-20 cm (VWC2), and 20-30 cm (VWC3) (Aquaterr M-300) with three repetitions at every relevé. We took average soil samples from the upper 10 cm layer of the soil for laboratory tests on relevé level. Concurrently, 100 cm^3 samples were also taken with sampling cylinders to calibrate the measured VWC and to measure the bulk density (BD).

2.3 Data processing, laboratory soil analysis and statistical testing

We classified the data collected during the vegetation survey into coenological tables. The coenological recordings were taken using the TURBOVEG database management software (Hennekens – Schaminée 2001), and then the statistical evaluation of the data was performed with the JUICE software package version 7.1 (Tichý 2002). The classification is based on the modified TWINSPAN method (Roleček et al. 2006). During the analysis, the maximum number of divisions was seven and the analysis was run using the average of the Simpson

index of dissimilarity as a measure of within-group heterogenity. The background information belonging to the formed groups (total cover (%), litter cover (%), etc.) come from the field observations. The diagnostic, constant, and dominant species of the established groups were defined following the method of Chytrý et al. (2002). The range of diagnostic species was determined by calculating the fidelity values based on the coefficient Φ. Fidelity values were calculated only for species that showed non-random occurrence across the clusters according to the Fisher's exact test (P<0.05). The use of numerical vegetation classification aims to reduce the subjective factors of the expert-based classification. We give a brief summary of both classifications, but in the later analyses we use the vegetation groups based on the modified TWINSPAN analysis.

We performed laboratory testing of the soil samples based on the methodological recommendations of Bellér (2000) in the soil laboratory of the Institute of Environment and Earth Sciences of the University of Sopron. The undisturbed samples from the sampling cylinders were measured at the end of the field days and then dried at 105 °C for three days, after which they were measured again. In this way, we obtained VWC for calibration, and BD. The average or disturbed samples – collected near the cylinders – were dried at room temperature. After that, the skeletal parts, roots, and snail shells were removed from the samples. The pH (H_2O) of the prepared soil samples was measured in a 1:2.5 soil:distilled water suspension (Motsara – Roy 2008). The determination of the ammonium-lactate-acetic acid soluble (AL) potassium and phosphorus contents is based on the methodology of Egnér et al. (1960), which showed the phosphorus (PAP) and potassium (PAK) contents that are available for the vegetation. Finally, the organic carbon content (TOC), and the total-nitrogen (TN) and sulphur (TS) content of the soils were determined according to international standards (ISO 10694: 1995 and ISO 13878: 1998) using the Elementar Vario MAX CNS elemental analyser (Elementar Analysesysteme, Langenselbold, Germany).

We used a digital elevation model (DEM) from the Lechner Knowledge Centre called DDM-5 to visualize elevation, which was generated by digitizing 1:10000 scale topographic maps (Telbisz et al. 2013). Digitalization of the on-site drawn vegetation maps and visualization of the DEM–was achieved by QGIS, version 3.18. Since elevation above sea level is not a good measure of microtopography in the present case – it provides no information about whether the given point is a bottom of a ditch or a top of a hummock – derived models are used to quantify the microrelief. The DEM is calculated into normalised elevation model and slope model. According to Diamond et al. (2019) hollows tend to have less-than-average elevation and less-than-average slope. This classification was compared with the manual delineation of hollows. The automated delineation has 14.6 % root mean square error (RMSE) against the manual one. At the level of TWINSPAN groups, the calculated values were compared to determine potential significant difference between them. For this purpose, one-way analysis of variance (ANOVA) was applied with post-hoc Tukey-test.

R environment (R Core Team 2014) provided the further place for statistical analyses. Pairwise correlation was calculated between soil parameters with Bonferroni-adjusted P values. Average values of the soil parameters were calculated at the level of the TWINSPAN groups. The soil parameters of the relevés assigned to the TWINSPAN groups were compered via ANOVA and homogenous groups were separated with Tukey's honestly significant test. To investigate the relationship between the soil parameters and the distribution of the dominant plants (cover percentages) among the TWINSPAN groups, canonical correspondence analysis (CCA) (Legendre – Legendre 2012, Oksanen et al. 2020) was applied. The soil parameters which showed high linear dependency were eliminated from the CCA; for this purpose both correlation analysis and calculation of variance inflation factor

(VIF) was performed. Variables which showed multicollinearity (VIF > 5) were left out from the CCA. Only tests with $P < 0.05$ are named as significant.

3 RESULTS

3.1 Results of the botanical survey

We investigated a total of seven association types in the study areas that were described in previous studies:

1. *Glycerietum maximae* Hueck 1931;
2. *Galio palustris-Caricetum ripariae* Bal.-Tul. et al. 1993;
3. *Caricetum acutiformis* Eggler 1933;
4. *Caricetum gracilis* Almquist 1929;
5. *Caricetum distichae* Steffen 1931;
6. *Cirsio cani-Festucetum pratensis* Májovsky – Ružičková 1975;
7. *Carici vulpinae-Alopecuretum pratensis* (Máthé – Kovács M. 1967) Soó 1971 corr. Borhidi 1996;

Table 1 introduces the average characteristics of the relevés on the plant association level. Association types typically appear together in the form of stripe or mosaic complexes in the areas. They are well separated by their species composition and physiognomy, but usually there is a 1-8 m wide transition zone of adjacent associations where these associations are mixed. At gradually rising elevation, the associations follow each other in a stripe-like manner, while in flat areas they appear in patchy patterns.

Table 1. Average characteristics of the plant associations (mean (standard error of mean))

Plant association	Nr. of relevés (pcs.)	Avg. Nr. of species (pcs.)	Plant coverage (%)	Litter coverage (%)	Exposed soil surface (%)	Average height (cm)
Galio palustris-Caricetum ripariae	13	6 (1.04)	75 (2.56)	4 (1.17)	7 (2.37)	60 (2.91)
Caricetum gracilis	25	9 (0.80)	77 (2.10)	2 (0.52)	5 (1.61)	51 (1.68)
Caricetum distichae	9	12 (1.02)	78 (2.04)	3 (1.08)	10 (3.85)	37 (3.12)
Glycerietum maximae	8	6 (0.73)	66 (3.10)	5 (2.45)	14 (3.97)	56 (6.44)
Caricetum acutiformis	10	5 (0.57)	79 (2.56)	3 (1.09)	9 (3.58)	66 (4.74)
Cirsio cani-Festucetum pratensis	12	22 (1.29)	82 (2.71)	2 (0.59)	7 (2.73)	50 (2.34)
Carici vulpinae-Alopecuretum pratensis	17	19 (0.96)	89 (3.14)	2 (0.52)	1 (0.31)	51 (3.29)

3.1.1 Vegetation of wet sites

The *Glycerietum maximae* association is typically associated with the marginal zone of watercourses, but it also appears in smaller hollows in wet meadows. Its species number is

very low; the predominance of *Glyceria maxima* is obvious. The typical species are *Symphytum officinale, Lythrum salicaria,* and *Ranunculus repens*. As the habitat becomes drier, the *Galio palustris-Caricetum ripariae* association becomes dominant. The boundary between the two associations is usually marked by a sharp difference – transition happens in 1-2 m – due to the frequency of dominant species cover, which is usually characterized by a homogeneous carpet-like setting. In addition to the predominant *Carex riparia*, some constant elements are *Lysimachia vulgaris, Persicaria amphibia,* and *Symphytum officinale.* The *Caricetum acutiformis* association appears in almost identical habitats. The two associations differ most obviously in their dominant species; their appearance is similar. Moving away from the water, an association of *Caricetum gracilis*, which is more species-rich, more resistant to abiotic and biotic stress, is present. While the previous associations appear mostly as smaller spots or narrow stripes, these acute sedge associations are extensive. Their appearance is diverse, several compositions can be observed, from completely homogeneous acute sedge spots to broken-up, mosaic, and significantly more diverse settings. At some places, the *Caricetum distichae* association is wedged into the acute sedge associations as small spots and does not form large, connected stands. Typically, the patch area does not exceed 50 m^2. The species diversity of both types of associations is moderate. In addition to *Carex acuta, C. disticha, Cirsium brachycephalum, C. canum* and *Galium palustre* are typical. Both types (4-5) are more resistant to mowing (i.e., cutting and removal of the cut biomass) than types 1-3. As a result of improper grassland management, associations 1-3 are easily transformed, most often into association type 4 (*Figure 2 A*), especially if types 1-3 are on edge habitats.

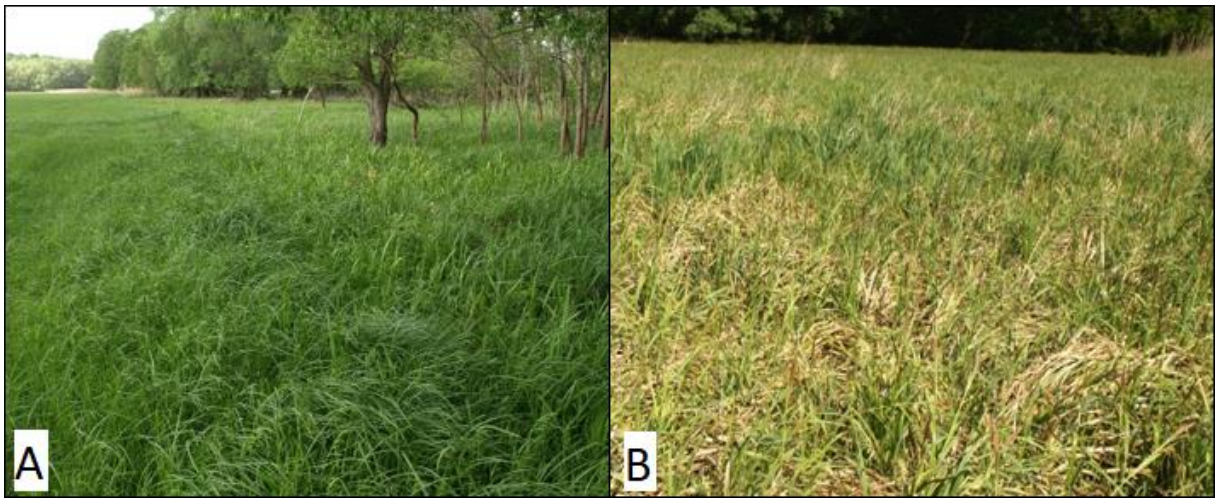

Figure 2. Effects of mowing (A) and accumulation of dry biomass on the soil surface (B)

The lack of grassland management makes the coenoses species-poor, mostly as a result of dry biomass accumulation (*Figure 2 B*), which makes many species unable to sprout. If sufficient water is available, the accumulation of sedge biomass is insignificant. However, this problem becomes common as the areas dry out.

3.1.2 Vegetation of wet-mesic sites

With the further decrease of the length of saturated periods, the dominance of sedge species also decreases; they are replaced by grass species. Typical associations in these areas are *Cirsio cani-Festucetum pratensis* and *Carici vulpinae-Alopecuretum pratensis*. Borhidi (2003) treats the association *Carici vulpinae-Alopecuretum pratensis* as a member of the *Deschampsion caespitosae* group. He mentions that the *Ranunculo repentis-*

Alopecuretum pratensis – which is poorer in *Magnocarion* species – is also closely related to it or that they are the same association. A more recent study sorts the *Ranunculo repentis-Alopecuretum pratensis* association into the *Arrhenatherion* group as a mesic-wet type (Lengyel et al. 2016). The most common habitats are colline and mountainous valleys. This association has a similar species composition as *Carici vulpinae-Alopecuretum pratensis*, but the proportion of the species of semi-dry grasslands and colline habitats is much higher. Therefore, we identified the more water-tolerant associations of wet mesotrophic wet meadows as *Carici vulpinae-Alopecuretum pratensis*.

The former is a typical plant community of mesic habitats; the latter of wet-mesic habitats. In many cases, they connect to each other via broader (4-8 m) transition zones. Their species composition is characterized by the fact that they do not have typical character species. Dominant species are generalists with a wide range of tolerance, so in many cases it is difficult to appropriately differentiate these plant associations. Typical species of the *Cirsio cani-Festucetum pratensis* association include *Festuca pratensis*, *Poa pratensis* and *Rumex acetosa*. Its stands at the Hanság are more degraded; they lack rare species. The *Carici vulpinae-Alopecuretum pratensis* association is less disturbed, even *Stellaria palustris* appearing in its stand. Typical species are *Alopecurus pratensis, Ranunculus acris*, and *Lathyrus pratensis.*

3.2 Results of the modified TWINSPAN analysis

According to the analysis results, the investigated plant communities do not differ as much from each other as we identified in the field. Of the six clusters formed *(Figure 3).*

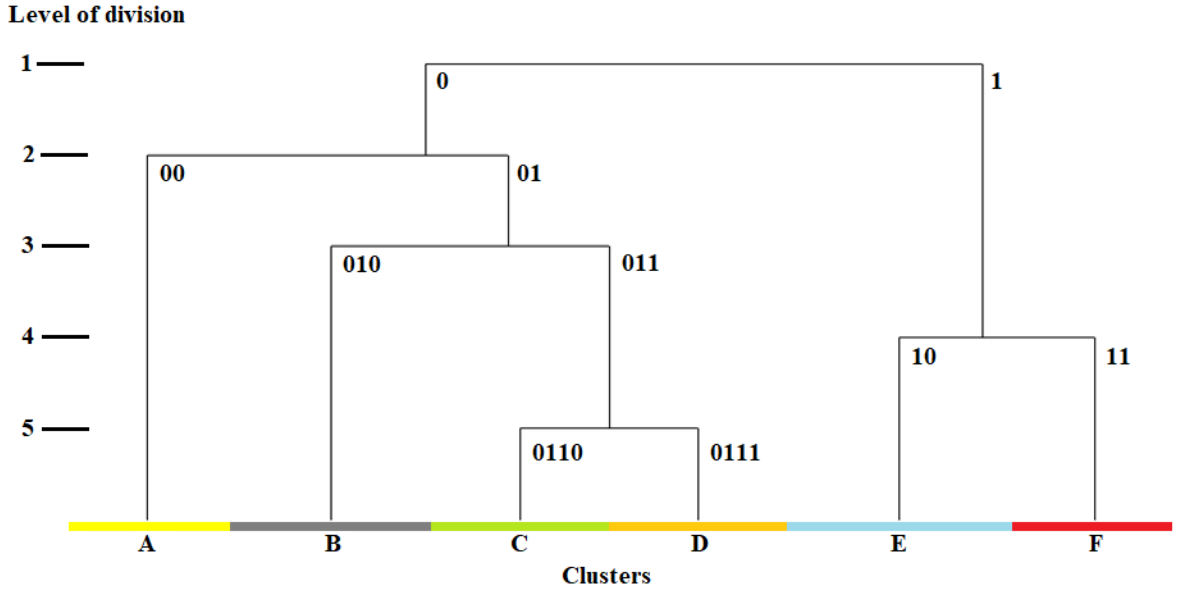

Figure 3. Modified TWINSPAN dendrogram of the 94 relevés

The first division brought the separation of the non-tussock tall-sedge beds (0) and the mesotrophic wet meadows (1). In the second division, the non-tussock tall-sedge beds (0) were divided into lesser groups: *Caricetum gracilis* × *Caricetum distichae group* (00) and a combination of *Galio palustris-Caricetum ripariae group* (01) This group (01) was divided into two subgroups: *Caricetum acutiformis* × *Caricetum ripariae* group (010) and the mixed group of *Galio palustris-Caricetum ripariae* associations (011). Group (011) collected the associations of wet and mesic habitats. This group is separated into two: the wet habitats were characterised by the *Galio palustris-Caricetum ripariae* × *Glycerietum maximae* group (0110)

and the wet-mesic habitats were populated by *Galio palustris-Caricetum repariae* × *Caricetum gracilis* group (0111).

The division of mesotrophic wet meadows (1) partitions into two subgroups. Both subgroups have transient characteristics. Their separation is caused by the different moisture regimes; group (10) occurs under more wet conditions while group (11) prefers less wet conditions.

Table 2 summarises vegetation characteristics of the formed TWINSPAN groups and the distribution of relevés between the two classification systems. The detailed interpretation of the TWINSPAN groups is in the following subsections.

Table 2. Average vegetation characteristics of the TWINSPAN groups (mean (standard error of mean)) and the distribution of relevés between the plant associations and TWINSPAN groups (CARR - Galio palustris-Caricetum repariae, CARG - Caricetum gracilis, CARD - Caricetum distichae, GLY -Glycerietum maximae, CARA - Caricetum acutiformis, FES - Cirsio cani-Festucetum pratensis, ALO - Carici vulpinae-Alopecuretum pratensis, SUM - summary)

Groups	Perc. cover (%)	Litter cover (%)	Exposed soil surface (%)	Avg. height (cm)	Avg. nr. of species (pcs.)	Nr. of relevés (pcs.)							
						CARR	CARG	CARD	GLY	CARA	FES	ALO	SUM
00	80 (3.03)	1 (0.50)	4 (1.69)	44 (2.09)	10 (0.75)		12	2					14
010	76 (2.28)	3 (0.76)	7 (2.18)	62 (3.40)	4 (0.39)	3	4			10			17
0110	71 (2.71)	5 (1.54)	11 (2.68)	59 (3.81)	6 (0.55)	7			8				15
0111	76 (1.50)	3 (0.69)	9 (2.83)	51 (3.24)	10 (0.77)	3	8	4					15
10	85 (2.95)	2 (0.63)	4 (1.65)	48 (3.06)	17 (0.84)		1	3			1	14	19
11	85 (2.85)	2 (0.50)	6 (2.41)	50 (2.13)	22 (0.93)						11	3	14

3.2.1 Caricetum gracilis × Caricetum distichae group (00)

This cluster shows a transitional character. The two associations usually form mosaic complexes with each other. Small patches (~50 m^2) of *Caricetum distichae* are wedged into the carpet-like *Caricetum gracilis* stands. There is considerable overlap in species composition but there are differences in their dominant species and physiognomy.

Diagnostic species: *Caltha palustris, Cardamine pratensis, Carex acuta, Carex vesicaria, Carex vulpina, Equisetum palustre, Lysimachia nummularia, Myosotis scorpioides, Persicaria dubia, Poa palustris, Ranunculus repens.*

Constant species: *Lychnis flos-cuculi, Rumex acetosa, Symphytum officinale, Taraxacum officinale*.

Dominant species: *Carex acuta, Carex disticha.*

3.2.2 Caricetum acutiformis × Caricetum ripariae group (010)

This group is created from two plant associations which are easy to distinguish in the field. However, both can be characterized as species-poor associations of hollows and wetter areas with a carpet-like setting. The associations share several species, and the physiognomy of the plant communities are determined by the dominant species. In most cases, *Carex riparia* and *C. acutiformis* are present together, but the dominant one has much higher cover percentage and more individuals. There is no evidence of codominance, which would imply the aggregation of the two associations. The TWINSPAN method aggregated these associations since their relevés were homogenous and since they have almost the same species with similar cover percentages. The difference is only shown in the dominant species (cover percentages).

Diagnostic species: *Carex acutiformis, Lythrum salicaria.*
Constant species: *Carex riparia, Lysimachia vulgaris, Symphytum officinale.*
Dominant species: *Carex acutiformis, Carex riparia.*

3.2.3 Galio palustris-Caricetum ripariae × Glycerietum maximae group (0110)

This is a transitional group of the wet areas. The group of mixed plant communities (0110) contains relevés of *Galio palustris-Caricetum ripariae* and *Glycerietum maximae* associations. This indicates that the assessment of differences between the investigated associations is not uniform. There is no significant difference in the species combination of the two types. However, the dominant species determines the appearance of the association, based on which they can be easily distinguished in the field. The program creates new groups based on the heterogeneity between the relevés. As these are quite similar based on their species composition, the analysis does not separate them into separate subgroups.

Diagnostic species: *Carex riparia, Glyceria maxima, Persicaria amphibia, Schoenoplectus lacustris, Stachys palustris, Urtica dioica.*
Constant species: *Iris pseudacorus, Ranunculus repens, Symphytum officinale*.
Dominant species: *Carex riparia, Glyceria maxima*.

3.2.4 Galio palustris-Caricetum ripariae × Caricetum gracilis group (0111)

This group is found in the transition zone of the wet and wet-mesic group. It is characterised by less wet conditions than in the case of 0110 group. These two groups often form stripe complexes or patch-complexes in micro-basins. Group 0111 is more species-rich than 0110 or the formerly introduced groups; however, it is more species poor than *Caricetum gracilis*. The species of the two associations mix equally and the two dominant species are often codominant.

Diagnostic species: *Agrostis stolonifera, Carex acuta, Cirsium arvense, Cirsium brachycephalum, Galium palustre, Iris pseudacorus, Persicaria amphibia, Phalaris arundinacea, Symphytum officinale, Thalictrum flavum.*
Constant species: *Cardamine pratensis, Carex riparia, Lysimachia vulgaris, Ranunculus repens.*
Dominant species: *Carex acuta, Carex disticha, Carex riparia.*

3.2.5 Carici vulpinae-Alopecuretum pratensis × Caricetum gracilis group (10)

This group of associations forms in the transition zone between mesotrophic wet meadows and non-tussock tall sedge beds and in the depressions of mesotrophic wet meadows. The presence of typical mesotrophic wet meadow species (*Alopecurus pratensis, Cardamine pratensis, Galium mollugo*) and an accumulation of aquatic species (*Iris pseudacorus,*

Phalaris arundinacea, Symphytum officinale) characterise the group. They are unstable plant communities, sensitive to changes in environment. The dominant species which is better adapted to the weather in a given year determines the community. They can experience significant change within a year.

Diagnostic species: *Alopecurus pratensis, Calamagrostis epigeios, Cardamine pratensis, Carex hirta, Carex otrubae, Cerastium tenoreanum, Festuca pratensis, Galium mollugo, Glechoma hederacea, Lychnis flos-cuculi, Phalaris arundinacea, Poa pratensis, Potentilla anserina, Potentilla reptans, Ranunculus repens, Taraxacum officinale, Vicia cracca*.

Constant species: *Cirsium arvense, Cirsium canum, Iris pseudacorus, Symphytum officinale.*

Dominant species: *Alopecurus pratensis, Carex disticha, Festuca pratensis*.

3.2.6 Carici vulpinae-Alopecuretum pratensis × *Cirsio cani-Festucetum pratensis group (11)*

The present cluster includes the typical mesotrophic wet meadows. In the absence of reliable character species, mesotrophic wet meadows are often difficult to distinguish from each other. They occur in a fairly wide range of habitats due to their broad-spectrum generalist species, which define the community. The observed *Cirsio cani-Festucetum pratensis* association is more species-poor than described by Borhidi (2003). The stands of the *Carici vulpinae-Alopecuretum pratensis* association are mostly small, with a wide transition to the mesotrophic wet meadows dominated by *Festuca* species. Considering the above-mentioned facts, it is understandable that they were not separated in the analysis. Nevertheless, we consider their field isolation to be necessary because they indicate the changes in the water balance of the habitat.

Diagnostic species: *Achillea millefolium, Anthoxanthum odoratum, Arrhenatherum elatius, Carex hirta, Carex praecox, Carex spicata, Cerastium brachypetalum, Cirsium canum, Colchicum autumnale, Dactylis glomerata, Daucus carota, Erigeron annuus, Festuca pratensis, Festuca rupicola, Fragaria viridis, Frangula alnus, Galium mollugo, Galium verum, Glechoma hederacea, Lathyrus tuberosus, Leontodon hispidus, Leucanthemum vulgare, Linaria vulgaris, Lotus corniculatus, Luzula campestris, Lychnis flos-cuculi, Myosotis arvensis, Myosotis ramosissima, Pastinaca sativa, Plantago lanceolata, Poa angustifolia, Poa pratensis, Potentilla reptans, Ranunculus acris, Rosa canina s.s., Rubus caesius, Rumex acetosa, Solidago gigantea, Veronica chamaedrys, Vicia hirsuta, Vicia tenuifolia*.

Constant species: *Alopecurus pratensis, Cirsium arvense, Potentilla anserina.*

Dominant species: *Alopecurus pratensis, Arrhenatherum elatius, Festuca pratensis.*

3.3 Results of soil analyses

During the field investigations, we described hydromorphic soils with topsoil of different thickness and organic matter (OM) content. Mollic Gleysols (meadow soils) were found in three cases (more mesic parts of the wet-mesic habitats). In wet habitats Histic Gleysols (histic meadow soils) were more common, which were present in 12 relevés. Transient types of the two soil types were found in six cases in wet-mesic habitats, especially in which wet character dominates and it associates with only a lower accumulation of OM. These are described as Mollic Gleysol (Hyperhumic). These soils have looser topsoil and higher OM

content (muck layer) than the described Mollic Gleysols, but they do not reach the requirements of histic properties.

The correlations between the individual soil parameters demonstrated that elevation and pH (H_2O) have no significant relationship with the other variables, except with each other ($r = 0.47$). All the other correlations proved to be significant. PAK shows a strong positive correlation ($0.50 < r < 0.60$) with PAP and TS, while it has a medium positive correlation with TN ($r = 0.47$) and a negative one with BD ($r = -0.45$). PAP is correlated strongly ($r > 0.60$) positively with TOC, TN, TS, VWC1, VWC2 and VWC3 and negatively with BD ($r = -0.76$). TOC, TN, and TS have strong positive connection with each other ($r > 0.95$), and with the VWC too ($r > 0.84$). The relation of BD and TN, TS is described as strong negative ($r < -0.89$). Between BD and the VWCs the connection strongly negative ($r < -0.85$). The group of moisture contents (VWC1, VWC2, VWC3) have correlation coefficients above 0.95 with each other, which indicates a strong positive relationship.

TOC and BD show a strong negative relationship (*Figure 4*) and the soil profiles of different classes cluster along these parameters. In the case of Mollic Gleysols, the lower TOC is associated with a high BD value, which indicates that the humic character does not dominate, but a relatively high, above 7%, TOC was observed as a result of OM accumulation. In the transitional group, TOC jumps, above 10%, but does not reach 20%. In parallel, BD decreases. As the histic character became predominant, a high TOC of over 20% was measured as a result of organic matter accumulation, which is accompanied by a very low BD.

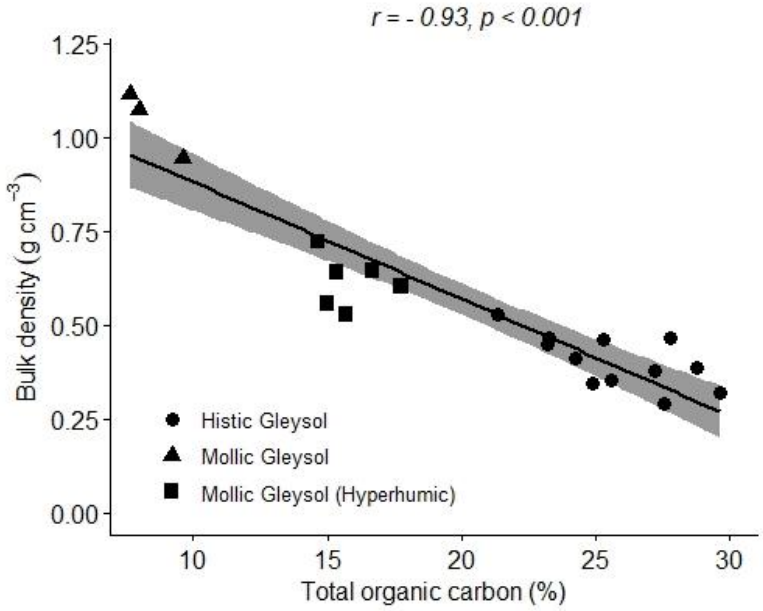

Figure 4. Relation of soil bulk density (BD) and total organic carbon (TOC) along different soil groups

3.4 Correlation between soil parameters and TWINSPAN groups

There is a correlation between the soil classes and the TWINSPAN groups (*Table 2*). On Mollic Gleysol, only group 11 can be found, while on Histic Gleysol, we typically find groups 010 and 0110, and group 0111. In the case of the transient Mollic Gleysol (Hyperhumic), the transient vegetation group 10 is predominant, but groups 00 and 11 also occur.

Table 2. Distribution of number of relevés among the TWINSPAN groups and soil classes

Soil classes	TWINSPAN groups					
	00	010	0110	0111	10	11
Mollic Gleysol						3
Mollic Gleysol (Hyperhumic)	1				3	2
Histic Gleysol		3	5	4		

The average soil parameters calculated for the TWINSPAN groups are presented in *Table 3*. Since group 00 has only one observation, it was omitted from the analyses and the values of that one relevé are presented in the table. Similarly to the classification by soil groups, there is no sharp separation between the individual TWINSPAN groups in terms of elevation, pH(H_2O), and PAK. For PAP, TOC, TN, and TS parameters, the TWINSPAN groups are divided into two groups. 00, 010, 0110 and 0111 form a group dominated by the histic character, while groups 10 and 11 are found in the other group, where the meadow soil character predominates.

Table 3. Soil params of the different TWINSPAN groups (mean (standard error of mean))

Soil parameters	TWINSPAN groups						F	Sign.
	00	010	0110	0111	10	11		
Nr. of elements (relevés) (pcs.)	1	3	5	4	3	5		
Elevation (m)	110	110^{a} (0.000)	109^{a} (1.304)	109^{a} (0.408)	110^{a} (1.155)	111.4^{a} (0.678)	1.31	NS
pH (H_2O)	6.9	6.2^{a} (0.082)	6.4^{a} (0.173)	6.5^{a} (0.225)	6.5^{a} (0.24)	6.7^{a} (0.094)	0.87	NS
Plant Available P (mg 100 g^{-1})	16.2	18.3^{a} (0.789)	15.3^{a} (2.286)	14.7^{a} (1.462)	6.2^{b} (0.681)	5.3^{b} (0.691)	13.54	***
Plant Available K (mg 100 g^{-1})	17.5	30.0^{a} (4.693)	24.6^{a} (5.55)	19.7^{a} (1.975)	14.9^{a} (1.187)	16.4^{a} (1.392)	2.38	NS
Total Organic C (%)	15.7	27.3^{a} (2.007)	25.5^{a} (1.17)	25.0^{a} (0.864)	15.5^{b} (0.633)	11.7^{b} (2.058)	20.5	***
Total N (%)	1.5	2.2^{a} (0.132)	2.2^{a} (0.103)	2.2^{a} (0.037)	1.4^{b} (0.07)	1.0^{b} (0.18)	18.65	***
Total S (%)	0.3	0.6^{a} (0.099)	0.6^{a} (0.035)	0.5^{a} (0.027)	0.2^{b} (0.021)	0.2^{b} (0.034)	20.74	***
Bulk Density (g cm^{-3})	0.5	0.4^{a} (0.042)	0.4^{a} (0.044)	0.4^{a} (0.019)	0.6^{ab} (0.047)	0.9^{b} (0.107)	10.22	***
Water Content 0-10 cm (%)	62.5	86.9^{a} (8.613)	95.0^{a} (2.165)	98.9^{a} (0.634)	78.0^{a} (11.018)	45.3^{b} (3.062)	22.39	***
Water Content 10-20 cm (%)	63.9	82.4^{a} (9.88)	91.9^{a} (3.547)	96.9^{a} (1.835)	72.4^{a} (14.601)	43.3^{b} (3.266)	13.49	***
Water Content 20-30 cm (%)	59.9	86.1^{a} (8.612)	92.5^{a} (2.593)	96.9^{a} (1.545)	75.5^{a} (12.35)	44.5^{b} (4.058)	16.86	***

Significance levels: $0 < *** \leq 0.001 < ** \leq 0.01 < * \leq 0.05 <$ NS

^{abc} represents homogenous subsets according to Tukey's honestly significant difference test

According to the BD of soils, the subsets are similar to the former case, but group 10 forms a transition and can be classified into both groups. Moisture contents show a uniform picture; only group 11 deviates from the other groups.

CCA was performed to show the correspondence of the main environmental factors with the composition of dominant plant species, (*Figure 5*). Soil and topographical variables were represented as arrows (eight altogether). Arrow length indicates the importance of the environmental variable. To avoid multicollinearity, variables showing higher variance inflation factors than five were omitted. The analysis was based on 21 relevés pictured by points and coloured according to their TWINSPAN group. The plant species were indicated by crosses. The location of the plant species relative to the arrows or axes represent the environmental conditions or gradients associated with the occurrence of the species.

The CCA model proved to be significant according to the permutation test (F = 1.748, *P* = 0.004). The total inertia is 4.746 from which 53.8% was described by the constrained axes. The first axis explained 18.4% of the total variation (34.2% of the constrained inertia), while the second axis covered 14.9% of the total inertia (27.6% of the constrained one). The coefficient of multiple determination (R^2) is 0.538 and the adjusted coefficient of multiple determination ($R^2_{adj.}$) is 0.234. The species – environmental correlation is strong, r = 0.95 in the case of the Axis 1 and r = 0.89 for Axis 2.

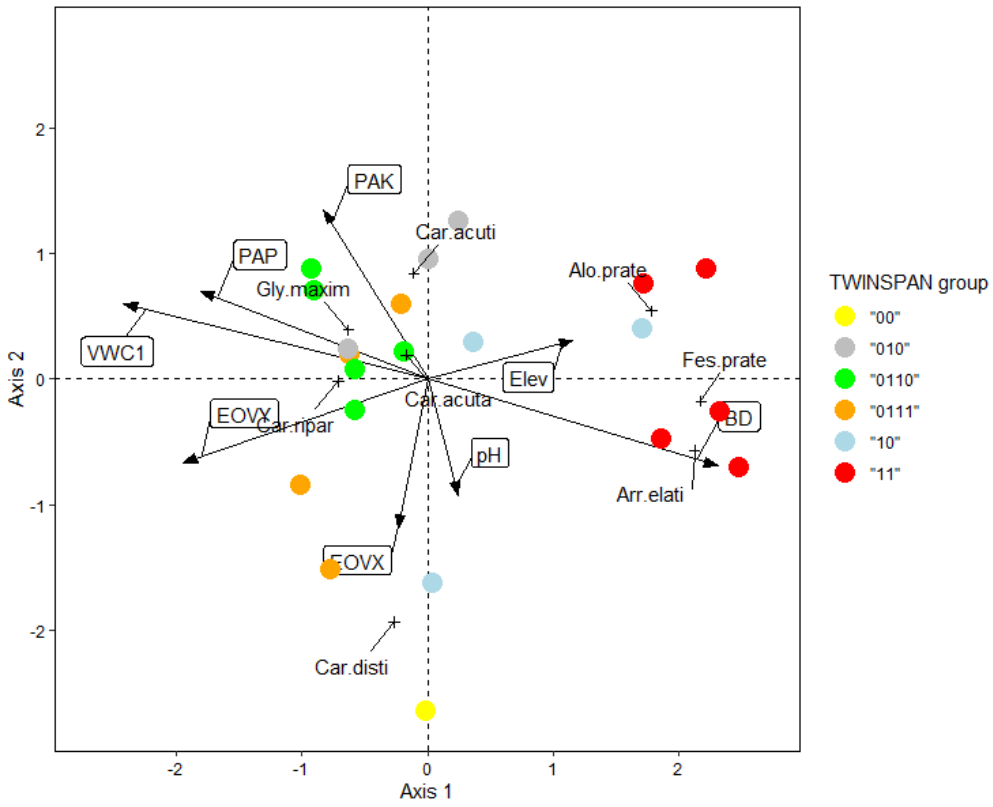

Figure 5. Results of the Canonical Correspondence Analysis (CCA) between the soil parameters (arrows) and cover percentage of the dominant species of the TWINSPAN groups (crosses), points represent the relevés grouped by the TWINSPAN groups. Abbreviations: Elev: Elevation (m), EOVY and EOVX: longitude and latitude in HD72 6 EOV reference system, pH: pH (H_2O), PAP: Plant Available Phosporus (mg 100 g^{-1}), PAK: Plant Available Potassium (mg 100 g^{-1}), BD: Bulk Density (g cm^{-3}), VWC: Volumetric Water Content of soil layer between 0 and 10 cm (%), Alo prate: Alopecurus pratensis, Arr. elati: Arrhenatherum elatius, Car acuta: Carex acuta, Car acuti: C. acutiformis, Car disti: C. disticha, Car ripar: C. riparia, Fes prate: Festuca pratensis, Gly maxim: Glyceria maxima

The most important factors are BD, VWC, EOVY, PAP, and PAK. The first axis has a strong positive correlation with BD (r = 0.818) and strong negative with VWC1, EOVY, PAP (r = -0.856, -0.687, -0.639 respectively) and medium positive with elevation (r = 0.409). The second axis was affected mostly by PAK (r = 0.446) and medium negative correlation was shown with EOVX (r = -0.394) and pH (r = -0.305).

3.5 Results of vegetation mapping

The reason for the fine mosaic pattern of vegetation formed in flat areas should also be investigated in the microrelief differences. Therefore, we fitted 5×5 m resolution digital elevation models to the study areas and made a comparison with the pattern of vegetation patches surveyed during vegetation mapping. The vegetation patches and the fine-scaled (10 cm increase in elevation) equiheight lines coincide in several cases (*Figure 6*).

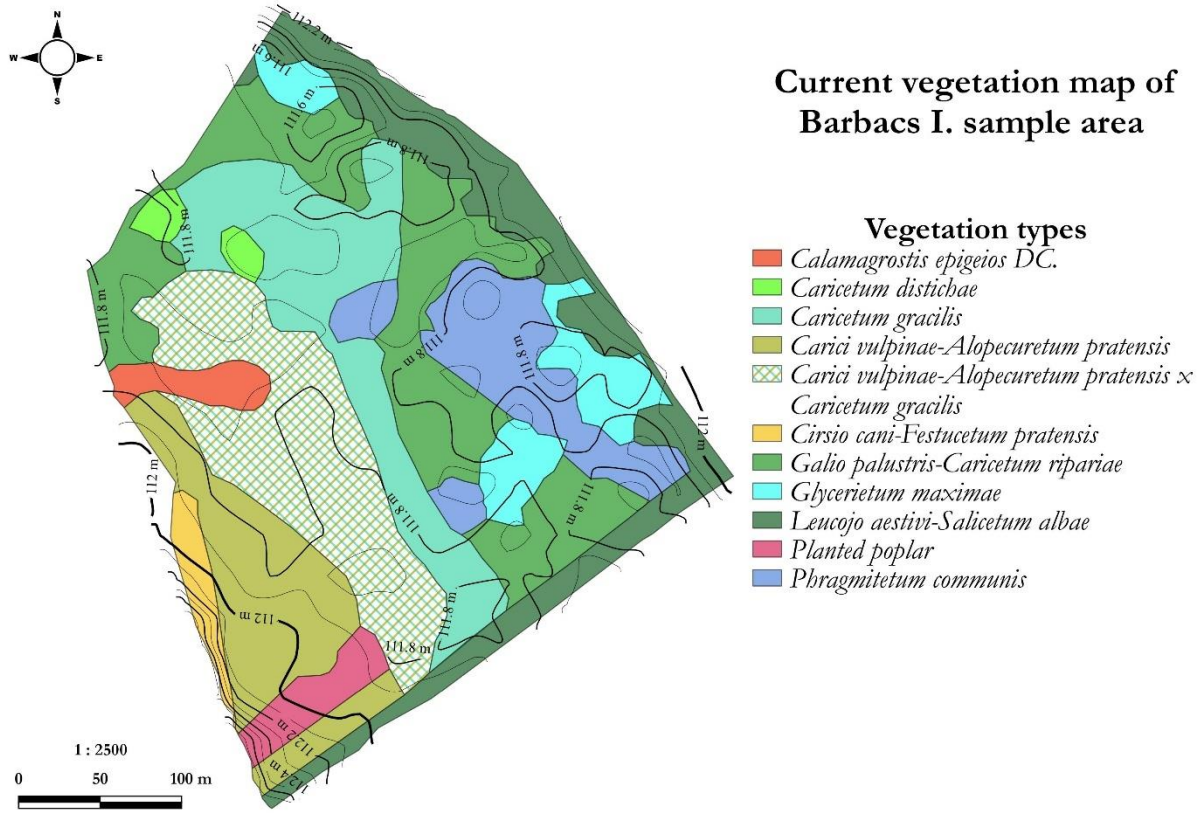

Figure 6. Current vegetation map of Barbacs I. sample area

The normalised elevation values of the TWINSPAN groups differ significantly (F = 32.94, $P < 0.001$). There are three subsets separated by Tukey's test. TWINSPAN group 00, 010, 0110, and 0111 are the ones which have average values lower than 0. Group 10 is a transient group and group 11 has the highest values and highest average. Normalised slope values show a different image. Significant difference among the groups is evident (F = 16.67, $P < 0.001$). The lowest values are accompanied with group 00 and 0111. Group 0110 shows a transition between subset a and b. Subset b (TWINSPAN group 010 and 10) are in the mid-range, while group 11 has again the highest average (*Figure 7*).

The TWINSPAN groups are assigned with the category of hummock or hollow according to the combined models of normalised elevation and slope on the level of relevés. The groups showed considerable differences (F = 18.04, $P < 0.001$). Tukey's test divided the group into

two subsets. TWINSPAN group 00, 010, 0110, and 0110 are assigned to the hollow subset and TWINSPAN group 10 and 11 classified into the hummock subset. TWINSPAN group 00 has relevés only in hollows, 0110 and 0111 have three and one hummock relevés respectively while the rest of the relevés are hollows. TWINSPAN group 010 has five hummock and 12 hollow relevés, group 10 has a similar distribution but with swapped groups (13 hummocks and six hollows). Group 11 has only hummock relevés.

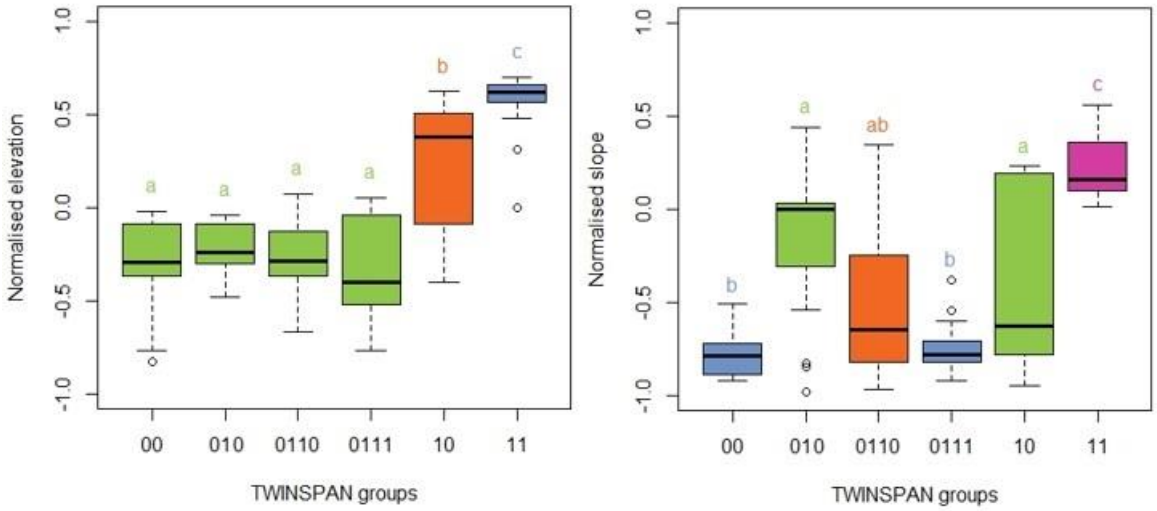

Figure 7. Normalised elevation and slope boxplots of the different TWINSPAN groups. Groups with different colours are significantly different.

4 DISCUSSION

During the vegetation mapping and the more detailed investigation, we found the earlier mentioned seven (i.e., subsection 3.1) plant associations (Zólyomi 1934, Járai-Komlódi 1960, Keszei–Takács 2008). The recorded relevés went under a TWINSPAN analysis, which resulted in six association groups. These groups overlap; the numerical analysis aggregates closely-related plant communities e.g., *Galio palustris–Caricetum rippariae* × *Glycerietum maximae* (0110) group. These two associations differ only in the dominant species. Our assumption is that the TWINSPAN method lowers the subjectivity of the expert-based description, and it provides more reliable data for further analyses. Beside the TWINSPAN analysis, other methods could be used and compared to classify the relevés.

The soil survey revealed different forms of Gleysols, which is the typical soil class of wet and wet-mesic meadows. The soil groups differed in nutrient contents, BD values, and VWCs, but not in pH, elevation, and PAK. Similar results are presented by Heil et al. (2008), but they found significant difference between soil groups and pH values. This is also supported by Ma et al. (2021) and Li et al. (2017). The soil groups spread among the TWINSPAN groups following a water gradient. Soils with more moisture content were found under more water tolerant TWINSPAN groups. Li et al. (2017) reported similar findings. The difference of the soil parameters of the TWINSPAN groups followed a similar pattern as in the case of WRB soil groups, except PAP, which showed significant difference only among the plant community groups. P content was found to be an important factor in plant composition of a site in several studies (Bigelow – Canham 2002, Amorim – Batalha 2007, Hammersmark et al. 2009, Mellado – Zamora 2015, Onur – Suha 2016). The plant associations follow the changes of the soil classes, but the finer pattern of the plant composition is not explained by the soil groups (Research question 1). The higher number of relevés and the periodical returns

to the same relevés could represent a more detailed relationship between the soils and plant communities. This can also help the land managers to set the optimal timing of mowing or grazing, e. g. only after the seeding of protected species.

The distribution of relevés according to their dominant species are organised along two gradients. The first axis represents soil porosity or wet to dry gradient. This axis separates the relevés of hollows, ditches, and the ones which are located on relatively elevated places. The species on the positive end of Axis 1 are typical species of mesic meadows, while the species around the origin are found in wet meadows. Jager et al. (2015) and Li et al. (2017) found soil physical parameters crucial for the distribution of plant communities. The second axis shows a nutrient uptake gradient. Generally, the higher pH values – in this context it means neutral pH levels – accompany the sites where the nutrient uptake is not limited by acidic pH. The positive correlation of the PAP, PAK levels and Axis 2 along with a negative relation with pH (H_2O) seems to be contradictious. The relevés affected by groundwater have lower pH values, which cause limited nutrient uptake, and the groundwater is usually richer in nutrients due to the fertilization of the adjacent arable lands. These processes can result in higher PAP, PAK or even TN levels than in relevés affected only rarely by groundwater. Species with higher nutrient needs occur on the negative end of this axis, while the positive values on this axis are accompanied by species which require lower nutrition levels. Groups of soil parameters show close relationship with the species composition of the study area, but soil physical parameters, therefore the water regime, seems to be a more fundamental factor than soil chemical characteristics (Research question 2). The larger number of relevés could result in a stronger connection between environmental and plan data.

The vegetation follows the changes in the microrelief of the sample areas (*Figure 6* and *Figure 7*). Differences in elevation in these areas are small. Between the highest and lowest point of the total area the difference in elevation is only 1.4 m. Even on the fields, the vegetation follows the 10–20 cm height differences. Where the surface rises "suddenly", the plant communities are arranged in stripes, and where the surface is nearly flat, they show a patchier arrangement. The analysis the DEM helped to make the correlation quantifiable between vegetation pattern and microtopography. Our findings support the results of Diamond et al. (2019) – as patch distribution is affected highly by the presence or by the lack of water. Some plant communities occur only in hollows and some are dry tolerant groups that were found on hummocks (Research question 3). Ladányi et al. (2016) described similar allocation of plant communities in a saline wetland. Future studies may use a higher spatial resolution DEM or even terrestrial laser scanning along with spatial statistics to find more fine-scaled relations.

Thus, it can be stated that the formation of different types of associations is highly dependent on the soil conditions of the area and can be closely related to it. However, in the formation of the fine mosaic pattern (in a lowland environment) the diversity of the microrelief and the differences in the period of flooding or saturated soil conditions play a crucial role (Jager et al. 2015, Li et al. 2017, Ma et al. 2021, Diamond et al. 2019, Diamond et al. 2020).

5. CONCLUSIONS

The present study examined the correlations between the characteristic soil types of the Hanság and Tóköz and the grassland plant associations that have developed on them. The soil classes of the sample areas and the physical and chemical properties of the topsoil were determined using laboratory tests. The plant associations of the areas and the microrelief categories produced from surface models showed close relationship. The patches of the

vegetation maps coincided with the hummock and hollows categories. The results of the plant association analysis were compared with the results of soil characteristics. We found that soil type determined the predominant vegetation type on a habitat level, but it is not responsible for the mosaic pattern formed by the associations. The distribution of the dominant species of the plant groups were closely determined by groups of soil parameters according to the CCA. We also found that the microrelief changes, and therefore the length of the saturated or flooded soil conditions, can be the reason behind the mosaic pattern of the vegetation pattern. According to our results, the vegetation follows the changes in the microtopography adequately, and it also indicates the minimal (10–20 cm) deviations reliably. Future studies should consider using more environmental parameters such as precipitation and groundwater fluctuation in multiple analyses.

Acknowledgements: Supported by the ÚNKP-20-3-II-29 New National Excellence Program of the Ministry for Innovation and Technology from the source of the National Research, Development and Innovation Fund.

REFERENCES

AMORIM, P. K. – BATALHA, M. A. (2007): Soil-vegetation relationships in hyperseasonal cerrado, seasonal cerrado, and wet grassland in Emas National Park (Central Brazil). Acta Oecologica 32: 319–327. https://doi.org/10.1016/j.actao.2007.06.003

BARTHA, D. – BIDLÓ, A. – KOVÁCS, G. – MARKOVICS, T. (1996): Termőhely és vegetáció kapcsolata a Bozsoki Zsidó-réten. [Interactions of site paramters and vegetation at the Zsidó-meadow at Bozsok (Hungary).] Erdészeti és Faipari tudományos Közlemények 40-41: 27–46. (in Hungarian)

BARTHOLY, J. – BIHARI, Z. – HORÁNYI, A. – KRÜZSELYI, I. – LAKATOS, M. – PIECZKA, I. – PONGRÁCZ, R. – SZABÓ, P. – SZÉPSZÓ, G. – TORMA, CS. (2011): Hazai éghajlati tendenciák. In: BARTHOLY, J. – BOZÓ, L. – HASZPRA, L. (ed.): Klímaváltozás-2011 / Klímaszcenáriók a Kárpát-medence térségére [Climate change–2011 / Climate scenarios of the Carpathian basin]. Magyar Tudományos Akadémia és az Eötvös Loránd Tudományegyetem Meteorológiai Tanszék, Budapest, pp: 145–169. (in Hungarian)

BEDFORD, B.L. – WALBRIDGE, M. R. – ALDOUS, A. (1999): Patterns in nutrient availability and plant diversity of temparate North American Wetlands. Ecology 80: 2151–2169. https://doi.org/10.2307/176900

BELLÉR, P. (2000): Talajvizsgálati módszerek [Methods of soil analysis]. Nyugat-Magyarországi Egyetem Kiadó, Sopron. 107 pp. (in Hungarian)

BERKI, I. – BIDLÓ, A. – BÖLÖNI, J. – VIG, P. (2019a): 38.1.2. Természetföldrajzi jellemzés [38.1.2. Geographical description]. In FÜHRER, E. (ed.): Magyarország erdészeti tájai. IV. Kisalföld erdészeti tájcsoport. [Forestry Region of Hungary IV. Kisalföld Forestry Region]. Agrárminisztérium Nemzeti Földügyi Központ, Budapest, Hungary, pp: 108-119 (in Hungarian)

BERKI, I. – BIDLÓ, A. – BÖLÖNI, J. – VIG, P. (2019b): 39.1.2. Természetföldrajzi jellemzés [39.1.2. Geographical description]. In FÜHRER, E. (ed.): Magyarország erdészeti tájai. IV. Kisalföld erdészeti tájcsoport. [Forestry Region of Hungary IV. Kisalföld Forestry Region]. Agrárminisztérium Nemzeti Földügyi Központ, Budapest, Hungary, pp: 184-198 (in Hungarian)

BIGELOW, S. W. – CANHAM, C. D. (2002): Community organization of tree species along soil gradient in a North-eastern USA forest. Journal of Ecology 90: 199–200. https://doi.org/10.1046/j.0022-0477.2001.00655.x.

BÍRÓ, M. – MOLNÁR, ZS. – ÖLLERER, K. – LENGYEL, A. – ULICSNI, V. – SZABADOS, K. – KIŠ, A. – PERIĆ, R. – DEMETER, L. – BABAI, D (2020): Conservation a herding cobenefit from traditional extensive wetland grazing. Agriculture. Ecosystems and Environment 300: 106983 https://doi.org/10.1016/j.agee.2020.106983

BORHIDI, A. (2003): Magyarország növénytársulásai [Plant associations of Hungary]. Akadémiai Kiadó, Budapest. 569 pp. (in Hungarian)

BORHIDI, A. – SÁNTA, A. (ed.) (1999): Vörös könyv / Magyarország növénytársulásairól 1-2. Környezetvédelmi Minisztérium Természetvédelmi Hivatalának Tanulmánykötetei [Red book on plant associations of Hungary], TermészetBÚVÁR Alapítvány Kiadó, Budapest, 362+404 pp. (in Hungarian)

BRAUN-BLANQUET, J. (1932): Plant sociology / the study of plant communities. McGraw-Hill Book Co., New York, London. 439 pp.

CHYTRÝ, M. – TICHÝ, L. – HOLT, J. – BOTTA-DUKÁT, Z. (2002). Determination of diagnostic species with statistical fidelity measures. Journal of Vegetation Science 13 (1): 79–90. https://doi.org/10.1111/j.1654-1103.2002.tb02025.x

DIAMOND, J. S. – MCLAUGHLIN, D. L. – SLESAK, R. A. – STOVALL, A. (2019): Pattern and structure of microtopography implies autogenic origins in forested wetlands, Hydrology and Earth System Sciences 23: 5069–5088. https://doi.org/10.5194/hess-23-5069-2019

DIAMOND, J. S. – MCLAUGHLIN, D. L. – SLESAK, R. A. – STOVALL, A. (2020): Microtopography is a fundamental organizing structure of vegetation and soil chemistry in black ash wetlands. Biogeosciences 17: 901–915. https://doi.org/10.5194/bg-17-901-2020

DURANEL, A. J. – ACREMAN, M. C. – STRATFORD, C. – THOMPSON, J. R. – MOULD, D. J. (2007): Assessing the hydrologicak suitability of floodplains for species–rich meadow restoration: a case study of the Thames floodplain, UK. Hydrology and Earth System Sciences 11: 170–179. https://doi.org/10.5194/hess-11-170-2007.

EGNÉR, H. – RIEHM, H. – DOMINGO, W.R. (1960): Untersuchungen über die chemische Bodenanalyse als Grundlage für die Beurteilung des Nährstoffzustandes der Böden. II. Chemische Extraktionsmethoden zur Phosphor- und Kaliumbestimmung. [Investigations of the chemical soil analysis as a basis for the assessment of the nutrient status of the soil. II. Methods of chemical extraction for phosphor- and potassiumdetermination.] Kungliga Lantbrukshögskolans Annaler 26:199–215. (in German)

FAO (2015): World Reference Soil Base for Soil Resources 2014, updated 2015 International soil classification system for naming soils and creating legends for maps (English). World Soil Resources Report No. 106. FAO, Rome, Italy, 109 pp.

FÜHRER, E. – HEIL, B. – HEILIG, D. –JAGODICS, A. – KOVÁCS, G. (2019a): 38.2.1. Termőhelyi viszonyok [38.2.1. Site parameters]. In FÜHRER, E. (ed.): Magyarország erdészeti tájai. IV. Kisalföld erdészeti tájcsoport. [Forestry Region of Hungary IV. Kisalföld Forestry Region]. Agrárminisztérium Nemzeti Földügyi Központ, Budapest, Hungary, pp: 123-135 (in Hungarian)

FÜHRER, E. – HEIL, B. – HEILIG, D. –JAGODICS, A. – KOVÁCS, G. (2019b): 39.2.1. Termőhelyi viszonyok [39.2.1. Site parameters]. In FÜHRER, E. (ed.): Magyarország erdészeti tájai. IV. Kisalföld erdészeti tájcsoport. [Forestry Region of Hungary IV. Kisalföld Forestry Region]. Agrárminisztérium Nemzeti Földügyi Központ, Budapest, Hungary, pp: 201-208 (in Hungarian)

HAMMERSMARKS, C. T. – RAINS, M. C. – WICKLAND, A. C. – MOUNT, J. F. (2009): Vegetation and watertable relationship in a hydrologically restored riparian meadow. Welands 29: 785–797. https://doi.org/10.1672/08-15.1

HENNEKENS, S. M. – SCHAMINÉE, J. H. J. (2001): TURBOVEG, a comprehensive data base management system for vegetation data. Journal of Vegetation Science 12 (4): 589–591. https://doi.org/10.2307/3237010

HU, S. – NIU, Z. – CHEN, Y. – LI, L. – ZHANG, H. (2017): Global wetlands: Potential distribution, wetaland loss, and status. Science of Total Environment 586: 319–327. https://doi.org/10.1016/J.scitotenv.2017.02.001

ISO 10694:1995 (1995): Soil Quality–Determination of Organic and Total Carbon Content after Dry Combustion (Elementary analysis, Internation Organization for Standardization: Deneva, Switzerland

ISO 13878:1998 (1998): Soil Quality–Determination of Total Nitrogen Content after Dry Combustion (Elementary analysis, Internation Organization for Standardization: Deneva, Switzerland

JAGER, N. R. D. – ROHWEDER, J. J. – YAO, Y. – HOY, E. (2015): The Upper Mississippi River Floodscape: Spatial Patterns of Flood Inundation and Associated Plant Community Distributions. Applied Vegetation Science 19: 164–172. https://doi.org/10.1111/avsc.12189.

JANISOVA, M. – UJHÁZY, K. – UHLIAROVA, E. (2013): Phytosociology and ecology of Avenual adsurgens subsp. adsurgens in Carpathian grasslands. Tuxemia 33: 371–398.

JANSSENS, F – PEETERS, A. – TALLOWIN, J. – BAKKER, J – BEKKER, R. FILLAT, F. –OOMES, M. (1998): Relationship between soil chemical factors and grassland diversity. Plant and Soil 202: 69–78. https://doi.org/10.1023/A:1004389614865

JÁRAI-KOMLÓDI M. (1960): Beiträge zur Kenntnis der Vegetation des Moorgebiets Hanság. – Annales Universitatis Scientiarum Budapestinensis de Rolando Eötvös Nominatae. Sectio Biologica 3: 229–234. (in German)

JOSSELYN, M. N. – FAULKNER, S. P. –PATRICK, W. H. (1990): Relationships between seasonally wet soils and occurrence of wetland plants in California. Journal: Wetlands 10: 7–26. https://doi.org/10.1007/BF03160820

KESZEI B. – TAKÁCS G. (2008): A HUFH30005 Hanság (Észak-Hanság) Natura 2000 terület élőhely-térképezése. – Kutatási jelentés [Habitat maps of HUFH30005 Hanság (North-Hanság) Natura 2000 area], Fertő-Hanság Nemzeti Park Igazgatóság, Sarród, 45 pp. (in Hungarian)

KIRÁLY, G. (ed.) (2009): Új magyar füvészkönyv. Magyarország hajtásos növényei. Határozókulcsok. [New Hungarian Herbal. The Vascular Plants of Hungary. Identification key] – Aggteleki Nemzeti Park Igazgatóság, Jósvafő. 616 pp. (in Hungarian)

HEIL, B. – KOVÁCS, G. – BIDLÓ, A. – ILLÉS, G. (2006): A dél-hansági láprekonstrukciót megalapozó termőhelyi vizsgálatok. [Foundational site survey before the wetland restoration in Southern Hanság] In: SIMON, L. (ed.): Talajvédelem különszám. 81–88. (in Hungarian)

KOVÁCS, M. (1957): Magyarország láprétjeinek ökológiai viszonyai (talaj- és mikroklíma-viszonyok) [Ecological conditions of the bogs of Hungary (soil and microclimate conditions]. A Magyar Tudományos Akadémia Biológiai Tudományok Osztályának Közleményei 1 (3-4): 387-454+2 táblázat. (in Hungarian)

LADÁNYI, Z. – BLANKA, V. – ÁRON, J. D. – RAKONCZAI, J. – MEZŐSI, G. (2016): Assessment of soil and vegetation changes due to hydrologically driven desalinization process in an alkaline wetland, Hungary. Ecological Complexity 25: 1–10. https://doi.org/10.1016/j.ecocom.2015.11.002.

LEGENDRE, P – LEGENDRE, L. (2012): Numerical Ecology, Third English edition. Elsevier. Amsterdam, The Netherlands. 625–673.

LENGYEL, A. – ILLYÉS, E. – BAUER, N. – CSIKY, J. – KIRÁLY, G. – PURGER, D. – BOTTA –DUKÁT, Z. (2016): Classification and syntaxonomical revision of mesic and semi-dry grasslands in Hungary. Preslia 88: 201–228.

LI, J. – CHEN, Q. – LI, Q. – ZHAO, C. – FENG, Y. (2021): Influence of plants and environmental variables ont he diversity of soil microbial communities in the Yelow River Delta Wetland, China. Chemosphere 274: 129967. https://doi.org/10.1016/j.chemosphere.2021.129967.

LI, W. – CUI, L. – SUN, B. – ZHAO, X. – GAO, C. – ZHANG, Y. – PAN, X. – LEI, Y. – MA, W. (2017): Distribution patterns of plant communities and their associations with environmental soil factors on the eastern shore of Lake Taihu, China. Ecosystem Health and Sustainability 3 (9): 1385004. https://doi.org/10.1080/20964129.2017.1385004

MA, M. – ZHU, Y. – ZHAO, N. (2021): Soil nutrient and vegetation patterns of alpine wetlends ont he Qinghai-Tibetian Plateau. Sustainability 13: 6221. https://doi.org/10.3390/su13116221

MELLADO, A. – ZAMORA, R. (2015): Spatial heterogenity of a parasitic plant drives the seed-dispersial patterns of zoochorous plant community in a generalist dispersal system. Functional Ecology 30: 459–467. https://doi.org/10.1111/1365-2435.12524.

MICHENER, M. C. (1983): Wetland site index for summarizing botanical studies. Wetlands 3: 180–191. https://doi.org/10.1007/BF03160740

ONUR, S. – SUHA, B. (2016): Crop yield prediction under soil salinity using satellite derived vegetation indices. Field Crop Research 192: 134–143. https://doi.org/10.1016/j.fcr.2016.04.028.

OKSANEN, J. – BLANCHET, F.G. – FRIENDLY, M. – KINDT, R. – LEGENDRE, D. – MCGLINN, D. – MINDCHIN, P.R. – O'HARA, B. – SIMPSON, G.L. – SOLYMOS, P. – STEVENS, M.H.H. – SZOECS, E. – WAGNER H. (2020): vegan: Community Ecology package. R package version 2.5-7.

PENNINGTON, M. R. – WALTERS, M. B. (2006): The response of planted trees to vegetation zonation and soil redox potential in created wetlands. Journal: Forest Ecology and Management. 233: 1–10. https://doi.org/10.1016/j.foreco.2006.04.026

RAJKAI, K. (1978): A talaj vízgazdálkodása és a természetes vegetáció közötti kölcsönhatás vizsgálata a Szilas-patak árterén [Investigation of the interaction between soil hydrology and natural vegetation of the Szilas-brook]. Agrokémia és Talajtan 27 (1-2): 31-48. (in Hungarian)

R CORE TEAM (2014): R: A language and environment for statistical computing. R Foundation for Statistical Computing, Vienna, Austria.

ROLEČEK, J. – TICHÝ, L. – ZELENÝ, D. – CHYTRÝ, M. (2009): Modified TWINSPAN classification in which the hierarchy respects cluster heterogeneity. Journal of Vegetation Science 20 (4): 596–602. https://doi.org/10.1111/j.1654-1103.2009.01062.x

SCOTT, M. L. – SLAUSON, W. L. – SEGELQUIST, C.A. – AUBLE, G. T. (1989): Correspondence between Vegetation and Soils in Wetlands and Nearby Uplands. Wetlands 9 (1): 41–60. https://doi.org/10.1007/BF03160767

SEABLOOM, E.W. – ADLER, P. B. – ALBERTI, J. – BIEDERMAN, L. – BUCKLEY, Y. M. – CADOTTE, M. W. – COLLINS, S.L. – DEE, L. – FAY, P. A. – FIRN, J. – HAGENAH, N. – HARPOLE, W. S. – HAUTIER, Y. – HECTOR, A. – HOBBIE, S. E. – ISBELL, F. – KNOPS, J. M. H. – KOMATSU, K. J. – LAUNGANI, R. – MACDOUGALL, A. – MCCULLEY, R. L. – MOORE, J. L. – MORGAN, J. W. – OHLERT, T. – PROBER, S. M. – RISCH, A. C. – SCHUETZ, M. – STEVENS, C. J. – BORER, E. T. (2020): Increasing effects of chronic nutrient enrichment on plant diversity loss and ecosystem productivity over time. Ecology 102: e03218. https://doi.org/10.1002/ecy.3218

STEFANOVITS, P. – FILEP, GY. – FÜLEKY, GY. (2010): Talajtan [Soil science]. Mezőgazda Kiadó, Budapest. 470 pp. (in Hungarian)

SWACHA, G. – BOTTA-DUKÁT, Z. – KĄCKI, Z. – PRUCHNIEWICZ, D. – ŻOØNIERZ, L. (2018): The effect of abandonment on vegetation composition and soil properties in Molinion meadows (SW Poland). PLoS ONE 13 (5): e0197363. https://doi.org/10.1371/journal.pone.0197363

TASI, J. – BAJNOK, M. – HALÁSZ, A. – SZABÓ, F. – HARKÁNYINÉ SZÉKELY, ZS. – LÁNG, V. (2014): Magyarországi komplex gyepgazdálkodási adatbázis létrehozásának első lépései és eredményei [Results and the first steps of the creation of the database on complex grassland management in Hungary]. Gyepgazdálkodási Közlemények 1-2: 57–64. (in Hungarian)

TELBISZ, T – SZÉKELY, B. – TIMÁR G. (2013): Digitális Terepmodellek [Digital Terrain Models]. Eötvös Loránd Tudományegyetem, Természettudományi Kar, Földrajz- és Földtudományi Intézet, Természetföldrajzi Tanszék, Budapest. 80 pp. (in Hungarian)

TICHÝ, L. (2002): JUICE, software for vegetation classification. Journal of Vegetation Science 13 (3): 451-453. https://doi.org/10.1111/j.1654-1103.2002.tb02069.x

ZÓLYOMI B. (1934): A Hanság növényszövetkezetei (összefoglalás). [Plantassociations of Hanság (Summary)] – Vasi Szemle 1: 146–174. (in Hungarian)

https://doi.org/10.37045/aslh-2021-0007 Acta Silv. Lign. Hung., Vol. 17, Nr. 2 (2021) 105–119

Mapping Forest Cover Changes using Sentinel-2A Imagery in the Municipality of Zubin Potok, Republic of Kosovo

Ferat KRASNIQI[a*] – Géza KIRÁLY[b]

[a] Department of Geography, Faculty of Mathematics and Natural Sciences, University of Prishtina "Hasan Prishtina", Prishtina, Kosovo
[b] Institute of Geomatics and Civil Engineering, Faculty of Forestry, University of Sopron, Sopron, Hungary

Abstract – This research aimed to investigate the changes in forest cover, utilizing Sentinel-2A imagery data. Annual results of deforestation, non-forest, and forest area in the Municipality of Zubin Potok (Kosovo) between 2016 and 2017 were presented and analyzed by applying the image difference change detection method on a Normalized Difference Vegetation Index (NDVI) product derived for both years. The study reveals that forest coverage in this municipality has changed due to human activity (harvested and burnt forests). The footprint of changes was evidenced by using Sentinel 2A band combinations and very high resolution (VHR) images available in Google Earth (GE). From the overall forest-covered area of 24,873.61 hectares, the detected changes during the annual period are as follows: 24,423.57 ha or 98.19 % is mapped as forest, 113.75 hectares or 0.46 % as non-forest, and 336.77 or 1.35 % of the area forest is mapped as deforestation. These results can be used to identify human-made deforestation and to develop monitoring forest plans for the coming years.

deforestation / reforestation / vegetation indexes / change detection / sample design / accuracy assessment

Kivonat – Az erdőterület-változása Sentinel-2A űrfelvételek alapján Zubin Potok község határában, Koszovóban. A tanulmány Sentinel-2A műholdfelvételek alapján egy erdősült terület változását vizsgálja. Az erdőterület éves változását 2016 és 2017 között Zubin Potok (Koszovó) községhatárában mutatja be és elemzi a felvételek vegetációs index (NDVI) alapú változása alapján. A tanulmány megállapítja az emberi tevékenység (fakivágás) és az erdőtűz okozta területváltozásokat a községhatárban. A változásokat a Sentinel-2A űrfelvétel és a Google Earth (GE) felvételek egyértelművé teszik. A teljes 24 873,61 hektáros erdőterületből az éves időszakban észlelt változások a következők: 24 423,57 ha vagy 98,19 % erdőként, 113,75 hektár vagy 0,46 % nem erdőként és 336,77 vagy 1,35 % -a az erdőt erdőirtásként ábrázolják. Ezek az eredmények felhasználhatók az ember által okozott erdőirtások azonosítására és a következő évekre vonatkozó erdőterv kidolgozására.

erdőirtás / erdőfelújítás / vegetációs indexek / változás vizsgálata / mintavétel kialakítása / pontosság-vizsgálat

*Corresponding author: ferat.krasniqi@uni-pr.edu; XKX-10000 PRISHTINA, Mother Theresa-Street, N.N, Republic of Kosovo.

1 INTRODUCTION

Recently, the increased amount of imagery data coming from remote sensing technology empowered the science community and beyond to study and research important aspects of land cover and use changes on the living environment. Information on land cover and land use change inventory are essential data for different environmental issue implementations such as; deforestation, estimated devastations, disaster observations, urban growth, land management, and land planning (Hussain et al. 2013). According to Achard et al. 2009, INPE 2014, FAO, JRC, SDSU, and UCL 2009 as cited in (Hojas-Gascón et al. 2015) "for more than a decade the monitoring of deforestation has successfully been carried out at regional levels using medium-spatial resolution satellite data, predominantly from the Landsat sensor, which has 30 m spatial resolution and a revisit frequency of 16 days". In 1997, the World Resources Institute (WRI) founded the Global Forest Watch (GFW) as an initiative for forest frontiers, reporting only on a few pilot countries at the beginning until growing as an online global platform that provides data and tools for anyone to enter and obtain information on how and where forest cover is changing (WRI 2019).

Another valuable online inventory of the land cover product is Copernicus – the European Union's Earth Observation Programme, served by imagery data from the Sentinel satellite family. The Copernicus Land Monitoring Service (CLMS) delivers spatial information on land cover use and its changes, vegetation, and other products in the field of environmental land applications to a wide array of clients in Europe and across the world (EEA 2018).

Various image transformation indexes among spectral bands of various satellite sensors have been created for monitoring vegetation status on a continental and global scale including the most broadly applied Normalized Difference Vegetation Index (NDVI) using the Advanced Very High Resolution Radiometer (AVHRR) sensor on board the NOAA series of satellites (CCRS 2019) and Moderate Resolution Imagine Spectroradimeter (MODIS) sensors on the Terra and Aqua satellites. These both have high temporal resolution (one day revisit time) and their reflectance data are convenient for time series vegetation dynamic analysis at regional and global scales. However, due to their very coarse spatial resolution of 1 km (AVHRR) and 250 m (MODIS), the investigation of phenological dynamics is problematic for finer or local scale vegetation status monitoring (Walker et al. 2012).

Furthermore, Landsat series of satellites provides the longest and richest archive (over 40 years) of systematically collected remotely sensed data (Goward et al. 2006) with valuable information and possibilities for enhanced knowledge of methods and extents of past forest changes and recovery (Banskota et al. 2014). In addition, a 30 m spatial resolution and 16-day repetitive temporal resolution makes Landsat data well suited for land cover monitoring of the Earth's surface (Gillanders et al. 2008). Concerning the diverse possibility of remotely sensed data from both optical and radar sensors, monitoring an environmental phenomenon employing temporal and spatial resolutions of the data is reduced to five days and higher spatial resolution to 10 m with the launch of the Sentinel-2 mission by ESA in June 2015. In remote sensing (RS) technology, the common intention of the change detection approach is to point out the geographic position of land cover changes, change calculation, and map result validation (Coppin et al. 2004, Im - Jensen 2005, Macleod - Congalton 1998).

The Normalized Difference Vegetation Index (NDVI) is a widely used vegetation index because it is useful in remotely sensed data calculation (Huete − Liu 1994) and strongly revealed global vegetation cover monitoring in the past two decades (Leprieur et al. 2000). According to Singh (1989), change detection is "the process of identifying differences in the state of an object or phenomenon by observing it at different times". Brothers and Fish as well as Malila and Singh, as cited (Macleod − Congalton 1998), reported: "four aspects of change

detection are important when monitoring natural resources: (1) detecting that changes have occurred, (2) identifying the nature of the change, (3) measuring the areal extent of the change, and (4) assessing the spatial pattern of the change". For improved understanding, the change detection method types are grouped into seven categories: 1. algebra, 2. transformation, 3. classification, 4. advanced models, 5. Geographical Information System GIS approaches 6. visual analysis, and 7. other approaches (Lu et al. 2004b). The change detection technique is one of the key implementations in remote sensing (RS), moreover using bi-temporal or multi-temporal data imagery (Campbell – Wynne 2011). According to Singh (1989, p. 990), "there are two basic approaches for change detection; (1) comparative analysis of independently produced classification for different dates and (2) simultaneous analysis of multi-temporal data". The image difference technique requires two accurately co-registered image data sets in order to generate a new subtracted image, the values of which indicate the changes (Hussain et al. 2013). Although different change detection techniques are currently available, they are difficult and require choosing an appropriate algorithm to achieve change detection results practically (Lu et al. 2004). Therefore, defining an appropriate threshold for mapping class change category is one of the most critical steps (Lu et al. 2005). The application of image thresholding in computer vision is to segment the objects based on the image pixel intensities by using a grayscale image as input and threshold, and the result is a binary image.

Checking accuracy assessment is an essential part of any project that deals with remotely sensed data. Many reasons that emphasize the significance of the accuracy assessment exist: "1) the need to know how well you are doing and to learn from your mistakes; 2) the ability to quantitatively compare methods; and 3) the ability to use the information resulting from your spatial data analysis in some decision-making process" (Congalton 2001, p. 321).

An error matrix table successfully describes a precise classification map by containing commission and omission mistakes. A commission error indicates the pixels or areas are wrongly assigned to that map category, while an omission error represents the pixels or areas correctly assigned to that map category (Congalton − Green 2009). Use of the error matrix table is also possible to calculate other measures of classification change validation such as overall accuracy as well as produce and user accuracy (Story − Congalton 1986).

The existing literature on the status of forest monitoring using remotely sensed data is quite applicable. Deforestation and reforestation are common environmental topics across the world. The direct human cause of forest land transformation to a non-forested land was defined as deforestation and the transformation of non-forest land (which was previously covered under forests) into the human-induced forest through the planting of seedlings, or the planting of natural seeds is defined as reforestation (UNFCCC 2002).

Based on the National Forest Inventory Kosovo 2012 Report (Tomter et al. 2013), forests cover an area of 481,000 hectares or 44.7 % of the total country land area, which is dominated by deciduous forest (93 %), coniferous forest (5 %), and mixed forest (2 %). Concerning the status of Kosovo loggings, according to this report, the annual permitted logging level allowed is about 1.4 million m^3. This level was exceeded by an estimated 1.6 million m^3 of annual loggings. In addition, 7% of loggings were conducted according to forest legislation and around 12,200 hectares, or 2.5 % of the total forest areas, were severely burned. The data analyzed from this report constitute the reason for increased study of the state of forests in Kosovo. Therefore, we have decided to investigate the forest changes in a one-year difference (2017-2016) in this study area and address the following research objectives: How can deforestation be detected and mapped? How can non-forested areas that have been previously deforested be detected and mapped? Is there any human intervention involved in the reforestation?

2 MATERIALS AND METHODS

2.1 Study area

Defining the study area was one of the research challenges. The forest area examined for this study is located in the municipality of Zubin Potok in the northern part of the Republic of Kosovo, located between the latitudes 42° 48.507'N and 43° 2.120'N and longitudes 20° 29.076'E and 20° 47.839'E. The area extends over 333 km^2 and has a population of 6,616 (KSA 2013). In its southern part, this municipality borders Istog and Skënderaj, while in its eastern part it borders Zveçan. Its entire western part borders Serbia (*Figure 1*). The area is characterized by mainly mountainous relief and scattered settlements. Its main economic branch is agriculture. The area is also home to an artificial accumulation of the lake of Ujman (Gazivoda). In addition to being of great importance for the municipality and the country, the lake is one of the largest artificial lakes in Kosovo with an extended surface of 9 km^2.

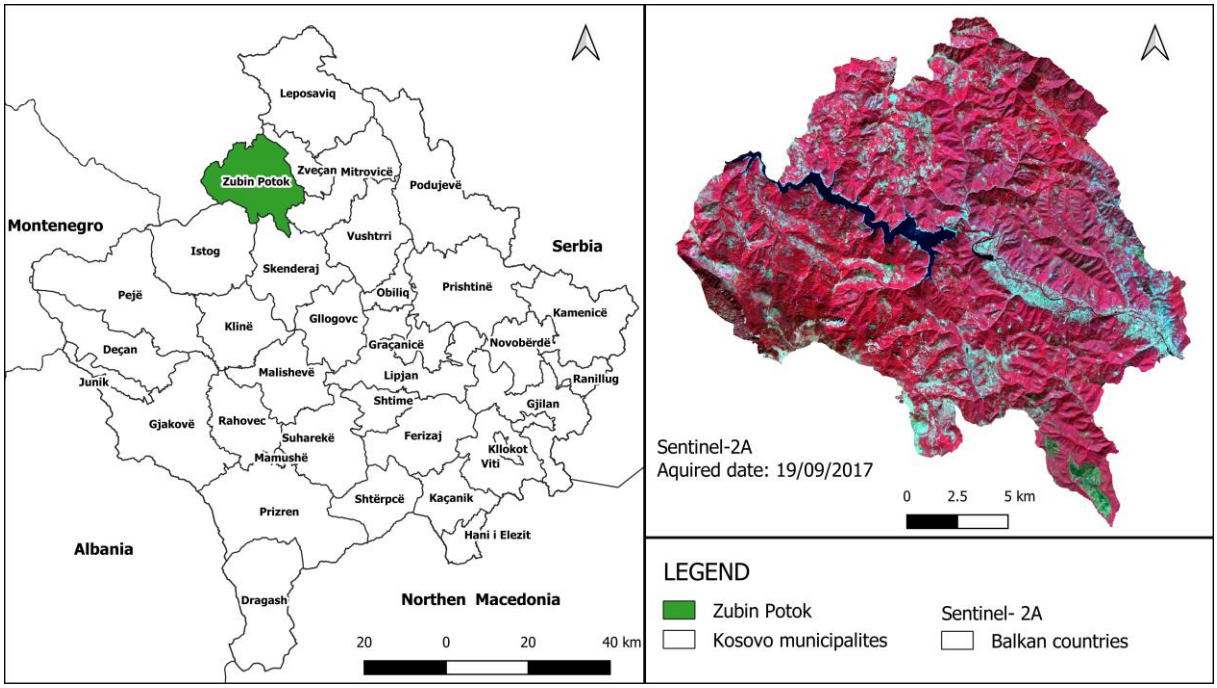

Figure 1. The geographical location of the study area in Kosovo (left), and Sentinel 2A color composite map (right). The map to the right of Figure 1 used in this study is a color composite image of these bands combination: NIR, RED, and GREEN. The red color on the map indicates forest vegetation; the green color represents deforestation, the blue color represents the water surface, the cyan, and other colors represent the surfaces not covered with forests (settlements, roads, bare land, agricultural areas, etc.).

According to CLC (CORINE Land Cover), 2018 inventory (EEA, 2018), 24,850.32 hectares (77.43 %) of the total area of the municipality – 33,385.6 ha (100 %) – is forest covered (deciduous, coniferous, and mixed), 3,207.28 ha (9.61 %) is semi-forested (meadows and shrubs), 4,133.42 hectares (12.38 %) are agricultural, 774.21 ha (2.32 %) waters (lakes and rivers), and 129.32 ha (0.39 %) of the surface is a built-up area.

2.2 Imagery Data and their Processing

The multi-spectral imagery data set of Sentinel satellite platforms 2A has been used as a primary source. Two cloud-free images were selected from 15/08/2016 and 19/09/2017 and

downloaded from the Copernicus Data and Information Access Services (DIAS) via the Mundi web services platform (https://mundiwebservices.com/). Sentinel-2A satellite has 13 spectral bands from visible through near-infrared to shortwave infrared: four image bands at 10 m, six bands at 20 m, and three other bands at 60 m spatial resolution (ESA 2015).

Table 1. The spatial and spectral resolution of Sentinel 2-A bands

Band number	Band name	Spatial resolution (m)	Central wavelength (nm)	Bandwidth (nm)
2	Blue	10	492.4	98
3	Green		559.8	45
4	Red		664.6	38
8	NIR		832.8	145
5	Vegetation Red Edge (VRE)	20	704.1	19
6	Vegetation Red Edge (VRE)		740.5	18
7	Vegetation Red Edge (VRE)		782.8	28
8a	Vegetation Red Edge (VRE)		864.7	33
11	SWIR		1613.7	143
12	SWIR		2202.4	242
1	SWIR	60	442.7	27
9	SWIR		945.1	26
10	SWIR		1373.5	75

Source: (https://earth.esa.int/web/sentinel/user-guides/sentinel-2-msi/resolutions/radiometric)

The Sentinel-2 mission is a constellation of two satellites (Sentinel-2A and Sentinel-2B) that provide high-resolution optical imagery on global coverage of Earth's land surface. Every ten days it revisits every single satellite and every five days with the combined constellation of the second satellite, making the data of great use for land monitoring studies (Addabbo et al. 2016).

Processing Level-1C and Level-2A of MSI Sentinel 2A products are freely available to users. The Level-2A processing of MSI Sentinel-2A data contains a Scene Classification and an Atmospheric Correction applied to Top-Of-Atmosphere (TOA) Level 1C orthoimage products (ESA 2015). The main output is an orthoimage Bottom-of-Atmosphere (BOA) corrected reflectance product, resampled and generated with an equal spatial resolution for all bands, and it can be used at the request of users in three levels of spatial resolution: 10 m, 20 m, and 60 m (ESA 2015). The metadata of Sentinel-2A, such as a product item, spacecraft name, processing level, product type delivered, and the date of acquired imageries is described in *Table 2*.

Table 2. Main metadata of the selected Sentinel-2A imageries

Product	Spacecraft name	Processing level	Acquisition time
S2A_MSIL2A_20160815T093042_S0100_R136_T34TDN_20160815T093218	Sentinel – 2A	Level-2A	2016-08-15
S2A_MSIL2A_20170919T093031_N0205_R136_T34TDN_20170919T093732	Sentinel – 2A	Level-2A	2017-09-19

2.3 Methodology

To complete the research objective, the following methodology was applied. A 10 m spatial resolution of Level-2A of MSI Sentinel-2A spectral bands: 2 (Blue), 3 (Green), 4 (Red), and 8 (NIR) covering the study area downloaded. Spatial and spectral subset and layer stacking of an orthoimage Sentinel-2A corrected reflectance images was realized by the raster tool in QGIS. The Sentinel-2A bands 4 (RED) and band 8 (NIR) that belong to the visible and near-infrared (VNIR) electromagnetic spectrum were selected for further use. $NDVI_{2016}$ and $NDVI_{2017}$ maps creation is the main step to proceed further with change detection analysis. NDVI is calculated by dividing the surface reflectance difference between near-infrared (NIR; 0.842 μm), and visible red (R; 0.665 μm) spectral bands by their sum, given in a value between -1 and 1 (Tucker et al. 1985):

$$NDVI = (NIR–R) / (NIR+R) \quad (1)$$

To conduct change detection analysis in the forest area, the following tasks such as image difference, image threshold, and refinement of the change detection results, were undertaken by using the Image Change Workflow tool in ENVI 5.3 software. The image difference method could be performed directly on a single band image or a single transformation image. The formula to calculate the difference change image is:

$$dNDVI_{(2016\text{-}2017)} = NDVI_{2016} – NDVI_{2017} \quad (2)$$

An image difference algorithm was applied by subtracting $NDVI_{2016}$ from $NDVI_{2017,}$ to create a difference NDVI ($dNDVI_{2016\text{-}2017}$) map. To detect and map the changes in the forest area, Otsu's threshold algorithm by auto-default settings is applied on the $dNDVI_{(2016\text{-}2017)}$ grayscale image. Otsu (1979) introduced the discriminant criterion η as a ratio between-class variance and total variance (total = between-class + within-class variance). He proved that the optimal threshold k maximizes the ratio η or equivalently maximizes the between-class variance. The equation below describes the calculation of the threshold using two options:
Within class variance:

$$\sigma_\omega^2(t) = \omega_0(t)\sigma_0^2(t) + \omega_1(t)\sigma_1^2(t) \quad (3)$$

Where ω_0 and $\omega_1$are the probabilities of the two clusters separated by a threshold (t), σ_0^2 and σ_1^2 are the class variances. From the L bins of the histogram is computed the class probability $\omega_{0,1}(t)$:

$$\omega_0(t) = \sum_{i=0}^{t-1} p(i) \quad (4)$$

$$\omega_1(t) = \sum_{i=t}^{L-1} p(i) \quad (5)$$

Between class variance:

$$\sigma_b^2(t) = \omega_0(t)\omega_1(t)[\mu_0(t) - \mu_1(t)]^2 \quad (6)$$

Where, ω express class probabilities; μ express class means. The class means $\mu_0(t)$, $\mu_1(t)$ and μ_T are computed:

$$\mu_0(t) = \frac{\sum_{i=1}^{t-1} ip(i)}{\omega_0(t)} \tag{7}$$

$$\mu_1(t) = \frac{\sum_{i=1}^{L-1} ip(i)}{\omega_1(t)} \tag{8}$$

$$\mu_T = \sum_{i=t}^{L-1} ip(i) \tag{9}$$

There is a possibility that all the following relations can be easily verified:

$$\begin{gathered} \omega_0\mu_0 + \omega_1\mu_{1=}\mu_T \\ \omega_0 + \omega_1 = 1 \end{gathered} \tag{10}$$

Repetitively the calculation of class means and class probabilities can be done. This brings an effective algorithm:

1. Compute the histogram and intensity level probabilities
2. Initialize $\omega_1(0)\ and\ \mu_1(0)$
3. Iterate through all possible thresholds: $t = 1, \ldots$ max. intensity
   3.1. Update ω_1 and μ_1
   3.2. Compute $\sigma_b^2(t)$
4. The max. $\sigma_b^2(t)$ value is the final threshold.

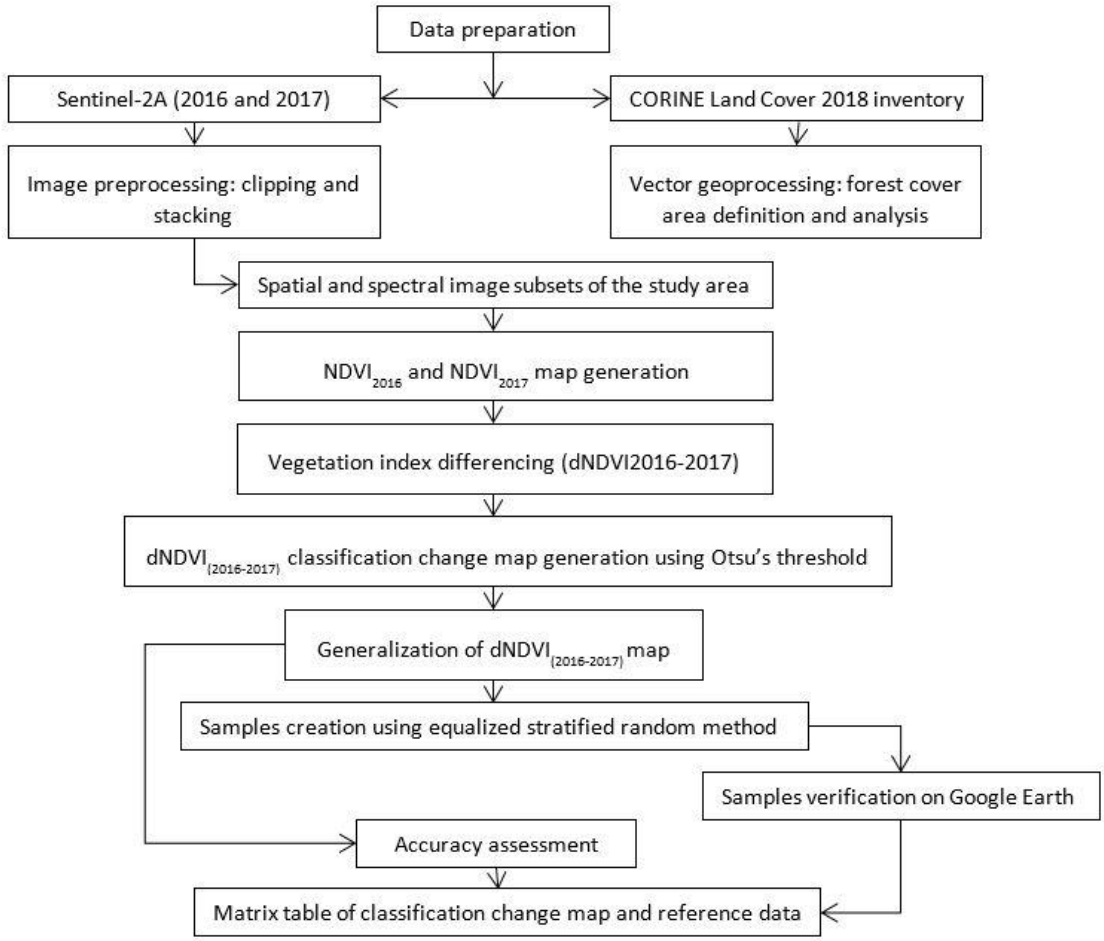

Figure 2. Flowchart depicting the working methodology in this research

3 RESULTS AND ANALYSIS

This paper analyzed forest cover changes in the Municipality of Zubin Potok from 2016 to 2017 by utilizing the vegetation index difference method of change detection algebra technique on the Sentinel-2A imagery data. Result interpretation is described in the following chapters.

3.1 NDVI maps

In this study, the RED (4) and NIR (8) bands of the Sentinel- 2A at 10m spatial resolution were used to generate $NDVI_{2016}$ and $NDVI_{2017}$ maps using the NDVI equation (1). In practice, water bodies, bare ground, artificial features, and other non-vegetative areas correspond below 0.1 NDVI values; and higher values indicate a higher photosynthetic activity such as shrubs, grasslands, crops, temperate, and tropical forest (Meneses-Tovar 2011/12).

Table 3. Normalized difference vegetation indexes ($NDVI_{2016}$ and $NDVI_{2017}$) basic statistics

Statistics	NDVI 2016	NDVI 2017
Minimum	-0.98	-0.88
Mean	0.86	0.84
StdDev	0.08	0.11
Maximum	0.99	1.00

Table 3 presents the basic statistics of $NDVI_{2016}$ and $NDVI_{2017}$ maps, such as minimum, mean, standard deviation, and maximum.

Figure 3 presents the $NDVI_{2016}$ and $NDVI_{2017}$ maps, and their values indicate the spatial distribution differences of forest cover between years. The color ramp from yellowish to reddish of the $NDVI_{2017}$ map in the southeastern part of the study indicates the area with negative values or no vegetation due to fires or forest cutting by human activity. However, more detailed interpretations of the NDVI maps will be explained by applying the vegetation index difference method.

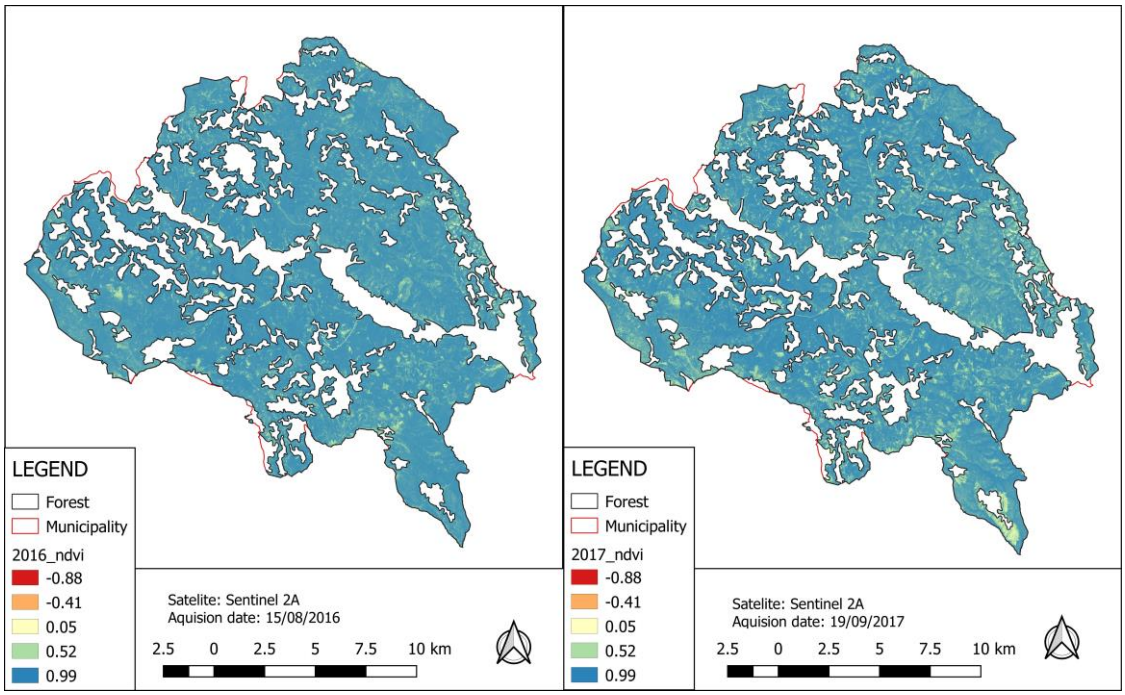

Figure 3. The Normalized difference vegetation indexes - $NDVI_{2016}$ (left) and $NDVI_{2017}$ maps (right) of the study area

3.2 Difference NDVI maps

By applying the image difference method on NDVI pairs, the result is the image difference NDVI output. The color ramp of the difference image $dNDVI_{2016\text{-}2017}$ map presented in *Figure 5* reveals the different intensity of pixels which indicate the differences in vegetation condition between annual years, either forest loss or forest growth. The histogram of the newly created difference image has both negative and positive pixel values. Pixels with negative and positive values indicate the changing area by scattering on the edges of the distribution curve (Singh 1989) when pixels with zero or close to zero values indicate unchanged by scattering around the zero (Lu et al. 2005). *Figure 4* shows the distribution curve of difference image $dNDVI_{(2016\text{-}2017)}$, while table 4 shows the basic statistics of difference $dNDVI_{(2016\text{-}2017)}$.

Table 4. Difference of $NDVI_{2016}$ and $NDVI_{2017}$ basic statistics

Minimum	Mean	StdDev	Maximum
-0.84	-0.01	0.05	1.02

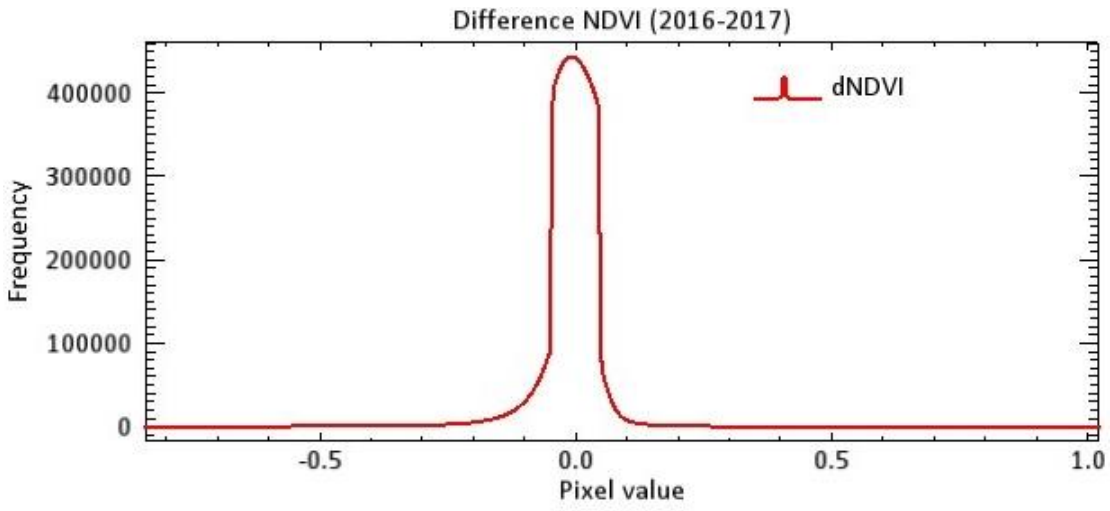

Figure 4. Histogram of $dNDVI_{(2016\text{-}2017)}$ map

3.3 Change classification map

The left map in *Figure 5* shows the spatial distribution of the $dNDVI_{(2016\text{-}2017)}$, and the map on the right of the figure determines the classification change forest in this study by selecting Otsu's automatic threshold. Of the three categories classes mapped inside the forest area, the forest class indicates the non-changed forest areas, the non-forest shows the previously deforested areas, and the deforestation class indicates cut-out forest areas between the years.

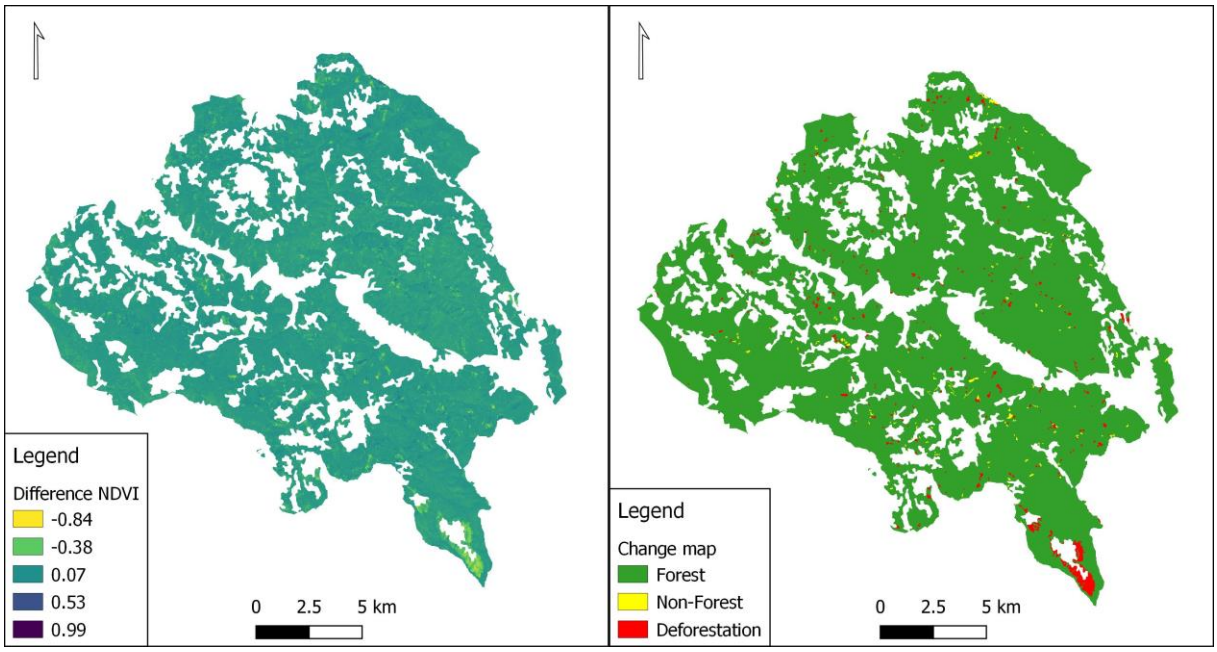

Figure 5. Difference NDVI$_{(2016-2017)}$ map (left) and classification change map (right)

Table 5 shows the distribution of these three classes. Forest class covers the most class area with 98.19%, the non-forest class has the least with 0.46%, and deforestation class covers 1.35% of the total area and represents clear-cutting forest activity. Also, the description of the sampling size for each category class is in included in this table.

Table 5. Map category and sample size statistics

Class name	Classification statistics		Sample size	
	Area (*ha*)	Percent (%)	Number per class	Total (%)
Forest	24423.57	98.19	50	33.33
Non-Forest	113.27	0.46	50	33.33
Deforestation	336.77	1.35	50	33.33
Total	24873.61	100.00	150	100

3.4 Sampling sites and verification

Without the possibility of verifying field classification samples, time series of very high resolution (VHR) images on the Google Earth platform were utilized. All the category class samples (150) were covered with images in Google Earth and verified in the periods before and after the detection of forest cover changes (August 2016 - September 2017). In *Figure 6*, the yellow polygons represent the areas covered with forests in 2016, while the polygons in *Figure 7* visually show the temporary removal of forest cover due to clear-cut. In *Figure 8*, the yellow polygons in the vast majority show the areas not covered with forests in 2016 that were deforested previously. On the other hand, in *Figure 9*, the yellow polygons clearly indicate that no artificial reforestation activities have occurred.

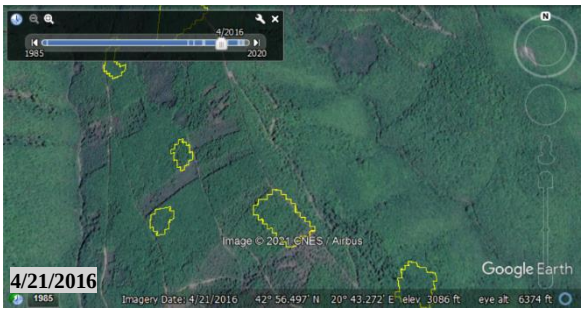

Figure 6. Yellow polygons indicate the forested area in 2016, visualized in GE

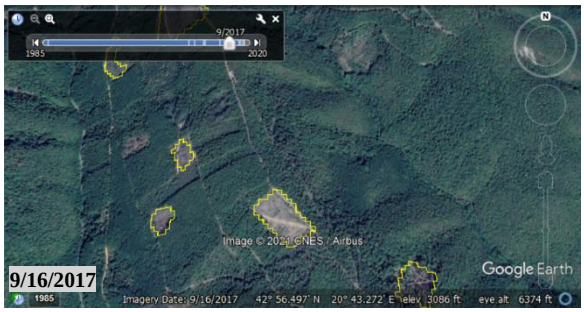

Figure 7. The clear-cut forested areas in 2017, interpreted and verified in GE

Figure 8. Example of the non-forested areas detected in 2016

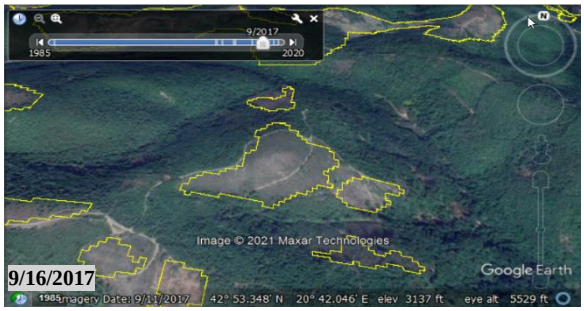

Figure 9. The yellow polygons of non-forested areas in 2017 shows no human reforestation

3.5 Validation of classification change

Quantitative accuracy assessment was utilized using the error (confusion) matrix in ENVI 5.3 software. *Table 6* presents the error matrix of the reference data and classification change in percentage and number of pixels of the study area. From 50 samples of deforestation area, reference data shows that 40 belong to the deforestation class, eight to non-forest, and one of them remain in the forest class. From 50 samples of non-forest areas, eight were placed incorrectly in the deforestation class and none in the forest class. Only one sample site of the forest class belongs to the deforestation class.

Table 6. Error matrix table of reference data and classification change

	Reference data pixel and (percent)				
Classification pixel and (percent)	Class name	Forest	Non-Forest	Deforestation	Total
	Forest	49 (94.23)	0 (0.00)	1 (2.04)	50 (33.33)
	Non-Forest	0 (0.00)	42 (85.71)	8 (16.33)	50 (33.33)
	Deforestation	3 (5.77)	7 (14.29)	40 (81.63)	50 (33.33)
	Total	52 (100.00)	49 (100.00)	49 (100.00)	150 (100.00)

The overall accuracy of classification change is calculated by dividing the total sum of diagonal correctly classified pixels (131) by the total number of reference points (150). The compounded overall accuracy was 87.33%. Producer accuracy is calculated by dividing each

diagonal pixel value class by the total of each column. *Table 7* shows that the highest producer's accuracy possesses forest area (94.23 %), then the non-forest areas ranges to (85.71 %), and the least have deforestation area around 81.63 %. User accuracy is calculated by dividing each of the diagonal pixel value classes by the total of each row. From the results of *Table 6*, the forest area has the highest user accuracy (98.00), followed by non-forest (84.00 %), and deforestation (80.00 %).

Table 7. Validation measurements of classification change

Class name	Commission error (%)	User accuracy (%)	Omission error (%)	Producer accuracy (%)
Forest	2.00	98.00	5.77	94.23
Non-Forest	16.00	84.00	14.29	85.71
Deforestation	20.00	80.00	18.37	81.63

4 DISCUSSION AND CONCLUSIONS

Acquiring spatial information on vegetation status using geospatial technologies has become necessary for sustainable forest management. In this research, we used medium-spatial resolution satellite imagery of the Sentinel 2-A platform to detect and map the deforestation process between 2016 and 2017 within the forest area. The image difference method is easy to apply to conduct a grayscale image by subtracted vegetation indices (VIs) of two dates NDVI, but it is difficult to manually setup the appropriate thresholds. The application of the Otsu's threshold on the image differenced NDVI monochrome image ($NDVI_{(2016-2017)}$) enabled us to detect and map the deforested and non-forested areas that were previously under forest. The results of accuracy assessment show that this approach is acceptable (overall accuracy was 87.33%). Researchers have used different forest classification approaches, change detection methods, and algorithms to evaluate the forest cover change process. They have also utilised multi-spectral images and VIs. The VIs of the NDVI, enhanced vegetation index (EVI), and leaf area index (LAI) had derived from multi-spectral images used by Elhag et al. (2021) for mapping spatial-temporal land cover distribution, mapping bare soil index (BSI), and in identifying the significant land cover changes over 20 years (1995-2015) in the Sougia catchment of Crete Island, Greece. The VIs of NDVI was derived from Landsat data, EVI was derived from MODIS time-series and used as an optimized index, and LAI as NDVI derivatives to define up to ten land cover classes. The supervised image classification method using Support Vector Machine (SCM) train algorithm was applied to create land cover maps for three periods: 1995, 2005, and 2015 and to assess the classification accuracy. Their results compared with CLC categories map as ground truth data. The overall accuracy of the SVM classification algorithm was over 87.00 % in three periods. As a change detection method, Elhag et al. (2021) used a post-classification comparison between the spanning times and revealed a significant depletion of -14% in the coniferous forest from 1995 to 2015. Nath and Acharjee (2013) used the NDVI index to generate maps by slicing five ranges of NDVI applying the Jenks Natural Breaks classification method in their study area. The final step in their research was the creation of the vegetation cover change map, where NDVI categories map (decreased, some decreased, some increase, and increased) of 1989 and 2010 had crossed and revealed significant changes. From the total area (2893.59) hectares, reduced class shows 44.40%, followed by some decrease 37.93% and remaining falls under some increase and increasing trend. Candra (2020) has developed a method to detect deforestation in his work in Kalimantan and Sumatera (Indonesia) using multitemporal satellite imagery from 2018-2019.

He called this method Multitemporal Deforestation Detection (MDD). The main idea was to determine the difference between the reflection values in the targeted image (image that has deforested pixels) and in the original one (image without change of forest pixels). To develop this algorithm, Candra took two main steps: a) Band selection – several pixels representing the deforestation from the target and original image are taken, and the change in their reflection values is calculated. The bands that have the most significant changes in values from the results are selected and the threshold is also selected by performing some observations. b) With the created algorithm, the combination is made using NDVI and difference normalized burn ratio (dNBR) - to increase the accuracy of the results. The commission error results of deforestation detection were a total of 0.63%, while, on the other hand, the omission error is 0.33%. Given that the errors are small, this then provides the user accuracy and producer accuracy higher accuracy. Concerning our study, the selection of Equalized Stratified Random sampling strategy samples for classification verification has reduced the overestimation of the classification result, especially for the forest and non-forest class, which were the target of the classification. As the verification process of the samples relayed only VHR Google Earth images, field verification seems necessary in future research, especially to check the regeneration process at the early stage, which is not visible from satellite images. The difficulty during this study was that the work was based solely on using Remote Sensing and GIS desktop software, making it impossible to directly access platforms that offer real-time data for spatial analysis and change detection.

Therefore, in the future, such research would be easier and more resource intensive using modern web-based platforms such as Google Earth Engine (GEE), which provides high-speed data analysis for large spatial extents using processing function and provide algorithms to gather data from multiple years, satellite sensors and models (Zurqani et al. 2018). The results of the image difference method applied in this study revealed that forest cover in this municipality has changed both from human (forest cutting) and natural factors (forest fire). Based on the Kosovo Green Report 2018 (Report, 2018), during 2017, around 2.040 m^3 of timber was confiscated from illegal loggers by communal authorities and 2.054 ha forests experienced fires in Kosovo. Illegal forest cutting is much related to the poor social and economic situation, especially in poor rural areas where forest resources are utilized for survival. From the overall forest-covered of 24,873.61 hectares, 24,423.57 ha or 98.19 % mapped as forest cover, 113.75 hectares or 0.46 % as non-forest, and 336.77 or 1.35 % of the area forest mapped as deforestation. The percentage of deforestation area is worthy of attention, and in the future, we intend to investigate spatial-temporal forest cover changes till to present time.

REFERENCES

ADDABBO, P. – FOCARETA, M. – MARCUCCIO, S. – VOTTO, C. – ULLO, L.S. (2016): Contribution of Sentinel-2 data for applications in vegetation monitoring. Acta IMEKO 5 (2): article 7. Identifier: IMEKO-ACTA-05 (2016)-02-07

BANSKOTA, A. – KAYASTHA, N. – FALKOWSKI, M. - WULDER, M.A. – FROESE, R. – WHITE, J.C. (2014): Forest monitoring using Landsat time-series data- A review. Canadian Journal of Remote Sensing 40 (5): 362–384. https://doi.org/10.1080/07038992.2014.987376

NATH, B. – SHUKLA ACHARJEE, SH. (2013): Forest Cover Change Detection using Normalized Difference Vegetation Index (NDVI) : A Study of Reingkhyongkine Lake's Adjoining Areas, Rangamati, Bangladesh. Indian Cartographer 33: 348–353. https://www.researchgate.net/publication/271908557

CAMPBELL, J. B. – WYNNE, R.H. (2011): Introduction to Remote Sensing (Fifth Edition ed.). The Guilford Press, New York. 662 p.

CANADA CENTRE FOR REMOTE SENSING. Fundamentals of Remote Sensing. Intermap Technologies Ltd, Calary and Ottawa, Canada. Online: https://www.nrcan.gc.ca/sites/www.nrcan.gc.ca/files/earthsciences/pdf/resource/tutor/fundam/pdf/fundamentals_e.pdf

CANDRA, S. D. (2021): Deforestation detection using multitemporal satellite images. In: Proceedings of the Fifth International Conferences of Indonesian Society for Remote Sensing. IOP Conference Series: Earth and Environmental Science. Indonesia. July 2020. 1–13. https://doi.org/10.1088/1755-1315/500/1/012037

CONGALTON, G. R. – GREEN, K. (2009): Assessing the Accuracy of Remotely Sensed Data: Principles and Practices (Second Edition). Taylor & Francis Group, New York. 200 p.

CONGALTON, G. R. (2001): Accuracy assessment and validation of remotely sensed. International Journal of Wildland Fire 10: 231–328. https://doi.org/10.1071/WF01031

COPPIN, P. - JONCKHEERE, I. - NACKAERTS, K. - MUYS, B. - LAMBIN, E. (2004): Review article digital change detection methods in ecosystem monitoring: a review. International Journal of Remote Sensing 25: 1565–1596. https://doi.org/10.1080/0143116031000101675

ELHAG, M. – BOTEVA, S. – AL-AMRI, N. (2021): Forest cover assessment using remote-sensing techniques in Crete Island, Greece. Open Geosciences 13 (1): 345–358. https://doi.org/10.1515/geo-2020-0235

ESA. (2015). SENTINEL-2 User Handbook.

EUROPEAN ENVIRONMENT AGENCY, (2018). Copernicus Land Monitoring Service. Online: https://land.copernicus.eu

GILLANDERS, S. N. – COOPS, N. C. – WULDER, M. A. – GERGEL, S. E. – NELSON, T. (2008): Multitemporal remote sensing of landscape dynamics and pattern change: describing natural and anthropogenic trends. Progress in Physical Geography 32 (5): 503–528. https://doi.org/10.1177/0309133308098363

GOWARD, S. – ARVIDSON, T. – WILLIAMS, D. – FAUNDEEN, J. – IRONS, J. – FRANKS, S. (2006): Historical record of Landsat global coverage: mission operations, NSLRSDA, and international cooperator stations. Photogrammetric Engineering and Remote Sensing 72 (10): 1155–1169.

HOJAS-GASCÓN, L. – BELWARD, A. – EVA, H. – CECCHERINI, G. – HAGOLLE, O. – GARICA, J. – CERUTTI, P. (2015): Potential improvement for forest cover and forest degradation mapping with the forthcoming Sentinel-2 program. The International Archives of the Photogrammetry, Remote Sensing and Spatial Information Sciences, XL-7/W3. https://doi.org/10.5194/isprsarchives-XL-7-W3-417-2015

HUETE, A. R. - LIU, H. (1994): An error and sensitivity analysis of the atmospheric- and soil-correcting variants of the NDVI for the MODIS-EOS. IEEE Transactions on Geoscience and Remote Sensing 32: 897−905. https://doi.org/10.1109/36.298018

HUSSAIN, M. – CHEN, D. – CHENG, A. – WEI, H. – STANLEY, D. (2013): Change detection from remotely sensed images: From pixel-based to object-based approaches. ISPRS Journal of Photogrametry and Remote Sensing 80: 91-106. https://doi.org/10.1016/j.isprsjprs.2013.03.006

IM, J. – JENSEN J.R. (2005): A change detection model based on neighbourhood correlation image analyses and decision tree classification. Remote Sensing of Environment 99: 326–340. https://doi.org/10.1016/j.rse.2005.09.008

KOSOVO STATISTIC AGENCY (2013): ESTIMATION of Kosovo population 2011. Online: http://ask.rks-gov.net/media/2129/estimation-of-kosovo-population-2011.pdf

LEPRIEUR, C. – KERR, Y. H. – MASTORCHIO, S. – MEUNIER, J. C. (2000): Monitoring vegetation cover across semi-arid regions: Comparison of remote observations from various scales. International Journal of Remote Sensing 21: 281−300. https://doi.org/10.1080/014311600210830

LU, D. – MAUSEL, P. – BATISTELLA, M. – MORAN, E. (2005, online 2007): Land-cover binary change detection methods for use in the moist tropical region of the Amazon: a comparative study. International Journal of Remote Sensing 26: 101–114. https://doi.org/10.1080/01431160410001720748

LU, D. – MAUSEL, P. – BRONDIZIO, E. – MORAN, E. (2004): Change detection techniques. International Journal of Remote Sensing 25: 2365–2407. https://doi.org/10.1080/0143116031000139863

MACLEOD D. R. – CONGALTON, G. R. (1998): A quantitative comparison of change-detection algorithms for monitoring eelgrass from remotely sensed data. Photogrammetric Engineering and Remote Sensing 64: 207–216.

MENESES-TOVAR, L. C. (2011/12): NDVI as indicator of degradation. Unasylva Vol. 62, http://www.fao.org/3/i2560e/i2560e07.pdf

MINISTRY OF AGRICULTURE, FORESTRY AND RURAL DEVELOPMENT (2018): Kosovo Green Report 2018. Online: https://www.mbpzhr-ks.net/repository/docs/Raporti_i_Gjelber_2018.pdf

OTSU, N. (1979). A threshold selection method from gray-level histograms. IEEE Trans. SMC 9: 62–66. https://doi.org/10.1109/TSMC.1979.4310076

SINGH, A. (1989). Review Article Digital change detection techniques using remotely-sensed data. International Journal of Remote Sensing 10: 989–1003. https://doi.org/10.1080/01431168908903939

STORY, M. - CONGALTON, R.G. (1986): Accuracy Assessment: A User's Perspective. Photogrammetric Engineering and Remote Sensing 52: 397–399.

TOMTER, S. M. – BERGSAKER, E. – MUJA, I. – DALE, T. – KOLSTAD, J. (2013): National Forest Inventory of Kosovo 2012. Ministry of Agriculture, Forestry and Rural Development. Online: https://nfg.no/wp-content/uploads/2019/01/Kosovo-National-Forest-Inventory-2012.pdf

TUCKER, C.J. – VANPRAET, C.L. – SHARMAN, M.J. – VAN ITTERSUM, G. (1985): Satellite remote sensing of total herbaceous biomass production in the Sengalese Sahel—1980–1984: Remote Sensing of Environment 17: 233–249. https://doi.org/10.1016/0034-4257(85)90097-5

UNFCCC. (2002). Report of the Conference of the Parties on its seventh session. UNFCCC. Online: https://unfccc.int/resource/docs/cop7/13a01.pdf. Morocco

ZURQANI, H. – POST, C. – MIKHAILOVA, E. – SCHLAUTMAN, A. – SHARP, J. (2018) Geospatial analysis of land use change in the Savannah Rover Basing using Google Earth Engine. International Journal of Applied Earth Observation and Geoinformation 69: 175–185 https://doi.org/10.1016/j.jag.2017.12.006

WALKER, J. J. – DE BEURS, K. M. – WYNNE, R. H. – GAO, F. (2012): Evaluation of Landsat and MODIS data fusion products for analysis of dryland forest phenology. Remote Sensing of Environment 117: 381–393. https://doi.org/10.1016/j.rse.2011.10.014

WRI (World Resource Institute) (2019): Global Forest Watch. WRI, Washington USA. Online: https://www.globalforestwatch.org/

https://doi.org/10.37045/aslh-2021-0008 Acta Silv. Lign. Hung., Vol. 17, Nr. 2 (2021) 121–133

Tissue Proportion, Fibre, and Vessel Characteristics of Young *Eucalyptus* Hybrid Grown as Exotic Hardwood for Wood Utilization

James Kudjo GOVINA[a, c*] – Emmanuel EBANYENLE[a] – Emmanuel APPIAH-KUBI[b] – Francis Wilson OWUSU[a] – James KORANG[a] – Haruna SEIDU[a] – Róbert NÉMETH[c] – Roland Walker MENSAH[a] – Ruth AMUZU[a]

[a] CSIR– Forestry Research Institute of Ghana, Kumasi, Ghana
[b] Department of Construction and Wood Technology, University of Education, Kumasi, Ghana
[c] Institute of Wood Technology and Technical Sciences, Faculty of Wood Engineering and Creative Industries, University of Sopron, Sopron, Hungary

Abstract – This study sought to determine selected anatomical properties of young *Eucalyptus* hybrid species (*E. grandis x E. urophylla*) grown in Ghana. Images of fibres from macerated wood, and micro–sections produced with microtome were analysed using a compound digital microscope associated with Motic Image Plus Software (MIPS), version 2.0, installed on a computer. Images were initially processed using ImageJ software. Study data were analysed using an R statistical package. The overall mean value for fibre length was 907.67 µm, whereas double fibre wall thickness was 7.76 µm. Both variables had higher mean values in sapwood than in heartwood. Nevertheless, the found values decreased from the butt to the top portion. Statistically, axial and radial positions had no influence on fibre characteristics. In a 1 mm^2 of the cross-section, the proportion of fibres was 38%, vessels were 19%, axial parenchyma were 22%, and radial parenchyma were 21% on average. Again, the radial and axial positions had no statistical influence on tissue proportion traits for the young eucalyptus wood. Mean value for vessel area was 9462.04 µm^2, whereas vessel frequency per mm^2 was about 14. Vessels were significantly larger in area (range 9982.50 – 13544.41 µm^2), yet reduced in frequency (range 6 – 17 per mm^2) for sapwood. In heartwood, vessel area was comparatively smaller (range 6321.15 – 7816.69 µm^2), whereas their frequency was high (range 15 – 18 vessels per mm^2). Axial and radial position had statistical influence on vessel frequency and area for the young *Eucalyptus* grown in a plantation in Ghana.

***Eucalyptus* / hybrid / fibre / tissue / parenchyma / vessel**

Kivonat – Fahasznosítás céljából termesztett *Eucalyptus* hibrid fajok fiatal egyedeinek szöveti szerkezete, rost– és edényjellemzői. Ez a cikk a Ghánában termesztett *Eucalyptus* hibrid fajok (*E. grandis x E. urophylla*) fiatal egyedeinek egyes anatómiai tulajdonságait írja le. A macerációval elkülönített farostok fotóit, ill. mikrotómmal készített anatómiai metszetek mikroszkopikus részleteit elemeztük egy összetett digitális mikroszkóppal, amely a számítógépre telepített Motic Image Plus Software (MIPS) 2.0 verziójához kapcsolódott. A képeket eredetileg ImageJ szoftverrel dolgoztuk fel. A nyert adatokat R statisztikai szoftvercsomag segítségével elemeztük. A rosthossz átlagértéke 907,67 µm, míg a kettős sejtfalfalvastagság 7,76 µm volt. Megállapítottuk, hogy a szijács hosszabb farostokat

*Corresponding author: ndvm36@uni-sopron.hu; H-9400 SOPRON, Bajcsy-Zs. u. 4, Hungary

tartalmaz, melyeknek kettős falvastagsága is nagyobb a gesztben mért értékekhez viszonyítva, ugyanakkor a különbségek statisztikailag nem szignifikánsak. Az említett értékek a tő felől a csúcs irányában csökkenő értékeket mutattak, de statisztikailag nem volt igazolható az eltérés. Statisztikailag tehát az axiális és radiális helyzetek nem befolyásolták a farostok jellemzőit. 1 mm^2 keresztmetszetet vizsgálva a farostok aránya 38%, az edényeké 19%, az axiális parenchimáké 22%, míg a bélsugár parenchimáké 21%. A radiális és axiális helyzetnek nincs statisztikai hatása a fiatal eukaliptusz faegyedekben a vizsgált sejttípusok arányára. Az edényterület átlagos értéke 9462,04 μm^2 volt, míg az edények darabszáma 14 körüli érték volt 1 mm^2–re vetítve. A szijácsban az edények területe a 9982,50 – 13544,41 μm^2 tartományban, mozgott, de darabszámuk kisebb volt a geszthez viszonyítva (6 – 17 db/mm^2). A gesztben az edények területe kisebb értéket adott (6321,15 – 7816,69 μm^2), míg darabszámuk nagyobb volt (15 – 18 db/mm^2). Vizsgálatainkkal megállapítottuk, hogy a ghánai ültetvényen termesztett fiatal *Eucalyptus* egyedek esetén az axiális és a radiális helyzet statisztikailag befolyásolta az edények mennyiségét (számát) és méretét (területét).

Eukapliptusz / hibrid / farost / szöveti szerkezet / parenchyma / edény

1 INTRODUCTION

Wildfires, illegal logging, overexploitation to meet domestic and foreign wood demand, and other factors put continuous pressure on natural forests in tropical timber producing countries. Experts have predicted that the raw material base for wood will soon shift from natural to plantation timber. Efforts to guarantee a sustainable future supply of wood include the introduction of fast-growing exotic species like *Tectona grandis*, *Cedrela odorata*, and *Eucalyptus* species. The genus *Eucalyptus* comprises fast-growing species that are able to adapt well to marginal soils in diverse climatic conditions (Willan 1951, Woods – Peseta 1996). These characteristics make *Eucalyptus* a suitable candidate genus for commercial timber plantations that can meet the increasing wood demand as well as mitigate some alarming climate change effects. Eucalyptus plantations are found currently in tropical, subtropical, and temperate areas. They amount to 8% of planted forests globally (Harwood 2011).

Wood from *Eucalyptus* species are useful for pulp and paper, solid wood products, veneer, fuelwood, posts, etc. In Kenya, eucalyptus is the third most grown genus after pine and cypress. It was originally introduced in Kenya to provide biomass for powering railway steam engines (Githiomi – Kariuki 2010). Until recently, eucalyptus was only planted in small scale research plot sizes and on private lands in Ghana, primarily for shade and ornamental purposes. Admittedly, general information on original eucalyptus species has been published; however, specific research on young stems is scarce. Presently, MIRO Forestry Ghana Limited, a private organisation, has adopted a breeding technology program for *Eucalyptus grandis* and *Eucalyptus urophylla*. The goal is to create a hybrid species for an improved tree form and enhanced growth. Nonetheless, little research focusing on the wood properties has been completed on bred *Eucalyptus* species.

As is the case with other tree species, silvicultural management, age, genetics, and growing sites influence the formation and quality of the woody biomass of eucalyptus (Zobel – van Buijtenen 1989, Savidge 2003, Roque 2004). In addition, wood quality can also vary with an individual tree and between trees of same species growing under same conditions (Plomion et al. 2001, Wimmer et al. 2002, Monteoliva et al. 2005, Quilhó et al., 2006, Sharma et al. 2015).

Generally, it has been argued that timber species that are fast-growing and less than ten years old produce mostly juvenile, inferior quality wood (Zobel – Sprague 1998, Moore – Cown 2017). Accordingly, properties of young eucalyptus wood need to be investigated for efficient utilization. The anatomical structure and characteristics of wood are known to

influence the most important properties, which include density, drying characteristics, shrinkage, permeability for preservation treatment, pulp yield, paper strength, etc. (Fujiwara et al. 1991, Ofori – Brentuo 2005, Bhat et al. 2007, Yahya et al. 2010, Zanuncio et al. 2016). Moglia et al. (2008), reported that fibre and vessel length significantly varied radially within a tree, whereas tissue proportion differed considerably between trees of same species. Amidon (1981) and Barauna et al. (2014) found that vessel frequency and diameter size greatly affected papermaking properties and wood permeability. The present study aimed to establish the anatomical properties that are fundamental to enhancing the utilisation potential of hybrid *Eucalyptus* species grown in Ghana. Specific anatomical properties considered for the present study were fibre characteristics (length, diameter, lumen width, and wall thickness), tissue proportion (fibre, vessel, axial and radial parenchyma), and vessel characteristics (frequency and area). These variables could influence utilisation properties of the young wood considerably.

2 MATERIALS AND METHODS

2.1 Study site

The study was conducted with materials from a plantation site owned by MIRO Forestry Ghana Limited located near Agogo in Asante Akyem North district of the Ashanti region of Ghana (*Figure 1*). The land is a degraded forest reserve forming part of the forest transition zone of Ghana. Between 2013 and 2018, the district, which is located on latitude 6º 37' 5" N and longitude 1º 12' 36" W, recorded monthly rainfall between 120 mm and 150 mm. The mean temperature ranged between 26ºC and 30ºC (MOFA 2018). Total plot size was 50 hectares.

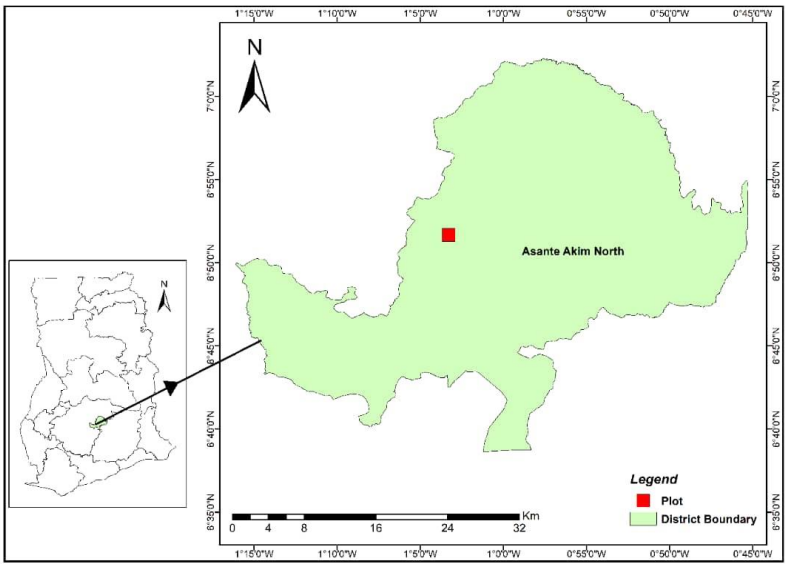

Figure 1. A map highlighting the Eucalyptus plot and Asante Akyem North District in the Ashanti region of Ghana.

2.2 Measurement of trees morphological features

The *Eucalyptus* hybrid (*E. grandis* and *E. urophylla*) trees were four years old, planted with 2.5 x 3m spacing, and were nurtured with MIRO's thorough silvicultural management and protection from annual wildfires. Fifty trees were randomly selected for height and diameter measurement. Diameter tape was used to measure stem diameters for the trees at breast height

position of 1.3 m. Tree heights were measured using a linear tape after the trees had been harvested close to the ground with a chainsaw. Respective stump heights were also added.

2.3 Sampling of wood materials

Six trees were randomly selected from the 50 harvested trees. MIRO donated only six trees for this destructive study. The trees were crosscut into three axial portions representing the butt, middle, and top position of tree. One 2 cm-wide wood disc was collected from the different stem height levels (butt, middle, and top) of all six trees. Eighteen (18) wood discs were labelled accordingly. Each disc was packaged in a sealed polythene and transported to the Wood Anatomy Laboratory within the Council for Scientific and Industrial Research's Forestry Research Institute of Ghana (CSIR–FORIG). The idea behind sampling from the axial position was to address any inherent variability that had naturally developed during growth of each tree. Again, there was a sharp visible distinction between sapwood and heartwood on the butt and middle discs. Therefore, one sample from heartwood and one from sapwood were taken from either side of the disc (Cherelli 2015). A total of 72 sub-samples were studied (4 sub–samples x 18 discs).

2.4 Fibre characteristics

Matchstick-sized wood pieces were taken from all sub-samples. These were placed in labelled vials and macerated using a solution of equal parts of hydrogen peroxide and glacial acetic acid. The vials containing the wood material were kept in a N53C-Genlab Oven at 60°C and monitored every 12 hours until the maceration was complete. The macerate was repeatedly washed with distilled water to guarantee total removal of acetic acid (Franklin 1945). A drop of glycerol was placed unto the macerate, and the fibres were put on a specimen slide where they were separated apart with a pin (*Figure 2*). The slides were studied under a digital Compound Microscope (National) operated alongside a Motic Image Plus software (MIPS). Images with X40 magnification (*Figure 2*) were employed for the measurement of fibre length, whereas images with X400 magnification (*Figure 3*) were used for diameter, lumen width, and wall thickness. Twenty-five (25) straight and unbroken fibres were measured for each sub-sample. This resulted in 50 fibres for sapwood and 50 fibres for heartwood, for a total of 100 fibres per disc.

2.5 Tissue proportion and vessel characteristics

Wood samples of approximately 2 cm in all dimensions were taken through a softening process following published protocols (Schweingruber 2007). After being softened, each sample was mounted on a sledge Microtome (HM 400, Microm, Walldorf, Germany) to cut microsections of about 10 – 20 μm from the cross-sectional surface (*Figure 4*). The thin sections were stained with safranin solution and further submitted to a gradual dehydration process. This was achieved by transferring the stained microsections from water through ethanol solution of 30 %, 50 %, 70 %, 90 %, and absolute ethanol. Furthermore, the sections were permanently mounted with Canada balsam and oven–dried at 60 °C (Schweingruber 2007, Tardif – Conciatori 2015). The best-mounted sections were selected, at least 3 slides per sub-sample, and studied under the microscope associated with MIPS to capture images. In ImageJ, the software scale is set using the scale of an individual image. Afterwards, a scale grid of 1 mm^2 was superimposed, at least 10 times, on original images representing a sub-sample. The individual tissue elements (fibre, vessel, axial parenchyma, radial parenchyma) within the 1 mm^2 area were counted at each placement and equated to 20.

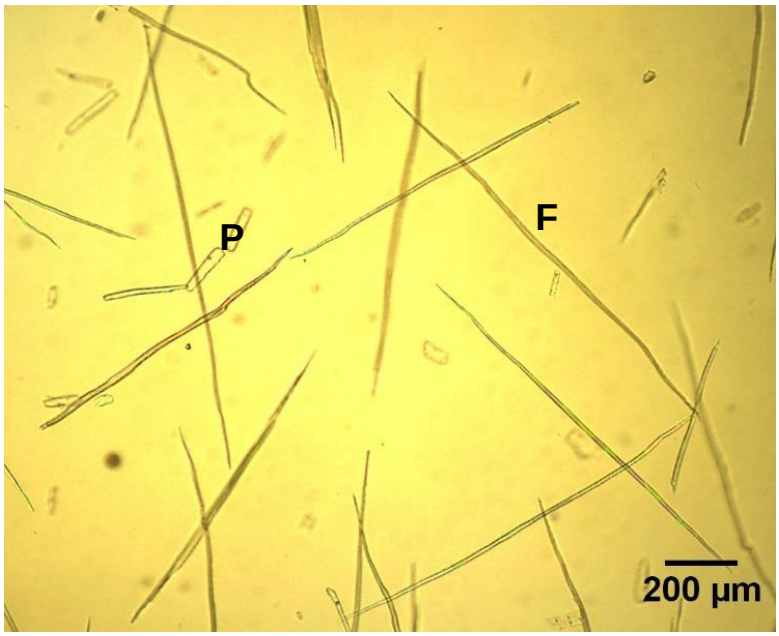

Figure 2. Fibres (F) and parenchyma cells (P) from macerated wood from 4-year-old Eucalyptus hybrid species grown in Ghana.

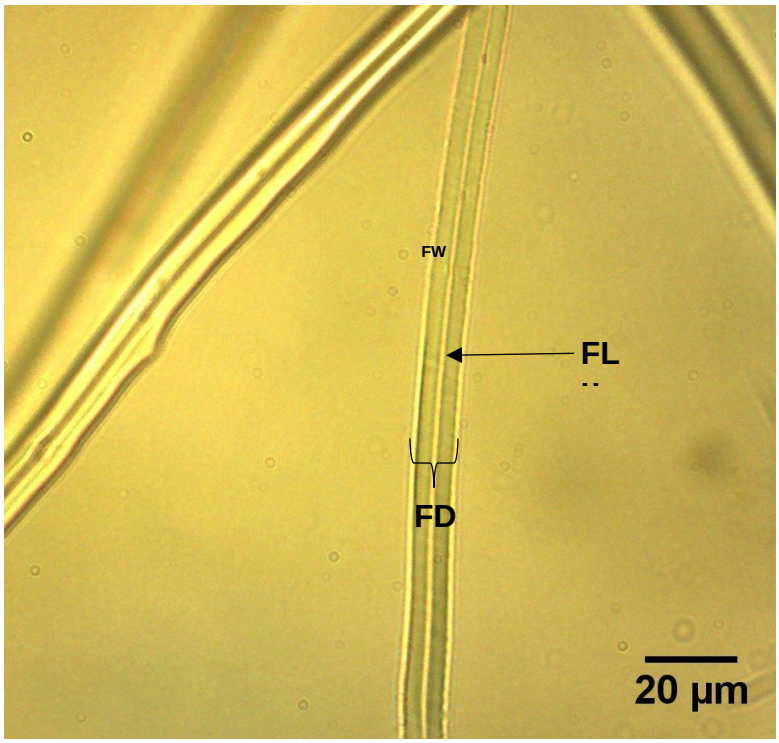

Figure 3. A magnified fibre from macerated wood from a 4-year-old Eucalyptus hybrid species. (FW): Fibre wall; (FD): Fibre diameter; (Flu): Fibre lumen.

For instance, if vessels are 3 out 20 spots, the proportional means are reported as percentages as (3/20)·100. Regarding vessel characteristics measurement, ImageJ software was used to analyse the same images captured to represent the sub-samples (Abràmoff et al. 2004). For vessel area, the images were converted into 8-bit format, inverted, and threshold set activated to convert all vessels into black dots. Using a feature called 'analyse particle' within ImageJ,

dot circularity was set between 0.75-1.00. Furthermore, the desired dot area was set above a pre-determined area of the smallest vessel. This excludes the many smaller dots representing cells such as axial parenchyma. Vessels were analysed as particles to estimate their area (*Figures 4* and *5*). A minimum of 45 vessels from three different images were feasible for area measurement for each sub-sample. Vessel frequencies were completed manually on the same-sized images.

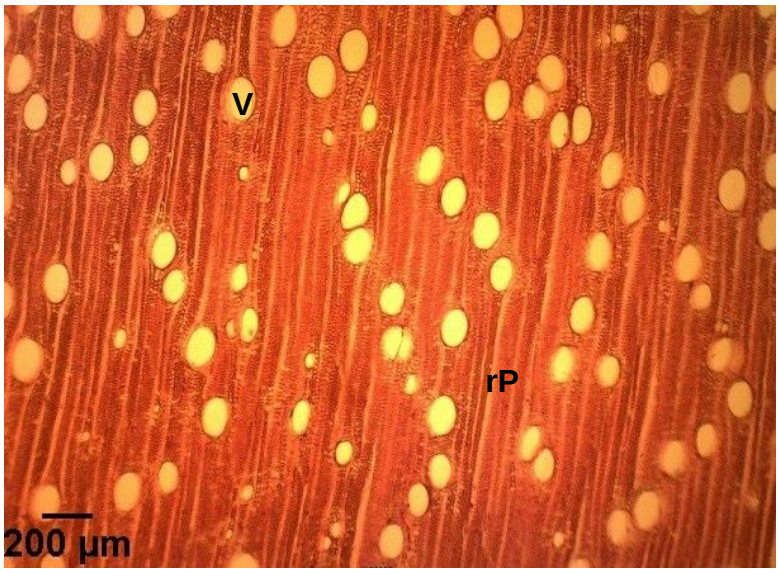

Figure 4. Cross-sectional image of wood from a 4-year-old Eucalyptus hybrid grown in Ghana. Image is at X40 magnification. V = vessel, rP = radial parenchyma

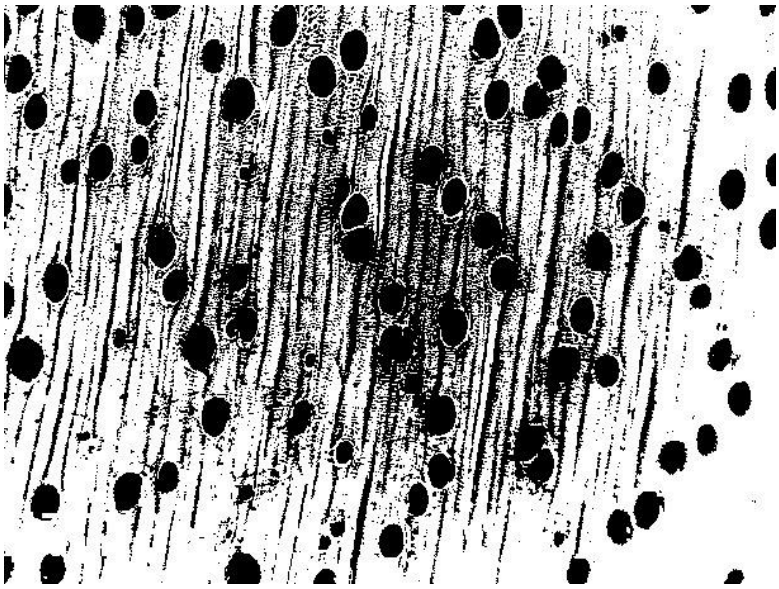

Figure 5. A processed image of a cross-section of wood from 4–year–old Eucalyptus hybrid species grown in Ghana. The vessels in the original image (Figure 4) are now seen as dark particles. Radial parenchyma now seen as black stripes.

2.6 Data analysis

The data generated from the study was organized with an Excel spreadsheet (Microsoft 365), and analysed using the R statistical package (Team 2014). The mean values and their corresponding standard deviations are reported in *Tables 2-4*. A one-way analysis of variance

(ANOVA) was employed to test if differences observed in the mean values were statistically significant. *P*-values from ANOVA outputs are included in the Tables presented above. Tukey's Honest Significant Difference was implemented to compare mean values with statistically significant differences, especially for variables with more than two categories.

3 RESULTS AND DISCUSSION

In general, the study results of morphological features, tissue proportion, fibre and vessel traits were comparable among the axial and radial positions as well as to values reported in the literature.

3.1 Morphological features

Mean merchantable height was 14.26 m, whereas the mean diameter at the butt section was 31.42 cm (*Table 1*). The mean height and diameters the present study found for eucalyptus trees grown in Ghana correspond with those reported in literature. In Brazil, Brito et al. (2019) reported a diameter at breast height (dbh) of 16.19 cm and a height of 17.07 m for clone materials of the same age. Likewise, Ramalho et al. (2019) reported a dbh range of 7.4-14.11 cm. Quilho et al. (2006) found an average dbh of 11.5 cm and an average commercial height of 17.8 m for 5-year-old *Eucalyptus urograndis* hybrid trees. The study results indicate that the hybrid eucalyptus trees have positively adapted to their growth conditions. It also suggests that *Eucalyptus* hybrid trees have sufficient crown development to provide adequate useful area for the trees (Miranda et al. 2009). The morphological findings reported in *Table 1* are important when considering the utilization of 4-year-old materials for solid wood applications such as utility poles. The impregnation of preservatives and their retention are influenced by the sapwood portion (Valle et al. 2013).

Table 1. Some morphological properties for 4-year-old Eucalyptus hybrid trees (E. grandis x E. urophylla) grown in Ghana. (Max): Maximum; (Min): Minimum; (Stdv): Standard Deviation. Total samples trees (n) = 50.

Variable	Min	Max	Mean	Stdv
Merchantable length (m)	11.55	16.87	14.26	2.20
Butt diameter (cm)	28.65	34.70	31.42	2.36
Top diameter (cm)	9.23	13.37	11.14	1.55
Sapwood width at butt (mm)	15	95	56	2.34
Sapwood width 3m from butt (mm)	37	76	53.50	1.58
Sapwood width at mid-length (mm)	40	60	47.83	0.78

3.2 Fibre biometry

The mean fibre length for the eucalyptus hybrid trees was 907 µm. The found value falls within the length range (800 to 1300 µm) reported in an earlier study and the InsideWood database (Wheeler 2011, Brito et al. 2021). Fibre length decreased from tree butt to the top portion (938.81 to 862.69 µm) as shown in *Table 2*.

The observed longitudinal variation agrees with other studies (Quilhó et al. 2006, Bhat et al. 2007). However, the abovementioned authors observed an initial increase in fibre length to about breast height before the decrease to the top portion. In the present study, the middle portion was at exactly the 50% mark of merchantable height reported in Table 1. Clearly, the middle portion was beyond the breast height of 1.3 m. Bamber (1985) reported a similar observation. Quilhó et al. (2006) studied eucalyptus hybrids (*E. grandis* and *E.*

urophylla) and reported 820 – 1040 µm for fibre length for trees from seed origin and 1010-1110 µm for five-and-half-year-old clones. Regarding the same hybrid grown in India, Sharma et al. (2015) reported 910-1140 µm for fibre length. Radially, the sapwood had longer mean fibre length (949.55 µm) than heartwood (862.77 µm). The differences between mean values for fibre length, for both axial and radial positions, were statistically insignificant.

Table 2. Mean values of fibre characteristics for 4-year-old eucalyptus hybrid (E. grandis x E. urophylla) grown in Ghana. (FL): Fibre Length; (FD): Fibre Diameter; (FLW): Fibre Lumen Width; (FDWT): Fibre Double Wall Thickness.

Positions	Levels	FL (µm)	FD (µm)	FLW (µm)	FDWT (µm)
Axial	Top	862.69 (81.85)	16.85 (1.82)	9.67 (1.11)	7.18 (1.07)
	Middle	923.26 (69.83)	16.49 (1.13)	8.77 (1.06)	7.72 (0.83)
	Butt	938.81 (77.86)	17.98 (1.51)	9.56 (1.33)	8.42 (1.92)
P–value		0.22	0.24	0.38	0.31
Overall mean		907.67 (40.25)	17.11 (0.78)	9.33 (0.49)	7.77 (0.62)
Radial	Heartwood	862.77 (82.86)	17.71 (1.33)	10.23 (1.50)	7.49 (1.16)
	Sapwood	949.55 (52.97)	16.49 (1.69)	8.48 (0.88)	8.00 (1.14)
P–value		0.06	0.19	0.034	0.45
Overall mean		906.16 (61.36)	17.10 (0.86)	9.36 (1.24)	7.76 (0.36)

The P–values for each variable are from a one–way ANOVA run at 95% confidence interval. In parenthesis are the standard deviation of the mean values. Total sampled trees (n) = 6.

Regarding fibre diameter (width), the mean value was 17.11 µm. This variable decreased from the butt to the middle, but slightly increased from the middle to the top portion (*Table 2*). The study finding on fibre diameter correlates with values reported in the literature. Carvalho and Nahuz (2001) reported 17.1 µm; Rao et al. (2002) reported 14.5 – 16.9 µm; Quilhó et al. (2006) reported 20 µm; Sharma et al. (2015) reported 14.3 – 16.8 µm. Across radial position, fibre diameter was higher in heartwood. The mean values for fibre diameter found by this study were not statistically different in either axial or radial directions.

The mean value of fibre double wall thickness (width) was 7.76 µm. The pattern for double wall thickness also decreased from the butt to the top, as with the fibre length. Radially, double wall thickness for fibres from sapwood were thicker than double wall thickness for fibres from heartwood. However, the reported mean values are comparable to those reported by Sharma et al. (2015) for 6-year-old *Eucalyptus* hybrid trees. The fibre double wall thickness exhibited mean values that were not statistically different.

This study revealed that fibre length and double wall thickness were comparatively higher in sapwood than in heartwood. This observation suggests that sapwood could be denser than heartwood in young wood. Similar observations have been reported in literature for both young and older *Eucalyptus species*; 6.5-year-old trees (Pillai et al. 2013), 10-year-old trees (Tomazello 1987), 15-year-old trees (Carrillo et al. 2015), 18-year-old trees (Trevisan et al. 2013) and 37-year-old trees (Melo et al. 2018). The authors attributed their observation to cambial age as particularly related *Eucalyptus* species.

3.3 Tissue proportion

Fibre carried a proportion of 37.54% and vessel elements carried 18.60%. Axial and radial parenchyma proportion were about 22% and 21% respectively (Table 3). Axial and radial variation in tissue proportion was recorded within trees. Study findings are compatible with studies on similar *Eucalyptus* hybrid species (Hu et al. 2008) and a 4.5-year-old

Eucalyptus tereticornis (Rao et al. 2002). However, the differences reported in the present study were statistically insignificant. Generally, the radial variation, though insignificant, was a little pronounced, but only at the butt section for the tissue proportional traits. Practically, the findings suggest that the studied wood materials may be utilized irrespective of its portion on the stem. Meanwhile, the service life of the young wood could be compromised as described in Brischke et al. (2006); a direct decay-influencing factor, among others, is a material natural resistance.

3.4 Vessel characteristics

Generally, vessels were exclusively solitary with a diffuse porous arrangement. Vessel characteristics affect the papermaking properties of wood and other technologies like impregnability (Amidon 1981, Barauna et al. 2014, Anupam et al. 2016). The mean values for vessel area, based on cross sectional view, for the 4-year-old *Eucalyptus* hybrid wood is 9462 μm^2 (*Table 4*). Vessel area was larger in sapwood than in heartwood. Same variable increased from the butt to the middle portion of the tree before a slight decrease at the top portion. Regarding vessel quantity, the estimated mean value was approximately 14 per mm^2. The top portions had highest vessel frequency followed by the butt before the middle portion. Statistically, the effect of axial and radial position on vessel quantity and size was highly significant. Practically, the results suggest that positions are important when considering the young wood for application. For instance, in cases where impregnation of preservatives is required, different portions of the stem would give different outputs.

Table 3. Mean tissue element proportion (%), based on cross section area, for 4-year-old Eucalyptus hybrid (E. grandis x E. urophylla) grown in Ghana.

Variable	Position	Heartwood	Sapwood	*P*–value
Fibre (%)	Top	–	35.13 (8.31)	0.60910
	Middle	38.67 (9.00)	38.33 (10.47)	
	Butt	37.00 (12.07)	41.00 (8.97)	
Overall mean		*37.54 (2.34)*		
Vessel (%)	Top	–	20.43 (5.50)	0.32011
	Middle	18.00 (6.90)	17.33 (7.76)	
	Butt	19.67 (6.94)	15.75 (5.68)	
Overall mean		*18.60 (1.90)*		
Axial parenchyma (%)	Top	–	23.40 (7.35)	0.2456
	Middle	21.00 (7.59)	22.33 (6.51)	
	Butt	21.67 (7.24)	23.25 (7.30)	
Overall mean		*22.51 (1.43)*		
Radial parenchyma (%)	Top	–	21.05 (7.27)	0.8270
	Middle	22.33 (6.66)	22.00 (8.82)	
	Butt	21.67 (11.75)	20.50 (8.72)	
Overall mean		*21.43(0.77)*		

The P–values for each variable are from a two–way ANOVA run at 95% confidence interval. In parenthesis are the standard deviation of the mean values. – is used because the top portion had not developed heartwood yet. Total sampled trees (n) = 6.

Tukey's Honest Significant Difference was employed to test where the significant difference existed among the axial positions. Regarding vessel area, the butt portion

contributed greatly compared to the middle and the top. Conversely, for vessel frequency, the top portion contributes greatly when compared to both butt and middle. The pattern of vessel characteristics in this study conforms to earlier reports ((Taylor 1973, McKimm – Ilic 1987, Leal et al. 2003). The axial and radial variations observed in this study for vessel characteristics can be attributed to cambial age as related to eucalyptus species, and reported in literature (Leal et al. 2003, Ramírez et al. 2009, Carrillo et al. 2015).

Table 4. Mean vessel frequency per mm^2 and area (μm^2) for 4-year-old Eucalyptus hybrid (E. grandis x E. urophylla) grown in Ghana. (VA): Vessel Area; (VF): Vessel Frequency.

Variable	Axial position	Heartwood	Sapwood	*P*–value
	Top	–	9503.73 (3573.25)	
VA (μm^2)	Middle	7816.69 (3993.39)	13544.41 (5955.02)	1.188e–05
	Butt	6321.15 (2729.22)	9982.50 (5037.37)	
Overall mean		*9462.04 (2717.98)*		
	Top	–	17.70 (1.93)	
VF/mm^2	Middle	15.00 (2.36)	6.60 (1.51)	1.371e–06
	Butt	15.50 (2.12)	11.40 (1.65)	
Overall mean		*13.98(4.31)*		

The P–values for each variable are from two-way ANOVA run at 95% confidence interval. In parenthesis are the standard deviations of the mean values. – is used because the top portion had not developed heartwood yet. Total sampled trees (n) = 6.

4 CONCLUSIONS

This study contributes to addressing the scarce scientific literature on eucalyptus in Africa. The focus on selected anatomical properties and morphological features is an important start for the resilient species. The height, diameters, and other morphological traits identified for the 4-year-old eucalyptus hybrid wood suggest that the hybrid species could qualify for numerous applications and further related tests. The axial and radial positions within the trees had no significant effect on fibre dimensions and tissue proportions. On the contrary, axial and radial positions had significant effect on vessel frequency and area. Meanwhile, the mean values found for all variables agreed with reported values of eucalyptus species grown through seed and clones in both native and cultivated lands. Comparatively, vessels were larger in area, but fewer by frequency in sapwood than in heartwood. Additionally, both vessel area and frequency increased from butt to top portion. The findings of this study highlight some of the fundamental information needed to support efficient utilization of eucalyptus wood, especially in Ghana. In this regard, it would be helpful to conduct further research to establish the effect of age, planting distances, etc., on wood properties of the *Eucalyptus* hybrid species in Ghana.

Acknowledgements: The authors wish to acknowledge the Directors and managements of Asuboa Wood Treatment Company Limited and MIRO (Ghana) Forestry Limited for funding this study and granting the research team access to their plantations at Agogo. Thanks to Mr. William Hagan Brown for helping to prepare the map for the study site.

REFERENCES

ABRÁMOFF, M. D. – MAGALHÃES, P. J. – RAM, S. J. (2004): Image processing with Image. Biophotonics International 11 (7): 36–42.

AMIDON, T. E. (1981): Effect of the wood properties of hardwoods on kraft paper properties. Technical Association of Pulp and Paper Industry 64(3): 123–126.

ANUPAM, K. – SHARMA, A. K. – LAL, P. S. – BIST, V. (2016): Physicochemical, morphological, and anatomical properties of plant fibers used for pulp and papermaking. In: *Fiber Plants*, Springer. pp 235–248. https://doi.org/10.1007/978-3-319-44570-0_12

BAMBER, R. (1985): The wood anatomy of eucalypts and papermaking. Technical Association of Australian and New Zealand Pulp and Paper Industry 38: 210–216.

BARAÚNA, E. E. P. – LIMA, J. T. – VIEIRA, R. D. S. – SILVA, J. R. M. D. – MONTEIRO, T. C. (2014): Effect of anatomical and chemical structure in the permeability of "Amapá" wood. Cerne 20 (4): 529–534. https://doi.org/10.1590/01047760201420041501

BHAT, K. – BHAT, K. – DHAMODARAN, T. (2007): Wood density and fiber length of *Eucalyptus grandis* grown in Kerala, India. Wood and Fiber Science 22 (1): 54–61.

BRISCHKE, C. – BAYERBACH, R. – OTTO, A. (2006): Decay–influencing factors: A basis for service life prediction of wood and wood–based products. Wood Material Science and Engineering 1 (3–4): 91–107. https://doi.org/10.1080/17480270601019658

BRITO, S. A. – VIDAURRE, G. B. – OLIVEIRA, J. T. S. – SILVA, J. M. G. – OLIVEIRA, R. F. – DIAS JUNIOR, A. F. – ARANTES, M. D. C. – MOULIN, J. C. – VALIN, M. – SIQUEIRA, L. – ZAUZA, E. A. V. (2021): Interaction between planting spacing and wood properties of *Eucalyptus* clones grown in short rotation. iForest–Biogeosciences and Forestry 14: 12–17. https://doi.org/10.3832/ifor3574-013

BRITO, S. A. – VIDAURRE, G. B. – OLIVEIRA, J. T. D. S. – SILVA, J. G. M. – RODRIGUES, B. P. – CARNEIRO, A. D. C. O. (2019): Effect of planting spacing in production and permeability of heartwood and sapwood of *Eucalyptus* wood. Floresta e Ambiente 26 (SPE1). https://doi.org/10.1590/2179-8087.037818

CARRILLO, I. – AGUAYO, M. G. – VALENZUELA, S. – MENDONÇA, R. T. – ELISSETCHE, J. P. (2015): Variations in wood anatomy and fiber biometry of *Eucalyptus globulus* genotypes with different wood density. Wood Research 60 (1): 1–10.

CARVALHO, M. – NAHUZ, M. (2001): The evaluation of the *Eucalyptus grandis* × *E. urophylla* hybrid wood through the production of small dimension sawnwood, pulpwood and fuelwood. Scientia Forestalis 59: 61–76.

CHERELLI, S. G. (2015): Heartwood and sapwood in eucalyptus: influence of species and age on technological properties. [Dissertation] Sao Paulo state university, Faculty of Agronomic Sciences.

FRANKLIN, G. (1945): Preparation of thin sections of synthetic resins and wood–resin composites, and a new macerating method for wood. Nature 155 (3924): 51. https://doi.org/10.1038/155051a0

FUJIWARA, S. – SAMESHIMA, K. – KURODA, K. – TAKAMURA, N. (1991): Anatomy and properties of Japanese hardwoods I. Variation of fibre dimensions and tissue proportions and their relation to basic density. Internation Association of Wood Anatomists 12 (4): 419–424. https://doi.org/10.1163/22941932-90000544

GITHIOMI, J. – KARIUKI, J. (2010): Wood basic density of *Eucalyptus grandis* from plantations in central rift valley, Kenya: variation with age, height level and between sapwood and heartwood. Tropical Forest Science, 281–286. https://www.jstor.org/stable/23616657

HARWOOD, C. (2011): New introductions–doing it right. In: proceedings of the "Farm Forestry Association conference on developing a eucalypt resource: learning from Australia and elsewhere" (Walker J. ed). University of Canterbury. Christchurch, New Zealand: Wood Technology Research Centre 43–54.

HU, J. – LIU, Y. – CHANG, S. – WU, Y. – ZHU, L. (2008): Radial variation of the micro–fibrillar angle and tissue proportion of *Eucalyptus urophylla* × *Eucalyptus grandis* families. Central South University for Forestry and Technology 28 (1): 30–34.

LEAL, S. – PEREIRA, H. – GRABNER, M. – WIMMER, R. (2003): Clonal and site variation of vessels in 7–year–old *Eucalyptus globulus*. International Association for Wood Anatomist 24 (2): 185–195. https://doi.org/10.1163/22941932-90000331

MCKIMM, R. – ILIC, Y. (1987): Characteristics of the wood of young fast–grown trees of *Eucalyptus nitens* Maiden with special reference to provenance variation. III. Anatomical and physical characteristics. Australian Forest Research 17 (1): 19–28.

MELO, L. E. L. – GOULART, S. L. – GUIMARÃES, B. M. R. – GUIMARÃES, N. R. M. – SARTORI, C. J. – LIMA, J. T. (2018): Prediction of microfibril angle for *Eucalyptus microcorys* wood by fiber length and basic density. Maderas. Ciencia y tecnología 20 (4): 553–562. http://doi.org/10.4067/S0718-221X2018005004301

MIRANDA, I. – GOMINHO, J. – PEREIRA, H. (2009): Variation of heartwood and sapwood in 18–year–old Eucalyptus globulus trees grown with different spacings. Trees *23* (2): 367–372. http://doi.org/10.1007/s00468-008-0285-9

MOGLIA, J. G. – BRAVO, S. – GEREZ, R. (2008): Anatomía comparada del leño de *Eucalyptus camaldulensis* (Myrtaceae) de dos orígenes, ensayados en Santiago del Estero [Comparative anatomy of the log of *Eucalyptus camaldulensis* (Myrtaceae) of two origins, tested in Santiago del Estero]. Boletín de la Sociedad Argentina de Botánica 43 (3–4): 239–246. (In Spanish)

MONTEOLIVA, S. – SENISTERRA, G. – MARLATS, R. (2005): Variation of wood density and fibre length in six willow clones (Salix spp.). International Association for Wood Anatomists 26 (2): 197–202. https://doi.org/10.1163/22941932-90000111

MOORE, J. R. – COWN, D. J. (2017): Corewood (juvenile wood) and its impact on wood utilisation. Current Forestry Reports, *3*(2), 107–118. http://doi.org/10.1007/s40725-017-0055-2

OFORI, J. – BRENTUO, B. (2005): Green moisture content, basic density, shrinkage and drying characteristics of the wood of *Cedrela odorata* grown in Ghana. Tropical Forest Science 17 (2): 211–223. http://www.jstor.org/stable/23616568

PILLAI, P. – PANDALAI, R. – DHAMODARAN, T. – SANKARAN, K. (2013): Wood density and heartwood proportion in eucalyptus trees from intensively–managed short–rotation plantations in Kerala, India. Journal of Tropical Forest Science 25 (2): 220–227. https://www.jstor.org/stable/23617037

PLOMION, C. – LEPROVOST, G. – STOKES, A. (2001): Wood formation in trees. Plant Physiology 127 (4): 1513–1523. https://doi.org/10.1104/pp.010816

QUILHÓ, T. – MIRANDA, I. – PEREIRA, H. (2006): Within–tree variation in wood fibre biometry and basic density of the urograndis eucalypt hybrid (*Eucalyptus grandis* × *E. urophylla*). International Association for Wood Anatomists 27(3): 243–254. https://doi.org/10.1163/22941932-90000152

RAMALHO, F. M. G. – PIMENTA, E. M. – GOULART, C. P. – DE ALMEIDA, M. N. F. – VIDAURRE, G. B. – HEIN, P. R. G. (2019): Effect of stand density on longitudinal variation of wood and bark growth in fast–growing eucalyptus plantations. iForest–Biogeosciences and Forestry 12 (6): 527–532. https://doi.org/10.3832/ifor3082-012

RAMÍREZ, M. – RODRÍGUEZ, J. – PEREDO, M. – VALENZUELA, S. – MENDONÇA, R. (2009): Wood anatomy and biometric parameters variation of *Eucalyptus globulus* clones. Wood Science and Technology 43 (1–2): 131–141. https://doi.org/10.1007/s00226-008-0206-5

RAO, R. – SHASHIKALA, S. – SREEVANI, P. – KOTHIYAL, V. – SARMA, C. – LAL, P. (2002): Within tree variation in anatomical properties of some clones of *Eucalyptus tereticornis* Sm. Wood Science and Technology 36 (3): 271–285. https://doi.org/10.1007/s00226-002-0139-3

ROQUE, R. M. (2004): Effect of management treatment and growing regions on wood properties of *Gmelina arborea* in Costa Rica. New Forests 28 (2): 325–330. https://doi.org/10.1023/B:NEFO.0000040965.76119.bc

SAVIDGE, R. A. (2003): Tree growth and wood quality. In: "Wood Quality and its Biological Basis" Barnett J. R. – Jeronimidis, G. eds). Blackwell Publishing, Victoria, 1–29.

SCHWEINGRUBER, F. H. (2007): Wood structure and environment: Springer Verlag, Berlin, pp. 278. https://doi.org/10.1007/978-3-540-48548-3

SHARMA, S. K. – SHUKLA, S. R. – SHASHIKALA, S. – POORNIMA, V. S. (2015): Axial variations in anatomical properties and basic density of *Eucalyptus urograndis* hybrid (Eucalyptus grandis × E. urophylla) clones. Forestry Research 26 (3): 739–744. https://doi.org/10.1007/s11676-015-0080-6

TARDIF, J. C. – CONCIATORI, F. (2015): Microscopic examination of wood: Sample preparation and techniques for light microscopy. *In*: "Plant microtechniques and protocols" (Yeung E, Stasolla C,

Sumner M, Huang B eds). Springer, Cham, pp. 373–415. https://doi.org/10.1007/978-3-319-19944-3_22

TAYLOR, F. (1973): Anatomical wood properties of South African grown *Eucalyptus grandis*. South African Forestry Journal 84 (1): 20–24. https://doi.org/10.1080/00382167.1973.9629286

TEAM, R. C. (2014): R: A language and environment for statistical computing. Vienna, Austria: R Foundation for Statistical Computing. Web site [online 11 november 2020] URL: http://www.R–project.org/

TOMAZELLO, F. M. (1987): Variação radial da densidade básica e da estrutura anatômica da madeira do *Eucalyptus globulus, E. pellita e E. acmenioides* [Radial variation of basic density and anatomical structure of *Eucalyptus globulus, E. pellita and E. acmenioides* wood]. Revista, Instituto de Pesquisa Florestais 36: 35–42.

TREVISAN, R. – DE SOUZA, J. T. – DENARDI, L. – HASELEIN, C. R. – SANTINI, E. J. (2013): Effect of thinning on the wood fibre length of *Eucalyptus grandis* W. Hill ex Maiden. Ciência Florestal 23 (2): 463–475.

VALLE, M. L. A. – SILVA, J. D. C. – LUCIA, R. M. D. – EVANGELISTA, W. V. (2013): Retention and penetration of CCA in wood of first and second rotation of *Eucalyptus urophylla* ST Blake. Ciência Florestal 23: 481–490. http://hdl.handle.net/1807/45303

WHEELER, E. A. (2011): Insidewood – a Web Resource for Hardwood Anatomy. International Association for Wood Anatomists 32 (2): 199–211. https://doi.org/10.1163/22941932-90000051

WILLAN, P. G. A. (1951): Rapid growth of Eucalyptus in Nyasaland. Empire Forestry Review 30 (1): 77. Accessed March 14, 2020. http://www.jstor.org/stable/42602074

WIMMER, R. – DOWNES, G. M. – EVANS, R. (2002): High–resolution analysis of radial growth and wood density in *Eucalyptus nitens*, grown under different irrigation regimes. Annals of Forest Science 59 (5–6): 519–524. https://doi.org/10.1051/forest:2002036

WOODS, P. V. – PESETA, O. (1996): Early growth of *Eucalyptus pellita* on a range of sites in Western Samoa. The Commonwealth Forestry Review 75 (4): 334–337. https://www.jstor.org/stable/42608909

YAHYA, R. – SUGIYAMA, J. – SILSIA, D. – GRIL, J. (2010): Some anatomical features of an Acacia hybrid, A. mangium and A. auriculiformis grown in Indonesia with regard to pulp yield and paper strength. Tropical Forest Science 22 (3): 343–351. https://www.jstor.org/stable/23616663

ZANUNCIO, A. V. J. – CARVALHO, A. G. – DAMÁSIO, R. A. P. – OLIVEIRA, B. S. – CARNEIRO, A. C. O. – COLODETTE, J. L. (2016): Relationship between the anatomy and drying in *Eucalyptus grandis* X *Eucalyptus urophylla* wood. Revista Árvore 40 (4): 723–729. https://doi.org/10.1590/0100-67622016000400016

ZOBEL, B. J. – SPRAGUE, J. R. (1998): Juvenile wood in forest trees. Springer Verlag: Berlin, Germany, pp. 299.

ZOBEL, B. J. – VAN BUIJTENEN, J. (1989): Wood variation–its causes and control. Springer Verlag: Berlin, Germany, pp. 363. https://doi.org/10.1007/978-3-642-74069-5_1

Guide for Authors

Acta Silvatica et Lignaria Hungarica publishes original reports and reviews in the field of forest, wood and environmental sciences. ASLH is published twice a year (Nr. 1 and 2) in serial volumes. It is online accessible under: http://aslh.nyme.hu

Submission of an article implies that the work has not been published previously (except in the form of an abstract or as part of a published lecture or academic thesis), that it is not under consideration for publication elsewhere. Articles should be written in English. All papers will be reviewed by two independent experts.

Authors of papers accepted for publication should sign the Publishing Agreement that can be downloaded from the homepage (http://aslh.nyme.hu).

All instructions for preparation of manuscripts can be downloaded from the homepage.

Contents and Abstracts of the Bulletin of Forest Science

Bulletin of Forest Science (Erdészettudományi Közlemények) is a journal supported by the Forest Research Institute of the Faculty of Forestry of the University of Sopron. The papers are in Hungarian, with English summaries. The recent issue (Vol. 11, 2021) contains the following papers. The full papers can be found and downloaded in *pdf* format from the journal's webpage (www.erdtudkoz.hu).

Vol. 11, Nr. 1, 2021

Abstract - Our aim was to assess the effects of feeding places for hunting wild boar (bait sites). We selected 3-3 sites, located in forest, clearing area and on road. 4 transects were arranged from the centre of the sites, each consisting of 22 1 m^2 quadrats, where vegetation surveys were carried out in several years and periods. For the seed bank experiment, soil samples were taken at the centre of each bait and control sites. Then, seedling emergence method was used. We also measured soil P, K and NO_3^-. Bait sites in clearings were the most invaded, possibly due to greater accessibility. Forest baits were the least weedy, road baits' degradation depends on their exposure and usage. The proportion of weeds was always higher in August, at clearings T4 weeds dominated. We detected a stress gradient: weeds were dominant in the centre, but with the distance they decreased, while natural species increased. At baits, the proportion of weeds in the seed bank was larger than in the control. Soil P, K and NO_3^- was also higher in the centre of baits. Besides degrading the vegetation, baits have negative effects on seed bank and soil as well, so they could be the focal points of biological invasions

https://doi.org/10.17164/EK.2021.001

Abstract - We examined the changes in the prevalence and abundance of Tree of Heaven in several forest stands in the Peszérierdő (Central Hungary), where logging activities were carried out or previously stump deposits were made. According to our results, selective thinning and clear-cutting can have a significant effect on the activation of the seed bank of Tree of Heaven. Due to the abrupt growth of light availability, the soil disturbance and the other effects of log transport, the forest management activities may result in a reforestation, where the Tree of Heaven becomes dominant. In comparison to the spontaneous spread measured in control stands, forest management activities resulted even in a hundred times higher growth in both the prevalences and abundances of Tree of Heaven from one year to

another. In the surveyed artificial reforestations, the stump deposits proved to be the main objects where this species can regenerate from. It can resprout from its stumps and root remnants as well, then propagate within a few years and invade the intact, young stands. In addition – based on our local observations –, we also highlight the verticillium wilt as a control possibility against the Tree of Heaven.
https://doi.org/10.17164/EK.2021.002

Csenge Veronika HORVÁTH, Flóra TINYA, Bence KOVÁCS and Péter ÓDOR:

The effect of different forestry treatments on the understory vegetation of a sessile oak-hornbeam forest

Abstract - In the framework of a multitaxon forest ecological experiment, we compared the effects of different treatments of rotation and selection silvicultural systems on the understory vegetation of a sessile oak–hornbeam forest stand. The five treatments were: clear-cutting, keeping a retention tree group in the clear-cut, preparation cutting, gap-cutting, and closed mature stands were used as control. We compared species richness, total cover and composition of the understory vegetation, and cover of four plant functional groups in the second and fourth year after the interventions across the treatments. Species richness and total cover increased the most until the fourth year in clear-cuts and gaps, moderately in preparation cuts and the least in retention tree groups. Species composition changed the most in clear-cuts: here the cover of non-forest herbs increased, while species typical of woodlands could prevail in gaps. Gaps and preparation cuts provided the most favourable conditions for forest herbs and for the cover increase of woody saplings, supporting that harvesting methods sustaining continuous forest cover could possibly integrate both conservation and timber production aims.
https://doi.org/10.17164/EK.2021.003

László BALI, Dániel ANDRÉSI, Katalin TUBA and Csaba SZINETÁR:

Ground-dwelling spider fauna of the Nyíri-forest near Kecskemét, Hungary

Abstract – During our survey, we investigated the ground-dwelling spider fauna of five forest sub-compartments (32-117 years old; with species as grey poplar, pedunculate oak and black locust) belonging to the Nyíri-forest of Central Hungary, using pitfall traps. Sampling was conducted during the year of 2016, through 190 days. We collected 1802 specimen of 39 spider species. *Pardosa alacris* was the most common species, with 361 specimen. Gnaphosidae was the most species rich spider family, with 8 species. Most of the trapped spiders were cursorial hunters. The community showed the highest activity during June. According to the indicator species, the surveyed forest can be considered open and relatively dry, and in a good condition regarding its naturality. The values of the Shannon diversity indices and the equitability were generally low. According to the ordination analysis, the samples collected from different forest sub-compartments separated from each other noticeably.
https://doi.org/10.17164/EK.2021.004

Balázs Gábor BALÁZS, Katalin TUBA and Ferenc LAKATOS:

The role of microorganisms in the ecology of bark beetles (Curculionidae, Scolytinae)

Abstract – Some bark beetle species (Curculionidae, Scolytinae), especially in coniferous forests, are major factors for mass mortality of trees. Although bark beetle species usually do not attack healthy trees, they can colonize weakened or dying trees. Some species may have massive outbreaks, especially under defined abiotic conditions (like hot and dry weather or

after wind and snow damage) and can have significant economic and ecological effect. Microorganisms associated with bark beetles such as fungi or bacteria play important roles in their colonization success, development, and gradation. This paper provides a review on the effects of microorganisms on the biology of bark beetles and interactions between bark beetles and their host plants. We present these interactions based on the holobiont theory, i.e., considering bark beetles and their associated microbiota as a whole.
https://doi.org/10.17164/EK.2021.005

Vol. 11, Nr. 2, 2021

Tamás KOLLÁR and Attila BOROVICS:

The updated methodological directives of data processing and maintainance of the Hungarian long term forestry experimental network, and its most important results

Abstract – The Hungarian long-term forestry experiment network was established in 1962, with the lead of Rezső Solymos, The Forest Research Institute has been running the network continuously since that time and its data are under research. The basic objectives of the network are unaltered since the establishment. The primary aim was to create a suitable basis for silvicultural and forest yield research in Hungary. The experiment plots take place in forest stands of common beech (*Fagus sylvatica*), sessile oak (*Quercus petraea*), Turkey oak (Quercus cerris), pedunculated oak (*Quercus robur*), hornbeam (*Carpinus betulus*), common ash (*Fraxinus excelsior*), Scots pine (*Pinus sylvestris*), black pine (*Pinus nigra*) and Norway spruce (*Picea abies*). More than 3000 plots, about 11000 survey reports (diameter, height, classification) are available, from which more than 6600 survey reports are digitally accessible. About 1200 plots are still monitored. The detailed methods of alignment, measurement and maintenance of the experimental plots and the most important publications of the long-term experiments are summarized. From these, the national forest yield tables and silvicultural treatment models are significant, but with the possession of new data, reformation is necessary.
https://doi.org/10.17164/EK.2021.006

Ferenc SZMORAD, Kristóf KELEMEN, Kata KENDERES and Tibor STANDOVÁR:

Assessment of composition, structure and dead wood supply in forests of the North Hungarian Mountains, Hungary

Abstract – The main objective of our project entitled „Multi-purpose assessment serving biodiversity conservation in the Carpathians region of Hungary”, supported by the Swiss-Hungarian Cooperation Program, was to develop a new forest state description methodology and to apply it to survey nearly 50,000 hectares of forests in three regions (Börzsöny, Mátra, Aggtelek Karst) of the North Hungarian Mountains. The present study evaluates the composition and structure of tree canopy and deadwood supply based on data collected by systematic sampling, fine spatial resolution and by recording numerous variables. The results show the compositional and structural richness of the Aggtelek karst, the lack of admixing tree species and a better supply of standing dead wood in the Mátra, the higher variation in canopy closure in the Börzsöny. There is no significant difference between the regions in terms of lying dead wood, and invasive trees species (black locust, tree of heaven). Among the practical conclusions, the dependence of certain characteristics (admixing trees, dead wood) on management is emphasised, and related management proposals are made.
https://doi.org/10.17164/EK.2021.007

Abstract – This paper analyses the drought induced growth responses of oak stands, Sessile oak (*Quercus petraea*) and Turkey oak (*Q. cerris*), along a precipitation gradient in Somogy County. 136 tree-ring samples were analysed and dendroecological metrics were also applied to assess the drought sensitivity of the species. Water deficit was estimated by using the soil water budget based water stress index. Results indicated a strong dependency of annual tree ring width on the water availability of current year summer but found different strategies of the two tree species against drought conditions. Turkey oak responded more sensitively to droughts than sessile oak revealed by the significantly lower resistance and higher recovery potential of this species. A linearly proportional increase of growth reduction with rising water stress was found for Turkey oak while the growth response of sessile oak decreased considerably with increasing aridity indicating lower growth plasticity of sessile oak to droughts there. Based on our findings it seems that Turkey oak copes better with droughts than sessile oak and may gain competitive advantages under the projected climate change.
https://doi.org/10.17164/EK.2021.008

Abstract – The satellite based remote sensing forest monitoring system of Farkas-erdő of Sárvár was created to utilize high resolution ESA Sentinel-2 images and cloud computing, where processing, analysing, and displaying of health state changes of forests takes place online, in the Google Earth Engine. The system aims to monitor the forest health state change constantly with high precision in the investigation period of 2017-2020, using maps and graphs made of vegetation and moisture indices. Remotely sensed data was compared to field-based damage reports for validation purposes.
https://doi.org/10.17164/EK.2021.009